TUDelft

Delft University of Technology

Novel genetic parts and cultivation strategies for yeast-based conversion of lignocellulosic feedstocks

Verhoeven, Maarten

DOI
10.4233/uuid:afd3a04b-1e86-4561-bc9e-87ad8e569de3

Publication date
2018

Document Version
Final published version

Important note
To cite this publication, please use the final published version (if applicable).
Please check the document version above.

Novel genetic parts and cultivation strategies for yeast-based conversion of lignocellulosic feedstocks

Maarten Verhoeven
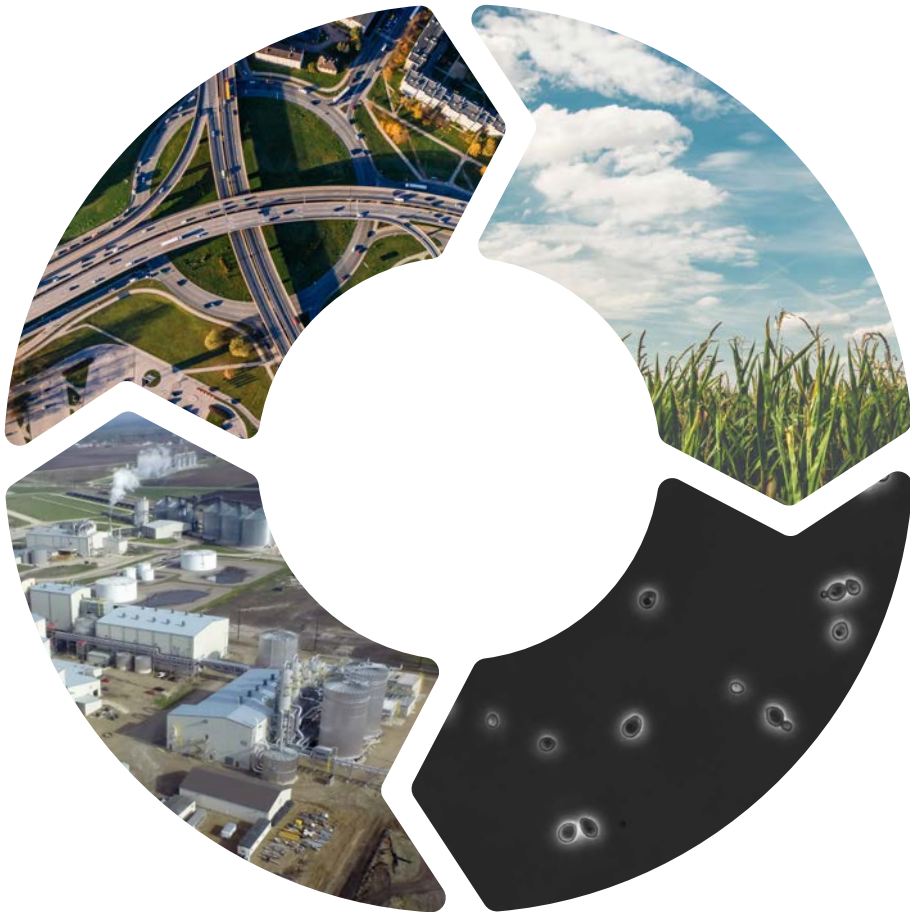
Novel genetic parts and cultivation strategies for yeast-based conversion of lignocellulosic feedstocks

Proefschrift

ter verkrijging van de graad van doctor
aan de Technische Universiteit Delft,
op gezag van de Rector Magnificus prof. dr. ir. T.H.J.J. van der Hagen
voorzitter van het College voor Promoties,
in het openbaar te verdedigen op
donderdag 6 september 2018 om 10:00 uur

door

Maarten Dirk VERHOEVEN

Ingenieur in Life Science and Technology
Technische Universiteit Delft, Nederland
geboren te Amersfoort, Nederland

Dit proefschrift is goedgekeurd door de promotoren.

Samenstelling promotiecommissie:

Rector magnificus,	voorzitter
Prof. dr. J.T. Pronk,	Technische Universiteit Delft, promotor
Prof. dr. ir. A.J.A. van Maris,	Technische Universiteit Delft, promotor

Onafhankelijke leden:

Prof. dr. P. A. S. Daran-Lapujade	Technische Universiteit Delft
Prof. dr. H. op den Camp	Radboud Universiteit Nijmegen
Prof. dr. B. Teusink	Vrije Universiteit Amsterdam
Dr. M. Oreb	Goethe-Universität Frankfurt am Main
Prof. dr. U. Hanefeld	Technische Universiteit Delft, reservelid

Overig lid:

Prof. dr. D. B. Jansen	Rijksuniversiteit Groningen

Table of Contents

Summary

The recent start-up of several full-scale 'second generation' ethanol plants marks a major milestone in the development of *Saccharomyces cerevisiae* yeast strains for fermentation of lignocellulosic hydrolysates of agricultural residues and energy crops. In contrast to the fermentation of hexose sugar-rich substrates, such as corn syrup or sugar cane bagasse, these hydrolysates contain mixtures of the hexose sugar D-glucose and the pentose sugars D-xylose and L-arabinose. While S*. cerevisiae* performs excellently in fermenting hexose sugars to ethanol, efficient utilization of pentose sugars required extensive metabolic and evolutionary engineering.

   Chapter 1 discusses the challenges imposed by second-generation industrial ethanol production on yeast strain characteristics and describes key metabolic engineering strategies that have been developed to address these challenges. Additionally, it outlines how proof-of-concept studies, often developed in academic settings, can be used for the development of robust strain platforms that meet the requirements for industrial application. Amongst the developments that are described, DNA-sequencing and genome-editing techniques have transformed the molecular toolbox for yeast strain and analysis. construction. In particular, CRISPR-Cas9-supported genome editing and identification of causal mutations that underly the improved performance of strains obtained by non-targeted strain improvement campaigns, have greatly accelerated research in this field. The goal of the PhD research project described in this thesis was to use these tools to design and test novel strategies to obtain *S. cerevisiae* strains with improved D-xylose and/or L-arabinose fermentation kinetics.

   Previous studies already demonstrated that combined overexpression of xylulokinase, pentose-phosphate-pathway enzymes and a heterologous xylose isomerase (XI), enables fast growth of *S. cerevisiae* on D-xylose. XI catalyzes the reaction from D-xylose to D-xylulose, which, after phosphorylation to D-xylulose-5-phosphate, can be channeled into the pentose-phosphate-pathway. In **Chapter 2**, single-step Cas9-assisted metabolic engineering was done to obtain a yeast strain expressing *Piromyces* XI that showed instantaneous, fast aerobic growth on D-xylose. However, anaerobic growth of the resulting strain required a 12-day adaptation period. Xylose-adapted anaerobic cultures were shown to carry mutations in *PMR1*, encoding a Golgi Ca^{2+}/Mn^{2+} ATPase. Deleting *PMR1* in the parental XI-expressing strain enabled its instantaneous anaerobic growth on D-xylose. In *pmr1* strains, intracellular Mn^{2+} concentrations were much higher than in the parental strain. XI activity assays in cell extracts and reconstitution experiments with purified XI apoenzyme showed superior enzyme kinetics with Mn^{2+} relative to other divalent metal ions. The results presented in this Chapter indicated that engineering of metal homeostasis can be a relevant approach for optimization of metabolic pathways involving metal-

dependent enzymes. Specifically, it identifies metal interactions of heterologous XIs as an underexplored aspect of engineering xylose metabolism in yeast.

Compared to levels of D-xylose in lignocellulosic hydrolysates, those of the pentose sugar L-arabinose are generally lower, but still economically relevant. Functional expression, in *S. cerevisiae*, of the *araA*, *araB* and *araD* genes from the gram-positive bacterium *Lactobacillus plantarum*, which encode an isomerase, kinase and epimerase, respectively, enable conversion of intracellular L-arabinose into D-xylulose-5P. Transport of L-arabinose in *S. cerevisiae* occurs via the Gal2 galactose transporter which, however, has a low affinity for this pentose sugar while, moreover, L-arabinose transport via Gal2 is inhibited by D-glucose. L-arabinose uptake is therefore an important rate-controlling step in the complete conversion of lignocellulosic feedstocks by engineered, pentose-metabolizing *S. cerevisiae* strains. In **Chapter 3**, chemostat-based transcriptome analysis yielded 16 putative sugar transporter genes whose transcript levels were at least three-fold higher in L-arabinose-limited cultures than in D-glucose-limited and ethanol-limited cultures in the filamentous fungus *Penicillium chrysogenum*. Five genes that encoded putative transport proteins showed an over 30-fold higher transcript level in L-arabinose-grown cultures than in D-glucose-grown cultures. One of these (Pc20g01790) restored growth on L-arabinose upon expression in an engineered L-arabinose-fermenting *S. cerevisiae* strain in which the endogenous L-arabinose transporter, encoded by *GAL2*, had been deleted. Sugar-transport assays indicated that this fungal transporter, designated as *Pc*AraT, is a high-affinity (K_m = 0.13 mM), high-specificity L-arabinose-proton symporter that does not transport D-xylose or D-glucose. An L-arabinose-metabolizing *S. cerevisiae* strain in which *GAL2* was replaced by *PcaraT* showed a 450-fold lower residual substrate concentration in L-arabinose-limited chemostat cultures than a congenic strain in which L-arabinose import depended on Gal2 ($4.2 \cdot 10^{-3}$ g L^{-1} and 1.8 g L^{-1}, respectively). Inhibition of L-arabinose transport by the most abundant sugars in lignocellulosic hydrolysates, D-glucose and D-xylose, was far less pronounced than observed with Gal2. Expression of *Pc*AraT in a hexose-phosphorylation-deficient, L-arabinose-metabolizing *S. cerevisiae* strain enabled growth in media supplemented with both 20 g L^{-1} L-arabinose and 20 g L^{-1} D-glucose. Under the same conditions, no growth was observed with a congenic strain in which L-arabinose transport exclusively depended on Gal2. Its high affinity and specificity for L-arabinose, combined with limited sensitivity to inhibition by D-glucose and D-xylose make *Pc*AraT a valuable transporter for application in metabolic engineering strategies aimed at engineering *S. cerevisiae* strains for efficient conversion of lignocellulosic hydrolysates.

In **Chapter 4**, an engineered glucose-phosphorylation-negative *S. cerevisiae* strain, expressing the L-arabinose pathway and *Pc*AraT, was constructed and subjected to laboratory evolution. Selection on L-arabinose in the presence of d-glucose was made possible by removing all the hexokinase encoding genes (first step of glycolysis). Anaerobic sequential batch cultivations on glucose-xylose-arabinose mixtures yielded evolved strains that grew on L-arabinose in the presence of D-glucose and D-xylose. Whole-genome

sequencing of four evolved strains showed that *GAL2* had been duplicated in all strains, with both copies encoding the same, strain-dependent amino-acid substitution at position 376 of Gal2. In one strain, one of the two *GAL*2 alleles additionally encoded a T89I substitution. Introduction of the N376I substitution in a non-evolved strain enabled growth on L-arabinose in the presence of D-glucose. In sugar-transport assays, Gal2^{N376S}, Gal2^{N376T} and Gal2^{N376I} exhibited a lower glucose sensitivity of L-arabinose uptake than wild-type Gal2 and a strongly increased K_m for D-glucose transport. The T89I substitution was also identified in *S. cerevisiae* IMS0010, a strain that was previously engineered and evolved for pentose/hexose co-consumption. Gal2$^{N376T, T89I}$ and Gal2^{T89I} showed a lower K_m for L-arabinose and a higher K_m for D-glucose than wild-type Gal2. Reverting Gal2$^{N376T, T89I}$ to Gal2^{N376} in an evolved strain negatively affected anaerobic growth on L-arabinose. Reverse engineering of *GAL2* mutations into a non-evolved strain indicated that improved utilization of L-arabinose was primarily due to the Gal2^{N376T} substitution, while the Gal2$^{N376T, T89I}$ substitution and expression of *Pc*AraT contributed to L-arabinose uptake when concentrations of this pentose sugar were low relative to those of D-glucose. Sequential batch cultures on sugar mixtures of a glucose-phosphorylation-negative yeast strain were successfully used to select for xylose- and glucose-insensitive growth on L-arabinose. Identification of causal mutations in *GAL2* provided insight into the evolution of a strain with two new, functionally different L-arabinose transporters. Combination of these two evolved Gal2 variants with a heterologously expressed fungal arabinose transporter enabled the fastest rate of anaerobic L-arabinose fermentation in *S. cerevisiae* reported to date.

Simultaneous fermentation of D-glucose and D-xylose can contribute to productivity and robustness of yeast-based processes for bioethanol production from lignocellulosic hydrolysates. **Chapter 5** explores a novel evolutionary engineering strategy for identifying mutations that contribute to simultaneous utilization of these sugars in batch cultures of *S. cerevisiae*. To force simultaneous utilization of D-xylose and D-glucose, *PGI1* and *RPE1* were deleted in an XI-based xylose-fermenting strain with a modified oxidative pentose-phosphate pathway. Laboratory evolution of this strain in serial batch cultures on glucose-xylose mixtures yielded mutants that rapidly co-consumed the two sugars. Whole-genome sequencing of evolved strains identified mutations in *HKX2*, *RSP5* and *GAL83*. Subsequent introduction of these mutations into a non-evolved xylose-fermenting *S. cerevisiae* strain improved co-consumption of D-xylose and D-glucose under aerobic and anaerobic conditions. Combined deletion of *HXK2* and introduction of a *GAL83*^{G673T} allele yielded a strain with a 2.5-fold higher xylose and glucose co-consumption ratio than its xylose-fermenting parental strain. These two modifications decreased the time required for full sugar conversion in anaerobic bioreactor batch cultures, grown on 20 g L^{-1} glucose and 10 g L^{-1} xylose, by over 24 h. This study demonstrates that combining laboratory evolution and genome resequencing of microbial strains engineered for forced co-consumption is a powerful approach for studying and improving simultaneous conversion of mixed substrates.

Current yeast-based second-generation bioethanol production strategies employ 'generalist' strains of *S. cerevisiae* to anaerobically ferment mixtures of pentose and hexose sugars to ethanol. **Chapter 6** explores an alternative strategy: the anaerobic fermentation of glucose-xylose-arabinose mixtures by a consortium of three 'specialist' *S. cerevisiae* strains. A xylose specialist strain was constructed by elimination of hexose phosphorylation in a xylose isomerase-based, xylose-fermenting *S. cerevisiae* strain, followed by laboratory evolution in anaerobic sequential batch reactors (SBRs) grown on 20 g L^{-1} of D-xylose, D-glucose and L-arabinose. A strain isolated from such an evolution experiment anaerobically grew and fermented D-xylose in the presence of 20 g L^{-1} of the other two sugars. A mixed-sugar fermenting consortium was formed by combining this strain with the previously constructed L-arabinose specialist strain, described in **Chapter 4**, and a pentose-non-fermenting laboratory strain of *S. cerevisiae*. In anaerobic batch cultures of the consortium on 20 g L^{-1} of each sugar, D-glucose and L-arabinose were rapidly and simultaneously converted. However, D-xylose fermentation was strongly impaired in the presence of the glucose and arabinose specialist strains. Prolonged cultivation of the consortium on sugar mixtures in SBR cultures strongly improved kinetics of mixed-sugar fermentation. The time required for complete sugar conversion by evolved consortium approached that of a previously described generalist *S. cerevisiae* strain. In contrast to the generalist strain, which showed progressive deterioration of fermentation kinetics during prolonged anaerobic SBR cultivation on a mixture of 20 g L^{-1} D-glucose, 10 g L^{-1} D-xylose and 5 g L^{-1} L-arabinose, fermentation kinetics of the evolved consortium remained stable. Deterioration of the performance of a 'generalist' pentose-fermenting strain during prolonged SBR cultivation on sugar mixtures identifies a key challenge in the implementation of yeast biomass recycling in the industrial fermentation of lignocellulosic hydrolysates. The stable performance, under the same conditions, of a consortium of three 'specialist' strains demonstrates a potential advantage of this mixed-culture approach in industrial processes. Further improvement of the kinetics of mixed-sugar fermentation by synthetic consortia will require additional research into the interactions between the specialist strains.

At present, fermentation performance of current engineered industrial *S. cerevisiae* strains is no longer a bottleneck in efforts to achieve the projected outputs of the first large-scale second-generation ethanol plants. The genetic parts and novel cultivation strategies presented in this thesis will, together with other academic and industrial yeast research, help to strengthen the economic value position of second-generation ethanol production by further improving fermentation kinetics, product yield and cellular robustness under process conditions.

Samenvatting

De recente ingebruikname van grootschalige 'tweede generatie' bio-ethanol fabrieken vormt een belangrijke mijlpaal in de ontwikkeling van *Saccharomyces cerevisiae* giststammen voor de fermentatie van lignocellulose-bevattende hydrolysaten die zijn gemaakt van agrarische reststromen en energiegewassen. In tegenstelling tot grondstoffen die rijk zijn aan hexose-suikers, zoals bijvoorbeeld maissiroop of suikerrietbagasse, bestaan deze hydrolysaten voornamelijk uit mengsels van de hexosesuiker D-glucose en de pentosesuikers D-xylose en L-arabinose. Terwijl *S. cerevisiae* uitstekend in staat is om hexosesuikers te fermenteren naar ethanol, verreist de efficiënte omzetting van pentose-suikers omvangrijke programma's op het gebied van "metabolic engineering" en laboratoriumevolutie.

Hoofdstuk 1 geeft een uiteenzetting van de uitdagingen bij tweede-generatie bio-ethanol productie op industriële schaal die betrekking hebben op de eigenschappen van de gebruikte giststammen. Dit hoofdstuk beschrijft de belangrijkste 'metabolic engineering' strategieën die zijn ontwikkeld om deze uitdagingen het hoofd te bieden. Verder wordt uiteengezet hoe verschillende 'proof of concept' studies, die vaak zijn ontwikkeld binnen universiteiten, gebruikt kunnen worden voor het ontwikkelen van robuuste platformstammen met de eigenschappen die nodig zijn voor industriële toepassing. Onder andere de ontwikkelingen in het bepalen van DNA-volgorden en nieuwe genetische modificatietechnieken hebben drastische veranderingen aangebracht in het gereedschap dat wordt gebruikt voor het maken en analyseren van giststammen. Met name de opkomst van op CRISPR-Cas9 gebaseerde genoommodificatie-technieken en daarnaast de mogelijkheid om causale mutaties op te sporen die verantwoordelijk zijn voor de verbeterde prestaties van stammen afkomstig uit stamverbeteringsprogramma's, hebben een stroomversnelling veroorzaakt in het onderzoeksveld. Het doel van het in dit proefschrift beschreven onderzoek was om, met behulp van deze 'moleculaire gereedschapskist', *S. cerevisiae*-stammen met verbeterde D-xylose en/of L-arabinose fermentatiekinetiek te ontwerpen, te construeren en te testen en zo nieuwe, verbeterde strategieën voor bio-ethanolproductie mogelijk te maken.

Eerder onderzoek heeft al aangetoond dat *S. cerevisiae* snel kan groeien op D-xylose na gecombineerde overexpressie van xylulokinase, enzymen uit de pentosefosfaat–route en een heteroloog xylose-isomerase (XI). XI katalyseert de omzetting van D-xylose in D-xylulose, dat vervolgens, na fosforylering tot D-xylulose-5-fosfaat, via de pentosefosfaat-route en glycolyse wordt omgezet in ethanol. Hoofdstuk 2 beschrijft hoe, op basis van deze strategie en met behulp van Cas9-gemedieerde genoommodificatie, razendsnel een aëroob op D-xylose groeiende giststam kon worden geconstrueerd. Voor anaërobe groei van deze stam bleek echter een adaptatieperiode van 12 dagen vereist. Analyse van de DNA-volgorde van anaëroob geadapteerde, D-xylose-gekweekte cultures

toonde aan dat deze mutaties bevatten in het *PMR1*-gen, dat voor een Golgi Ca^{2+}/Mn^{2+} ATPase codeert. Het uitschakelen van *PMR1* in de ouderstam maakte onmiddellijke groei op D-xylose onder anaërobe condities mogelijk. In *pmr1* stammen bleek de intracellulaire Mn^{2+}-concentratie vele malen hoger te zijn dan in de ouderstam. Essays van XI-enzymactiviteit met celextracten en reconstitutie-experimenten met gezuiverd XI apo-enzym toonden een betere enzymkinetiek met Mn^{2+} aan dan met andere divalente metaalionen. De in Hoofdstuk 2 gepresenteerde resultaten tonen aan dat het modificeren van intracellulaire metaalhomeostase een relevante manier kan zijn om metabole routes waarbij metaal-afhankelijke enzymen betrokken zijn, te optimaliseren. Meer in het bijzonder laat dit werk zien dat metaalinteracties van XI-enzymen een onderbelicht aspect zijn in het onderzoek aan D-xylose-metabolisme door gemodificeerde gisten.

   Naast D-xylose is de pentose-suiker L-arabinose in over het algemeen lagere, maar nog steeds economisch relevante hoeveelheden aanwezig in lignocellulose bevattende hydrolysaten. Intracellulaire conversie van deze pentose-suiker naar D-xylulose-5-fosfaat kan in *S. cerevisiae* worden bewerkstelligd door functionele expressie van de *araA*, *araB* en *araD* genen uit de Gram-positieve melkzuurbacterie *Lactobacillus plantarum*, die respectievelijk coderen voor een isomerase, kinase en epimerase. In *S. cerevisiae* wordt L-arabinose-transport gefaciliteerd door de Gal2 galactosetransporter die echter slechts een lage affiniteit heeft voor deze pentosesuiker. Bovendien wordt L-arabinose-transport via Gal2 sterk geremd door D-glucose. De opname van L-arabinose wordt daarom beschouwd als een belangrijke snelheidsbepalende stap in de volledige omzetting van lignocellulose bevattende substraten in ethanol met behulp van genetische gemodificeerde, pentose-consumerende *S. cerevisiae*-stammen. **Hoofdstuk 3** beschrijft onderzoek in chemostaatcultures van de schimmel *Penicillium chrysogenum*. In dit onderzoek werden door transcriptoomanalyse 16 veronderstelde suiker-transportergenen geïdentificeerd waarvan het transcriptieniveau tenminste driemaal hoger lag in L-arabinose-gelimiteerde cultures dan in D-glucose- en ethanol-gelimiteerde cultures. Vijf van deze genen hadden zelfs een meer dan 30 maal hoger transcriptie-niveau bij groei op L-arabinose dan bij groei op D-glucose. Expressie van één van deze genen (Pc20g01790) herstelde de groei op L-arabinose van genetisch gemodificeerde L-arabinose-fermenterende *S. cerevisiae*-stammen waarin *GAL2*, het gen dat codeert voor de endogene L-arabinose transporter, was verwijderd. Transportmetingen met radioactieve suikers toonden aan dat deze schimmeltransporter, die *Pc*AraT werd genoemd, een L-arabinose-proton symporter is met een hoge affiniteit (K_m = 0.13 mM) en specificiteit, die niet in staat is om D-xylose of D-glucose te transporteren. Een L-arabinose-consumerende *S. cerevisiae* stam waarin *GAL2* werd vervangen door *Pc*araT liet in L-arabinose-gelimiteerde chemostaatcultures een 450-maal lagere residuele substraatconcentratie zien dan een stam waarin import van L-arabinose afhankelijk was van Gal2 (respectievelijk $4.2 \cdot 10^{-3}$ g L^{-1} en 1.8 g L^{-1}). Remming van L-arabinose-transport door de meest voorkomende suikers in lignocellulose bevattende substraten, D-glucose en D-

xylose, was veel minder sterk voor PcaraT in dan voor Gal2. Heterologe expressie van PcAraT stelde een hexose–fosforylering-deficiënte en L-arabinose-consumerende *S. cerevisiae* stam in staat om te groeien in media waaraan zowel 20 g L^{-1} L-arabinose als 20 g L^{-1} D-glucose was toegevoegd. Onder dezelfde condities was een vergelijkbare stam, waarbij L-arabinose transport via Gal2 plaatsvond, niet in staat om te groeien. Door een hoge affiniteit en specificiteit, gecombineerd met lage remming door D-glucose en D-xylose, is PcaraT een waardevolle transporter voor gebruik in metabolic engineering strategieën met het doel om *S. cerevisiae* stammen te maken voor efficiënte omzetting van lignocellulose bevattende hydrolysaten in bio-ethanol.

Hoofdstuk 4 beschrijft onderzoek waarin een gemodificeerde hexose–fosforylering-deficiënte *S. cerevisiae* stam, die de L-arabinose route en PcAraT aan boord had, werd geconstrueerd en vervolgens gebruikt voor een in het laboratorium uitgevoerd evolutieprogramma. Door het verwijderen van alle genen die coderen voor hexokinase (het eerste enzym in de omzetting van D-glucose) was het mogelijk te selecteren voor groei op L-arabinose in de aanwezigheid van hexosesuikers. Langdurig kweken in anaërobe sequentiële batchcultures op glucose-xylose-arabinose mengsels leverden geëvolueerde stammen die in staat waren om te groeien op L-arabinose in aanwezigheid van D-glucose en D-xylose. Analyse van de volledige genoomsequentie van vier van deze geëvolueerde stammen onthulde een duplicatie van Gal2, waarbij bovendien in beide kopieën een, stam-specifieke, aminozuursubstitutie aanwezig was op positie 376 van het eiwit. Een van de stammen bevatte nog een extra mutatie in een van de twee *GAL2* allelen, resulterend in een T89I aminozuursubstitutie. De introductie van de N376I-substitutie in een niet-geëvolueerde stam bevestigde de functie van deze mutatie, aangezien deze groei mogelijk maakte in de aanwezigheid van D-glucose. Suikertransportmetingen met de Gal2^{N376S}, Gal2^{N376T} en Gal2^{N376I} varianten lieten vervolgens een lagere D-glucose-gevoeligheid van L-arabinosetransport zien dan werd waargenomen met wild-type Gal2 en ook een sterk verhoogde K_m voor D-glucosetransport. De T89I substitutie werd eveneens aangetoond in *S. cerevisiae* IMS0010, een stam die in voorgaand onderzoek was gemodificeerd en geëvolueerd voor pentose/hexose co-consumptie. Zowel de Gal2$^{N376T, T89I}$ variant als de Gal2^{T89I} variant leidde tot een hogere K_m voor D-glucose dan werd waargenomen in wild-type Gal2. Het terugzetten van Gal2$^{N376T, T89I}$ naar Gal2^{N376T} in de geëvolueerde stam verminderde het vermogen om anaëroob te groeien op L-arabinose. De 'reverse engineering' van de *GAL2* mutaties in niet-geëvolueerde stammen gaf aan dat een verbeterd gebruik van L-arabinose voornamelijk optrad vanwege de Gal2^{N376T}-mutatie terwijl de Gal2$^{N376T, T89I}$-mutatie, in combinatie met de expressie van PcAraT, voornamelijk bijdroeg waarbij de concentratie van L-arabinose relatief laag was ten opzichte van die van D-glucose. Sequentiële batchcultures op suikermengsels van een hexose–fosforylering-deficiënte giststam werden succesvol ingezet om te selecteren voor xylose- en glucose-ongevoelige en tegelijkertijd L-arabinose-prefererende mutanten. De identificatie van causale mutaties in *GAL2* levert bovendien meer inzicht in de evolutie van een giststam met twee nieuwe, maar zich wel functioneel anders gedragende, L-

arabinose-transporters. De combinatie van de de geëvolueerde *GAL2* varianten en de heterologe L-arabinose-transporter *PcAraT* resulteerde in de hoogste anaërobe fermentatiesnelheid van L-arabinose die tot nu toe in de literatuur is vermeld.

Gelijktijdige fermentatie van D-glucose en D-xylose kan positief bijdragen aan de productiviteit en robuustheid van op gist gebaseerde processen voor bioethanolproductie uit hydrolysaten van lignocellulose-bevattende grondstoffen. **Hoofdstuk 5** verkent een nieuwe strategie voor evolutie in het laboratorium die specifiek was gericht op het identificeren van mutaties die bijdrage aan simultaan gebruik van deze suikers in batchcultures van *S. cerevisiae*. Om gelijktijdig verbruik van D-xylose en D-glucose te forceren, werden de genen *PGI1* en *RPE1* uitgeschakeld in een op XI gebaseerde xylose-fermenterende stam met een gemodificeerde oxidatieve pentosefosfaatroute. Laboratoriumevolutie van deze stam in sequentiële batchcultures op glucose-xylose-mengsels resulteerde in mutanten die in staat waren om beide suikers snel te co-consumeren. De genoomsequenties van geëvolueerde stammen verschilden op een aantal plekken van dat van de ouderstam, onder andere door mutaties in *HXK2, RSP5* en *GAL83*. Introductie van deze mutaties in een niet-geëvolueerde, xylose-fermenterende, *S. cerevisiae* stam resulteerde in aanzienlijke verbeteringen in de D-xylose en D-glucose co-consumptie-eigenschappen, zowel onder aërobe als onder anaërobe omstandigheden. Het uitschakelen van *HXK2*, gecombineerd met introductie van de aminozuursubstitutie *GAL83*^{G673T}, leverde een stam op met een 2.5 maal hogere D-xylose en D-glucose co-consumptieratio dan die van de xylose-fermenterende ouderstam. Deze twee modificaties verminderden de tijd die nodig was voor volledige conversie van 20 g L^{-1} D-glucose en 10 g L^{-1} D-xylose in anaërobe batchcultures in bioreactoren met meer dan 24 uur. De in dit Hoofdstuk beschreven resultaten tonen aan dat laboratorium-evolutie van microbiële stammen die zijn ontwikkeld voor geforceerde co-consumptie, met daaropvolgend genoomsequencing, een krachtige methode is om simultane conversie van mengsubstraten te bestuderen en te verbeteren.

De huidige, op gist gebaseerde tweede generatie bioethanol-productiestrategieën gebruiken 'generalisten'stammen van *S. cerevisiae* om mengsels van pentoses en hexoses anaëroob te fermenteren tot ethanol. **Hoofdstuk 6** verkent een alternatieve strategie: anaërobe fermentatie van glucose-xylose-arabinose mengsels door een consortium van drie 'specialisten'stammen van *S. cerevisiae*. Een xylose-specialiststam werd geconstrueerd door hexosefosforylering uit te schakelen in een XI-gebaseerde, xylose-fermenterende *S. cerevisiae*-stam, waarna laboratoriumevolutie werd uitgevoerd in anaërobe sequentiële batchreactoren (SBRs) met 20 g L^{-1} D-xylose, D-glucose en L-arabinose. Een stam die uit een van deze evolutieexperimenten werd geïsoleerd, was in staat om te groeien onder anaërobe condities en daarbij alleen D-xylose om te zetten in de aanwezigheid van 20 g L^{-1} van de andere twee suikers. Vervolgens werd een mengcultuur van suikerfermenterende specialisten werd opgezet door deze stam te combineren met de L-arabinose specialist die is beschreven in **Hoofdstuk 4** en een niet-pentose-fermenterende laboratoriumstam van *S. cerevisiae*. In anaërobe batchculturen

van dit consortum op een mengsel met 20 g L^{-1} van elke suiker werden zowel D-glucose en L-arabinose snel, en tegelijkertijd, omgezet. D-xylose fermentatie werd echter sterk vertraagd in de aanwezigheid van de glucose- en arabinosespecialisten. Langdurig kweken van het consortium op diverse suikermengsels in SBR-culturen resulteerde in een sterk verbeterde fermentatiekinetiek. De tijd die nodig was voor de omzetting van alle suikers door het geëvolueerde consortium benaderde die van fermentaties gedaan met een eerder beschreven 'generaliststam' van *S. cerevisiae*. In tegenstelling tot deze generaliststam, die een progressieve verslechtering van de fermentatiekinetiek liet zien gedurende langdurig kweken op 20 g L^{-1} D-glucose, 10 g L^{-1} D-xylose en 5 g L^{-1} L-arabinose in SBR-systemen, bleef de fermentatiekinetiek van het consortium stabiel. De verslechtering in prestatie van de 'generalist' pentose-fermenterende stam gedurende langdurige groei op suikermengsels in SBR-cultures brengt een belangrijke uitdaging aan het licht met betrekking tot de implementatie van gistbiomassa recycling in industriële fermentatie van lignocellulose-bevattende hydrolysaten. De stabiele prestaties, onder dezelfde condities, van een consortium bestaande uit drie specialistenstammen demonstreert een mogelijk voordeel van deze mengcultuur-aanpak in industriële processen. Verdere verbetering op het gebied van fermentatiekinetiek van de synthetische consortia zal extra onderzoek vereisen naar de interacties tussen de specialistenstammen.

Op dit moment zijn de fermentatie-eigenschappen van de huidige gemodificeerde industriële *S. cerevisiae* stammen niet langer een knelpunt voor het bereiken van beoogde opbrengsten voor de eerste grootschalige 'tweede generatie' bio-ethanol fabrieken. De genetische onderdelen en nieuwe fermentatiestrategieën die zijn gepresenteerd in dit proefschrift zullen, samen met resultaten uit ander universitair en industrieel onderzoek, helpen om de economische waarde van tweede generatie bio-ethanol productie te vergroten, door fermentatiekinetiek, productierendement en celrobuustheid onder procescondities verder te verbeteren.

Chapter 1: Introduction

This Chapter is based on a published review paper (M.L. Jansen, J.M. Bracher, I. Papapetridis, M.D. Verhoeven, H. de Bruijn, P.P. de Waal, A.J.A. van Maris, P. Klaassen, and J.T. Pronk, 2017. '*Saccharomyces cerevisiae* strains for second-generation ethanol production: from academic exploration to industrial implementation'.

Abstract

The recent start-up of several full-scale 'second generation' ethanol plants marks a major milestone in the development of *Saccharomyces cerevisiae* strains for fermentation of lignocellulosic hydrolysates of agricultural residues and energy crops. After discussing the challenges that these novel industrial contexts impose on yeast strains, this mini-review describes key metabolic engineering strategies that have been developed to address these challenges. Additionally, it outlines how proof-of-concept studies, often developed in academic settings, can be used for the development of robust strain platforms that meet requirements for industrial application. Fermentation performance of current, engineered industrial *S. cerevisiae* strains is no longer a bottleneck in efforts to achieve the projected outputs of the first large-scale second-generation ethanol plants. Academic and industrial yeast research will continue to strengthen the economic value position of second-generation ethanol production by further improving fermentation kinetics, product yield and cellular robustness under process conditions.

1

Introduction

Alcoholic fermentation is a key catabolic process in most yeasts and in many fermentative bacteria, that concentrates the heat of combustion of carbohydrates into two thirds of their carbon atoms ($(CH_2O)_n \rightarrow \frac{1}{3}n\ C_2H_6O + \frac{1}{3}n\ CO_2$). Its product, ethanol, has been used as an automotive fuel for over a century [15]. With an estimated global production of 100 Mton [16], ethanol is the largest-volume product in industrial biotechnology. Its production is, currently, mainly based on fermentation of cane sugar or hydrolysed corn starch with the yeast *Saccharomyces cerevisiae.* Such 'first generation' bioethanol processes are characterized by high ethanol yields on fermentable sugars (> 90 % of the theoretical maximum yield of 0.51 g ethanol·(g hexose sugar)$^{-1}$), ethanol titers of up to 21 % (w/w) and volumetric productivities of 2 to 3 kg·m^{-3}·h^{-1} [17-19].

Over the past two decades, a large international effort, involving researchers in academia, research institutes and industry, aimed to access abundantly available agricultural and forestry residues, as well as fast-growing energy crops, as alternative feedstocks for fuel ethanol production [20]. Incentives for this effort, whose relative impact depends on geographical location and varies over time, include reduction of the carbon footprint of ethanol production [21], prevention of competition with food production for arable land [22, 23], energy security in fossil-fuel importing countries [24] and development of rural economies [25]. Techno-economic forecasts of low-carbon scenarios for global energy supply almost invariably include liquid biofuels as a significant contributor [26]. Moreover, successful implementation of economically and environmentally sustainable 'second generation' bioethanol processes can pave the way for similar processes to produce other biofuels and commodity chemicals [27].

In contrast to starch, a plant storage carbohydrate that can be easily hydrolysed, the major carbohydrate polymers in lignocellulosic plant biomass (cellulose, hemicellulose and, in some cases, pectin) contribute to the structure and durability of stalks, leaves and roots [28]. Consistent with these natural functions and with their chemical diversity and complexity, mobilization of these polymers by naturally occurring cellulose-degrading microorganisms requires complex arrays of hydrolytic enzymes [29, 30].

The second-generation ethanol processes that are now coming on line at demonstration and full commercial scale (**Table 1**) are mostly based on fermentation of lignocellulosic biomass hydrolysates by engineered strains of *S. cerevisiae*. While this yeast has a strong track record in first-generation bioethanol production and its amenability to genetic modification is excellent, *S. cerevisiae* cannot hydrolyse cellulose or hemicellulose. Therefore, in conventional process configurations for second-generation bioethanol production, the fermentation step is preceded by chemical/physical pretreatment and enzyme-catalysed hydrolysis by cocktails of fungal hydrolases, which can either be produced on- or off site (**Figure 1**, [31]). Alternative process configurations, including simultaneous saccharification and fermentation (SSF) and consolidated bioprocessing (CBP) by yeast cells expressing heterologous hydrolases are intensively investigated [32,

33]. However, the high temperature optima of fungal enzymes and low productivity of heterologously expressed hydrolases in *S. cerevisiae* have so far precluded large-scale implementation of these alternative strategies for lignocellulosic ethanol production [32, 34]. This mini-review will, therefore, focus on the development of yeast strains for conventional process designs.

Table 1 | Overview of operational commercial-scale (demonstration) plants for second-generation bioethanol production. Data for US and Canada reflect status in May 2017 (source: [35, 36], data for other countries (source: [35, 36] reflect status in 2016.

Company/Plant	Country (State)	Feedstock	Capacity ML·y^{-1}
DuPont Cellulosic Ethanol LLC - Nevada	USA (IA)	Corn stover	113.6
Poet-DSM Advanced Biofuels LLC - Project Liberty[1]	USA (IA)	Corn cobs/corn stover	75.7
Quad County Cellulosic Ethanol Plant	USA (IA)	Corn fiber	7.6
Fiberight Demonstration Plant	US (VA)	Waste stream	1.9
ICM Inc. Pilot integrated Cellulosic Biorefinery	US (MO)	Biomass crops	1.2
American Process Inc. – Thomaston Biorefinery	USA (GA)	Other	1.1
ZeaChem Inc. – Demonstration plant	US (OR)	Biomass crops	1.0
Enerkem Alberta Biofuels LP	Canada (AB)	Sorted municipal solid waste	38
Enerkem Inc.-Westbury	Canada (QC)	Woody biomass	5.0
Iogen Corporation	Canada (ON)	Crop residue	2.0
Woodlands Biofuels Inc. – Demonstration plant	Canada (ON)	Woody biomass	2.0
GranBio	Brazil	Bagasse	82.4
Raizen	Brazil	Sugarcane bagasse/straw	40.3
Longlive Bio-technology Co. Ltd. – commercial demo	China	Corn cobs	63.4
Mussi Chemtex / Beta Renewables	Italy	*Arundo donax*, rice straw, wheat straw	75
Borregaard Industries AS – ChemCell Ethanol	Norway	Wood pulping residues	20

[1] With expansion capacity to 94.6 ML per year

Over the past decade, the authors have collaborated in developing metabolic engineering concepts for fermentation of lignocellulosic hydrolysates with engineered *S. cerevisiae* strains and in implementing these in advanced industrial strain platforms.

1

Based on their joint academic-industrial vantage point, this paper reviews key conceptual developments and challenges in the development and industrial implementation of *S. cerevisiae* strains for second generation bioethanol production processes.
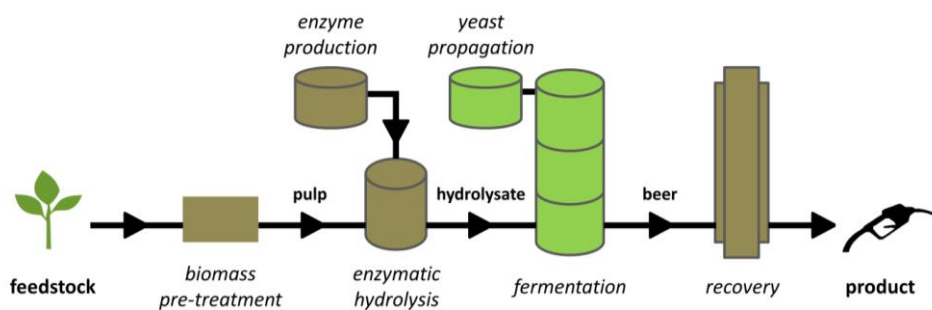
Figure 1 | Schematic process-flow diagram for ethanol production from lignocellulose, based on physically separated processes for pretreatment, hydrolysis and fermentation, combined with on-site cultivation of filamentous fungi for production of cellulolytic enzymes and on-site propagation of engineered pentose-fermenting yeast strains.

Fermenting lignocellulosic hydrolysates: challenges for yeast strain development

A wide range of agricultural and forestry residues, as well as energy crops, are being considered as feedstocks for bioethanol production [37]. Full-scale and demonstration plants using raw materials such as corn stover, sugar-cane bagasse, wheat straw and switchgrass are now in operation (**Table 1**). These lignocellulosic feedstocks have different chemical compositions, which further depend on factors such as seasonal variation, weather and climate, crop maturity and storage conditions [38]. Despite this variability, common features of feedstock composition and biomass-deconstruction methods generate several generic challenges that have to be addressed in the development of yeast strains for second-generation bioethanol production.

Pentose fermentation

For large-volume products such as ethanol, maximizing the product yield on feedstock and, therefore, efficient conversion of all potentially available substrate molecules in the feedstock is of paramount economic importance [39]. In addition to readily fermentable hexoses such as glucose and mannose, lignocellulosic biomass contains substantial amounts of D-xylose and L-arabinose. These pentoses, derived from hemicellulose and pectin polymers in plant biomass, cannot be fermented by wild-type *S. cerevisiae* strains. D-Xylose and L-arabinose typically account for 10-25 % and 2-3 %, respectively, of the carbohydrate content of lignocellulosic feedstocks [40]. However, in some feedstocks, such as corn fiber hydrolysates and sugar beet pulp, the L-arabinose content can be up to

10-fold higher [41, 42]. Early studies already identified metabolic engineering of *S. cerevisiae* for efficient, complete pentose fermentation as key prerequisite for its application in second-generation ethanol production [43-46].

Acetic acid inhibition. Since hemicellulose is acetylated [47], its complete hydrolysis inevitably results in the release of acetic acid. Bacterial contamination during biomass storage, pretreatment and/or fermentation may further increase the acetic acid concentrations to which yeasts are exposed in the fermentation process. First-generation bioethanol processes are typically run at pH values of 4-5 to counter contamination with lactic acid bacteria [48]. At these low pH values, undissociated acetic acid (pKa = 4.76) easily diffuses across the yeast plasma membrane. In the near-neutral pH environment of the yeast cytosol, the acid readily dissociates and releases a proton, which forces cells to expend ATP for proton export via the plasma-membrane ATPase to prevent cytosolic acidification [49-51]. The accompanying accumulation of the acetate anion in the cytosol can cause additional toxicity effects [52-54]. Acetic acid concentrations in some lignocellulosic hydrolysates exceed 5 g·l^{-1}, which can cause strong inhibition of anaerobic growth and sugar fermentation by *S. cerevisiae* [55]. Acetic acid tolerance at low culture pH is therefore a key target in yeast strain development for second-generation ethanol production.

Inhibitors formed during biomass deconstruction. In biomass deconstruction, a trade-off exists between the key objective to release all fermentable sugars at minimal process costs and the need to minimize generation and release of compounds that compromise yeast performance. Biomass deconstruction generally encompasses three steps: (i) size reduction to increase surface area and reduce degree of polymerization, (ii) thermal pretreatment, often at low pH and high pressure, to disrupt the crystalline structure of cellulose while already (partly) solubilizing hemicellulose and/or lignin and (iii) hydrolysis with cocktails of fungal cellulases and hemicellulases to release fermentable sugars [56-58]. Several inhibitors of yeast performance are generated in chemical reactions that occur during biomass deconstruction and, especially, in high-temperature pretreatment. 5-Hydroxymethyl-2-furaldehyde (HMF) and 2-furaldehyde (furfural) are formed when hexoses and pentoses, respectively, are exposed to high temperature and low pH [52, 59, 60]. These furan derivatives inhibit yeast glycolysis, alcoholic fermentation and TCA cycle [61-63] while, additionally, depleting intracellular pools of NAD(P)H and ATP [64]. Their further degradation, during biomass deconstruction, yields formic acid and levulinic acid [59, 60], whose inhibitory effects overlap with those of acetic acid [52]. Inhibitor profiles of hydrolysates depend on biomass structure and composition as well as on the type and intensity of the biomass deconstruction method used [64, 65]. During pressurized pretreatment at temperatures above 160 °C, phenolic inhibitors are generated by partial degradation of lignin. This diverse class of inhibitors includes aldehydes, ketones, alcohols and aromatic acids [64]. Ferulic acid, a phenolic compound that is an integral part of the lignin fraction of herbaceous plants [66, 67] is a potent inhibitor of *S. cerevisiae* fermentations [68]. The impact of phenolic inhibitors on membrane integrity and other cellular

functions depends on the identity and position of functional groups and carbon-carbon double bonds [69].

Concentrations of inorganic salts in hydrolysates vary depending on the feedstock used [70]. Moreover, high salt concentrations in hydrolysates can originate from pH adjustments during pretreatment [71]. Salt- and osmotolerance can therefore be important additional requirements in yeast strain development [72].

The inhibitors in lignocellulosic hydrolysates do not always act independently but can exhibit complex synergistic effects, both with each other and with ethanol [52, 73, 74], while their impact can also be modulated by the presence of water-insoluble solids [75]. Furthermore, their absolute and relative impact can change over time due to variations in feedstock composition, process modifications, or malfunctions in biomass deconstruction. While process adaptations to detoxify hydrolysates have been intensively studied [71, 76-78], the required additional unit operations typically result in a loss of fermentable sugar and are generally considered to be too expensive and complicated. Therefore, as research on optimization of biomass deconstruction processes continues, tolerance to the chemical environments generated by current methods is a key design criterion for yeast strain development.

Yeast strain development for second-generation ethanol production: key concepts

For almost three decades, yeast metabolic engineers have vigorously explored strategies to address the challenges outlined above. This quest benefited from rapid technological development in genomics, genome editing, evolutionary engineering and protein engineering. **Box 1** lists key technologies and examples of their application in research on yeast strain development for second-generation ethanol production.

Xylose fermentation. Efficiently linking D-xylose metabolism to glycolysis requires two key modifications of the *S. cerevisiae* metabolic network (**Figure 2**) [8, 79]: introduction of a heterologous pathway that converts D-xylose into D-xylulose and, simultaneously, alleviation of the limited capacity of the native *S. cerevisiae* xylulokinase and non-oxidative pentose-phosphate pathway (PPP). Two strategies for converting D-xylose into D-xylulose have been implemented in *S. cerevisiae*: (i) simultaneous expression of heterologous xylose reductase (XR) and xylitol dehydrogenase (XDH) and (ii) expression of a heterologous xylose isomerase (XI).

Box 1 | Overview of key technologies used for development of *Saccharomyces cerevisiae* strains for second-generation bioethanol production and examples of their application.

Metabolic engineering Application of recombinant-DNA techniques for the improvement of catalytic and regulatory processes in living cells, to improve and extend their applications in industry [80].	Metabolic engineering of pentose-fermenting strains commenced with the functional expression of pathways for XR/XDH- [81, 82] or XI-based [83] xylose utilization and pathways for isomerase-based arabinose utilization [84, 85]. Further research focused on improvement of pathway capacity [7, 86], engineering of sugar transport [87, 88], redox engineering to decrease byproduct formation and increase ethanol yield [4, 89-96] and expression of alternative pathway enzymes [97, 98]. Expression of heterologous hydrolases provided the first steps towards consolidated bioprocessing [32, 99-101].
Evolutionary engineering Application of laboratory evolution to select for industrially relevant traits [102]. Also known as adaptive laboratory evolution (ALE).	Evolutionary engineering in repeated-batch and chemostat cultures has been intensively utilized to improve growth and fermentation kinetics on pentoses (e.g., [9, 11, 13, 14, 93, 103-105] and inhibitor tolerance [106-110].
Whole genome (re)sequencing Determination of the entire DNA sequence of an organism.	Availability of a high-quality reference genome sequence is essential for experimental design in metabolic engineering. When genomes of strains that have been obtained by non-targeted approaches (e.g. evolutionary engineering or mutagenesis) are (re)sequenced, the relevance of identified mutations can subsequently be tested by their reintroduction in naïve strains, non-evolved strains and/or by classical genetics (reverse engineering; [111]). This approach has been successfully applied to identify mutations contributing to fast pentose fermentation [112-114] and inhibitor tolerance (e.g., [107, 115].
Quantitative trait loci (QTL) analysis QTL identifies alleles that contribute to (complex) phenotypes based on their meiotic co-segregation with a trait of interest [116, 117]. In contrast to whole-genome (re)sequencing alone, QTL analysis can identify epistatic interactions.	QTL analysis currently enables resolution to gene or even nucleotide level [118]. QTL analysis has been used to identify alleles contributing to high-temperature tolerance [119], ethanol tolerance [118] and improved ethanol-to-glycerol product ratios [120]. The requirement of QTL analysis for mating limits its applicability in aneuploidy and/or poorly sporulating industrial *S. cerevisiae* strains.
Protein engineering Modification of the amino acid sequences of proteins with the aim to improve their catalytic properties, regulation and/or stability in industrial contexts [121].	Protein engineering has been used to improve the pentose-uptake kinetics, reduce the glucose sensitivity and improve the stability of yeast hexose transporters (e.g., [122-124]; [123, 125-128]). The approach has been utilized to improve the redox cofactor specificity of XR and/or XDH to decrease xylitol formation [94, 129-132]. Directed evolution of xylose isomerase yielded XI variants with increased enzymatic activity [133]. Directed evolution of native yeast dehydrogenases has yielded strains with increased HMF tolerance [134].
Genome editing Where 'classical' genetic engineering encompass iterative, one-by-one introduction of genetic modifications, genome editing techniques enable simultaneous introduction of multiple (types of) modifications at different genomic loci [135].	The combination of CRISPR-Cas9-based genome editing [136, 137] with *in vivo* assembly of DNA fragments has enabled the one-step introduction of all genetic modifications needed to enable *S. cerevisiae* to ferment xylose [138, 139]). Recent developments have enabled the application of the system in industrial backgrounds [140]. CRISPR-Cas9 has been used in reverse engineering studies to rapidly introduce multiple single-nucleotide mutations observed in evolutionary engineering experiments in naïve strains (e.g., [141]).

1

The first *S. cerevisiae* strains engineered for xylose utilization were based on expression of XR and XDH from the xylose-metabolising yeast *Scheffersomyces stipitis* [81]. Due to the non-matching redox-cofactor preferences of these enzymes, these strains produced large amounts of the by-product D-xylitol [44, 81, 142]. Modification of these cofactor preferences by protein engineering resulted in reduced xylitol formation under laboratory conditions [5, 132]. A much lower xylitol formation by XR/XDH-based strains in lignocellulosic hydrolysates was attributed to NADH-dependent reduction of furfural, which may contribute to *in situ* detoxification of this inhibitor [1, 143-146]. A potential drawback of XR/XDH-based strains for application in large-scale anaerobic processes is that, even after prolonged laboratory evolution, their anaerobic growth rates are very low [93].

Combined expression of a fungal XI [147] and overexpression of the native *S. cerevisiae* genes encoding xylulokinase and non-oxidative PPP enzymes enabled anaerobic growth of a laboratory strain on D-xylose. In anaerobic cultures of this strain, in which the aldose-reductase encoding *GRE3* gene was deleted to eliminate xylitol formation, ethanol yields on D-xylose were the same as on glucose [7]. This metabolic engineering strategy, complemented with laboratory evolution under anaerobic conditions, has been successfully reproduced in different *S. cerevisiae* genetic backgrounds and/or with different XI genes [98, 99, 148-151].

Laboratory evolution (**Box 1**) for faster D-xylose fermentation and analysis of evolved strains identified high-level expression of XI as a major contributing factor [11, 150, 152]. Multi-copy introduction of XI expression cassettes, optimization of their codon usage, and mutagenesis of their coding sequences have contributed to higher D-xylose fermentation rates [98, 133, 153]. Whole genome sequencing of evolved D-xylose consuming strains that express *Piromyces* XI identified mutations affected stress-response regulators and, thereby, increased expression of yeast chaperonins that assisted functional expression of XI [114]. Consistent with this observation, co-expression of the *Escherichia coli* GroEL and GroES chaperonins enabled *in vivo* activity of *E. coli* XI in *S. cerevisiae* [154]. A positive effect of mutations in the *PHO13* phosphatase gene on xylose fermentation rates in XI- and XR/XDH-based strains has been attributed to transcriptional upregulation of PPP-related genes by an as yet unknown mechanism [155-158]. Additionally, Pho13 has been implicated in dephosphorylation of the PPP intermediate sedoheptulose-7-phosphate (Xu *et al.* 2016). For other mutations in evolved strains, e.g. in genes involved in iron-sulfur cluster assembly and in the MAP-kinase signaling pathway [3, 113], the mechanisms by which they affect D-xylose metabolism remain to be identified.
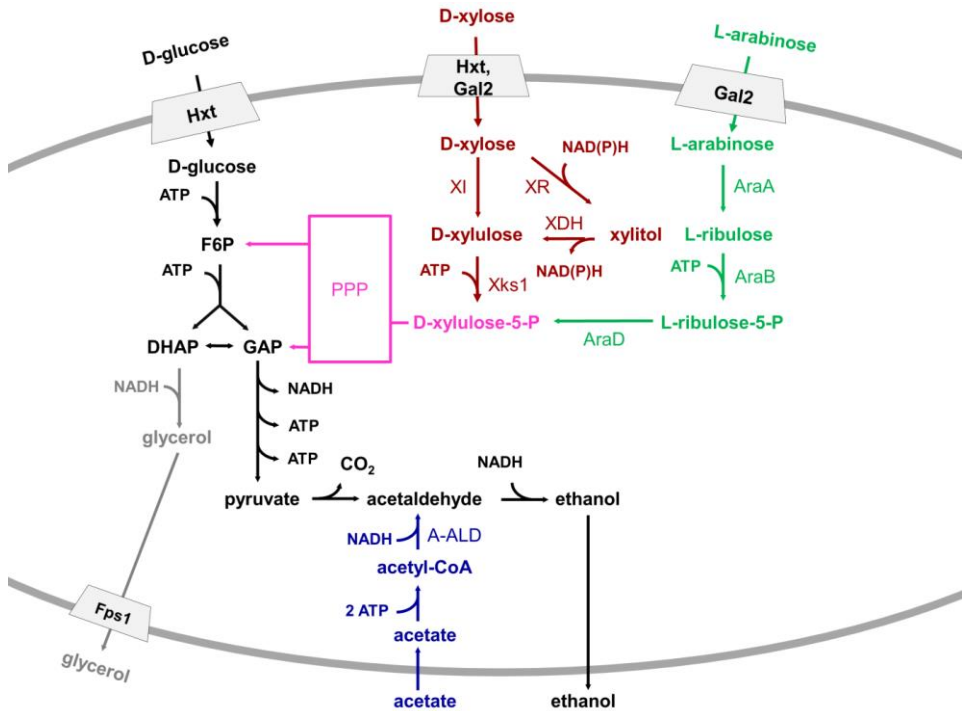
Figure 2 | Key strategies for engineering carbon and redox metabolism in *S. cerevisiae* strains for alcoholic fermentation of lignocellulosic feedstocks. Colours indicate the following pathways and processes: **Black**: native *S. cerevisiae* enzymes of glycolysis and alcoholic fermentation; **Magenta:** native enzymes of the non-oxidative pentose-phosphate pathway (PPP), overexpressed in pentose-fermenting strains; **Red:** conversion of D-xylose into D-xylulose-5-phosphate by heterologous expression of a xylose isomerase (XI) or combined expression of heterologous xylose reductase (XR) and xylitol dehydrogenase (XDH), together with the overexpression of (native) xylulokinase (Xks1); **Green:** conversion of L-arabinose into D-xylulose-5-phosphate by heterologous expression of a bacteria AraA/AraB/AraD pathway; **Blue:** expression of a heterologous acetylating acetaldehyde dehydrogenase (A-ALD) for reduction of acetic acid to ethanol; **Grey:** native glycerol pathway.

Arabinose fermentation. The metabolic engineering strategy for constructing L-arabinose-fermenting *S. cerevisiae* is based on heterologous expression of a bacterial pathway for conversion of L-arabinose into xylulose-5-phosphate, involving L-arabinose isomerase (AraA), L-ribulokinase (AraB) and L-ribulose-5-phosphate-4-epimerase (AraD) [159]. Together with the non-oxidative PPP and glycolysis, these reactions enable redox-cofactor-balanced alcoholic fermentation of L-arabinose (**Figure 2**).

Combined expression of *Bacillus subtilis* or *B. licheniformis araA* and *E. coli araBD* [85, 86, 160] allowed aerobic growth of *S. cerevisiae* on L-arabinose. Anaerobic growth of *S. cerevisiae* on arabinose was first achieved by expressing the *Lactobacillus plantarum araA, B* and *D* genes in an XI-based xylose-fermenting strain that already overexpressed the enzymes of the non-oxidative PPP (**Figure 2**), followed by evolutionary engineering under anaerobic conditions [84]. Increased expression levels of *GAL2*, which encodes a galactose transporter that also transports L-arabinose [161], was essential for L-arabinose

fermentation [85, 88, 162, 163]. Increased expression of the transaldolase and transketo-lase isoenzymes Nqm1 and Tkl2 contributed to an increased rate of arabinose fermentation in strains evolved for fast arabinose fermentation [163]. The set of arabinose isomerase genes that can be functionally expressed in *S. cerevisiae* was recently expanded by co-expression of *E. coli araA* with the *groEL* and *groES* chaperonins [154].

Engineering of sugar transport and mixed-substrate fermentation. In early *S. cerevisiae* strains engineered for pentose fermentation, uptake of D-xylose and L-arabinose exclusively relied on their native hexose transporters. While several of the 18 *S. cerevisiae* Hxt transporters (Hxt1-17 and Gal2) transport D-xylose, their K_m values for this pentose are one to two orders of magnitude higher than for glucose [123, 164-167]. High-affinity glucose transporters, which are only expressed at low glucose concentrations [168], display a lower K_m for D-xylose than low-affinity glucose transporters [164, 165]. The galactose transporter Gal2, which also catalyses high-affinity glucose transport [167] also has a much higher K_m for L-arabinose than for glucose [88, 162].

The higher affinities of Hxt transporters for glucose, combined with the transcriptional repression of Gal2 [169, 170] and other high-affinity Hxt transporters [168, 171] at high glucose concentrations, contribute to a sequential use of glucose and pentoses during mixed-substrate cultivation of engineered strains that depend on Hxt-mediated pentose uptake. Furthermore, the high K_m values of Hxt transporters for pentoses cause a deceleration of sugar fermentation during the pentose-fermentation phase. This 'tailing' effect is augmented by accumulation of ethanol and by the reduced inhibitor tolerance of *S. cerevisiae* at low sugar fermentation rates [10, 172, 173]. Intensive efforts have been made to generate yeast strains that can either co-consume hexoses and pentose sugars or sequentially consume all sugars in hydrolysates in an economically acceptable time frame [174, 175].

Evolutionary engineering experiments played a major role in accelerating mixed-sugar utilization by engineered pentose-fermenting strains [9, 11, 13, 93, 103]. Repeated batch cultivation on a sugar mixture can favour selection of mutants that rapidly ferment one of the sugars, while showing deteriorated fermentation kinetics with other sugars in the mixture. In practice, such trade-off scenarios can increase rather than decrease the time required for complete conversion of sugar mixtures [13]. A modified strategy for repeated batch cultivation, designed to equally distribute the number of generations of selective growth on each of the individual substrates in a mixture, enabled acceleration of the anaerobic conversion of glucose-xylose-arabinose mixtures by an engineered *S. cerevisiae* strain [13].

Recently constructed glucose-phosphorylation-negative, pentose-fermenting *S. cerevisiae* strains enabled evolutionary engineering experiments for *in vivo* directed evolution of Hxt variants that supported growth on D-xylose or L-arabinose in the presence of high glucose concentrations [112, 123, 126, 176]. Several of the evolved *HXT* alleles were confirmed to encode transporters whose D-xylose-transport kinetics were substantially

less sensitive to glucose inhibition [112, 123, 126, 176]. Remarkably, independent evolutionary engineering studies aimed at selecting glucose-insensitive D-xylose and L-arabinose Hxt transporters yielded single-amino-acid substitutions at the exact corresponding positions in Hxt7(N370), Gal2 (N376), and in a chimera of Hxt3 and Hxt6 (N367) [112, 123, 176]. Additional Hxt variants with improved relative affinities for pentoses and glucose were obtained by *in vitro* directed evolution and knowledge-based protein engineering [123, 125] (**Box 1**).

Low-, moderate- and high-affinity pentose transporters from pentose-metabolizing filamentous fungi or non-*Saccharomyces* yeasts, have been functionally expressed in *S. cerevisiae* [88, 177-187]. Expression and/or activity of several of these transporters were further improved by directed evolution [122, 179, 186] or evolutionary engineering [175, 188]. Such high-affinity transporters may be suited to 'mop up' low concentrations of pentoses towards the end of a fermentation process. Since high-affinity sugar transporters are typically proton symporters, care should be taken to avoid scenarios in which their simultaneous expression with Hxt-like transporters, which mediate facilitated diffusion, causes futile cycles and negatively affects inhibitor tolerance.

Inhibitor tolerance. Yeast enzymes involved in detoxification of specific inhibitors provide logical targets for metabolic engineering. For example, overexpression of native NAD(P)$^+$-dependent alcohol dehydrogenases stimulates conversion of furfural and HMF to the less toxic alcohols furanmethanol and furan-2,5-dimethanol, respectively [189-191]. Similarly, combined overexpression of the aldehyde dehydrogenase Ald5, the decarboxylase Pad1 and the alcohol acetyltransferases Atf1 and Atf2 increased resistance to several phenolic inhibitors [192].

Genome-wide expression studies have revealed intricate, strain- and context-dependent stress-response networks as major key contributors to inhibitor tolerance [54, 64, 193-197]. An in-depth transcriptome analysis implicated *SFP1* and *ACE2*, which encode transcriptional regulators involved in ribosomal biogenesis and septum destruction after cytokinesis, respectively, in the phenotype of an acetic-acid and furfural-tolerant strain. Indeed, overexpression of these transcriptional regulators significantly enhanced ethanol productivity in the presence of these inhibitors [198].

Whole-genome resequencing of tolerant strains derived from evolutionary engineering, mutagenesis and/or genome shuffling has yielded strains with increased tolerance whose causal mutations could be identified [10, 106, 107, 115, 199]. Physiological and evolutionary engineering experiments demonstrated the importance of high sugar fermentation rates for acetic acid tolerance [110, 173]. When the acetic-acid concentration in anaerobic, xylose-grown continuous cultures was continually increased over time, evolving cultures acquired the ability to grow at acetic-acid concentrations that prevented growth of the non-evolved *S. cerevisiae* strain. However, after growth in the absence of acetic acid, full expression of their increased tolerance required pre-exposure

to a lower acetic-acid concentration. This observation indicated that the acquired tolerance was inducible rather than constitutive [110]. Constitutive tolerance to acetic acid was shown to reflect the fraction of yeast populations able to initiate growth upon exposure to acetic acid stress [200]. Based on this observation, an evolutionary engineering strategy that involved alternating batch cultivation cycles in the presence and absence of acetic acid was successfully applied to select for constitutive acetic acid tolerance [107].

Exploration of the natural diversity of inhibitor tolerance among *S. cerevisiae* strains [201-203] is increasingly used to identify genes and alleles that contribute to tolerance. In particular, combination of whole genome sequencing and classical genetics is a powerful approach to identify relevant genomic loci, genes and even nucleotides [116] (Quantitative Trait Loci (QTL) analysis, see **Box 1**). For example, Meijnen *et al.* (2016) used whole-genome sequencing of pooled tolerant and sensitive segregants from crosses between a highly acetic-acid tolerant *S. cerevisiae* strain and a reference strain to identify mutations in five genes that contributed to tolerance[204].

Reduction of acetic acid to ethanol: converting an inhibitor into a co-substrate. Even small improvements of the product yield on feedstock can substantially improve the economics of biotechnological processes for manufacturing large-volume products such as ethanol [205, 206]. In industrial, anaerobic ethanol production processes, a significant amount of sugar is converted into the byproduct glycerol [207]. Glycerol formation, catalyzed by the two isoforms of glycerol-3-phosphate dehydrogenase (Gpd1 and Gpd2) and of glycerol-3-phosphate phosphatase (Gpp1 and Gpp2), is required during anaerobic growth of *S. cerevisiae* for reoxidation of NADH generated in biosynthetic reactions [208, 209]. Metabolic engineering strategies to diminish glycerol formation focused on modification of intracellular redox reactions [207, 210] or modulation of *GPD1* and *GPD2* expression [211]. Replacement of *GPD1* and *GPD2* with a heterologous gene encoding an acetylating acetaldehyde dehydrogenase (A-ALD) and supplementation of acetic acid eliminated glycerol formation in anaerobic *S. cerevisiae* cultures [89]. By enabling NADH-dependent reduction of acetic acid to ethanol (**Figure 2**), this strategy resulted in a significant increase in the final ethanol yield, while consuming acetic acid. This engineering strategy has recently been extended by altering the redox-cofactor specificities of alcohol dehydrogenase [90] and 6-phosphogluconate dehydrogenase [91]. These further interventions increased the availability of cytosolic NADH for acetate reduction and should, upon implementation in industrial strains, further improve *in situ* detoxification of acetic acid. The A-ALD strategy was also shown to decrease xylitol formation in XR/XDH-based xylose-fermenting engineered strains by reoxidation of excess NADH formed in the XDH reaction [4, 96].

Development of industrial yeast strains and processes. Much of the research discussed in the preceding paragraphs was based on laboratory yeast strains, grown in synthetic media whose composition can be different from that of industrial lignocellulosic

hydrolysates. **Table 2** provides examples of ethanol yields and biomass-specific conversion rates that have been obtained with engineered *S. cerevisiae* strains in synthetic media.

While data on the performance of current industrial strains on industrial feedstocks are proprietary, many scientific publications describe the fermentation of hydrolysates by D-xylose-fermenting strains (either XI or XR-XDH-based, but so far without arabinose pathways). These studies cover a wide variety of feedstocks, biomass deconstruction and fermentation strategies (batch, fed-batch, SSF), aeration regimes and nutritional supplementations (e.g. yeast extract, peptone, low-cost industrial supplements, trace elements, nitrogen sources). However, with few exceptions, these data are restricted to final ethanol yields and titers, and do not include quantitative information of the biomass-specific conversion rates (q_{xylose}, $q_{ethanol}$, expressed in g·(g biomass)$^{-1}$·h^{-1} that are essential for strain comparison and process design. **Table 3** summarizes results studies on fermentation of biomass hydrolysates that include or enable calculation of biomass-specific conversion rates and ethanol yields.

Despite the heterogeneity of the studies included in **Tables 2 and 3**, the available data clearly illustrate that, while even 'academic' strain platforms can exhibit high ethanol yields in hydrolysates, conversion rates under these conditions are much lower than in synthetic media. Improving kinetics and robustness in industrial hydrolysates is therefore the single most important objective in industrial yeast strain development platforms.

In the authors' experience, aspects such as spatial and temporal heterogeneity, hydrostatic pressure and CO_2 concentrations, which are highly important for down-scaling aerobic industrial fermentation processes [212], do not represent substantial challenges in down-scaling second-generation ethanol processes. Provided that anaerobic conditions can be maintained, strain performance can therefore be adequately assessed in small-scale systems. Access to hydrolysates whose composition and concentration are fully representative for the target industrial substrate(s) may be necessary for strain development. This requirement is not a trivial one due to feedstock variability, the plethora of pretreatment options and the limited scalability and continuous innovation in biomass deconstruction [213, 214].

Table 2 | Ethanol yields ($Y_{E/S}$, g ethanol·(g sugar)⁻¹) and biomass-specific rates of xylose and/or arabinose consumption and ethanol production (q_{xylose}, $q_{arabinose}$ and $q_{ethanol}$, respectively, g·(g biomass)⁻¹·h⁻¹) in cultures of *S. cerevisiae* strains engineered for pentose fermentation, grown in synthetic media. Asterisks (*) indicate values estimated from graphs in the cited reference.

S. cerevisiae strain	Pentose fermentation strategy	Key genetic modifications	Fermentation conditions	$Y_{E/S}$ g·g⁻¹	$q_{ethanol}$ g·g⁻¹·h⁻¹	q_{xylose} g·g·h⁻¹	$q_{arabinose}$ g·g·h⁻¹	Reference
TMB3400	XR/XDH (*S. stipitis XYL1, XYL2*)	*SsXYL1, SsXYL2* + *XKS1*↑, random mutagenesis	Anaerobic batch (bioreactor), 5 % xylose	0.33	0.04	0.13	-	[1]
GLBRCY87	XR/XDH (*S. stipitis XYL1, XYL2*)	*SsXYL1, SsXYL2, SsXYL3*, evolved on xylose and hydrolysate inhibitors	Semi-anaerobic batch (flask) 5 % glucose and 5% xylose	0.34*	0.036*	0.13	-	[3]
SR8	XR/XDH (*S. stipitis XYL1, XYL2*)	*SsXYL1, Ss XYL2, Ss XYL3, ald6Δ*, evolved on xylose	Anaerobic batch (reactor), 4 % xylose	0.39	0.25	0.64	-	[4]
TMB3421	XR/XDH (*S. stipitis XYL1, XYL2*)	*S. stipitis XYL1N272D/P275Q, XYL2* + *XKS1*↑ *TAL1*↑ *TKL1*↑ *RPE1*↑ *RKI1*↑ *gre3Δ*, evolved on xylose	Anaerobic batch (reactor), 6 % xylose	0.35	0.20	0.57	-	[5]
RWB 217	XI (*Piromyces XylA*)	*Piromyces XylA* + *XKS1*↑ *TAL1*↑ *TKL1*↑ *RPE1*↑ *RKI1*↑, *gre3Δ*	Anaerobic batch (reactor), 2 % xylose	0.43	0.46	1.06	-	[7]
RWB 218	XI (*Piromyces XylA*)	Derived from RWB 217 after evolution on glucose/xylose mixtures	Anaerobic batch (reactor) 2 % xylose	0.41	0.49	1.2	-	[9]
H131-A3-AL[CS]	XI (*Piromyces XylA*)	*XylA, Xyl3, XKS1*↑ *TAL1*↑ *TKL1*↑ *RPE1*↑ *RKI1*↑, *gre3Δ*, evolved on xylose	Anaerobic batch (reactor), 4 % xylose	0.43	0.76	1.9	-	[11]
IMS0010	XI/AraABD (*Piromyces XylA, L. plantarum AraA, B,D*	*XylA; XKS1*↑ *TAL1*↑ *TKL1*↑ *RPE1*↑ *RKI1*↑*AraT, AraA, AraB, AraD*, evolved on glucose, xylose, arabinose mixtures	Anaerobic batch (reactor), 3 % glucose, 1.5 % xylose and 1.5 % arabinose	0.43	-	0.35	0.53	[13]
GS1.11-26	XI/AraABD (*Piromyces XylA, L. plantarum AraA, B, D. K. lactis ARAT*).	*XylA, XKS1*↑ *TAL1*↑ *TKL1*↑ *RPE1*↑ *RKI1*↑ *XylA HXT7*↑ *KlAraT, AraA, AraB, AraD, TAL2*↑ *TKL2*↑, several rounds of mutagenesis and evolution on xylose	Semi-anaerobic batch (flask), synthetic medium, 3.5 % xylose	0.46	0.48	1.1	-	[14]

Table 3 | Ethanol yields on consumed sugar ($Y_{E/S}$, g ethanol·(g sugar)$^{-1}$) and biomass-specific rates of glucose and xylose consumption and ethanol production ($q_{glucose}$, q_{xylose} and $q_{ethanol}$, respectively, g·(g biomass)$^{-1}$·h^{-1}) in cultures of *S. cerevisiae* strains engineered for pentose fermentation, grown in lignocellulosic hydrolysates. Asterisks (*) indicate specific conversion rates estimated from graphs in the cited reference; daggers (†) indicate crude estimates of biomass-specific rates calculated based on the assumption that biomass concentrations did not change after inoculation, these estimates probably overestimate actual biomass-specific conversion rates. [1] Abbreviations of supplements: YE, yeast extract; YP, yeast extract and peptone; YNB, Yeast Nitrogen Base.

S. cerevisiae strain	Description	Feedstock, pretreatment conditions, hydrolysate sugar composition[3]	Fermentation conditions, added nutrients[1]	$Y_{E/S}$ g·g^{-1}	$q_{glucose}$ g·g·h^{-1}	$q_{ethanol}$ g·g·h^{-1}	q_{xylose} g·g·h^{-1}	Ref.
TMB3400	XR/XDH *S. stipitis XYL1* and *XYL2*; *XKS1*↑	Spruce, two-step dilute acid hydrolysis, 1.6 % glucose, 0.4 % xylose, 1 % mannose, 1 % galactose,	Anaerobic batch (flasks), (NH$_4$)$_2$HPO$_4$ NaH$_2$PO$_4$ MgSO$_4$, YE	0.41	0.021	0.005	0.005	[1]
GLBRCY87	XR/XDH *S. stipitis XYL1, XYL2* and *XYL3* evolved on xylose and hydrolysate inhibitors	Corn Stover, ammonia fiber expansion, 8 % glucose, 3.8 % xylose.	Semi-anaerobic batch (flasks), pH 5.5, Urea, YNB	0.28	1.4*	0.27*	0.04	[3]
GLBRCY87	XR/XDH *S. stipitis XYL1, XYL2* and *XYL3* evolved on xylose and hydrolysate inhibitors	Switchgrass, ammonia fiber expansion, 6.1 % glucose, 3.9 % xylose.	Semi-anaerobic batch (flasks), Urea, YNB	0.35	1.65*	0.28*	0.07	[3]
MEC1122	XR/XDH, industrial host strain *S. stipitis XYL1*(N272D/P275Q) and *XYL2*, *XKS1*↑ *TAL1*↑	Corn cobs, autohydrolysis (202 °C), liquid fraction acid-treated. 0.3 % glucose, 2.6 % xylose.	Oxygen limited batch (flasks), cheese whey, urea, YE, K$_2$O$_5$S$_2$	0.3	-	0.12†,*	0.25†	[6]
RWB 218	XI *Piromyces XylA*, *XKS1*↑ *TAL1*↑ *TKL1*↑ *RPE1*↑ *RKI1*↑, *gre3*Δ, evolved on glucose/xylose mixed substrate	Wheat straw hydrolysate, steam explosion, 5 % glucose, 2 % xylose	Anaerobic batch (reactor), (NH$_4$)$_2$PO$_4$	0.47	1.58†	1.0†	0.32†	[8]
GS1.11-26	XI, AraABD *Piromyces XylA*, *XKS1*↑ *TAL1*↑ *TKL1*↑ *RPE1*↑ *RKI1*↑ *HXT7*↑*AraT, AraA, AraB, AraD, TAL2*↑ *TKL2*↑, several rounds of mutagenesis and evolution on xylose	Spruce (no hydrolysis), acid pre-treated, 6.2 % glucose, 1.8 % xylose, 1 % mannose	Semi-anaerobic batch (flasks), YNB, (NH$_4$)$_2$SO$_4$, amino acids added,	0.43	2.46†	0.3†	0.11†	[10]
XH7	Multiple integrations of *RuXylA*; *XKS1*↑ *TAL1*↑ *TKL1*↑ *RPE1*↑ *RKI1*↑ *pho13*Δ *gre3*Δ, evolved on xylose	Corn stover, steam explosion, 6.2 % glucose, 1.8 % xylose	Semi-anaerobic batch (flasks), urea	0.39	0.14	0.080	0.096	[12]
LF1	Selection mutant of XH7 further evolved on xylose and hydrolysates with MGT transporter introduced	Corn stover, steam explosion, 8.7% glucose, 3.9% xylose	Semi-anaerobic batch (flasks), urea	0.41	0.57	0.34	0.23	[12]

1

Due to the complex, multigene nature of inhibitor tolerance, screening of natural and industrial *S. cerevisiae* strains is a logical first step in the development of industrial strain platforms. The power of this approach is illustrated by the Brazilian first-generation bioethanol strain PE-2. Stable maintenance of this strain in non-aseptically operated industrial reactors, over many production campaigns [215], was attributed to its innate tolerance to the sulfuric-acid washing steps that are employed between fermentation cycles to combat bacterial contamination [216]. In contrast to most laboratory strains, robust industrial strains of *S. cerevisiae* are heterozygous diploids or polyploids which, additionally, are prone to whole-chromosome or segmental aneuploidy [217, 218]. Acquiring high-quality, well annotated genome sequences (**Box 1**) of these complex genomes is an important prerequisite for interpreting the results of strain improvement campaigns and for targeted genetic modification.

Episomal expression vectors carrying auxotrophic marker genes, which are commonly used in academic research, do not allow for stable replication and selection, respectively, in complex industrial media [219-221]. Instead, industrial strain development requires chromosomal integration of expression cassettes. Even basic academic designs of xylose- and arabinose-fermenting strains encompass the introduction of 10-12 different expression cassettes [84, 163], some of which need to be present in multiple copies (e.g. for high-level expression of XI genes [11, 152, 222]). Additional genetic modifications, on multiple chromosomes in the case of diploid or polyploid strains, are required to reduce by-product formation, improve inhibitor tolerance and/or improve product yields. Genetic modification of complex industrial yeast genomes has now been strongly accelerated by novel, CRISPR-based genome editing tools (**Box 1**).

Non-targeted strategies for strain improvement (**Box 1**) including mutagenesis with chemical mutagens or irradiation, evolutionary engineering, recursive breeding and/or genome shuffling remain essential for industrial strain improvement. Down-scaling, automation and integration with high-throughput screening of the resulting strains in hydrolysates strongly increases the success rates of these approaches (e.g. for ethanol tolerance, [223]). In non-targeted strain improvement campaigns, it is important to maintain selective pressure on all relevant aspects of strain performance, to avoid trade-offs between, for example, fermentation kinetics with different sugars (glucose, xylose and arabinose), and/or inhibitor tolerance [10, 13, 109].

Even when kinetics of yeast growth and fermentation in hydrolysates are suboptimal (**Table 2**) due to the impact of inhibitors and/or strain characteristics, industrial fermentation processes need to achieve complete sugar conversion within acceptable time limits (typically 72 h or less). This can be accomplished by increasing the initial yeast biomass densities, which, in second generation processes, are typically 2- to 8-fold higher than the initial concentrations of 0.125-0.25 $g \cdot l^{-1}$ that are used in first-generation processes without biomass recycling [224]. Several second-generation bioethanol plants therefore include on-site bioreactors for cost-effective generation of the required yeast biomass. Precultivation in the presence of mild concentrations of inhibitors can prime

yeast cells for improved performance upon exposure to stressful conditions [225-227]. Especially when biomass propagation uses non-lignocellulosic feedstocks [228, 229] and/or is operated aerobically to maximize biomass yields, yeast strain development must take into account the need to maintain pentose- fermentation kinetics and inhibitor tolerance during biomass propagation.
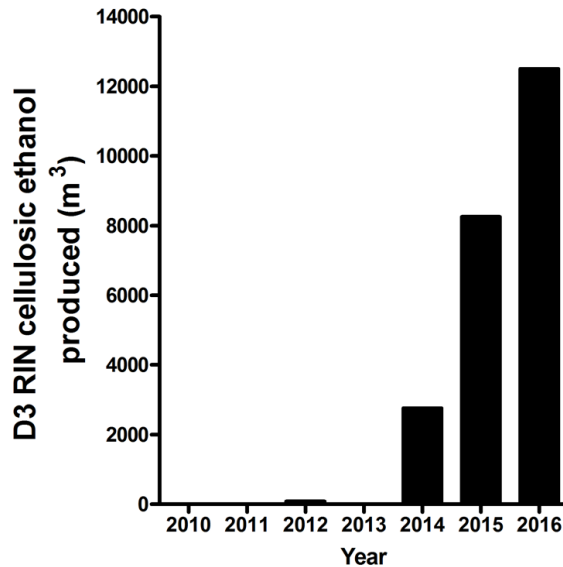
Figure 3 | Annual production volumes of cellulosic ethanol in the USA from 2010 until November 2016. Numbers are based on RIN D code 3 RIN (Renewable Identification Number) credits generated (accounted as cellulosic ethanol, [230].

Full-scale implementation: status and challenges

Vigorous lab-scale optimization of each of the unit operations in yeast-based ethanol production from lignocellulosic feedstocks enabled the design, construction and operation of processes at pilot scale. Recently, several industrial parties started or announced the first commercial-scale cellulosic ethanol plants, most of which rely on yeast for the fermentation step (**Table 1**). Actual cellulosic ethanol production volumes in the United States of America, derived from registered RIN (Renewable Identification Numbers) credits [230], indicate an increase in recent years (**Figure 3**). However, based on these numbers and estimates for plants elsewhere in the world, the global production volume of cellulosic ethanol is still below 1 % of that of first-generation processes. This places actual production volumes years behind earlier projections [231] and indicates that currently installed commercial-scale plants still operate below their nominal capacity. For obvious reasons,

33

industrial parties cannot always be fully transparent on factors that impede acceleration and intensification of cellulosic ethanol production. However, presentations at conferences and trade fairs enable a few general observations. Many aspects of full-scale plants can be assessed prior to commercialization by carefully down-scaling all process steps. Such down-scaling is crucial for optimal process development and equipment design (sizing, layout, mixing requirements, scheduling etc. [212, 232, 233]). As indicated above, most aspects of the performance of engineered yeast strains in full-scale plants can be, and indeed have been, adequately predicted from such lab-scale studies. Other aspects, such as impacts of seasonal and regional variation of plant biomass and other in-process streams, are more difficult to predict. Additionally, continued optimization of upstream unit operations in commercial-scale plants requires continual 'tuning' of yeast strain characteristics to address impacts on the fermentation process.
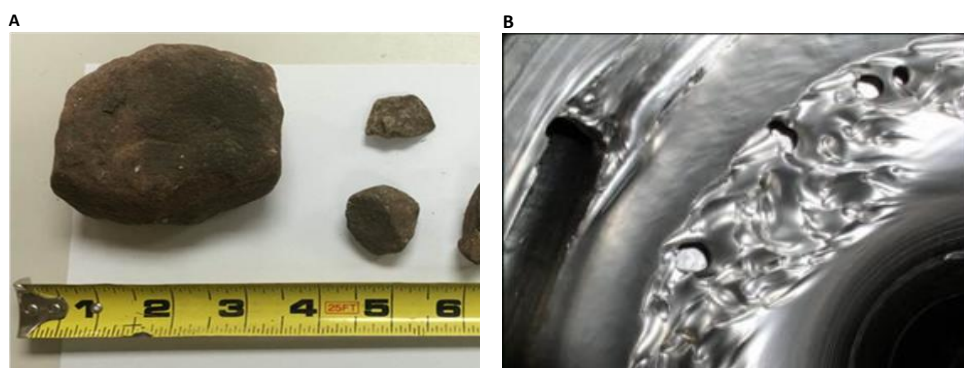
Figure 4 | Problems not encountered in shake flask cultures: non-yeast-related challenges in large-scale processing of lignocellulosic biomass. **A**. Small rocks collected from corn stover (picture courtesy of POET-DSM Liberty). **B**. Example of severely eroded equipment (picture courtesy of Iogen Corporation [238]).

An aspect that may have been underestimated in down-scaled experiments is bacterial contamination. Yield losses caused by contamination with lactic acid bacteria (LAB) is a well-known problem in first-generation bioethanol production [48, 234]. The longer pretreatment and fermentation times in current cellulosic ethanol processes, caused by inhibitors in the hydrolysates, allow LAB more time to compete with the engineered yeast strains than in first-generation processes. Moreover, concentrations of ethanol, a potent inhibitor of LAB, are typically lower in second generation processes [235]. While requiring constant attention, bacterial contamination is a manageable problem that can be addressed with currently available technology and without insurmountable additional costs. Strict attention for hygiene aspects in all aspects of plant design and operation, e.g. by avoiding dead legs, implementing full drainability and robust cleaning-in-place (CIP) procedures, is crucial in this respect. For example, installing appropriate valves and filters should be an integral part of plant design and be combined with measures to minimize survival and propagation of bacterial contaminants that do

make it into the process. As a last and sometimes inevitable resort, antibacterial compounds can be used to minimize bacterial load and impact [236].

An important factor that appears to have escaped attention in most small-scale studies is that the agricultural residues entering a factory contain an abundance of non-plant solids. Rocks, sand and metal particles coming off agricultural fields and/or equipment can rapidly damage and erode expensive equipment (**Figure 4**). In pilot- and commercial-scale plants, clogging of pipes and reactors during biomass handling and pre-treatment remains a point of attention. These challenges, which can result in significant down-time of plants, can either be addressed by elimination of high-density solids during harvesting and storage of the biomass or by installing extra unit operations in factories. For example, Beta Renewables installed a biomass washing step at their Crescentino plant [237]. While these engineering solutions cannot be easily down-scaled and retrofitting of existing processes may be complicated and expensive, they are technologically surmountable.

Scope and outline of this thesis

As discussed above, the pentose sugars D-xylose and L-arabinose constitute a significant fraction of the carbohydrates found in hydrolysates of lignocellulosic feedstocks. The pioneering research on enabling D-xylose and L-arabinose fermentation in *Saccharomyces cerevisiae* done by Kuyper *et al.* and Wisselink *et al.* at the Industrial Microbiology Section at the Delft University of Technology has contributed to the realization of the first full-scale second-generation plants for yeast-based production of bioethanol. Since then, fast developments in DNA sequencing and genome editing techniques have expanded the available toolbox for strain construction and reverse engineering of evolved phenotypes. The goal of this thesis is to use these strategies to design and test novel strategies for obtaining and applying *S. cerevisiae* strains with improved D-xylose and/or L-arabinose fermentation kinetics. **Chapter 1** provides an introduction to this research by reviewing previous research on alcoholic fermentation of lignocellulosic feedstocks in academia and the of the results from this work in the development of yeast strains that now perform second-generation bioethanol production on an industrial scale. The study provides an overview of metabolic engineering strategies that have been used to improve pentose fermentation kinetics, ethanol yield and cellular robustness during cultivation on these hydrolysates.

Previously, Kuyper *et al.* used metabolic engineering to construct D-xylose fermenting *S. cerevisiae* strains based on functional expression of a fungal xylose isomerase originating from *Piromyces* SP E2. The required strain construction, which also involved overexpression of pentose-phosphate-pathway enzymes and xylulokinase, was performed in a time-consuming, step-by-step manner. In **Chapter 2** this strategy was repeated in a single step using CRISPR/Cas9-mediated genome editing. While the resulting strain was immediately able to grow on xylose aerobically, it reproducibly required a 12-day adaptation period before anaerobic growth. Whole-genome resequencing was applied to investigate the basis for this apparent 'lag phase' and, in anaerobically adapted cultures, identified mutations in *PMR1*, which encodes a Golgi Ca^{2+}/Mn^{2+} ATPase. Further research, in collaboration with enzymology specialists at Groningen University, focused on understanding the relationship between intracellular metal homeostasis and xylose fermentation.

Chapter 3 describes the identification and heterologous expression of a high-affinity fungal L-arabinose transporter in *S. cerevisiae*. Transcriptome data on L-arabinose-limited chemostat cultures *Penicillium chrysogenum* were used to characterize the transporter landscape of this filamentous fungus. After testing functional expression of 5 putative *P. chrysogenum* transporter genes in *S. cerevisiae*, the study focussed on the only gene among this set of 5 that enabled aerobic growth of an engineered L-arabinose-fermenting *S. cerevisiae* strain on this pentose. A variety of growth studies and transporter kinetics essays

were conducted to determine the potential of this fungal transporter for improving L-arabinose uptake by engineered *S. cerevisiae* strains.

In consolidated pentose and hexose fermenting yeast strains, simultaneous consumption of these sugars can contribute to productivity and culture robustness. **Chapter 4** focused on improving the uptake of L-arabinose in the presence of glucose. To this end, an L-arabinose consuming, glucose-phosphorylation-negative *S. cerevisiae* strain, expressing the fungal L-arabinose transporter described in Chapter 3, was subjected to anaerobic laboratory evolution on a glucose-xylose-arabinose mixture. Single-cell isolates from the evolved cultures were analysed by whole-genome sequencing and reverse engineering was applied to determine which mutations that contribute to the acquired D-glucose-insensitive, L-arabinose fermenting phenotype. Analysis of L-arabinose transport kinetics, performed in collaboration with specialists at Groningen University, was used to quantify the effects individual and combined mutations on L-arabinose uptake affinity and specificity of the galactose transporter Gal2.

Chapter 5 presents a novel evolutionary engineering strategy for identifying mutations that contribute to simultaneous utilization of D-xylose and D-glucose. Targeted mutations in central metabolic pathways were used to force co-utilization of these sugars in a xylose-isomerase-based xylose-fermenting strain. Subsequently, the strain was subjected to laboratory evolution in serial batch cultures on glucose-xylose mixtures. Whole-genome sequencing of evolved isolates and subsequent reverse engineering was used to identify mutations that improved simultaneous consumption of D-glucose and D-xylose in engineered *S. cerevisiae* strains.

Chapter 6, explores a radically different strategy for fermentation of sugar mixtures. Rather than using consolidated pentose-glucose fermenting strains, this Chapter explores the construction, performance and stability of a consortium of three 'specialist' *S. cerevisiae* strains for anaerobic fermentation of glucose-xylose-arabinose mixtures. To this end, a xylose-fermenting, glucose-phosphorylation-negative *S. cerevisiae* strain was constructed using a combination of metabolic- and evolutionary engineering. A consortium, comprised of this xylose specialist, the L-arabinose-fermenting strain described in Chapter 4 and a pentose-non-fermenting laboratory strain, was the characterized in anaerobic batch cultures on sugar mixtures. Prolonged cultivation in sequential batch reactor cultivation on sugar mixtures, whose composition resembled that in hydrolysates, was then used to compare performance and stability of the consortium with that of a consolidated hexose- and pentose-fermenting strain (previously constructed by Wisselink *et al.*). Based on this comparison, the potential advantages of mixed-sugar by consortia of 'specialist' strains is evaluated.

Chapter 2: Mutations in *PMR1* stimulate xylose isomerase activity and anaerobic growth on D-xylose of engineered *Saccharomyces cerevisiae* by influencing manganese homeostasis

Maarten D. Verhoeven*, Misun Lee*, Lycka Kamoen, Marcel van den Broek, Dick B. Janssen, Jean-Marc G. Daran, Antonius J.A. van Maris & Jack T. Pronk
*These authors contributed equally to the presented work

Abstract

Combined overexpression of xylulokinase, pentose-phosphate-pathway enzymes and a heterologous xylose isomerase (XI) is required but insufficient for anaerobic growth of *Saccharomyces cerevisiae* on D-xylose. Single-step Cas9-assisted implementation of these modifications yielded a yeast strain expressing *Piromyces* XI that showed fast aerobic growth on D-xylose. However, anaerobic growth required a 12-day adaptation period. Xylose-adapted cultures carried mutations in *PMR1*, encoding a Golgi Ca^{2+}/Mn^{2+} ATPase. Deleting *PMR1* in the parental XI-expressing strain enabled instantaneous anaerobic growth on D-xylose. In *pmr1* strains, intracellular Mn^{2+} concentrations were much higher than in the parental strain. XI activity assays in cell extracts and reconstitution experiments with purified XI apoenzyme showed superior enzyme kinetics with Mn^{2+} relative to other divalent metal ions. This study indicates engineering of metal homeostasis as a relevant approach for optimization of metabolic pathways involving metal-dependent enzymes. Specifically, it identifies metal interactions of heterologous XIs as an underexplored aspect of engineering xylose metabolism in yeast.

Background

In conventional feedstocks for fermentative production of fuel ethanol, such as corn starch and cane sugar, carbohydrates predominantly occur as dimers or polymers of hexose sugars. These hexose sugars can be efficiently and rapidly fermented by *Saccharomyces cerevisiae*. Economically feasible ethanol production from non-food lignocellulosic feedstocks additionally requires efficient, anaerobic fermentation of D-xylose and L-arabinose [206, 239] . Although wild-type *S. cerevisiae* strains cannot ferment these pentose sugars, they can slowly convert D-xylulose [240]. In yeast species that can grow on D-xylose, such as *Scheffersomyces stipitis*, its metabolism is initiated by a two-step conversion into D-xylulose by the combined activity of a xylose reductase (XR) and a xylitol dehydrogenase (XDH) [241]. The different redox cofactor preferences of XR and XDH represent a challenge in their use for constructing D-xylose-fermenting *S. cerevisiae* strains. This redox problem causes the production of substantial amounts of xylitol by anaerobic cultures of such engineered strains [44, 81, 142]. Elegant engineering strategies in which cofactor specificities of XR and/or XDH were altered, have not yet completely eliminated the formation of this by-product [5, 132].

In bacteria, D-xylose conversion is often initiated by its direct isomerization to D-xylulose, catalysed by xylose isomerase (XI) (EC 5.3.1.5). Until 2003, attempts to express heterologous XI genes in *S. cerevisiae* yielded no or very low XI activities under physiologically relevant conditions [242-245]. Then, multi-copy expression of a newly discovered xylose isomerase gene (*xylA*) from the anaerobic fungus *Piromyces* sp. E2 [147] was shown to yield high XI activity in cell extracts of *S. cerevisiae* [83, 246]. *Piromyces xylA* shows strong sequence similarity with *Bacteroides* XI genes, suggesting that the fungus acquired the gene by horizontal gene transfer. Indeed, expression of XI genes from *Bacteroides* species also yielded XI activity in *S. cerevisiae* [8, 247].

Consistent with the slow growth of wild-type *S. cerevisiae* strains on D-xylose[240], functional expression of *xylA* by itself only enabled very slow aerobic growth on D-xylose [83, 246]. Kuyper *et al.* (2005a) [7] reported that expression of *xylA* combined with constitutive overexpression of the genes encoding the native *S. cerevisiae* xylulokinase (*XKS1*), ribulose 5-phosphate epimerase (*RPE1*, EC 5.3.1.1), ribulose 5-phosphate isomerase (*RKI1*, EC 5.3.1.6), transketolase (*TKL1*, EC 2.2.1.1) and transaldolase (*TAL1*, EC 2.2.1.2) was sufficient to enable anaerobic growth on D-xylose, at a specific growth rate of 0.07 h^{-1}. Several subsequent studies confirmed that overexpression of a heterologous XI, combined with overexpression of xylulokinase and the enzymes of the non-oxidative pentose-phosphate pathway, is required for fast anaerobic fermentation of D-xylose [11, 14]).

Laboratory evolution experiments designed to further improve the kinetics of xylose fermentation revealed expression of the heterologous XI as a key factor, as reflected by amplification of the XI gene via formation of extra-chromosomal circular DNA [152] or increased numbers of XI genes on the yeast chromosomes [11]. Other studies demonstrated improved xylose fermentation in yeast strains in which XI expression was

increased by random mutagenesis, codon optimization or by mutations influencing protein folding [98, 114, 133]. Additional mutations that improve pentose-fermentation kinetics, mainly identified by resequencing of laboratory-evolved strains, affected structural genes encoding native yeast hexose transporters [112, 123, 126, 248] and in the 'secondary' transaldolase and transketolase isoenzymes *NQM1* and *TKL2* [7, 11, 163].

Over a decade of intensive research on D-xylose fermentation by XI-based, engineered *S. cerevisiae* strains yielded many important insights into their physiology. However, one important and industrially relevant aspect remains incompletely understood. While an initial study [7] reported that combined overexpression of *xylA*, xylulokinase and non-oxidative pentose-phosphate pathway enzymes was sufficient to enable anaerobic growth of *S. cerevisiae* on D-xylose, subsequent reports indicated that anaerobic growth on xylose required additional, as yet unidentified mutations [11, 98].

The aim of the present study was to investigate the molecular basis for anaerobic growth of engineered *xylA*-expressing, D-xylose-metabolizing *S. cerevisiae*. To this end, we used CRISPR-Cas9 mediated genome editing for single-step construction of an *S. cerevisiae* strain that grew aerobically on D-xylose as sole carbon source. After adaptation to anaerobic growth in xylose-grown bio-reactor batch cultures, we showed that mutations in a single gene enabled anaerobic growth on xylose. Via a combination of physiological and enzymological analyses, we investigated how these mutations affected intracellular metal homeostasis and D-xylose metabolism.

Results

One-step construction of a xylose-utilizing *Saccharomyces cerevisiae* strain. To construct a xylose-metabolizing *S. cerevisiae* strain, nine copies of an expression cassette containing *Piromyces xylA*, as well as single expression cassettes for constitutive overexpression of the native yeast genes for xylulokinase (*XKS1*) and for the enzymes of the non-oxidative branch of the pentose-phosphate pathway (*RKI1, RPE1, TKL1, TKL2* and *TAL1*) were introduced in *S. cerevisiae* CEN.PK113-7D. Additionally, an expression cassette for *NQM1,* a paralog of *TAL1* whose duplication has been shown to enhance pentose fermentation by engineered *S. cerevisiae* [163], was introduced. Combination of *in vivo* assembly [249] and CRISPR/Cas9-mediated chromosomal integration [137] enabled a one-step introduction of all expression cassettes in the *GRE3* locus, thereby inactivating *GRE3*, which encodes a non-specific aldose reductase that can reduce xylose to xylitol [250]. The nine copies of the *xylA* cassette were introduced as tandem repeats to facilitate adaptation of the *xylA* copy number by homologous recombination. Transformants obtained after plating on xylose synthetic medium (SMX) plates were restreaked thrice on the same medium. The genome of the resulting strain IMX696 (Table 1), in which correct integration of the cassettes was confirmed by diagnostic PCR using primers listed in Table S3, was sequenced to assess whether mutations had occurred during growth on SMX plates. No single-nucleotide polymorphisms (SNPs), insertion/deletions in coding regions or

changes in chromosomal copy numbers were observed. However, read-depth analysis revealed the presence of 36 rather than 9 copies of the *xylA* cassette. This amplification of *xylA* is consistent with earlier reports that showed a positive impact of high *xylA* copy numbers on xylose metabolism by engineered *S. cerevisiae* strains [11, 114, 152]. In aerobic shake-flask cultures on SMX, strain IMX696 exhibited a specific growth rate of 0.21 h^{-1} (Fig. 1).

Table 1 | *Saccharomyces cerevisiae* strains used in this study.

Strain	Relevant genotype/description	Reference
CEN.PK 113-7D	*MATa MAL2-8c SUC2*	[251]
IMX581	*MATa ura3-52 MAL2-8c SUC2 can1*□*::cas9*-natNT2	[137]
IMX696	*MATa ura3-52 MAL2-8c SUC2 CAN1::cas9*-natNT2 *gre3:: [pTDH3_RPE1- pPGK1_TKL1- pTEF1_TAL1- pPGI1_NQM - pTPI1_RKI1- pPYK1_TKL2- (pTPI1_xylA_tCYC1)*36 pTEF1_XKS1]* pUDE335	This study
IMS0488	Single-cell line isolated after adaptation of IMX696 to anaerobic growth on xylose (reactor 1)	This study
IMS0489	Single-cell line isolated after adaptation of IMX696 to anaerobic growth on xylose (reactor 2)	This study
IMX906	*MATa ura3-52 MAL2-8c SUC2 CAN1::cas9*-natNT2 *gre3:: [pTDH3_RPE1- pPGK1_TKL1- pTEF1_TAL1- pPGI1_ NQM1- pTPI1_RKI1- pPYK1_TKL2- (pTPI1_xylA_tCYC1)*36 pTEF1_XKS1] pmr1*□*::amdSYM* pUDE335	This study
IMX979	IMX906 with *PMR1* reintegrated at *PMR1* locus	This study
IMK692	*MATa MAL2-8c SUC2 pmr1*□*::amdSYM*	This study

Native gene terminator sequences were used for expression of *RPE1, TKL1, TAL1, NQM1, RKI1, TKL2* and *XKS1.*

Anaerobic growth on xylose requires prolonged adaptation. Anaerobic growth of the engineered xylose-fermenting strain IMX696 was investigated in nitrogen-sparged bioreactor cultures on SMX, supplemented with the anaerobic growth factors Tween-80 and ergosterol. In duplicate experiments, CO_2 production, which was continuously monitored in the off-gas of the bioreactors, was only observed after 12 days of incubation (Supplementary Fig. S1). To investigate this slow adaptation to anaerobic growth on xylose in more detail, the experiment was repeated, with regular analysis of culture viability, metabolite concentrations and growth (Fig. 2). Again, no significant xylose consumption occurred during the first 12 days of the experiment. A subsequent increase in biomass concentration coincided with the conversion of D-xylose to ethanol and glycerol. The specific growth rate after the onset of anaerobic growth was estimated at 0.11 h^{-1} based on biomass dry weight measurements during the mid-exponential growth phase. Biomass and ethanol yields on xylose were 0.086 ± 0.01 g biomass (g D-xylose)$^{-1}$ and 0.382 ± 0.01 g ethanol (g D-xylose)$^{-1}$, respectively (Fig. 2a, Supplementary Fig. S2a). The dynamics of adaptation to anaerobic growth were further investigated by plating culture samples on

synthetic medium with either glucose (SMD) or D-xylose (SMX). Colony counts on these plates were determined after aerobic and anaerobic incubation (Fig. 2b-e). On anaerobic SMX plates, colonies were first observed after 10 d, at which time they represented a fraction of only $1.8 \cdot 10^{-4}$ of the number of cells that were plated. Subsequently, consistent with the exponential growth observed by biomass dry weight measurements, the fraction of cells capable of anaerobic growth of xylose rapidly increased (Fig. 2b). When culture samples were plated on SMD, aerobic and anaerobic plates showed similar trends in colony counts (Fig. 2d-e). Conversely, plating on SMX revealed a strong trade-off between the ability to grow aerobically and anaerobically on xylose. On aerobically incubated SMX plates cell counts did not increase, not even when exponential growth on xylose took off during the final days of the bioreactor experiments and strongly increasing colony counts were observed on anaerobically incubated SMX plates (Fig. 2c).
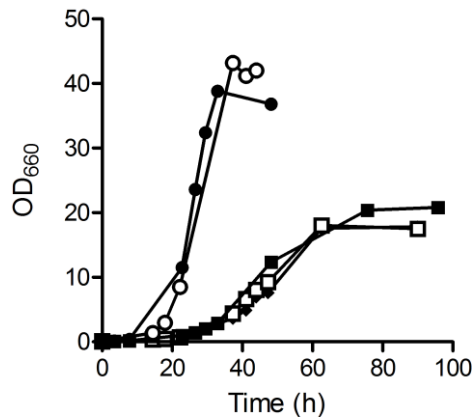
Figure 1 │ Growth of *S. cerevisiae* strains with different *PMR1* alleles in aerobic cultures on xylose. Aerobic growth curves in shake-flask cultures grown on synthetic medium with 20 g l^{-1} xylose. Symbols indicate the following *S. cerevisiae* strains: ●, IMX696 (*xylA*, PPP↑, *XKS1*↑), ■, IMX906 (*xylA*, PPP↑, XKS1↑, *pmr1Δ*), ○, IMX979 (*xylA*, PPP↑, XKS1↑, *PMR1*), ◆, IMS0488 (isolate from IMX696 culture adapted to anaerobic growth on xylose carrying Pmr1^{G249V} mutation) and □ IMS0489 (isolate from IMX696 culture adapted to anaerobic growth on xylose carrying Pmr1^{W387*} mutation). Data shown are from a single flask experiment for each strain. For all strains, data obtained from independent duplicate experiments differed by less than 5%.
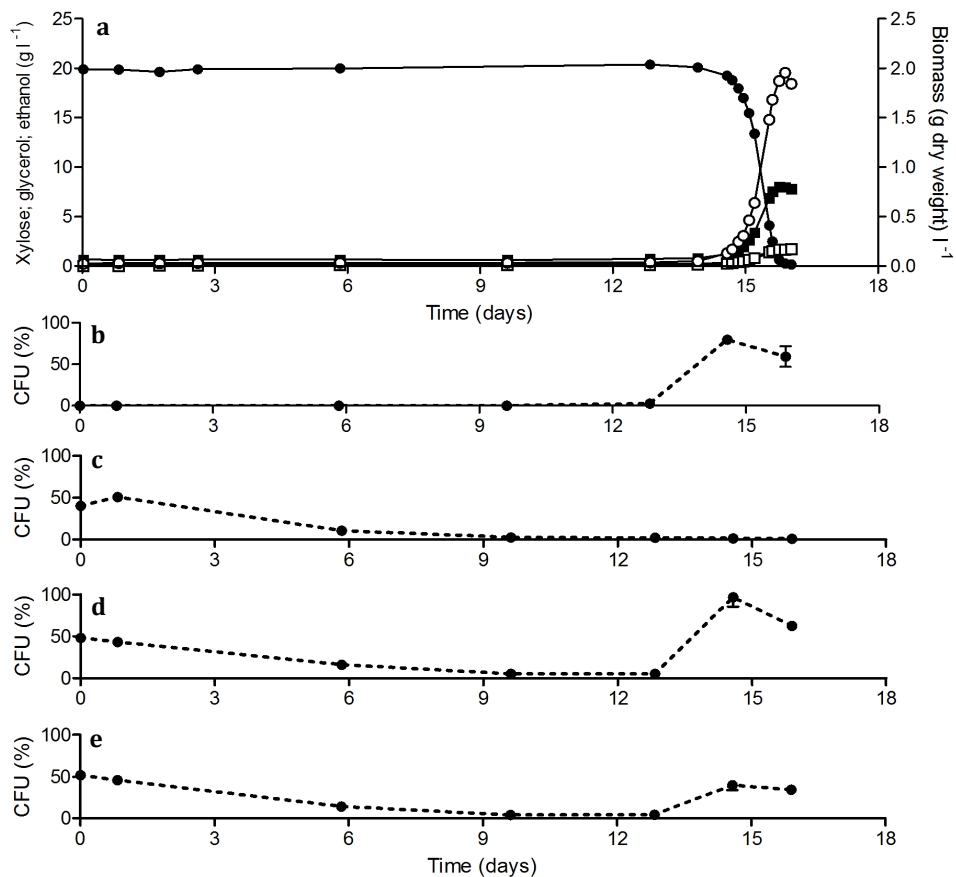
Figure 2 │ Anaerobic growth of *S. cerevisiae* IMX696 (*xylA*, PPP↑, *XKS1*↑) on xylose requires a prolonged adaptation period. (**a**) Growth, D-xylose consumption and product formation after inoculation of aerobically pregrown cells in anaerobic bioreactors containing synthetic medium with xylose (20 g l⁻¹). Symbols: ●, xylose, ■, ethanol, ○, biomass, □, glycerol. (**b**) Colony-forming units (CFU) on anaerobically incubated xylose medium reflect adaptation to growth on xylose in the absence of oxygen. (**c**) CFU on aerobically incubated xylose medium reflect trade-off between aerobic and anaerobic growth on xylose. (**d**) and (**e**) CFU on anaerobically and aerobically incubated glucose medium, respectively, showing that oxygen sensitivity of cells adapted to anaerobic growth on xylose is not carbon-source dependent. Data shown in figure are from one of two independent replicates, the replicate experiment is shown in Supplementary Fig. S2.

Table 2 | Single-nucleotide mutations in engineered *S. cerevisiae* strains adapted to anaerobic growth on xylose.

Strain	Gene	Nucleotide change	Amino acid change	Change in codon
IMS0488	*PMR1*	G746T	G249V	gGt/gTt
IMS0489	*PMR1*	G1161A	W387*	tgG/tgA

Strains IMS0488 and IMS0489 were isolated from independent anaerobic batch cultures of strain IMX696 (*xylA*, PPP↑, *XKS1*↑). The genome sequence of IMX696 was used as a reference.* introduction of stop codon.
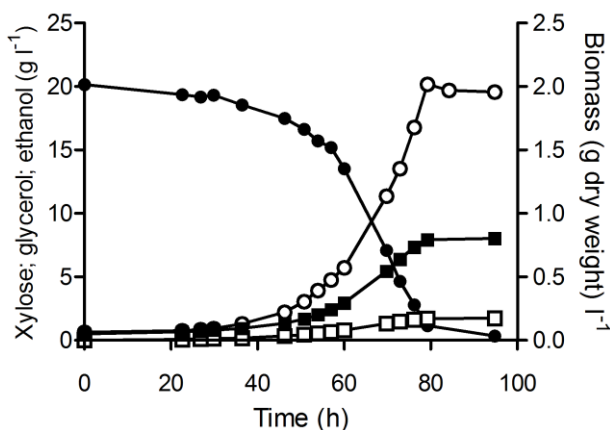
Figure 3 │ Deletion of *PMR1* enables anaerobic growth on xylose of engineered *S. cerevisiae* without prior adaptation phase. Growth and product formation of *S. cerevisiae* strain IMX906 (*xylA*, PPP↑, *XKS1*↑, *pmr1*Δ) on xylose (20 g l^{-1}) in anaerobic bioreactors. Symbols: ●, xylose, ■, ethanol, ○, biomass, □, glycerol. The data shown are from one of two independent replicates.

Mutations in PMR1 enable anaerobic growth on xylose. To investigate the role of the *PMR1* mutations in the adaptation to anaerobic growth on xylose, the gene was deleted in the parental strain IMX696. In replicate anaerobic bioreactor cultures on xylose, the resulting strain IMX906 grew within 24 h and completely consumed all sugar within 70 h (Fig. 3). The specific growth rate of both cultures was 0.08 h^{-1}, while biomass and ethanol yields on xylose were 0.086 g ± 0.01 biomass (g xylose)$^{-1}$ and 0.40 g ± 0.01 ethanol (g xylose)$^{-1}$, respectively. To further investigate the role of the *PMR1* deletion in the instantaneous anaerobic growth of strain IMX906 on xylose, the wild-type *PMR1* allele was reintegrated in this strain. The resulting strain IMX979 showed a lag phase of over 250 h in duplicate anaerobic bioreactor cultures on xylose (Supplementary Fig. S1), thereby confirming the key role of *PMR1* inactivation in the ability of engineered, XylA-based *S. cerevisiae* to grow anaerobically on xylose.

The plate count experiments during the anaerobic adaptation phase on xylose suggested a trade-off between aerobic and anaerobic growth on xylose (Fig. 2b-c). This possible trade-off was further explored by growth experiments in aerobic shake flasks on SMX. In these experiments, strains in which *PMR1* was mutated or deleted consistently showed a lower specific growth rate than strains that carried a wild-type *PMR1* allele (0.10 h^{-1} and 0.21 h^{-1}, respectively; Fig. 1). Furthermore, aerobic xylose-grown shake-flask cultures of strains with mutated *PMR1* alleles accumulated ethanol to 3-4 fold higher concentrations than corresponding cultures of strains with wild-type *PMR1* alleles (Supplementary Fig. S3). Consistent with previous results [252], aerobic shake flask cultures growing on glucose also revealed an approximately 50 % reduced growth rate of the *pmr1Δ* strain IMK692 (Supplementary Fig. S4).

Mutations in PMR1 affect intracellular metal concentrations in xylose-metabolizing S. cerevisiae strains. Pmr1 is an ATP-dependent transporter that imports Ca^{2+} and Mn^{2+} into the Golgi complex [253]. Based on the observation that *pmr1* null mutants accumulate Ca^{2+} and Mn^{2+} intracellularly, Pmr1 has also been implicated in secretion of divalent metal ions via the Golgi complex [254]. To explore a possible relation between metal homeostasis and anaerobic growth on xylose, we analysed intracellular concentrations of Ca^{2+}, Mn^{2+}, Mg^{2+} and Fe^{2+} in biomass samples from anaerobic mid-exponential phase bioreactor cultures using inductively coupled plasma mass spectrometry. Contents of Mg^{2+}, Ca^{2+} and Fe^{2+} were similar in all analysed strains, with Mg^{2+} accounting for over 80% of the analysed divalent metal ions, followed by Ca^{2+}, and with Fe^{2+} accounting for less than 1 % of the measured metals. Conversely, large differences were observed for the Mn^{2+} content. While in strains with a wild-type *PMR1* allele, Mn^{2+} represented less than 0.2% of the measured metal ions, 12- to 29-fold higher Mn^{2+} contents were observed in strains with mutated *PMR1* alleles, irrespective of whether they were grown on xylose or glucose (Table 3). The observation that mutations in *PMR1* affected cellular contents of Mn^{2+} but not those of Ca^{2+} is consistent with a previous study [255].

Table 3 | Impact of the deletion of *PMR1* on intracellular metal ion concentrations.

S. cerevisiae strain (relevant genotype)	Carbon source	µmol (g dry biomass)$^{-1}$				
		Mg^{2+}	Ca^{2+}	Fe^{2+}	Mn^{2+}	Total
IMX696 (*xylA*, *PPP*↑, *XKS1*↑)	glucose	60 ± 1	8.8 ± 1.6	0.56 ± 0.02	0.069 ± 0.001	69 ± 2
IMX906 (*xylA*, *PPP*↑, *XKS1*↑, *pmr1Δ*)	glucose	64 ± 1	12 ± 2	0.51 ± 0.02	1.2 ± 0.1	77 ± 2
IMX906 (*xylA*, PPP↑, *XKS1*↑, *pmr1Δ*)	xylose	50 ± 1	4.0 ± 0.7	0.36 ± 0.01	1.4 ± 0.1	56 ± 1
CEN.PK113-7D (reference strain)	glucose	61 ± 1	6.8 ± 1.3	0.44 ± 0.01	0.046 ± 0.001	68 ± 2
IMK692 (*pmr1Δ*)	glucose	72 ± 1	6.7 ± 1.2	0.46 ± 0.02	0.86 ± 0.06	80 ± 2

S. cerevisiae strains were grown in anaerobic bioreactors on xylose or glucose (20 g l^{-1}). Data represent average and mean deviation calculated from analyses on independent duplicate cultures.

Activity and metal content of xylose isomerase expressed in *S. cerevisiae* strains.
Laboratory evolution studies have identified XI activity as a key factor in rapid fermentation of xylose to ethanol [11, 152, 246]. XI enzymes are known to be metal dependent, with pronounced differences in metal binding and impact of metal identity on enzyme kinetics [256]. To examine the impact of Mn^{2+} on XylA activity, XI activities were assayed in cell extracts of strains IMX906 (*pmr1Δ*) and its parental strain IMX696 after aerobic and anaerobic growth on SMD in shake-flask cultures (Supplementary Figure S5). Cell extracts from both strains exhibited similar activities in assays without added metal ions. These activities do not necessarily reflect *in vivo* metal binding as they may, for example, have been influenced by binding of metals released during preparation of cell extracts, e.g. by disruption of vacuoles. Addition of Mn^{2+} and, to a lesser extent, of Mg^{2+} to the XI assays yielded significantly higher XI activities than observed in the absence of added metals. Conversely, addition of Ca^{2+} led to lower activities.

For a further analysis of the effect of Mn^{2+} on XylA activity, we purified the enzyme from the controlled anaerobic bioreactor cultures that were also used to determine cellular metal contents (Supplementary Fig. S6). Concentrations of Mg^{2+}, Ca^{2+}, Fe^{2+} and Mn^{2+} were measured in purified protein samples and the amount of each metal per enzyme active site was calculated (Table 4). These analyses showed that the isolated enzymes contained fewer than two metal ions per subunit, indicating that their metal binding sites were not fully occupied. In independent replicate experiments, large and

consistent differences were observed in the Mn^{2+} contents of XylA isolated from strains with wild-type and mutated *PMR1* alleles (0.017 and 0.30 mol Mn (mol XylA subunit)$^{-1}$, respectively, Table 4). The higher Mn^{2+} content of XylA isolated from xylose- or glucose-grown cells of the *pmr1Δ* strain coincided with a ca. 2-fold higher specific activity than measured with enzyme purified from the *PMR1* strain (Table 4). Although metal binding may have changed during cell disruption and enzyme purification, this correlation does indicate that Mn^{2+}-loaded XylA is a better catalyst than the Mg^{2+}-loaded enzyme. Addition of 1 mM $MgCl_2$ to purified enzyme preparations enhanced their XI activities, consistent with incomplete metal loading in the cell and/or metal loss during purification and activity assays.

Mn2+ binding results in superior catalytic efficiency of XylA. To accurately analyse the effect of different metals on catalytic properties of XylA, apoenzyme was prepared from XylA isolated from xylose-grown cultures of strain IMX906. Subsequently, XI activities were measured after reconstitution of apo-XylA with Mg^{2+}, Ca^{2+} or Mn^{2+} (Table 5). The activities of Mn^{2+}- and Mg^{2+}-reconstituted apo-XylA were higher than activities in non-metal-supplemented assays with XylA purified from yeast cultures (Table 4). The reconstituted enzyme showed the highest catalytic efficiency in the presence of Mn^{2+}, with a k_{cat}/K_M ratio that was 4-fold and 1500-fold higher than with Mg^{2+} and Ca^{2+}, respectively. Both the highest k_{cat} and the lowest K_M were observed with Mn^{2+} and contribute to the superior catalytic efficiency with this metal cofactor (Table 5). When XylA apoenzyme was reconstituted with mixtures of divalent metals that resembled those observed in intracellular metal content analyses (Table 3) of strains IMX696 (*PMR1*) and IMX906 (*pmr1Δ*), a 80-90% increase of XI activity was observed as the fraction of Mn^{2+} was increased from 0.002 to 0.01 (Supplementary Table S1).

Table 4 | Impact of *PMR1* deletion on metal content and activity of XylA.

S. cerevisiae strain (relevant genotype)	Carbon source	mol metal/mol XylA monomer				Sp. activity (U/mg XylA protein)	
		Mg^{2+}	Ca^{2+}	Fe^{2+}	Mn^{2+}	no metal added	Mg^{2+} added (1 mM)
IMX906 (*xylA*, PPP↑, *XKS1*↑, *pmr1Δ*)	xylose	0.18 ± 0.01	0.54 ± 0.11	0.06 ± 0.01	0.38 ± 0.04	2.39 ± 0.61	2.68 ± 0.5
IMX906 (*xylA*, PPP↑, *XKS1*↑, *pmr1Δ*)	glucose	0.20 ± 0.06	0.66 ± 0.07	0.064 ± 0.02	0.30 ± 0.03	1.35 ± 0.14	2.10 ± 0.1
IMX696 (*xylA*, PPP↑, *XKS1*↑)	glucose	0.22 ± 0.06	0.93 ± 0.41	0.086 ± 0.04	0.017 ± 0.004	0.60 ± 0.24	1.68 ± 0.1

XylA protein was isolated from *S. cerevisiae* cultures grown on xylose or glucose (20 g l^{-1}) in anaerobic bioreactors. Data represent average and mean deviation of analyses on XylA isolated from independent duplicate cultures.

Table 5 | Kinetic parameters of XylA measured after reconstituting apo-XylA with different divalent metal ions.

Metal	Kinetic parameters		
	k_{cat} (s^{-1})	K_M (mM)	k_{cat}/K_M (s^{-1}·M^{-1})
Mg^{2+}	2.8 ± 0.2	5.5 ± 0.4	500
Mn^{2+}	7.8 ± 0.1	3.9 ± 0.2	2000
Ca^{2+}	0.6 ± 0.06	420 ± 90	1.3

k_{cat} and K_M values represent average and mean deviation of independent duplicate experiments, calculated for each metal.

Discussion

One-step, Cas9-assisted integration of a heterologous XI (*Piromyces* XylA) and overexpression of native yeast genes encoding xylulokinase and enzymes of the non-oxidative pentose-phosphate pathway (PPP) enabled fast aerobic growth on xylose by *S. cerevisiae*, thus illustrating the efficiency of Cas9-based genome editing in this yeast [136, 137]. Nine copies of the *xylA* cassette were incorporated in tandem to facilitate expansion or compression of the *xylA* copy number by homologous recombination. This approach was validated by the four-fold higher *xylA* copy number in transformants isolated on xylose medium and its decrease in independent replicate cultures after subsequent adaptation to anaerobic growth. The observed amplification of *xylA* was consistent with the previously reported positive impact of high *xylA* copy numbers on xylose metabolism [11, 14, 152]. In line with earlier studies [11, 98], this metabolic engineering strategy did not enable anaerobic growth on xylose. In principle, the engineered XI-based pathway should allow for efficient, redox-cofactor-balanced alcoholic fermentation on this sugar. However, anaerobic growth on xylose requires much higher fluxes through XI since the ATP yield of anaerobic, fermentative metabolism of this sugar is approximately eight-fold lower than that of its aerobic, respiratory dissimilation (assuming an *in vivo* P/O ratio of 1.0) [257].

In independent replicate cultures, anaerobic growth on xylose required a two-week adaptation, which was shown to reflect the accumulation of spontaneous mutants with single-nucleotide mutations in *PMR1*. The observation that single, easily acquired point mutations enabled this adaptation may explain an earlier report that overexpression of XylA, xylulokinase and PPP enzymes sufficed to enable anaerobic growth of *S. cerevisiae* on xylose [7]. Here, we demonstrate that inactivation of *PMR1* caused both a strongly elevated intracellular Mn^{2+} concentration and an increased loading of heterologously expressed XylA with Mn^{2+}. Moreover, *in vitro* studies showed that loading of XylA apoenzyme with Mn^{2+} led to higher enzyme activities than binding of other divalent metal ions present in the yeast cytosol.

Consistent with the conclusion that intracellular Mn^{2+} homeostasis affects anaerobic xylose metabolism through its impact on *in vivo* XylA activity, none of the five *S. cerevisiae* enzymes that subsequently convert D-xylose into glycolytic intermediates (xylulokinase, ribulose-5-phosphate isomerase, ribulose-5-phosphate 3- epimerase, transaldolase and transketolase) have been documented to be Mn^{2+} dependent (BRENDA database [258]). Our results do not exclude the possibility that altered Mn^{2+} levels influenced pentose metabolism by mechanisms other than influencing XylA activity. However, a key role of XylA is consistent with the observation that acquisition of mutations in *PMR1* coincided with a decrease of the *xylA* copy number from 36 to 25. This decrease, which occurred during the course of a single batch culture, suggests that mutations in *PMR1* may have affected a trade-off between the need for a high *in vivo* activity of XylA and the metabolic burden associated with its high-level synthesis. As demonstrated in a study on the energetic impacts of galactose-induced synthesis of the enzymes of the Leloir pathway

[259], such a metabolic burden is much more pronounced in anaerobic cultures than in aerobic, respiring cultures due to the lower ATP yield from fermentative sugar dissimilation.

The mutations in *PMR1* that enabled anaerobic growth on xylose negatively affected aerobic growth. High intracellular Mn^{2+} concentrations have previously been implicated in impaired mitochondrial function [252], which is consistent with the increased accumulation of ethanol in aerobic shake-flask cultures of *pmr1* strains (Supplementary Fig. 3). Moreover, TORC1 signalling, which is involved in regulation of mitochondrial respiratory functions, is inhibited by Mn^{2+} and Pmr1 has been identified as a negative regulator of *TOR1*, which encodes a subunit of the TORC1 complex [260]. Additionally, Mn^{2+}-induced apoptosis mediated by Ndi1 [261, 262], a mitochondrial NADH dehydrogenase, may have contributed to low colony counts observed when cultures adapted to anaerobic growth on xylose were plated under aerobic conditions (Fig. 1c). The reduced growth rate in aerobic cultures of strains carrying *PMR1* mutations should be considered when their anaerobic industrial application is preceded by an aerobic biomass propagation phase.

Despite the pivotal role of the functional expression of a heterologous XI in *S. cerevisiae* [8] and the well documented role of metal ions in the active sites of XIs from taxonomically diverse organisms [263], the impact of metal loading on the performance of heterologously expressed XIs in *S. cerevisiae* has previously not been investigated. Similar to bacterial XIs [256], apo-XylA isolated from yeast could be activated with different metals. The results of this study suggest that metal loading can have a large effect on the *in vivo* catalytic performance of the enzyme.

The pronounced influence of cellular metal content on XI activity was in agreement with its promiscuity towards metal cofactors found in the *in vitro* analyses. However, while the fraction of the XI-bound Mn^{2+} increased by more than 10-fold in strains that carried mutations in *PMR1*, cellular contents of Mn^{2+} were still at least 40 times lower than the combined Mg^{2+} and Ca^{2+} contents (Tables 3 and 4). This observation suggests that the affinity of XylA for Mn^{2+} is higher than for the other divalent metal ions. Functional expression of heterologous XIs in *S. cerevisiae* initially represented a formidable challenge in engineering *S. cerevisiae* for anaerobic xylose fermentation [242-245]. After *Piromyces* XylA [147], XI genes from several eukaryotes and prokaryotes sources were shown to also be functionally expressed in *S. cerevisiae*, including those from *Orpinomyces* sp. [151], *Arabidopsis thaliana* [148], *Clostridium phytofermentans* [98], *Bacteroides thetaiotaomicron* [8], *Bacteroides stercoris*, *Prevotella ruminicula TC2-24* [149] and *Sorangium cellosum* [150]. In view of the key catalytic role of metal ions in all known xylose isomerases, we expect that *in vivo* activity of these and other XIs in yeast cells will also be affected by engineering of metal homeostasis.

Mutations in *PMR1* have been identified in two previous studies on adaptive laboratory evolution of XylA-based, engineered *S. cerevisiae* strains. P Klaassen, BEM Gielesen, GP Van Suylekom, P Sarantinopoulos, WHM Heijne and A Greeve [264] identified a mutation in *PMR1* (Y38C) in a strain evolved for fermentation of L-arabinose and xylose

to ethanol. Recently, J Hou, C Jiao, B Peng, Y Shen and X Bao [114], reported a mutation in *PMR1* (G698V) in a respiratory-deficient XylA based *S. cerevisiae* strain obtained by adaptive laboratory evolution on xylose medium. Our results strongly suggest that, in both studies, the mutations in *PMR1* may have contributed to the selected phenotypes. Additionally, the superior catalytic efficiency of Mn^{2+}-loaded XylA may explain a recent report that $MnSO_4$ supplementation enhanced growth on xylose of acetate-stressed cultures of a XylA-based xylose-fermenting *S. cerevisiae* strain [265].

Our study demonstrates the importance of metal homeostasis and enzyme loading in XI-based yeast metabolic engineering strategies for anaerobic conversion of xylose-containing lignocellulosic feedstocks into fuels and chemicals. Inactivation of *PMR1*, combined with overexpression of PPP enzymes, xylulokinase and *xylA* was shown to be sufficient to enable anaerobic growth of *S. cerevisiae* on xylose. Beyond xylose utilization, engineering of metal homeostasis has the potential to improve *in vivo* performance of other metal-dependent heterologous enzymes or pathways.

Methods

Strains and maintenance. All *S. cerevisiae* strains used in this study (Table 1) originate from the CEN.PK lineage [251, 266]. Frozen stock cultures were stored at -80 °C in 30% (vol/vol) glycerol.

Plasmid and strain construction. Plasmids used in this study are presented in Supplementary Table S2. Expression cassettes required for xylose fermentation were introduced into the *GRE3* locus of *S. cerevisiae* strain IMX581 by simultaneous in-vivo assembly and integration [249]. Expression cassettes for *RPE1*, *RKI1*, *TAL1*, *NQM1*, *TKL1*, *TKL2* and *XKS1* were obtained by fusing constitutive promoter sequences, ORFs and terminator sequences amplified from CEN.PK113-7D in a fusion-PCR [267] using the primers specified in Supplementary Table S3. Plasmid pYM-N18 [268] was used as a template for the *TEF1* promoter. The resulting fragments were cloned into pJET-1.2 blunt-end vectors. Correct assembly was verified by sequencing as described below. PCR amplification of expression cassettes and plasmids was performed using Phusion Hot Start II High Fidelity DNA Polymerase (Thermo Scientific, Waltham, MA), according to the manufacturer's protocol. Integration in *GRE3* locus was mediated by a chimeric CRISPR/Cas9 editing system [136, 137] with gRNA expressed from an episomal plasmid[137]. The plasmid backbone was PCR amplified from pMEL10 using primers 5792-5980 (Supplementary Table S3). A plasmid insert containing the 20bp gRNA-targeting sequence was obtained by PCR amplification with primers 5978-5979 using pMEL10 as template. The resulting fragment was fused to the plasmid backbone with the Gibson Assembly Cloning kit (New England Biolabs, Ipswich, MA), yielding plasmid pUDE335. *E. coli* DH5a cells were transformed with 1 μL of the Gibson-assembly mix using a Gene PulserXcell Electroporation System (Biorad,

Hercules, CA). Plasmid DNA was isolated from *E. coli* cultures using a Sigma GenElute Plasmid kit (Sigma-Aldrich, St. Louis, MO). The presence of the *GRE3* cutting gRNA was confirmed by PCR-amplification using primer pair 2528-960 followed by digestion with FastDigest *ClaI* (Thermo Scientific).

The coding region of the *Piromyces* sp. E2 xylose isomerase gene [Genbank: CAB76571.1] was codon optimized according to the codon preference of highly expressed glycolytic genes in *S. cerevisiae*[86]. The codon-optimized sequence, flanked by the constitutive *TPI1* promoter and *CYC1* terminator, was synthesized by GeneArt GmbH (Regensburg, Germany). After subsequent transformation of the pMK-RQ (GeneArt) based vector pUDR350 into *E. coli,* nine different expression cassettes of *xylA* were made, flanked by 60 bp synthetic recombinant sequences (Supplementary Fig. S7). For XylA expression in *E. coli*, a codon-optimized synthetic *xylA* was cloned into pBAD/myc-His-derived plasmid.

Yeast transformation was performed using the lithium acetate protocol [269]. Strain IMX696 was obtained by adding 200 pmol of each of the 15 fragments combined with 500 ng of plasmid pUDE335. After one hour of incubation in synthetic medium with glucose (SMD) the cells were plated on SM plates with xylose as the carbon source (SMX). Correct assembly of all fragments in the *GRE3* locus was confirmed by diagnostic PCR (Dreamtaq, Thermo Scientific) using primers listed in Table S3. Deletion of *PMR1* in *S. cerevisiae* strains IMX696 and CEN.PK113-7D was done by integrating an *amdSYM*-based deletion cassette [270], which was derived by PCR amplification from pUG-*amdSYM* using primers 8638/8639 as template. After transformation, cells were plated on glucose synthetic medium with acetamide as the nitrogen source (SMD-Ac). Gene deletion was confirmed by diagnostic PCR and the resulting strains were named IMX906 and IMK692, respectively. To reintegrate *PMR1*, the *PMR1* ORF was PCR-amplified from CEN.PK113-7D and transformed into strain IMX906. After overnight incubation in SMD-Ac, cells were plated on SMD plates supplemented with 2.3 g l^{-1} fluoroacetamide (SMD-Fac). Correct integration of *PMR1* in the resulting strain, IMX969, was confirmed by diagnostic PCR.

Cultivation and media. Shake-flask cultures were grown at 30 °C in an orbital shaker at 200 rpm, using 500-ml flasks containing 100 ml medium. Physiological characterization of aerobic growth was performed in shake flasks containing SMX or SMD with urea as sole nitrogen source to prevent acidification. Prior to filter sterilization, media were adjusted to pH 5.0 with 2 M KOH. For pre-cultures, SM adjusted to pH 6.0 was autoclaved at 120 °C for 20 min after which a 50 w/v % solution of sterile glucose or xylose was added to obtain a final sugar concentration of 20 g l^{-1}, together with filter-sterilized vitamin solution [51]. Glucose and xylose solutions were autoclaved separately (20 min at 110 °C). For plates, 2% agar was added to media prior to autoclaving. Frozen stocks (1 ml aliquots in 30 % glycerol) were inoculated directly into pre-culture shake flasks. In late exponential phase an aliquot was transferred to a second pre-culture to obtain an initial OD$_{660}$ of 0.1. Flasks or anaerobic bioreactors used for characterization were inoculated from these cultures at

an initial OD_{660} of between 0.1 and 0.2. Anaerobic batch cultures were conducted in 2-l bioreactors (Applikon, Delft, The Netherlands) with a working volume of 1 l. Biomass for metal content analysis was grown in 3-l bioreactors (Applikon) with a working volume of 2 l were used. Bioreactor cultures were grown at 30 °C, pH 5.0, and stirred at 800 rpm. To ensure anaerobic conditions, bioreactors were equipped with Viton O-rings and Norprene tubing. During cultivation, nitrogen gas (<10 ppm oxygen) was continuously sparged through the cultures at $0.5 \, l \, min^{-1}$. After autoclaving , synthetic medium used for anaerobic cultivation was supplemented with $0.2 \, g \, l^{-1}$ sterile antifoam C (Sigma-Aldrich), as well as Tween 80 ($420 \, mg \, l^{-1}$) and ergosterol ($10 \, mg \, l^{-1}$) dissolved in ethanol [271].

Analytical methods. Cell dry weight (CDW) measurements were done using pre-weighed nitrocellulose filters (pore size, 0.45 μm; Gelman Laboratory, Ann Arbor, MI) to filter 10 ml of culture. Before weighing the sample, filters were washed with demineral-ised water and dried in a microwave oven (Bosch, Stuttgart, Germany) for 20 min at 360 W. Growth was monitored by optical density (OD) measurements at a wavelength of 660 nm using a Libra S11 spectrophotometer (Biochrom, Cambridge, United Kingdom). A cor-relation between OD measurements and CDW was used to estimate CDW in samples for which no direct CDW measurements were taken. This correlation was based on at least six points during the exponential phase.

CO_2 and O_2 concentrations in bioreactor exhaust gas were measured using an NGA 2000 analyzer (Rosemount Analytical, Orrville, OH) after the gas was cooled by a condenser (2°C) and dried with a Permapure MD-110-48P-4 dryer (Permapure, Toms River, NJ). Metabolite levels in culture supernatants obtained by centrifugation were measured via high-performance liquid chromatography (HPLC) analysis on an Agilent 1260 HPLC (Agilent Technologies, Santa Clara, CA) fitted with a Bio-Rad HPX 87H column (Bio-Rad, Hercules, CA). The column was eluted at 60°C with $0.5 \, g \, l^{-1}$ H_2SO_4 at a flow rate of $0.6 \, ml \, min^{-1}$. Detection was by means of an Agilent refractive-index detector and an Agilent 1260 VWD detector. Correction for ethanol evaporation were done for all biore-actor experiments as described previously [89].

Viability of strain IMX696 during anaerobic cultivation was assessed by plating culture samples. The number of cells per ml was measured using a Z2 Coulter Counter (Beckman Coulter, Woerden, The Netherlands) after which dilutions were plated in dupli-cate on SMX and SMG agar plates and incubated at 30°C. To limit exposure to oxygen, cells that were used to determine anaerobic viability measurements were sampled directly into a container flushed with argon and immediately transferred into an anaerobic chamber (5% H_2, 6% CO_2, and 89% N_2, Sheldon MFG Inc., Cornelius, OR) for plating and incubation. Colony-forming units (CFU) were counted after incubation at 30 °C for 4 days (aerobic growth) or 8 days (anaerobic growth).

DNA sequence analysis. Genomic DNA of strains IMX696, IMS0488 and IMS0489 was isolated using the QIAGEN Blood & Cell Culture DNA Kit with 100/G Genomics-tips (QIAGEN, Valencia, CA) according to the manufacturer's protocol. From these DNA samples, 350-bp insert libraries were constructed using the Nextera XT DNA kit (Illumina, San Diego, CA). Paired-end sequencing (100-bp reads) of genomic or plasmid DNA was performed with an Illumina HiSeq 2500 sequencer (Baseclear BV, Leiden, The Netherlands). Data were mapped to the CEN.PK113-7D genome or to in silico-generated plasmid sequences using the Burrows-Wheeler alignment tool [272] and processed with Pilon[273]. Identified single-nucleotide differences were inspected with the Integrated Genomics Viewer [274] (IGV). The chromosomal copy number variance (CNV) was estimated using the Poisson mixture model based algorithm Magnolya [275]. The copy number of *xylA* was estimated by comparing the read depth to the average read depth of all chromosomes. Raw sequence data of strains IMX696, IMS0488 and IMS0489 are deposited at the NCBI Sequence Read archive (www.ncbi.nlm.nih.gov/sra) under BioProject ID PRJNA349142.

Purification of xylose isomerase. Cell pellets were resuspended in 10 mM MOPS, pH 7.0, containing protease inhibitors (cOmplete ULTRA tablets, Roche) and disrupted using a high pressure homogenizer (Constant Systems Ltd, Low March, United Kingdom). Samples were passed through the apparatus twice at 39 kpsi and cell debris was removed by centrifugation at 35,000 x g for 45 min at 4 ˚C. A single-step purification procedure based on anion-exchange chromatography was applied to minimize the loss of protein-bound metals. Cell-free extracts were loaded on a strong anion-exchange column (Resource Q, GE Healthcare, Chicago, IL) equilibrated with 10 mM MOPS, pH 7.0. A gradient elution was applied using 10 mM MOPS, pH 7.0, containing 0 - 200 mM KCl. XylA eluted at approximately 40 mM KCl. Protein concentrations were determined using the theoretical extinction coefficient at 280 nm ($\varepsilon280$, XI = 73,800 M^{-1} cm^{-1}) calculated by the ProtParam tool (http://web.expasy.org/protparam/).

Metal content analysis. Metal concentrations were analysed with an inductively coupled plasma mass spectrometer (ICP-MS, Varian 820). All measurements were performed 5 times for each sample and yttrium was used as an internal standard. Purified protein samples were lyophilized and analysed for contents of magnesium, calcium, iron and manganese. Prior to measurement, samples were dissolved in 1 % nitric acid solution. All analyses were performed on protein samples isolated from two replicate cultures. For intracellular metal analysis, cells were prepared with a protocol adopted from Eide *et al*. [276]. The harvested cells were washed three times each with 1 µM EDTA solution and subsequently with deionized water (Milli-Q) and suspended in 1 ml 30 % (w/v) nitric acid and incubated at 60 ˚C for 4 h. Cell lysates were centrifuged at 16,000 x g and supernatants were collected. Pellets were washed with 1 ml deionized water and the supernatants were collected as before. The 2 ml of final sample solution containing approximately 15 %

(w/v) nitric acid were then subjected to the measurements. The metal content was determined with samples from two separate bioreactor batch cultures.

Preparation of cell extracts. Cell extracts were prepared following a previously published procedure with minor modifications [246]. To limit loss of metals during preparation, no EDTA was added prior to sonication. Cells were washed and suspended in 10 mM MOPS buffer pH 7.0 to avoid precipitation of $MnCl_2$ and 10 mM DTT was added. After sonication (4 bursts of 30 s with 30 s intervals at 0 °C, amplitude 8 μm) using a Soniprep 150 sonicator (Beun de Ronde BV, Abcoude, The Netherlands), cell debris was removed by centrifugation (4 °C, 20 min at 48,000g) and the clear supernatant was used for XylA assays.

Enzyme activity assays. Activity of XylA was measured with a coupled enzyme assay using D-sorbitol dehydrogenase [277]. D-sorbitol dehydrogenase (SDH) was obtained from Roche Diagnostics GmbH (Mannheim, Germany). Reactions were performed at 30 ˚C and pH 7.0 (20 mM MOPS buffer). The decrease in absorbance at 340 nm was monitored in either a spectrophotometer (Jasco, Easton, MD) or a Synergy Mx microtiter plate reader (BioTek Instruments, Winooski, VT). Reaction mixtures included 5, 200 or 500 mM xylose, 250 μM NADH and 1 U ml^{-1} of SDH. Addition of 0.03 to 1 μM (depending on the substrate concentration and the metal added) XI or cell free extract into the mixture initiated the reaction. For measuring XylA activity in the presence of different metal cofactors, samples of apo-XylA were prepared by overnight incubation of the purified enzyme with 10 mM EDTA. Subsequently, EDTA was removed by buffer exchange to 20 mM MOPS, pH 7.0 and 1 mM of divalent metal solutions ($MgCl_2$, $MnCl_2$ or $CaCl_2$) were added in the reaction. For kinetic analyses, D-xylose was added at concentrations ranging from 0.5 mM to 1.50 M.

Acknowledgements

Supplementary Material

Table S1 | Activity of XylA in the presence of different metal mixtures.

Xylose (mM)	XylA activities (U·(mg protein)$^{-1}$)			
	Mg^{2+}	Mn^{2+}	Mix 1 Mg:Ca:Mn 0.85:0.15:0.001	Mix 2 Mg:Ca:Mn 0.84:0.14:0.02
5	1.73 ± 0.19	4.03 ± 0.44	1.87 ± 0.42	3.53 ± 0.73
200	3.13 ± 0.10	7.05 ± 0.67	3.35 ± 0.06	6.02 ± 0.45

XylA was expressed in *E. coli*, purified and EDTA-treated. Enzyme activities were measured in the presence different metal (mixtures), total concentration 1 mM. The molar fractions in metal mixes 1 and 2 represent the intracellular metal composition of IMX696 and IMX906, respectively (see Table 3 and main text). Reactions were performed at 30 °C and pH 7.0 with saturating concentration (200 mM) and near K_M (5 mM) of xylose. The values represent average and mean deviation of measurements with XylA isolated from independent duplicate *E. coli* cultures.

Table S2 | Plasmids used in this study.

Plasmid	Characteristics	Origin
pMEL10	2 μm ori, *KlURA3*, p*SNR52*-gRNA.CAN1.Y-t*SUP4*	Mans *et al.* (2015)[33]
pJET1.2Blunt	Multi-purpose cloning vector	ThermoFisher
pUD344	pJET1.2Blunt + TagA_p*PGI1_NQM1*_TagB	This study
pUD345	pJET1.2Blunt + TagB_p*TPI1_RKI1*_Tagc	This study
pUD346	pJET1.2Blunt + TagC_p*PYK1_TKL2*_TagF	This study
pUD347	pJET1.2Blunt + TagG_p*TDH3_RPE1*_TagH	This study
pUD348	pJET1.2Blunt + TagH_p*PGK1_TKL1*_TagI	This study
pUD349	pJET1.2Blunt + TagI_p*TEF1_TAL1*_TagA	This study
pUD350	pMK-RQ_p*TPI1_xylA*_t*cyc*	This study
pUD353	pJET_Blunt_p*TEF1_XKS1*_t*XKS1*	This study
pUDE335	2 μm ori, *KlURA3*, p*SNR52*-gRNA.*GRE3*.Y-t*SUP4*	This study
pUG-AmdSYM	Template of AmdSYM cassette for *PMR1* deletion	Solis-Escalante *et al.* (2013)[63]

Native gene terminator sequences were used for expression of *RPE1, TKL1, TAL1, NQM1, RKI1, TKL2* and *XKS1*.

Table S3 | Oligonucleotide primers used in this study.

Construction of cassettes containing constitutively expressed-pentose-phosphate-pathway and *XKS1* genes:

Primer nr.:	Purpose:	Template:	Sequence 5' -> 3':
5924	*PGI1* promoter fragment	CEN.PK113-7D	ACTATATGTGAAGGCATGGCTATGGCACGG-CAGACATTCCGCCAGATCATCAATAGGCACCAGGGCACTACTTCTACACATCAACG
5925	*PGI1* promoter fragment	CEN.PK113-7D	TTTTAGGCTGGTATCTTGATTCTAAATCG
5926	*NQM1* ORF fragment	CEN.PK113-7D	TCGATTTAGAATCAAGATACCAGCCTAAAAAT-GTCAGAACCTTCAGAGAAAAAAC
5927	*NQM1* ORF fragment	CEN.PK113-7D	GTTGAACATTCTTAGGCTGGTCGAATCATT-TAGACACGGGCATCGTCCTCTCGAAAGGTGGCCCAAGAGGATATTAAGTACTAATGTGG
3847	fusion-PCR of pPGI1 and *NQM1*	pPGI1 + *NQM1* fragment	ACTATATGTGAAGGCATGGCTATGG
3276	fusion-PCR of pPGI1 and *NQM1*	pPGI1 + *NQM1* fragment	GTTGAACATTCTTAGGCTGGTCGAATC
5928	*TPI1* promoter fragment	CEN.PK113-7D	CACCTTTCGAGAGGACGATGCCCGTGTCTAAAT-GATTCGACCAGCCTAAGAATGTTCAACGCGGCCGTGTTTAAAGATTAC
5929	*TPI1* promoter fragment	CEN.PK113-7D	CCGCGGAGTTTATGTATG
5930	*RKI1* ORF fragment	CEN.PK113-7D	CTTAAATCTATAACTACAAAAAAACACATACA-TAAACTCCGCGGATGGCTGCCGGTGTCCC
5931	*RKI1* ORF fragment	CEN.PK113-7D	CTAGCGTGTCCTCGCATAGTTCTTAGATT-GTCGCTACGGCATATACGATCCGTGAGACGTATCATAGGTGAGAAAGAGATGGAGAAT-GTAGTACTGC
4672	fusion-PCR of pTPI1 and *RKI1*	pTPI1+ *RKI1* fragment	CACCTTTCGAGAGGACGATG
3277	fusion-PCR of pTPI1 and *RKI1*	pTPI1+ *RKI1* fragment	CTAGCGTGTCCTCGCATAGTTCTTAGATTG
5932	*PYK1* promoter fragment	CEN.PK113-7D	ACGTCTCACGGATCGTATATGCCGTAGCGA-CAATCTAAGAACTATGCGAGGACACGCTAGGGTAGCGCCCTGGTCAAACTTCAGAAC
5933	*PYK1* promoter fragment	CEN.PK113-7D	TGTGATGATGTTTTATTTGTTTTGATTGGTGTC
5934	*TKL2* ORF fragment	CEN.PK113-7D	CACCAATCAAAACAAATAAAACATCATCA-CAATGGCACAGTTCTCCGACATTGATAAACTTGC
5935	*TKL2* ORF fragment	CEN.PK113-7D	TGCCGAACTTTCCCTGTATGAAGCGATCTGAC-CAATCCTTTGCCGTAGTTTCAACGTATGGCAGCCCATACACTCAAAGC
3283	fusion-PCR of pPYK1 and *TKL2*	pPYK1 + *TKL2* fragment	ACGTCTCACGGATCGTATATGC
3288	fusion-PCR of pPYK1 and *TKL2*	pPYK1 + *TKL2* fragment	TGCCGAACTTTCCCTGTATGAAGC

5912	*TDH3* promoter fragment	CEN.PK113-7D	GCCAGAGGTATAGACATAG-CCAGACCTACCTAATTGGTGCATCAGGTGGTCATGGCCCTTCCGGGAGTTTATCATTATCAAT-ACTCG
5913	*TDH3* promoter fragment	CEN.PK113-7D	CCGTCGAAACTAAGTTCTTGG
5914	*RPE1* ORF fragment	CEN.PK113-7D	TTAGTTTTAAAACACCAAGAACT-TAGTTTCGACGGATGGTCAAACCAATTATAGCTCCCAGTATCC
5915	*RPE1* ORF fragment	CEN.PK113-7D	GTCACGGGTTCTCAGCAATTCGAGCTAT-TACCGATGATGGCTGAGGCGTTAGAGTAATCTCTTCTCCGGCCTCCATCACCAC
4870	fusion-PCR of pTDH3and *RPE1*	pTDH3 + *RPE1* fragment	GCCAGAGGTATAGACATAGCC
3290	fusion-PCR of pTDH3and *RPE1*	pTDH3 + *RPE1* fragment	GTCACGGGTTCTCAGCAATTCG
5916	*PGK1* promoter fragment	CEN.PK113-7D	AGATTACTCTAACGCCTCAGCCAT-CATCGGTAATAGCTCGAATTGCTGAGAACCCGTGACTGCCCTTATCTTGTGCAGTTAGAC
5917	*PGK1* promoter fragment	CEN.PK113-7D	TGTTTTATATTTGTTGTAAAAAGTAGATAAT-TACTTCC
5918	*TKL1* ORF fragment	CEN.PK113-7D	GGAAGTAATTATCTACTTTTTACAACAAA-TATAAAACAATGACTCAATTCACTGACATTGATAAGC
5919	*TKL1* ORF fragment	CEN.PK113-7D	GCCTACGGTTCCCGAAGTATGCTGCTGATGTCT-GGCTATACCTATCCGTCTACGTGAATAATGAATGCGACCGATATTTTTGG
3291	fusion-PCR of pPGK1 and *TKL1*	pPGK1 + *TKL1* fragment	CTCTAACGCCTCAGCCATCATCG
4068	fusion-PCR of pPGK1 and *TKL1*	pPGK1 + *TKL1* fragment	GCCTACGGTTCCCGAAGTATGC
5920	*TEF1* promoter fragment	pYM-N18	TATTCACGTAGACGGATAGGTATAGCCAGA-CATCAGCAGCATACTTCGGGAACCGTAGGCAGCTCATAGCTTCAAAATGTTTCTACTCC
5921	*TEF1* promoter fragment	pYM-N18	AAAACTTAGATTAGATTGCTATGCTTTCT-TTCTAATGAGC
5922	*TAL1* ORF fragment	CEN.PK113-7D	GCTCATTAGAAAGAAAGCATAG-CAATCTAATCTAAGTTTTATGTCTGAACCAGCTCAAAAGAAACAAAAGG
5923	*TAL1* ORF fragment	CEN.PK113-7D	GTGCCTATTGATGATCTGGCGGAATGTCT-GCCGTGCCATAGCCATGCCTTCACATATAGTCATTGTGATCCTCCTATGTTGTAGTATAGTGC
3274	fusion-PCR of pTEF1 and *TAL1*	pTEF1+ *TAL1* fragment	TATTCACGTAGACGGATAGGTATAGC
3275	fusion-PCR of pTEF1 and *TAL1*	pTEF1+ *TAL1* fragment	GTGCCTATTGATGATCTGGCGGAATG

2

| 6278 | *XKS1* ORF fragment | CEN.PK113-7D | GCAATGACAAATTCAAAAGAAGACGCCGA-CATAGAGGAGAAGCATATGTACAATGAGCCGGTCCAGTGCTTCCACATC |
| 6279 | *XKS1* ORF fragment | CEN.PK113-7D | GCTCATTAGAAAGAAAGCATAG-CAATCTAATCTAAGTTTTATGTTGTGTTCAGTAATTCAGAGACAG |

Primers used for amplification of integration fragments:

Primer nr.:	Purpose:	Template:	Sequence:
7133	fl_*RPE1*_H fragment fw	pUD347	TATAATATTTCATTATCGGAACTCTAGA-TTCTATACTTGTTTCCCAATTGTTGCTGGTAGGGCCCTTCCGGGAGTTTATC
3290	fl_*RPE1*_H fragment rv	pUD347	GTCACGGGTTCTCAGCAATTCG
3291	H_*TKL1*_I fragment fw	pUD348	CTCTAACGCCTCAGCCATCATCG
4068	H_*TKL1*_I fragment rv	pUD348	GCCTACGGTTCCCGAAGTATGC
3274	I_*TAL1*_A fragment	pUD349	TATTCACGTAGACGGATAGGTATAGC
3275	I_*TAL1*_A fragment	pUD349	GTGCCTATTGATGATCTGGCGGAATG
3847	A_ *NQM1* _B	pUD344	ACTATATGTGAAGGCATGGCTATGG
3276	A_ *NQM1* _B	pUD344	GTTGAACATTCTTAGGCTGGTCGAATC
4672	B_*RKI1*_C fragment	pUD345	CACCTTTCGAGAGGACGATG
3277	B_*RKI1*_C fragment	pUD345	CTAGCGTGTCCTCGCATAGTTCTTAGATTG
3283	C_*TKL2*_F fragment	pUD346	ACGTCTCACGGATCGTATATGC
3288	C_*TKL2*_F fragment	pUD346	TGCCGAACTTTCCCTGTATGAAGC
7138	F_*xylA*_P fragment	pUD350	CTGATAGTGCTGTAAGTCGCCTCCATCTTAG-CAGAGCTGTCCCTGAATGCGTACTCGTGAGCGATACCCTGCGATCTTC
7136	F_*xylA*_P fragment	pUD350	CATACGTTGAAACTACGGCAAAGGATT-GGTCAGATCGCTTCATACAGGGAAAGTTCGGCACGCGCAGATTAGCGAAGC
7139	P_*xylA*_Q fragment	pUD350	GAGCTGAATGTATATGCTGCGGGATCATTGCA-CAGCTCTGAGAGCCCTGCAACGCGATATGCGATACCCTGCGATCTTC
7137	P_*xylA*_Q fragment	pUD350	TCACGAGTACGCATTCAGGGACAGCTCT-GCTAAGATGGAGGCGACTTACAGCACTATCAGCGCGCAGATTAGCGAAGC
7142	Q_*xylA*_E fragment	pUD350	AGCGATCTGCGAGACCGTATAGCCATGAC-GAGGTCGCAATCTTGCGGACAGTGTAGCTCAGCGATACCCTGCGATCTTC

7140	Q_*xylA*_E fragment	pUD350	ATATCGCGTTGCAGGGCTCTCAGAGCTGTG-CAATGATCCCGCAGCATATACATTCAGCTCCGCGCAGATTAGCGAAGC
7141	E_*xylA*_G fragment	pUD350	TGAGCTACACTGTCCGCAAGATT-GCGACCTCGTCATGGCTATACGGTCTCGCAGATCGCTCGCGCAGATTAGCGAAGC
6285	E_*xylA*_G fragment	pUD350	AAGGGCCATGACCACCTGATGCAC-CAATTAGGTAGGTCTGGCTATGTCTATACCTCTGGCGCGATACCCTGCGATCTTC
6273	G_*xylA*_D fragment	pUD350	GCCAGAGGTATAGACATAG-CCAGACCTACCTAATTGGTGCATCAGGTGGTCATGGCCCTTCGCGCAGATTAGCGAAGC
6284	G_*xylA*_D fragment	pUD350	AATCACTCTCCATACAGGGTTTCATACATTTCT-CCACGGGACCCACAGTCGTAGATGCGTGCGATACCCTGCGATCTTC
6283	D_*xylA*_M fragment	pUD350	ACGCATCTACGACTGTGGGTCCCGTGGAGAAAT-GTATGAAACCCTGTATGGAGAGTGATTGCGATACCCTGCGATCTTC
6275	D_*xylA*_M fragment	pUD350	ACGAGAGATGAAGGCTCACCGAT-GGACTTAGTATGATGCCATGCTGGAAGCTCCGGTCATCGCGCAGATTAGCGAAGC
6287	M_*xylA*_N fragment	pUD350	ATGACCGGAGCTTCCAGCATGGCATCATACT-AAGTCCATCGGTGAGCCTTCATCTCTCGTGCGATACCCTGCGATCTTC
6276	M_*xylA*_N fragment	pUD350	TTCTAGGCTTTGATGCAAGGTCCACATATCT-TCGTTAGGACTCAATCGTGGCTGCTGATCCGCGCAGATTAGCGAAGC
6288	N_*xylA*_O fragment	pUD350	GATCAGCAGCCACGATTGAGTCCTAAC-GAAGATATGTGGACCTTGCATCAAAGCCTAGAAGCGATACCCTGCGATCTTC
6277	N_*xylA*_O fragment	pUD350	ATACTCCCTGCACAGATGAGTCAAGCTATT-GAACACCGAGAACGCGCTGAACGATCATTCCGCGCAGATTAGCGAAGC
6289	O_*xylA*_L fragment	pUD350	GAATGATCGTTCAGCGCGTTCT-CGGTGTTCAATAGCTTGACTCATCTGTGCAGGGAGTATGCGATACCCTGCGATCTTC
6627	O_*xylA*_L fragment	pUD350	GCCGTAGCTTCCGCAAGTATGCCGTAGTTGAAG-AGCATTTGCCGTCGGTTCAGGTCATATCGCGCAGATTAGCGAAGC
7135	L_*XKS1*_fl fragment	pUD353	ATATGACCTGAACCGACGGCAAATGCTCT-TCAACTACGGCATACTTGCGGAAGCTACGGCCATAGCTTCAAAATGTTTCTACTCC
7134	L_*XKS1*_fl fragment	pUD353	TGTGGCACCGCAATCATTACTAT-GGCTAGTGCTATCATTGCTGTTTGACGCACTGATGGGGTCCAGTGCTTCCACATCAATTTG
8638	*PMR1* KO cassette	pUG-AmdSYM	CAAGACGAAGCAAGGCCAGCACAGACGTAAG-CTTAAGTGTAAGTAAAAGATAAGATAATTCAGCTGAAGCTTCGTACGC

8639	*PMR1* KO cassette	pUG-AmdSYM	ACATATGTTCCCATTAATTAGTACATT-TACCTCAATAGGGTTGGGCGTCCTCATGAAAGAGCATAGGCCACTAGTGGATCTG
8640	*PMR1* reintgration	CEN,PK113-7D	CCATGGCTACTGCTATTTCG
8641	*PMR1* reintgration	CEN,PK113-7D	AGGGCGTTGATAGGATG

Primers used for construction of plasmid containing the gRNA cutting in *GRE3*:

Primer nr.:	Purpose:	Template:	
5792	pUDE335 backbone	pMEL10	GTTTTAGAGCTAGAAATAGCAAGTTAAAATAAG
5980	pUDE335 backbone	pMEL10	CGACCGAGTTGCTCTTG
5978	pUDE335 gRNA	pMEL10	ATTTTAACTTGCTATTTCTAGCTCTAAAACT-TTATGACGTATACGTTTACGATCATTTATCTTTCACTGCGG
5979	pUDE335 gRNA	pMEL10	TATTGACGCCGGGCAAGAGC
2528	restriction analysis of gRNA	pUDE335	TCTTTCCTGCGTTATCCC
960	restriction analysis of gRNA	pUDE335	GTGGATGATGTGGTCTCTAC

Primers used for verifying integration of fragments:

Primer nr.:	Purpose:	Sequence:
6640	checking PPP integration	CTAGATGTGGTCAGCCATTC
976	checking PPP integration	CACCAGTGTCGGCAACAACG
6717	checking PPP integration	CTCATTAGAAAGAAAGCATAGCAATC
5603	checking PPP integration	CGCAAGTTTATCAATGTCGG
4656	checking PPP integration	CCTTCCCATATGATGCTAGG
7056	checking *xylA* integration	AGAGGTGGTGGTTTCGTTAC
6632	checking *xylA* integration	AGCGTCGTAGTAGTGGAAAGC
7370	checking *xylA* integration	TGCTGTAAGTCGCCTCCATC
3293	checking *xylA* integration	GAGCTGAATGTATATGCTGCGGGATC
7369	checking *xylA* integration	AGCGATCTGCGAGACCGTATAG
4692	checking *xylA* integration	AAGGGCCATGACCACCTG
5231	checking *xylA* integration	AATCACTCTCCATACAGGG
3354	checking *xylA* integration	ACGCATCTACGACTGTGGGTC
4184	checking *xylA* integration	ATGACCGGAGCTTCCAGCATG
3843	checking *xylA* integration	GATCAGCAGCCACGATTG
3837	checking *xylA* integration	GAATGATCGTTCAGCGCG
6921	checking *xylA* integration	AGAGGTGGTGGTTTCGTTAC
3286	checking *xylA* integration	GCCGTAGCTTCCGCAAGTATG
8640	checking *PMR1* KO/integration	CCATGGCTACTGCTATTTCG
8641	checking *PMR1* KO/integration	AGGGCGTTGATAGGATG
9	checking *PMR1* KO/integration	CGCACGTCAAGACTGTCAAG
10	checking *PMR1* KO/integration	TCGTATGTGAATGCTGGTCG
8792	checking *PMR1* KO/integration	GTTGGACTGTCTCTGTTAGG
8793	checking *PMR1* KO/integration	CTTCGTCCACGGATAAAG

2
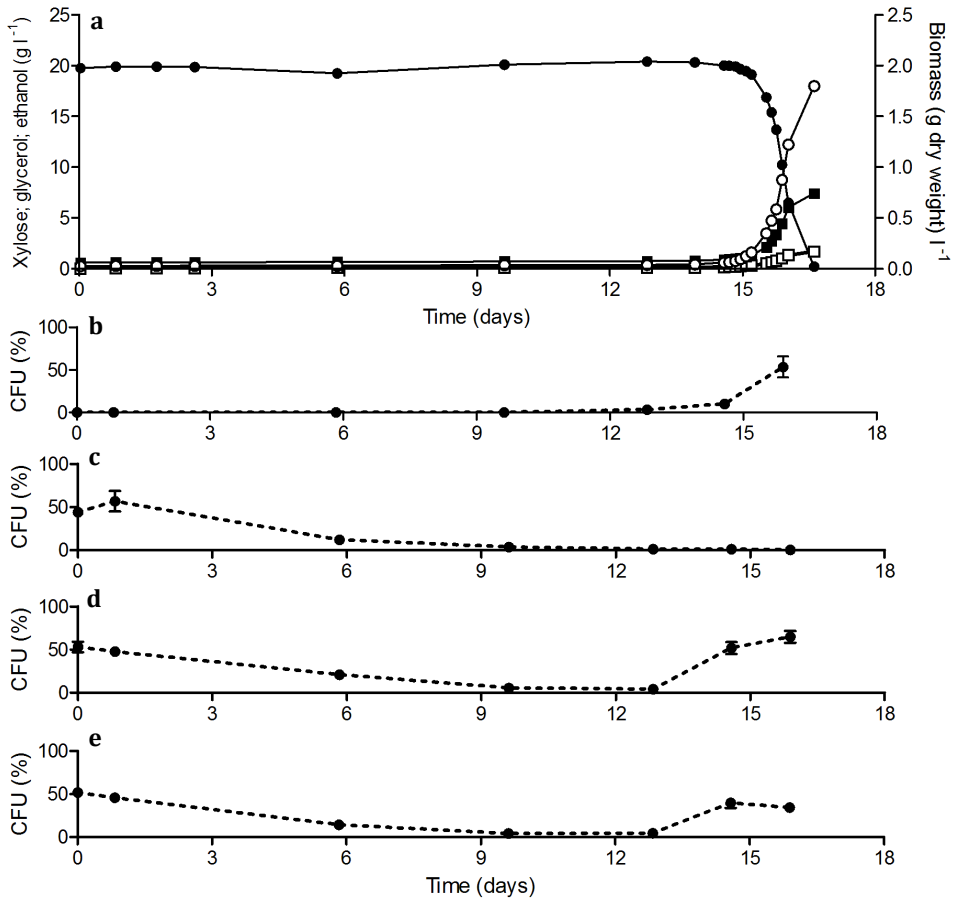
Figure S2 │ Anaerobic growth of *S. cerevisiae* IMX696 (*xylA*, PPP↑, *XKS1*↑) on xylose, independent replicate of experiment shown in Fig. 1. (**a**) Growth, xylose consumption and product formation after inoculation of aerobically pregrown cells in anaerobic bioreactors containing synthetic medium with xylose (20 g l⁻¹). Symbols: ●, xylose, ■, ethanol, ○, biomass, □, glycerol. (**b**) Colony-forming units (CFU) on anaerobically incubated xylose medium reflect adaptation to growth on xylose in the absence of oxygen. (**c**) CFU on aerobically incubated xylose medium reflect trade-off between aerobic and anaerobic growth on xylose. (**d**) and (**e**) CFU on anaerobically and aerobically incubated glucose medium, respectively, showing that oxygen sensitivity of cells adapted to anaerobic growth on xylose is not carbon-source dependent. Data shown in Figure are from one of two independent replicates.

2

Figure S3 │ **Growth of *S. cerevisiae* strains on xylose in aerobic shake-flask cultures**; (**a**) IMX696 (*xylA*, PPP↑, *XKS1*↑). (**b**) IMS0488 (isolated from culture of strain IMX696 adapted to anaerobic growth on xylose). Both strains were grown in aerobic shake flasks on synthetic medium containing 20 g l^{-1} xylose. Symbols: ●, xylose, ■, ethanol and ○, biomass. The data shown in the figure are from a single shake-flask experiment of each strain. Data from duplicate experiments with each strain differed by less than 5%.
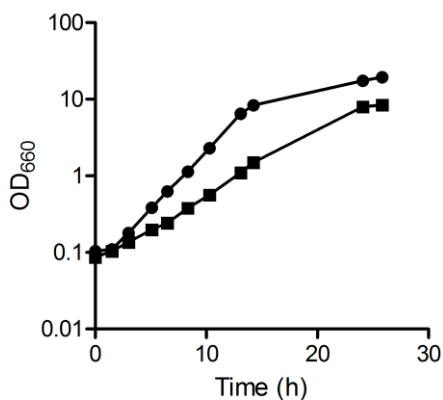
Figure S4 │ **Impact of a *PMR1* deletion on aerobic growth of *S. cerevisiae* CEN.PK113-7D on glucose.** Growth was monitored in aerobic shake-flask cultures grown on synthetic medium with 20 g l^{-1} glucose. Symbols indicate the following *S. cerevisiae* strains: ●, CEN.PK113-7D and ■, IMK692 (*pmr1Δ*). Data shown are from a single flask experiment for each strain. For both strains, data obtained from independent duplicate experiments differed by less than 5%.
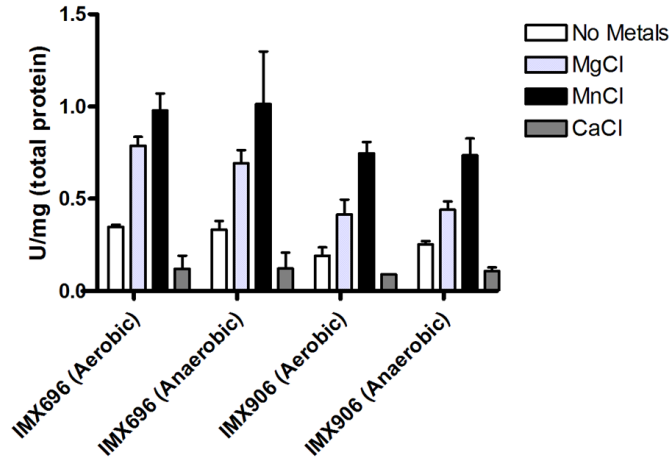
Figure S5 │ XylA activity measured in cell extracts and the effect of divalent metals. XI activity measured in cell-free extracts prepared from exponentially growing shake-flask cultures of *S. cerevisiae* strains IMX696 (*xylA*, PPP↑, *XKS1*↑) and IMX906 (*xylA*, PPP↑, *XKS1*↑, *pmr1Δ*), pre-grown under aerobic and anaerobic conditions on glucose. 25-50 μl of the extract was used in a 1 ml reaction mixture containing 20 mM MOPS buffer pH 7.0, 0.25 mM NADH, 500 mM xylose, 2U sorbitol dehydrogenase and 10mM of the divalent metal ion indicated. The activity values represent average and mean deviation of independent duplicate experiments.
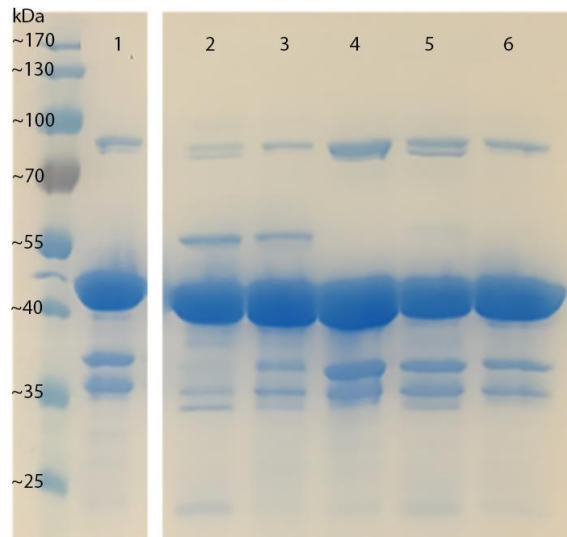
Figure S6 │ **SDS-polyacrylamide gel electrophoresis of xylose isomerases isolated from different engineered *S. cerevisiae* strains.** Lane 1: IMX906 ((*xylA*, *PPP*↑, *XKS1*↑, *pmr1Δ*) grown on glucose; Lane 2: IMX696 (*xylA*, *PPP*↑, *XKS1*↑) grown on glucose; Lane 3: IMX906 grown on xylose; Lane 4: IMX696 grown on glucose; Lane 5: IMX696 grown on glucose; Lane 6: IMX906 grown on xylose.
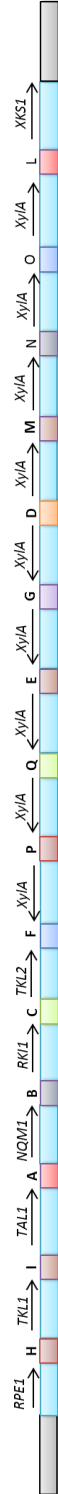
Figure S7 | Schematic overview of the integrated construct that enables xylose consumption in iMX696 (*xylA*, PPP↑, *XKS1*↑). The construct consists of 15 cassettes containing 60bp homologous sequences named A to Q. The fragments were transformed with pUD335 allowing for a Cas9-induced double-strand break in *GRE3*. Correct integration of all the fragments in *GRE3* was verified by diagnostic PCR.

Chapter 3: The *Penicillium chrysogenum* transporter *Pc*AraT enables high-affinity, glucose insensitive L-arabinose transport in *Saccharomyces cerevisiae*

Jasmine M. Bracher*, Maarten D. Verhoeven*, H. Wouter Wisselink, Barbara Crimi, Jeroen G. Nijland, Arnold J.M. Driessen, Paul Klaassen, Antonius J.A. van Maris[c], Jean-Marc G. Daran & Jack T. Pronk

*These authors contributed equally to the presented work

Abstract

Background: L-Arabinose occurs at economically relevant levels in lignocellulosic hydrolysates. Its low-affinity uptake via the *Saccharomyces cerevisiae* Gal2 galactose transporter is inhibited by D-glucose. Especially at low concentrations of L-arabinose, uptake is an important, rate-controlling step in the complete conversion of these feedstocks by engineered, pentose-metabolizing *S. cerevisiae* strains.

Results: Chemostat-based transcriptome analysis yielded 16 putative sugar transporter genes in the filamentous fungus *Penicillium chrysogenum* whose transcript levels were at least three-fold higher in L-arabinose-limited cultures than in D-glucose-limited and ethanol-limited cultures. Of five genes, that encoded putative transport proteins and showed an over 30-fold higher transcript level in L-arabinose-grown cultures compared to D-glucose-grown cultures, only one (Pc20g01790) restored growth on L-arabinose upon expression in an engineered L-arabinose-fermenting *S. cerevisiae* strain in which the endogenous L-arabinose transporter, *GAL2,* had been deleted. Sugar-transport assays indicated that this fungal transporter, designated as *Pc*AraT, is a high-affinity (K_m = 0.13 mM), high-specificity L-arabinose-proton symporter that does not transport D-xylose or D-glucose. An L-arabinose-metabolizing *S. cerevisiae* strain in which *GAL2* was replaced by *PcaraT* showed 450-fold lower residual substrate concentrations in L-arabinose-limited chemostat cultures than a congenic strain in which L-arabinose import depended on Gal2 ($4.2 \cdot 10^{-3}$ g L^{-1} and 1.8 g L^{-1}, respectively). Inhibition of L-arabinose transport by the most abundant sugars in hydrolysates, D-glucose and D-xylose, was far less pronounced than observed with Gal2. Expression of *Pc*AraT in a hexose-phosphorylation-deficient, L-arabinose-metabolizing *S. cerevisiae* strain enabled growth in media supplemented with both 20 g L^{-1} L-arabinose and 20 g L^{-1} D-glucose, which completely inhibited growth of a congenic strain in the same condition that depended on L-arabinose transport via Gal2.

Conclusion: Its high affinity and specificity for L-arabinose, combined with limited sensitivity to inhibition by D-glucose and D-xylose make *Pc*AraT a valuable transporter for application in metabolic engineering strategies aimed at engineering *S. cerevisiae* strains for efficient conversion of lignocellulosic hydrolysates.

Background

At an annual production of 100 Mton [16], bioethanol produced by the yeast *Saccharomyces cerevisiae* is by volume the largest fermentation product in industrial biotechnology. Cane sugar and corn starch, which are still the predominant feedstocks for bioethanol production, almost exclusively yield sucrose and D-glucose as fermentable sugars. Alternative lignocellulosic feedstocks, derived from agricultural residues or energy crops, contain cellulose, hemicellulose and, in some cases, pectin [28]. The pentoses D-xylose and L-arabinose typically represent 10 to 25 % and 2 to 3 %, respectively, of the monomeric sugars in lignocellulosic hydrolysates [40]. Some industrially relevant hydrolysates, however, contain higher L-arabinose concentrations. For instance, in hydrolysates of corn fibre and sugar beet pulp, L-arabinose represents 16 and 26 % of the total sugar content, respectively [42, 278].

While pentose sugars are not natural substrates of *S. cerevisiae*, their efficient conversion to ethanol and, ultimately, other bulk products, is essential to ensure economically viable processes [39]. Extensive metabolic and evolutionary engineering has been applied to enable efficient xylose fermentation, based on expression of either a heterologous xylose reductase and xylitol dehydrogenase, or a heterologous xylose isomerase (reviewed by [175] and [279]). Construction of yeast strains capable of L-arabinose fermentation involved functional expression of bacterial genes encoding L-arabinose isomerase (AraA), L-ribulokinase (AraB), and L-ribulose-5-phosphate-4-epimerase (AraD) [84-86, 154, 160]. Additional overexpression of *S. cerevisiae* genes encoding enzymes of the non-oxidative pentose-phosphate pathway (*RPE1, RKI1, TAL1,* and *TKL1*) strongly improved rates of D-xylose and L-arabinose fermentation [7, 84]. In *S. cerevisiae* strains whose metabolic pathways have been intensively optimized for pentose fermentation by metabolic and evolutionary engineering, uptake of L-arabinose and D-xylose is an important rate-controlling step [280-282].

Several *S. cerevisiae* plasma-membrane hexose-transporter proteins are able to transport D-xylose and/or L-arabinose but invariably exhibit a high K_m for these pentoses [88, 123, 161, 162, 164-167]. This low affinity causes sluggish pentose conversion ('tailing') towards the end of anaerobic batch cultures. Amongst the set of 18 *S. cerevisiae* hexose transporters (Hxt1-17 and Gal2), only the galactose transporter Gal2 and, with much lower activities, Hxt9 and Hxt10 support L-arabinose import [88, 161]. Gal2 has a high affinity for D-glucose and galactose but its affinity for L-arabinose is low (K_m= 57 – 371 mM) [88, 184]. Consequently, engineered strains in which L-arabinose transport depends on Gal2 fail to grow at low L-arabinose concentrations [88]. Moreover, even when D-glucose-induced transcriptional repression of *GAL2* [169, 170, 283] is prevented, kinetic competition prevents L-arabinose consumption by such strains in the presence of D-glucose.

So far, few heterologous L-arabinose transporters have been functionally expressed and characterized in *S. cerevisiae* [88, 184, 186]. In these previous studies, *S. cerevisiae* strains harbouring a functional L-arabinose fermentation pathway but no native

hexose transporters proved to be excellent platforms for characterization of heterologous L-arabinose transporters. In such experiments, transporters from the yeasts *Scheffersomyces stipitis* (*Ss*AraT), *Pichia guilliermondii* (*Pg*Axt1) and from the plant *Arabidopsis thaliana* (*At*Stp2) were shown to support L-arabinose transport in *S. cerevisiae*. These transporters exhibited K_m values of 0.13 – 4.5 mM but low transport capacities, while also exhibiting severe D-glucose inhibition [88, 184]. Inhibition by D-xylose was only studied for *Pg*Axt1, where it completely blocked L-arabinose uptake [184]. Conversely, L-arabinose transporters from the fungi *Neurospora crassa* (Lat-1) and *Myceliophthorum thermophilum* (*Mt*Lat-1) supported high-capacity, low-affinity (K_m = 58 and 29 mM, respectively) L-arabinose uptake and were also strongly affected by D-glucose inhibition [186]. The strong inhibition of these transporters by D-glucose and/or D-xylose precludes the simultaneous utilization of D-glucose and L-arabinose in *S. cerevisiae* strains depending on these transporters for L-arabinose uptake.

The filamentous fungus *P. chrysogenum* and its genome have been intensively studied in relation to its role in the production of β-lactam antibiotics [284, 285]. *P. chrysogenum* is able to hydrolyse arabinoxylan to L-arabinose by its Axs5 extracellular arabinofuranohydrolase, followed by uptake and metabolism of L-arabinose as a carbon and energy source [286-288]. This ability implies the presence of one or more membrane transporters capable of importing L-arabinose across the plasma membrane of this fungus.

The goal of this study was to explore the *P. chrysogenum* genome for L-arabinose transporters that can be functionally expressed in *S. cerevisiae* and support D-glucose- and D-xylose insensitive, high-affinity transport of L-arabinose. To this end, transcriptomes of L-arabinose-, ethanol- and D-glucose-limited chemostat cultures of *P. chrysogenum* were compared, and putative L-arabinose transporter genes were tested for their ability to support L-arabinose transport upon expression in an *S. cerevisiae* strain engineered for L-arabinose fermentation in which *GAL2* had been deleted. A *P. chrysogenum* transporter identified in this screen, *Pc*AraT, was subjected to more detailed analysis, including kinetic sugar-uptake studies with radiolabelled substrates, *in vivo* studies on uptake inhibition, and physiological studies with engineered *S. cerevisiae* strains in L-arabinose-limited chemostat cultures.

Materials and Methods

Microbial strains, growth media and maintenance. All *S. cerevisiae* strains constructed and used in this study (Table 1) are derived from the CEN.PK lineage [251]. Yeast strains were grown on synthetic medium (SM) [51] or on YP medium (10 g L^{-1} Bacto yeast extract, 20 g L^{-1} Bacto peptone). For shake-flask cultures on synthetic medium, ammonium sulfate was replaced with urea as nitrogen source to minimize acidification. The resulting SM-urea contained 38 mmol L^{-1} urea and 38 mmol L^{-1} K$_2$SO$_4$ instead of (NH$_4$)$_2$SO$_4$. SM and YP media were autoclaved at 121°C for 20 min, or filter sterilized using 0.2-μm bottle-top

3

filters (Thermo Scientific, Waltham MA). Subsequently, synthetic media were supplemented with 1 ml L^{-1} of a sterile-filtered vitamin solution [51]. SM, SM-urea and YP media were further supplemented with 20 g L^{-1} D-glucose or L-arabinose, by adding concentrated solutions autoclaved at 110°C for 20 min, yielding SMD or SMA, SMD-urea or SMA-urea and YPD or YPA, respectively. Yeast cultures were grown in 100 mL medium in 500-mL shake flasks at 30 °C and at 200 rpm in an Innova Incubator (New Brunswick Scientific, Edison NJ). Solid SMD, SMA, YPD and YPA contained 1.5 % Bacto agar and when indicated, 200 mg L^{-1} G418 (Invivogen, San Diego CA)*.* Solid medium with ethanol and glycerol as carbon source (YPEG, SMEG, YPEG-G418) contained 2 % ethanol and 3 % glycerol. Selection and counter selection of the *amdSYM* marker cassette were performed as described previously [270]. *Escherichia coli* strains were grown in 5 ml Lysogeny Broth (10 g L^{-1} Bacto tryptone, 5 g L^{-1} Bacto yeast extract, 5 g L^{-1} NaCl) supplemented with 100 mg L^{-1} ampicillin in 25 ml shake flasks at 37 °C and 200 rpm in an Innova 4000 shaker (New Brunswick Scientific). Before storage at -80 °C, yeast and *E. coli* cultures were mixed with glycerol (30 % v/v). *Penicillium chrysogenum* DS17690 was kindly provided by DSM Anti-infectives (Delft, The Netherlands) and grown in mineral medium (pH 5.5), containing 3.5 g $(NH_4)_2SO_4$, 0.8 g KH_2PO_4, 0.5 g $MgSO_4 \cdot 7H_2O$ and 10 ml of trace element solution (15 g L^{-1} $Na_2EDTA \cdot 2H_2O$, 0.5 g L^{-1} $Cu SO_4 \cdot 5H_2O$, 2 g L^{-1} $ZnSO_4 \cdot 7H_2O$, 2 g L^{-1} $MnSO_4 \cdot H_2O$, 4 g L^{-1} $FeSO_4 \cdot 7H_2O$, and 0.5 g L^{-1} $CaCl_2 \cdot 2H_2O$) per litre of demineralised water. The mineral medium was supplemented with 7.5 g L^{-1} D-glucose. Precultivation for chemostat cultures was carried out on mineral medium with 7.5 g L^{-1} D-glucose, 7.5 g L^{-1} L-arabinose, or 5.8 g L^{-1} ethanol as carbon source.

Molecular biology techniques. DNA fragments were amplified by PCR amplification with Phusion Hot Start II High Fidelity Polymerase (Thermo Scientific) and desalted or PAGE-purified oligonucleotide primers (Sigma-Aldrich, St. Louis, MO) performed according to the manufacturers' instructions. Diagnostic PCR reactions were run with DreamTaq polymerase (Thermo Scientific). Oligonucleotide primers used in this study are listed in Additional File 6. PCR products were separated by electrophoresis on 1 % (w/v) agarose gels (Thermo Scientific) in TAE buffer (Thermo Scientific) and, if required, purified with a Zymoclean Gel DNA Recovery kit (Zymo Research, Irvine, CA) or a GenElute PCR Clean-Up Kit (Sigma-Aldrich). Yeast or *E. coli* plasmids were isolated with a Zymoprep Yeast Plasmid Miniprep II kit (Zymo Research), or a Sigma GenElute Plasmid kit (Sigma-Aldrich), respectively. A YeaStar Genomic DNA kit (Zymo Research) or an SDS/lithium acetate protocol [289] was used to isolate yeast genomic DNA. Yeast strains were transformed using the lithium acetate/polyethylene glycol method [269]. Single-colony isolates were obtained from three consecutive re-streaks on selective solid agar plates, followed by analytical PCR analysis of the relevant genotype. *E. coli* DH5α cultures were transformed by chemical transformation [290]. After isolation, plasmids were verified by restriction analysis and analytical PCR.

Table 1 | *Saccharomyces cerevisiae* strains used in this study.

Strain	Relevant genotype	Reference
CEN.PK 113-7D	*MAT*a *URA3 HIS3 LEU2 TRP1 MAL2-8c SUC2*	[251]
CEN.PK 113-5D	*MAT*a *ura3-52 HIS3 LEU2 TRP1 MAL2-8c SUC2*	[251]
CEN.PK102-12A	*MAT*a *ura3-52 his3-D1 leu2-3,112 TRP1 MAL2-8c SUC2*	[251]
IMX080	CEN.PK102-12A *glk1::SpHis5, hxk1::KlLEU2*	[291]
IMX581	CEN.PK113-5D *can1::cas9-natNT2*	[137]
IMX486	IMX080 *gal1::cas9-AMDS*	This study
IMX604	IMX486 *ura3-52 gre3::pTDH3-RPE1, pPGK1-TKL1, pTEF1-TAL1, pPGI1-NQM1, pTPI1-RKI1, pPYK1-TKL2*	This study
IMX658	IMX604 *ura3-52 gal80::(pTPI-AraA-tCYC1c)*9, pPYK-AraB-tPGI1, pPGK-AraD-tTDH3*	This study
IMX660	IMX658 *hxk2::KlURA3*	This study
IMX728	IMX658 *hxk2::PcaraT*	This study
IMX844	IMX660 *gal2::KANMX*	This study
IMX869	IMX728 *gal2::KanMX*	This study
IMX918	IMX581 *gre3::pTDH3-RPE1, pPGK1-TKL1, pTEF1-TAL1, pPGI1-NQM1, pTPI1-RKI1, pPYK1-TKL2*	This study
IMX928	IMX918 *gal80::(pTPI-AraA-tCYC1)*9, pPYK-AraB-tPGI1, pPGK-AraD-tTDH3*	This study
IMX929	IMX918 *gal80::(pTPI-AraA-tCYC1)*9, pPYK-AraB-tPGI1, pPGK-AraD-tTDH3*, pUDE348	This study
IMX1504	IMX928, *gal2Δ*, pUDR245	This study
IMX1505	IMX928 *gal2::Pc13g04640* (from pPWT111), pUDR245	This study
IMX1506	IMX928 *gal2::Pc13g08230* (from pPWT113), pUDR245	This study
IMX1507	IMX928 *gal2::Pc16g05670* (from pPWT116), pUDR245	This study
IMX1508	IMX928 *gal2::pc20g0179 (PcaraT)* (from pPWT118), pUDR246	This study
IMX1509	IMX928 *gal2::Pc22g14520* (from pPWT123), pUDR245	This study
DS68616	*MAT*a, *ura3-52, leu2-112, gre3::loxP, loxP-pTPI-TAL1, loxP-pTPI-RKI1, loxP-pTPI-TKL1, loxP-pTPI-RPE1, leu2::pADH1-XKS1-tCYC1-LEU2, ura3::URA3-pTPI1-XylA-tCYC1*	DSM, The Netherlands
DS68625	DS68616 *his3::loxP, hxt2::loxP-kanMX-loxP, hxt367::loxP-hphMX-loxP, hxt145::loxP-natMX-loxP, gal2::loxP-zeoMX-loxP*	[112]
DS68625-*PcaraT*	DS68625, pRS313-*PcaraT*	This study
DS68625-*GAL2*	DS68625, pRS313-*GAL2*	This study
DS68625-mcs	DS68625, pRS313-mcs (empty)	This study

Table 2 | Plasmids used in this study.

Plasmid	Characteristic	Source
p414-*TEF1p-Cas9-CYC1t*	*CEN6/ARS4* ampR *pTEF1-cas9-tCYC1*	[136]
pUG-*amdSYM*	Template for *amdSYM* marker	[270]
pUG-72	Template for *KlURA3* marker	[292]
pUG6	Template for *KanMX* marker	[293]
pUDE327	2 μm, *KlURA3*, *pSNR52*-gRNA.*HXK2.Y*	[294]
pUDE335	2 μm, *KlURA3*, *pSNR52*-gRNA.*GRE3*.Y	[295]
pUDE348	2 μm, *KlURA3*, *pSNR52*-gRNA.*GAL80.Y*	This study
pUDR246	2 μm, *KlURA3*, *pSNR52*-gRNA.*GAL2.Y pSNR52*-gRNA.*GAL2.Y*	This study
pUDR245	2 μm, *KlURA3*, *pSNR52*-gRNA.*GAL2.Y pSNR52*-gRNA.*GAL2.Y*	This study
pMEL10	*pSNR52*-gRNA.*CAN1.Y-tSUP4*	[137]
pROS10	2 μm, *KlURA3*, *pSNR52*-gRNA.*CAN1.Y pSNR52*-gRNA.*ADE2.Y*	[137]
pUD344	pJET1.2Blunt TagA-*pPGI1-NQM1*-TagB	[295]
pUD345	pJET1.2Blunt TagB-*pTPI1-RKI1*-TagC	[295]
pUD346	pJET1.2Blunt TagC-*pPYK1-TKL2*-TagF	[295]
pUD347	pJET1.2BluntTagG-*pTDH3-RPE1*-TagH	[295]
pUD348	pJET1.2Blunt TagH-*pPGK1-TKL1*-TagI	[295]
pUD349	pJET1.2Blunt TagI-*pTEF1-TAL1*-TagA	[295]
pUD405	pJET1.2Blunt Gal2-flanked KanMX	This study
pPWT111	ampR KanMX, amdSYM, *pADH1*-Pc13g04640-*tPMA1*	This study
pPWT113	ampR KanMX, amdSYM, *pADH1*-Pc13g08230-*tPMA1*	This study
pPWT116	ampR KanMX, amdSYM, *pADH1*-Pc16g05670-*tPMA1*	This study
pPWT118	ampR KanMX, amdSYM, *pADH1*-Pc20g01790 *(PcaraT)-tPMA1*	This study
pPWT123	ampR KanMX, amdSYM, *pADH1*-Pc22g14520-*tPMA1*	This study
pUD354	*pMK-RQ-pTPI1-araA-tADH3*	This study
pUD355	*pMK-RQ-pPYK1-araB-tPGI1*	This study
pUD356	*pMK-RQ-pPGK1-araD-tTDH3*	This study
pRS313-mcs	*CEN6, ARSH4, HIS3-pHXT7, tHXT7*	[112]
pRS313-*PcaraT*	*CEN6, ARSH4, HIS3,* ampR, *pHXT7-PcaraT-tHXT7*	This study
pRS313-*GAL2*	*CEN6, ARSH4, HIS3,* ampR, *pHXT7-GAL2-tHXT7*	This study

Plasmid construction. Plasmids used in this study are shown in Table 2. All synthesized gene expression cassettes were constructed by GeneArt (Regensburg, Germany). Genes encoding the five putative transporters Pc13g04640 [Genbank: CAP91533.1] Pc13g08230 [Genbank: CAP91892.1], Pc16g05670 [Genbank: CAP93237.1], Pc20g01790 (*PcaraT*)[Genbank: CAP85508.1], Pc22g14520 [Genbank: CAP98740.1] were codon-pair optimized [296] for expression in *S. cerevisiae* and cloned into the plasmid pPWT007 [297] resulting in pPWT111, 113, 116, 118 and 123 respectively, harbouring each an expression cassette consisting of the *ADH1* promoter, the codon-optimized open-reading frame of a putative transporter gene, and the *PMA1* terminator. Expression cassettes for the coding regions of *L. plantarum* L-arabinose isomerase *araA* [Genbank: ODO63149.1], L-ribulose kinase *araB* [Genbank: ODO63147.1] and L-ribulose-5P epimerase *araD* [Genbank: ODO63148.1] were codon optimized according to the glycolytic codon preference in *S. cerevisiae* [86] and provided by GeneArt in pMK-RQ based cloning vectors named,

3

pUDE354, pUDE355 and pUDE356, respectively. The episomal plasmids used to express guide RNAs (gRNAs) were constructed from PCR amplified fragments that were ligated using the Gibson Assembly Cloning Kit (New England Biolabs, Ipswich, MA). gRNA plasmids pUDR246 and pUDR245 were constructed using pROS10 as a template [137], with oligonucleotide primers listed in Additional File 6. pUDE348 was derived from pMEL10 by first PCR amplifying the plasmid backbone using primers 5792-5980. The gRNA sequence was introduced in the gRNA expression cassette with primers 6631-5979 using pMEL10 [137] as a template. Subsequently, both fragments were combined using the Gibson Assembly Cloning kit. pUD405 was obtained by integration of a Gal2-flanked KanMX cassette obtained from pUG6 with primers 944 & 945 into a pJET1.2 blunt vector according to the manufacturers' instructions. Construction of the low-copy-number centromeric plasmid pRS313-mcs was described previously [112]. *GAL2* was amplified from genomic DNA of *S. cerevisiae* DS68616 [112] and *PcaraT* was amplified from plasmid pPWT118 using primers F *GAL2* Xbai & R *GAL2* Cfr9i and primers F *PcaraT* Xbai & R *PcaraT* Cfr9i, respectively and cloned into pRS313-mcs, resulting in plasmids pRS313-*PcaraT* & pRS313-*GAL2*.

Strain construction. Gene expression cassettes were PCR amplified with oligonucleotide primers shown in Supplementary Table S1 and genomic DNA of CEN.PK113-7D or plasmids described in Table 2. Gene knock-outs and construct integrations were introduced with a chimeric CRISPR/Cas9 editing system [137]. To enable CRISPR/Cas9 mediated editing in strain IMX080, the *Sp*Cas9 expression cassette was amplified from p414-*pTEF1-cas9-tCYC1* (Addgene plasmd # 43802) and integrated into the *GAL1* locus via *in-vivo* assembly, together with the *amdSYM* marker, yielding strain IMX486. For overexpression of the non-oxidative pentose-phosphate pathway (PPP), IMX486 and IMX581 were co-transformed with gRNA plasmid pUDE335 and repair fragments flanked with either 60 bp homologous to *GRE3* or with synthetic tags [298] assisting homologous recombination of the PPP expression cassettes (*gre3$_{flank}$-pTDH3-RPE1- TagH, TagH-pPGK1-TKL1-TagI, TagI-pTEF1-TAL1-TagA, TagA-pPGI1-NQM1-TagB, TagB-pTPI1-RKI1-TagC, TagC-pPYK1-TKL2-gre3$_{flank}$*). After counter selection of the *URA3*-based plasmid pUDE335, the resulting strains, IMX604 and IMX918, respectively, were co-transformed with pUDE348 and repair fragments flanked with either 60 bp homologous to *GAL80* or with synthetic tags [298] (*GAL80$_{flank}$-pTPI1-araA-TagG, TagG-pTPI1-araA-TagA, TagA- pTPI1-araA-TagB, TagB-pTPI1-araA-TagC, TagC-pTPI1-araA-TagD, TagD-pTPI1-araA-TagM, TagM-pTPI1-araA-TagN, TagN-pTPI1-araA-TagO, TagO-pTPI1-araA-TagI, TagI-pPYK1-araB-TagK, TagK-pPGK1-araD-GAL80$_{flank}$*) resulting in nine copies of *araA* and a single copy of *araB* and *araD* integrated in the *GAL80* locus. After verification of the resulting strains IMX929 and IMX658, respectively, plasmid pUDE348 was counter selected in IMX929 to yield strain IMX928. Disruption of *HXK2* in IMX658 was done by PCR-amplification and transformation of the *KlURA3*-based deletion cassette from pUG-72 [292] to obtain strain IMX660

upon transformation and plating in solid SMA. *GAL2* was disrupted in IMX660 by transformation with a KanMX cassette amplified from pUD405 with primers 944 & 945 flanked with 60 bp homologous to *GAL2*. Transformants were incubated for 2 h in YPE before plating on YPEG-G418, yielding strain IMX844. Expression of *PcaraT* in IMX658 was achieved by transforming IMX658 with the gRNA plasmid pUDE327 together with an expression cassette of *PcaraT* (pADH1-*PcaraT*-tPMA1) with flanking regions homologous to the *HXK2* locus amplified with the primer pair 7660 & 7676. Counter selection of the pUDE327 and subsequent transformation of a DNA fragment derived from CEN.PK113-7D using primers 2641-1522 repaired uracil auxotrophy and resulted in strain IMX728. *GAL2* was disrupted in IMX728 by transformation with a KanMX cassette amplified from pUD405 with primers 944 & 945 flanked with 60 bp homologous to *GAL2*. Transformants were incubated for 2 h in YPE before plating on YPEG-G418, yielding strain IMX869. Strains IMX1505-1509 were constructed by co-transforming pUDR245 or pUDR246 and a *GAL2*-flanked expression cassette (pADH1-ORF-tPMA1) amplified from pPWT111, 113, 116, 118 or 123, respectively, amplified with the primer pair 10585 & 10584. IMX1504, harbouring a knockout of *GAL2,* was constructed by co-transforming pUDR245 and a repair fragment based on the annealed primers 9563 and 9564. Transformation of *GAL2* and *PcaraT* plasmids, and the pRS313-mcs plasmid (as an empty plasmid/control) into the hexose transporter deletion strain DS68625 yielded strains DS68625-*GAL2*, DS68625-*PcaraT*, and DS68625-mcs.

Growth experiments in shake flasks. Thawed 1 ml aliquots from frozen stock cultures were used to inoculate shake-flask precultures on SM-urea supplemented with either D-glucose (20 g L^{-1}), L-arabinose (20 g L^{-1}), or both sugars (both 20 g L^{-1}). These precultures were used to inoculate a second culture, which was subsequently used to inoculate a third culture, which was inoculated at an initial OD$_{660}$ of 0.1 and used to monitor growth. Optical densities at 660 nm were measured with a Libra S11 spectrophotometer (Biochrom, Cambridge, United Kingdom). Maximum specific growth rates (μ_{max}) were derived from at least four consecutive data points derived from samples taken during the exponential growth phase of each culture.

Spot plates. L-arabinose metabolising *S. cerevisiae* strains expressing putative *P. chrysogenum* L-arabinose transporter genes (IMX1504-1509) were grown on SMD medium and a total number of approximately 10^4, 10^3, 10^2, and 10^1 cells were spotted on duplicate agar plates as described previously [141, 299] containing either 20 g L^{-1} L-arabinose or D-glucose as carbon source (pH 6). Cell numbers were estimated from calibration curves of OD$_{660}$ versus cell counts determined with an Accuri flow cytometer (Becton Dickinson B.V., Breda, The Netherlands), derived from exponentially growing shake-flask cultures of *S. cerevisiae* CEN.PK113-7D on SMD medium. SMA and SMD plates were incubated at 30 °C for 97 and 41 h, respectively.

Chemostat cultivation. Aerobic carbon-limited chemostat cultures of *P. chrysogenum* were grown at 25 °C in 3-L turbine-stirred bioreactors (Applikon, Schiedam, The Netherlands) with a working volume of 1.8 L and a dilution rate of 0.03 h^{-1} as described previously [300], with the exception that, in addition to cultures grown on 7.5 g L^{-1} D-glucose, chemostat cultures were also grown on either 7.5 g L^{-1} L-arabinose or 5.8 g L^{-1} ethanol. Aerobic, L-arabinose-limited chemostat cultures of *S. cerevisiae* were grown at 30 °C in 2-L Applikon bioreactors with a working volume of 1 L and at a dilution rate of 0.05 h^{-1}. SMA (7.5 g L^{-1} L-arabinose) supplemented with 0.15 g L^{-1} antifoam Pluronic PE 6100 was used as culture medium for the initial batch phase and for chemostat cultivation, with the exception of the initial batch phase of strain IMX929 which was grown on 20 g L^{-1} L-arabinose. Cultures were stirred at 800 rpm, kept at pH 5.0 by automatic addition of 2 M KOH, and sparged with 0.5 L min^{-1} air. Upon completion of the batch phase, chemostat cultivation was initiated, ensuring a constant culture volume with an electric level sensor. When after at least five volume changes, biomass dry weight and CO_2 production varied by less than 2 % over two consecutive volume changes, the culture was considered to be in steady state.

Analytical methods. *P. chrysogenum* biomass dry weight was determined in duplicate by filtration of 10 mL culture sample over pre-weighed glass fibre filters (Type A/E, Pall Life Sciences, Hoegaarden, Belgium). After filtration, filters were washed with demineralised water and dried for 10 min at 600 W in a microwave oven (Bosch, Stuttgart, Germany) prior to reweighing. Biomass dry weight in *S. cerevisiae* culture samples was determined with a similar procedure using nitrocellulose filters (0.45 μm pore size; Gelman Laboratory, Ann Arbor, MI) and drying for 20 min in a microwave oven at 360 W output. Optical density (OD) of the cultures was determined at 660 nm with a Libra S11 spectrophotometer (Biochrom, Cambridge, United Kingdom). Determination of CO_2 and O_2 concentrations in the bioreactor exhaust gas and HPLC analysis of metabolite concentrations in culture supernatant samples were performed as described previously [295].

Sampling, RNA extraction, microarrays analysis, and data analysis. Samples (60 mL) from *P. chrysogenum* chemostat cultures were rapidly filtered over a glass fibre filter (Type A/E, Pall Life Sciences) and further processed for total RNA extraction by phenol-chloroform extraction [300]. The cRNA sample preparation (cDNA synthesis, purification, *in vitro* transcription, labelling, purification, fragmentation and biotinylation) was performed according to Affymetrix recommendations [284]. Eventually cRNA samples were hybridized onto custom-made *P. chrysogenum* GeneChip microarrays (array code DSM_PENa520255F). Data Acquisition, hybridization, quantification of processed array images, and data filtering were performed using the Affymetrix GeneChip Operating Software (GCOS version 1.2). Global array normalization was performed by scaling the global fluorescence intensity of each microarray to 100. The scaling factors of the individual arrays were highly similar and ranged from 0.21 to 0.35. Subsequently, significant variations

3

in expression were statistically estimated by comparing replicate array experiments using the Significance Analysis of Microarray software (SAM version 2.0) [301] with the multiclass setting. A false discovery rate of 1 % was applied to minimize the chance of false positive hits. Genes with an over 3-fold higher transcript level in arabinose-grown cultures than in D-glucose-grown cultures and a less than 3-fold difference in ethanol- and D-glucose-grown cultures were deemed to show arabinose-specific expression. Transcriptome data of strain DS17690 grown on D-glucose, ethanol or arabinose are accessible at NCBI Genome Omnibus database   [https://www.ncbi.nlm.nih.gov/geo/] under accession number GSE12632, GSE24212, and GSE10449, respectively [300].

Analysis of sugar uptake kinetics. Uptake experiments with [^{14}C] L-arabinose, [^{14}C] D-xylose, or [^{14}C] D-glucose, labelled at the first carbon atom (50-60 mCi/mmol) (ARC St. Louis, MO), were performed with *S. cerevisiae* hexose transporter deletion strains (DS68625) harbouring a low copy plasmid with constitutively expressed *PcaraT* (pRS313-*PcaraT*) or *GAL2* (pRS313-*GAL2*). The experimental workflow was carried out as described previously [112] with [^{14}C] L-arabinose concentrations of 0.5 to 2000 mmol L^{-1}, [^{14}C] D-xylose concentrations of 0.5 to 500 mM, or [^{14}C] D-glucose concentrations of 0.1 to 500 mmol L^{-1}. Transport competition experiments were carried out in the presence of 50 mmol L^{-1} [^{14}C] L-arabinose and 0 to 500 mmol L^{-1} D-glucose or D-xylose, and at [^{14}C] L-arabinose concentration of 2 mmol L^{-1} together with increasing D-glucose and xylose concentrations of 0 to 20 mM. Maximum biomass-specific transport rates ('V$_{max}$') calculated from transport assays were expressed as nmol sugar transported per mg biomass dry weight per minute [nmol (mg biomass)$^{-1}$ min^{-1}]. As this V$_{max}$ is influenced by the expression level of the relevant transporter, it is not solely dependent on intrinsic transporter kinetics. The impact of proton-gradient uncoupling on transport activity was determined in 200 µl synthetic medium at a [^{14}C]-L-arabinose concentration of 2 mmol L^{-1}, by comparing transport rates upon addition of either 10 µmol L^{-1} CCCP (0.5 µl of a stock solution dissolved in 100 % DMSO), 0.5 µL DMSO (control), or 0.5 µL water.

Phylogenetic methods. Protein sequences used for generation of a phylogenetic tree were derived from NCBI (https://www.ncbi.nlm.nih.gov/) and the *Saccharomyces* Genome Database (https://www.yeastgenome.org/). Mafft was used to generate a CLUSTAL format alignment of all sequences, using the L-INS-i method default settings (https://mafft.cbrc.jp/alignment/server/) [302, 303]. Alignments were further processed using neighbour-joing and a 500-times bootstrap. The resulting Newick tree file was visualized and midpoint rooted in iTOL (https://itol.embl.de/) [304]. Gene accession numbers were: *ScGAL2*: P13181, *PcaraT*: CAP85508, *SsaraT*: XP_001382755, *Atstp2*: OAP13698, *Kmaxt1*: GZ791039, *Pgaxt1*: GZ791040, *Amlat1*: AY923868, *Amlat2*: AY923869, *Nclat-1*: EAA30346, *Mtlat-1*: XP_003663698.

3

Results

Chemostat-based transcriptome analysis of *Penicillium chrysogenum* for identification of possible L-arabinose transporter genes. Filamentous fungi exhibit a much broader range of carbon source utilization than *S. cerevisiae* and, similar to many other ascomycetous fungi, *P. chrysogenum* can grow on L-arabinose as sole carbon source [286, 305]. To identify candidate structural genes for L-arabinose transporters in *P. chrysogenum*, carbon-limited chemostat cultures of strain DS17690 were grown at a dilution rate of 0.03 h⁻¹ on different carbon sources. To discriminate between alleviation of carbon repression and L-arabinose induction, duplicate D-glucose-, L-arabinose-, and ethanol-limited chemostat cultures were performed. RNA was extracted from steady-state cultures and gene expression levels were obtained using Affymetrix DNA-arrays [300]. A total of 540 genes were differentially expressed over the three conditions. Of these differentially expressed genes, 137 exhibited an over 3-fold higher transcript level in L-arabinose-limited cultures than in D-glucose-limited cultures, as well as a less than three-fold difference in transcript level between ethanol- and D-glucose-limited cultures. Genes whose transcript levels in L-arabinose- and ethanol-limited cultures were both at least 2-fold higher than in D-glucose-grown cultures were not considered for further analysis as their regulation could have reflected unspecific D-glucose (de)repression. An annotation screen indicated that 16 of the identified 'arabinose-induced' genes encoded putative transporters, whose transcript levels were 3.4 to 52-fold higher in the L-arabinose-limited cultures than in the D-glucose-limited cultures (Table 3). Five of these genes, whose transcript levels were at least 30-fold higher in L-arabinose-limited cultures than in D-glucose-limited cultures, shared similarity with the *S. cerevisiae* maltose transporter Mal31, the *Neurospora crassa* D-glucose transporter Rco-3, the *Kluyveromyces lactis* high-affinity D-glucose transporter Hgt1 and the *S. cerevisiae* allantoate transporter Dal5. These five transporter genes (Pc13g08230, Pc16g05670, Pc20g01790, Pc22g14520, and Pc13g04640, respectively) were selected for further functional analysis.

***Pc*AraT: A *P. chrysogenum* L-arabinose transporter that can be functionally expressed in *S. cerevisiae*.** *S. cerevisiae* strains in which *HXT* transporter genes have been deleted and which express heterologous pathways for pentose metabolism have proven to be powerful platforms for screening and characterization of heterologous pentose transporter genes [88, 184, 306]. To enable screening for *P. chrysogenum* L-arabinose transporters, *S. cerevisiae* strains were first engineered for L-arabinose consumption.

Table 3 | Putative transporter genes that showed higher relative transcript levels in aerobic, L-arabinose-limited chemostat cultures of *Penicillium chrysogenum* than in corresponding D-glucose- and ethanol-limited cultures. *P. chrysogenum* DS1769 was grown in L-arabinose-, D-glucose-, or ethanol-limited chemostat cultures (dilution rate = 0.03 h⁻¹, pH 6.5, T = 25 °C). Genes indicated in bold were selected for further analysis based on a ≥ 30-fold higher transcript level in L-arabinose-limited cultures than in D-glucose-limited cultures. Data represent average ± mean deviation of globally scaled (target 100) Affymetrix microarrays for independent duplicate chemostat cultures.

Gene	Strong similarity to	Relative transcript levels under different nutrient limitations			Ethanol versus glucose (ratio)	L-Arabinose versus glucose (ratio)
		Glucose	L-Arabinose	Ethanol		
Pc13g08230	*S. cerevisiae* maltose transport protein Mal31	13 ± 1	664 ± 3	17 ± 1	1.4	53
Pc16g05670	*Neurospora crassa* glucose transporter rco-3	63 ± 28	3176 ± 40	69 ± 1	1.1	51
Pc20g01790 (*PcaraT*)	*Kluyveromyces lactis* high-affinity glucose transporter HGT1	32 ± 6	1415 ± 42	46 ± 3	1.4	44
Pc22g14520	*S. cerevisiae* allantoate permease Dal5	19 ± 2	770 ± 104	28 ± 1	1.5	41
Pc13g04640	*K. lactis* high-affinity glucose transporter HGT1	29 ± 5	971 ± 32	53 ± 7	1.8	34
Pc21g10190	*K. lactis* high-affinity glucose transporter HGT1	12 ± 1	167 ± 26	12 ± 1	1.0	14
Pc12g00190	*Candida albicans* ABC transporter CDR4	13 ± 2	164 ± 24	29 ± 2	2.2	12
Pc14g01680	*Escherichia coli* L-fucose permease fucP	106 ± 14	1269 ± 172	68 ± 1	0.64	12.0
Pc21g12210	*Aspergillus nidulans* quinate transport protein qutD	12 ± 0	118 ± 1	12 ± 1	1	9.8
Pc06g01480	*S. cerevisiae* maltose transport protein Mal31	459 ± 85	3551 ± 102	226 ± 3	0.5	7.7
Pc13g10030	*S. cerevisiae* high-affinity nicotinic acid permease Tna1	125 ± 25	827 ± 33	216 ± 3	1.7	6.6
Pc21g09830	*K. lactis* high-affinity glucose transporter HGT1	185 ± 9	842 ± 1	126 ± 3	0.68	4.6
Pc16g02680	*S. cerevisiae* allantoate permease Dal5	80 ± 29	360 ± 14	113 ± 6	1.4	4.5
Pc12g05440	*S. cerevisiae* maltose transport protein Mal31	596 ± 201	2633 ± 64	104 ± 8	0.17	4.4
Pc13g15590	*S. cerevisiae* glucose permease Rgt2	12 ± 1	48.0 ± 1.0	12 ± 1	1	4.0
Pc13g06440	*S. cerevisiae* high-affinity nicotinic acid permease Tna1	66 ± 23	225 ± 11	48 ± 5	0.73	3.4

3

Using CRISPR/Cas9-mediated *in-vivo* assembly [137], the overexpression cassettes for all structural genes involved in the non-oxidative pentose-phosphate pathway (*TAL1, NQM1, TKL1, TKL2, RKI1, RPE1*) were stably integrated into the *GRE3* locus, thereby inactivating synthesis of the Gre3 aldose reductase. Subsequently, nine copies of an expression cassette for overexpression of codon-optimized *Lactobacillus plantarum* L-arabinose isomerase AraA and single copies of *L. plantarum* AraB (L-ribulokinase) and AraD (L-ribulose-5-phosphate-4-epimerase) expression cassettes were integrated into the *GAL80* locus, using a strain-construction strategy previously described for expression of a D-xylose pathway into *S. cerevisiae* [295]. This integration inactivated *GAL80* and thereby alleviated transcriptional repression by D-glucose of *GAL2*, which encodes the major L-arabinose transporter in *S. cerevisiae* [307, 308]. The resulting strain IMX929 was able to grow in liquid media supplemented with L-arabinose as sole carbon source and was used as a platform strain to test if any of the five selected putative *P. chrysogenum* transporter genes, placed under the control of the constitutive ADH1 promoter, could support L-arabinose transport in *S. cerevisiae*. To this end, single copies of codon-optimized expression cassettes were integrated into the *GAL2* locus of the L-arabinose metabolizing *S. cerevisiae* strain IMX928, a uracil auxotrophic daughter strain of IMX929, thereby inactivating the *GAL2* gene. Consistent with previous studies [88, 184], inactivation of *GAL2* in strain IMX928 yielded a strain (IMX1504) that was unable to grow on SMA plates (Fig. 1). All five strains in which *GAL2* had been replaced by putative *P. chrysogenum* transporter genes (IMX1505-1509) showed vigorous growth on SMD plates. However, only strain IMX1508, which expressed the *P. chrysogenum* gene Pc20g01790, showed growth on L-arabinose (Fig. 1). Based on this observation, Pc20g01790 was designated *PcaraT* (*P. chrysogenum* Arabinose Transporter). A Blast-p search revealed strong homology of Pc20g01790 with the *K. lactis* gene *HGT1*, which encodes a high-affinity D-glucose and galactose transporter [309, 310].

PcaraT encodes a high-affinity, high-specificity L-arabinose transporter. Sugar transport kinetics of *Pc*AraT were analysed using ^{14}C-labelled L-arabinose, D-xylose and D-glucose. To dissect transporter kinetics of *Pc*AraT and Gal2, their structural genes were separately expressed in *S. cerevisiae* DS68625 [112]. Each gene was introduced on a centromeric plasmid and expressed from the *HXT7* promoter. In strain DS68625, the major hexose transporter genes (*HXT1-7* and *GAL2*) are deleted, while its inability to metabolize L-arabinose enables the specific analysis of sugar uptake rather than the combination of radioactive sugar uptake and metabolism. The negative control strain DS68625-mcs (DS68625 transformed with the 'empty' centromeric plasmid pRS313-mcs) did not show significant [14C] L-arabinose uptake, while expression of either Gal2 or *Pc*AraT (strains DS68625-*GAL2* and DS68625-*PcaraT*, respectively) restored L-arabinose transport (Table 4). In kinetic analyses, the K_m of *Pc*AraT for L-arabinose (0.13 mmol L^{-1}), was found to be three orders of magnitude lower than that of Gal2 (335 mmol L^{-1}), while its transport capacity (V_{max}) was 14-fold lower than that of Gal2 (5.3 and 75 nmol (mg biomass)$^{-1}$ min^{-1},

respectively) (Table 4). *Pc*AraT was found to be highly L-arabinose specific, as its expression in strain DS68625 did not support transport of either [^{14}C] D-glucose or [^{14}C] D-xylose. Consistent with earlier reports [88, 184], expression of Gal2 in strain DS68625 enabled transport of D-glucose (K_m = 1.9 mmol L^{-1}, V_{max} = 26 nmol (mg biomass)$^{-1}$ min^{-1}, while Gal2 has previously been shown to enable low-affinity D-xylose transport (K_m = 226 mmol L^{-1}; [123]).
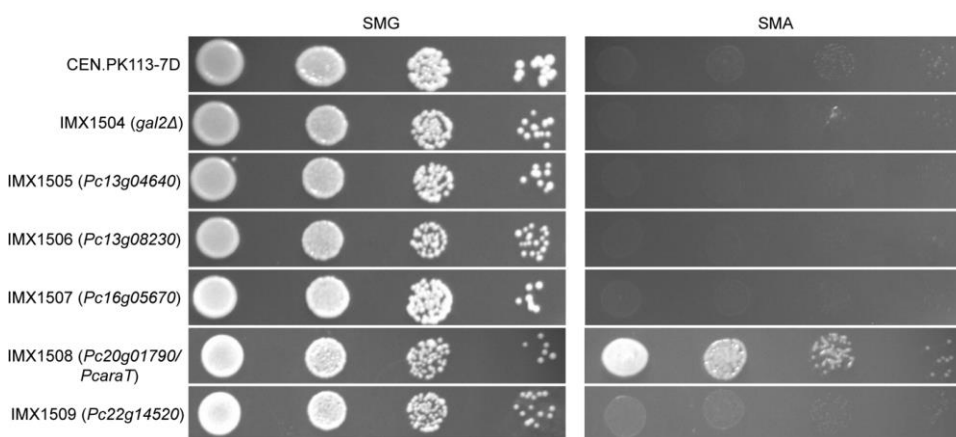
Fig. 1 | Impact of the expression of putative *P. chrysogenum* sugar transporter genes in an L-arabinose metabolizing *S. cerevisiae* strain in which *GAL2* was deleted. Strains were pregrown on liquid SMD and spotted on plates containing 20 g L^{-1} D-glucose (SMD, left) or L-arabinose (SMA, right) as carbon source. Codes on left hand side indicate *S. cerevisiae* strain names and, in brackets, the systematic name of the corresponding over-expressed *P. chrysogenum* gene. CEN.PK113-7D is a control strain that was not engineered for L-arabinose metabolism. SMD and SMA plates were incubated at 30 °C for 47 and 91 h, respectively. The experiment was performed in duplicate, data shown are from a single representative experiment.

The impact of the presence of D-glucose and D-xylose on L-arabinose transport by Gal2 and *Pc*AraT was investigated in transport assays with 50 mmol L^{-1} [^{14}C] L-arabinose and increasing concentrations of non-radioactive D-glucose or D-xylose. In these assays, both transporters exhibited a reduced L-arabinose transport capacity in the presence of D-glucose or D-xylose (Table 4, Additional File 4). At a concentration of 100 mmol L^{-1} (i.e., twice the concentration of L-arabinose), D-xylose and D-glucose inhibited L-arabinose uptake rate via Gal2 by 29 and 85 %, respectively. In contrast, L-arabinose transport via *Pc*AraT was less impaired at this concentration of D-xylose and, especially, D-glucose (22 and 63 % inhibition, respectively). To study the transport mechanism of *Pc*AraT, the impact of the protonophore uncoupler CCCP on transport kinetics was tested. Transport of L-arabinose via Gal2, which mediates facilitated diffusion of sugars [311], was not affected by CCCP, while this uncoupler completely abolished transport via *Pc*AraT. These results indicate that *Pc*AraT mediates proton-coupled import of L-arabinose.

Table 4 | Kinetic data for the *S. cerevisiae* transporter Gal2 and *P. chrysogenum* *Pc*AraT derived from uptake studies with ¹⁴C-labelled L-arabinose, D-glucose, and D-xylose. Sugar transport kinetics were measured by uptake of ¹⁴C-radiolabelled sugars by *S. cerevisiae* DS68625, an engineered strain lacking the Hxt1-7 and Gal2 transporters, expressing either *GAL2* or *PcaraT*. Transport inhibition was determined at 50 mmol L⁻¹ [¹⁴C] L-arabinose and 100 mmol L⁻¹ of either D-glucose or D-xylose and expressed relative to the transport rate observed in the absence of D-xylose or D-glucose. Values are represented as average ± mean deviation of duplicate experiments. Graphs used to calculate kinetic parameters are shown in Additional files 1-4. ARA = L-arabinose; GLC = D-glucose; XYL = D-xylose.

	Gal2	*Pc*AraT
$K_{m, ARA}$ [mmol L⁻¹]	335 ± 21	0.13 ± 0.03
$V_{max, ARA}$ [nmol (mg biomass)⁻¹ min⁻¹]	75 ± 5.2	5.3 ± 0.2
$K_{m, GLC}$ [mmol L⁻¹]	1.9	-
$V_{max, GLC}$ [nmol (mg biomass)⁻¹ min⁻¹]	26	-
L-arabinose transport inhibition by glucose	85 %	63 %
$K_{m, XYL}$ [mmol L⁻¹]	226 [20]	-
$V_{max, XYL}$ [nmol (mg biomass)⁻¹ min⁻¹]‡	91 [20]	-
L-arabinose transport inhibition by D-xylose	29 %	22 %

-, no transport

Functional expression of *PcaraT* in an L-arabinose-fermenting *S. cerevisiae* strain enables L-arabinose consumption in the presence of D-glucose. The ability to transport L-arabinose in the presence of D-glucose is a highly relevant characteristic in the construction of platform *S. cerevisiae* strains for conversion of lignocellulosic hydrolysates [279]. To investigate whether expression of *PcaraT* can confer this ability, a set of three strains was constructed that (i) could not metabolize D-glucose due to the deletion of *HXK1, HXK2, GLK1* and *GAL1* [20, 62] (ii) (over)expressed non-oxidative PPP enzymes and the *L. plantarum* AraA, AraB and AraD genes to enable L-arabinose metabolism, and (iii) had different genotypes with respect to L-arabinose transport (*GAL2, PcaraT/gal2Δ* and *gal2Δ* in strains IMX660, IMX869 and IMX844, respectively). Since these 'arabinose specialist strains' cannot grow on D-glucose, the impact of the presence of D-glucose on L-arabinose metabolism can be directly measured via its effect on growth. As anticipated, strain IMX844 (*gal2Δ*) was unable to grow on synthetic medium supplemented with either 20 g·L⁻¹ L-arabinose or a mix of 20 g·L⁻¹ of each, L-arabinose and D-glucose. In contrast, the L-arabinose specialist strains IMX660 (*GAL2*) and IMX869 (*PcaraT/gal2Δ*) grew on synthetic medium with L-arabinose as the sole carbon source at specific growth rates of 0.240 ± 0.001 h⁻¹ and 0.099 ± 0.001 h⁻¹, respectively (Fig. 2A). However, when 20 g L⁻¹ D-glucose was added to the L-arabinose medium, strain IMX660 (*GAL2*) did not show growth during a 120 h batch cultivation experiment (Fig. 2B), while strain IMX869 (*PcaraT/gal2Δ*) grew at 60 % of the specific growth rate observed in the absence of D-glucose (μ = 0.057 ± 0.003 h⁻¹ versus 0.099 ± 0.001 h⁻¹, Fig. 2B). This result indicated that

expression of *Pc*AraT in strain IMX869 enabled uptake of ʟ-arabinose in the presence of ᴅ-glucose.
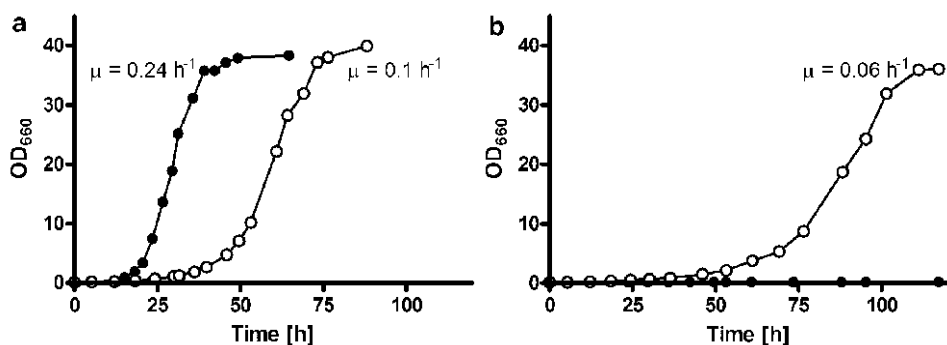
Fig. 2 | Growth curves of *S. cerevisiae* ʟ-arabinose specialist strains, engineered for ʟ-arabinose consumption and disabled for ᴅ-glucose consumption by deletion of the hexose kinase genes *HXK1*, *HXK2*, *GLK1* and *GAL1,* and expressing either *GAL2* (IMX660, filled circles) or the *P. chrysogenum* transporter *Pc*AraT (IMX869, open circles) as the sole ʟ-arabinose transporter. To assess the ability of Gal2 and *Pc*AraT to support import of ʟ-arabinose by growing cultures in absence **(a)** and presence **(b)** of ᴅ-glucose, specific growth rates were estimated from shake-flask cultures on synthetic media supplied with 20 gL^{-1} ʟ-arabinose **(b)** and on synthetic media supplied with ʟ-arabinose and ᴅ-glucose (20 g L^{-1} each, **(b)**)

Low residual substrate concentrations in chemostat cultures confirm high-affinity ʟ-arabinose transport kinetics of *Pc*AraT. To further evaluate the *in vivo* impact of ʟ-arabinose transport via *Pc*AraT, biomass-specific ʟ-arabinose consumption rates and residual substrate concentrations were analysed in ʟ-arabinose-limited, aerobic chemostat cultures, grown at a dilution rate of 0.05 h^{-1}. Under these conditions, the ʟ-arabinose-metabolizing strain IMX1508 (*PcaraT/gal2Δ*) exhibited a residual ʟ-arabinose concentration of only $4.2 \cdot 10^{-3}$ g L^{-1}, compared to 1.8 g L^{-1} in cultures of strain IMX929 (*GAL2*) (Table 5). In these growth experiments, different promoters were used for expression of *PcaraT* and *GAL2* (pADH1 and derepressed pGAL2, respectively). However, while this may moderately affect expression levels of the two transporters, this cannot explain the over 1000-fold difference in residual ʟ-arabinose concentration. This difference was entirely consistent with the conclusion from the kinetic analyses of [14]C-ʟ-arabinose uptake, in which both transporter genes were expressed from the same promoter (pHXT7) and which also indicated that *PcaraT* encodes an ʟ-arabinose transporter with a much higher affinity for ʟ-arabinose than Gal2. In shake-flask batch cultures grown on an initial ʟ-arabinose concentration of 7.5 g L^{-1}, these strains exhibited initial specific growth rates of 0.085 h^{-1} and 0.13 h^{-1}, respectively. Based on this observation and on the high K$_m$ of Gal2 for ʟ-arabinose [88, 162], this study), the *in vivo* activity of *Pc*AraT can be expected to exceed that of Gal2 when ʟ-arabinose concentrations are below ca. 4 g L^{-1}.

In duplicate steady-state chemostat cultures, the biomass-specific ʟ-arabinose consumption rate of strain IMX1508 (*PcaraT*) was approximately 14 % higher than the

one of strain IMX929 (*GAL2*; 0.8 ± 0.1 and 0.7 ± 0.1 mmol g^{-1} h^{-1}), reflecting the slightly lower biomass yield of the former strain. This difference in biomass yield is close to the difference of 8.1 % that, based on published estimates of the P/O ratio and proton stoichiometry of the plasma-membrane ATPase in aerobic *S. cerevisiae* cultures (both close to 1.0, [271, 312]), would be expected if L-arabinose uptake via *Pc*AraT occurred via symport with a single proton.

Table 5 | Physiological data derived from steady-state chemostat cultures of engineered, L-arabinose-metabolizing *S. cerevisiae* strains. Strains expressing either *GAL2* (IMX929) or *PcaraT* (IMX1508) as sole functional L-arabinose transporter were grown in aerobic, L-arabinose-limited chemostat cultures (7.5 g L^{-1} L-arabinose, dilution rate = 0.05 h^{-1}, pH 5, T = 30 °C). Data are derived from independent triplicate experiments and presented as average ± mean deviation.

	IMX929 (*GAL2*)	IMX1508 (*PcaraT*)
Residual L-arabinose [g L^{-1}]	1.77 ± 0.19	0.004 ± 0.002
$Y_{X/S}$ [g biomass (g L-arabinose)$^{-1}$]	0.48 ± 0.06	0.40 ± 0.01
$q_{\text{L-arabinose}}$ [mmol g^{-1} h^{-1}]	0.70 ± 0.10	0.80 ± 0.08

Discussion

Chemostat-based transcriptome analysis of *Penicillium chrysogenum* proved to be an efficient method to identify candidate genes for L-arabinose transporters in this fungus. In comparison with similar studies in batch cultures, use of chemostat cultures offered several advantages. First, chemostat cultivation at a fixed dilution rate eliminated the impact of specific growth rate on transcriptional regulation [313]. Furthermore, use of L-arabinose-limited chemostat cultures of *P. chrysogenum*, in which residual concentrations of this pentose were very low, enabled a focus on the identification of high-affinity transporters. Finally, the use of both D-glucose- and ethanol-limited cultures as references helped to eliminate transcriptional responses of *P. chrysogenum* that were specific to either of these two carbon sources, e.g. as a result of CreA-mediated D-glucose repression of relevant transporter genes [314, 315]. Although this study was focused on L-arabinose transport, the *P. chrysogenum* transcriptome dataset from D-glucose, ethanol and arabinose grown cultures generated in this study (available via GEO, [https://www.ncbi.nlm.nih.gov/geo/] under accession numbers GSE12632, GSE24212, and GSE104491, respectively) may contribute to studies on other aspects on metabolism and metabolic regulation in this industrially relevant fungus.

Of five putative transporter genes that showed an over 30-fold higher transcript level in L-arabinose-limited chemostat cultures of *P. chrysogenum* than in D-glucose-limited cultures, only *PcaraT* was shown to encode an L-arabinose transporter that is functional in *S. cerevisiae*. While the low K_m of this transporter observed upon its expression in *S. cerevisiae* is consistent with its upregulation in L-arabinose-limited cultures of *P. chrysogenum*, this observation does not necessarily imply that *Pc*AraT is the only or even

the most important L-arabinose transporter active in these cultures. Problems in protein folding, plasma-membrane (mis)targeting, post-translational modification and/or protein turnover [164, 316] may have affected expression of the other candidate genes. Indeed, in screening of cDNA libraries encoding putative heterologous transporters, typically only few of the candidate genes are found to enable transport of the substrate upon expression in *S. cerevisiae* [181, 317].

Several studies have used *gal2Δ* strains of *S. cerevisiae* to analyse transport kinetics of heterologous L-arabinose transporters (Table 6, Fig. 3). Two studies that estimated K_m and V_{max} of Gal2 upon its reintroduction in such a strain found different results (Table 6)[88, 184]. At L-arabinose concentrations of about 10 mmol L^{-1} these studies reported Gal2-mediated transport rates of 0.3 and 8.9 nmol (mg biomass)$^{-1}$ min^{-1} respectively, as compared to a value of 2.5 nmol (mg biomass)$^{-1}$ min^{-1} observed in the present study. One of the previous studies [184] used a strain that also expressed a functional bacterial L-arabinose pathway, thereby raising the possibility that apparent uptake rates were enhanced by subsequent metabolism of L-arabinose. Moreover, in different studies, *GAL2* was expressed from different promoters (*pTDH3, pADH1, and pHXT7*) and either high-copy number (2µ) [88, 184] or low-copy number centromeric (this study) expression plasmids. D-Glucose transport kinetics via Gal2 determined in this study (K_m = 1.9 mmol L^{-1}, V_{max} = 26 nmol (mg biomass)$^{-1}$ min^{-1}) were similar to previously reported values (1.5 mmol L^{-1} and 27 nmol (mg biomass)$^{-1}$ min^{-1} [123].

L-arabinose transport rates in L-arabinose-limited chemostat cultures of both Gal2- and *Pc*AraT-dependent strains were higher than the V_{max} values calculated from transporter assays with radioactively labelled L-arabinose. A similar difference between transport assays and rates of L-arabinose uptake in growing cultures was reported by Knoshaug *et al.* [184]. These discrepancies suggest that either the transport assays did not accurately reflect zero-trans-influx kinetics [318] or that differences in experimental conditions and/or cellular energy status between transport assays and chemostat cultures influenced L-arabinose uptake. Assuming that *Pc*AraT mediates symport of L-arabinose with a single proton, the L-arabinose consumption rate in aerobic, L-arabinose-limited chemostat cultures of the strain IMX1508 (*Pc*AraT *gal2Δ*) (0.8 mmol (g biomass) h^{-1}; Table 5) would, under anaerobic conditions, correspond to an ATP production rate of ca. 0.3 mmol ATP (g biomass)$^{-1}$ h^{-1}. This rate of ATP production is well below the reported ATP requirement of anaerobic *S. cerevisiae* cultures for cellular maintenance (ca. 1 mmol ATP (g biomass)$^{-1}$ h^{-1} [72]. Consistent with this observation, no growth on L-arabinose as sole carbon source was observed in anaerobic shake flask cultures of the L-arabinose specialist strain IMX869 strain (*Pc*AraT *gal2Δ*) (data not shown).

Table 6 | Comparison of key characteristics of Gal2, *Pc*AraT and heterologous L-arabinose transporters that were previously expressed in *S. cerevisiae*.
n.d = not determined; GLC = D-glucose; XYL = D-xylose

Protein	Origin	K_m [mM]	V_{max} [nmol (mg bio-mass)$^{-1}$ min^{-1}]	Glucose transport	Xylose transport	Mechanism	Ref
ScGal2	*S. cerevisiae*	335 ± 21.0[a] 57 ± 11[b] 371 ± 19[c]	75 ± 5 [a] 2.2 ± 0.3 [b] 18 ± 0.8[c]	✓	✓	facilitated diffusion	[a]This study [b][19] [c][26]
PcAraT	*P. chrysogenum*	0.13 ± 0.03	5.3 ± 0.2	✗	✗	H+ symport	This study
SsAraT	*Scheffersomyces stipitis*	3.8 ± 1.7	0.4 ± 0.1	✓	✗	n.d	[19]
AtStp2	*Arabidopsis thaliana*	4.5 ± 2.2	0.6 ± 0.1	✗	✗	H+ symport	[19]
KmAxt1	*Kluyveromyces marxianus*	263 ± 57	57 ± 6	✗	✓	facilitated diffusion	[26]
PgAxt1	*Pichia guilliermondii*	0.13 ± 0.04	18 ± 0.8	✗	✓	H+ symport	[26]
AmLat1	*Ambrosiozyma monospora*	0.03*	0.2 ± 0.0	✗	✗	n.d	[70, 73]
AmLat2	*A. monospora*	n.d	4 ± 0	✗	✗	n.d	[70, 73]
NcLat-1	*Neurosporacrassa*	58 ± 4	1945 ± 50	✓	n.d	H+ symport	[30]
MtLat-1	*Myceliophthora. thermophila*	29 ± 4	172 ± 6	✗	n.d	H+ symport	[30]

*K_m of *Am*Lat1 was determined as a GFP-fusion protein [2]
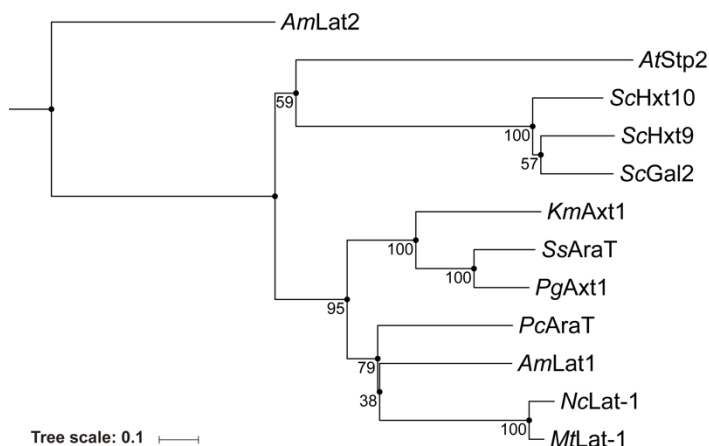
Fig. 3 | Phylogenetic tree of *S. cerevisiae* Gal2, *Pc*AraT, and other heterologous ʟ-arabinose transporters that have previously been functionally expressed in *S. cerevisiae.* Species names are added in two-letter code in front of protein names. Numbers are derived from a 500-times bootstrap iteration. Characteristics and literature references for each transporter are provided in Table 6. Accession numbers: *Sc*Gal2: P13181, *Pc*AraT: CAP85508, *Ss*AraT: A3LQQ5-1, *At*Stp2: OAP13698, *Km*Axt1: GZ791039, *Pg*Axt1: GZ791040, *Am*-Lat1: AY923868, *Am*Lat2: AY923869, *Nc*Lat-1: EAA30346, *Mt*Lat-1: G2QFT5-1.

Differences in experimental protocols for strain-construction and sugar-uptake studies, as well as the different kinetics observed in transport assays and growing cultures, complicate quantitative comparisons between different studies. Nevertheless, some important differences can be discerned between the heterologous ʟ-arabinose transporters that have hitherto been expressed in *S. cerevisiae* (Table 6, Fig. 3). Protein sequence alignment of *Pc*AraT and transporters that were previously shown to mediate ʟ-arabinose import in *S. cerevisiae* showed that *Pc*AraT clusters with *Ambriosozyma monospora Am*-Lat1 (Fig. 3). In terms of its low K_m, *Pc*AraT most closely resembled *Am*Lat1 and the *Pichia guillermondii Pg*Axt1 transporter. However, expression in *S. cerevisiae* of *Am*Lat1 [2, 317] led to ~25-fold lower reported V_{max} of ʟ-arabinose uptake than found in the present study for *Pc*AraT. In contrast to *Pc*AraT, *Pg*Axt was able to transport ᴅ-glucose, which might contribute to the strong inhibition of the latter transporter by ᴅ-glucose [184]. Although *Pc*AraT resembled *A. thaliana* Stp2 [88] in being partially inhibited by ᴅ-glucose despite an inability to transport this sugar, *Pc*AraT enabled consumption of ʟ-arabinose in batch cultures containing 20 g L^{-1} ᴅ-glucose.

In common with other high-affinity sugar transporters in yeasts and fungi [184, 319], the observation that *Pc*AraT mediates ʟ-arabinose-proton symport should be taken into account in future strain designs, since simultaneous activity of proton symport and facilitated diffusion, e.g. via Gal2, may result in energy-consuming futile cycles [279].

In the lignocellulosic hydrolysates now used in the first industrial-scale plants for 'second generation' bioethanol production, L-arabinose generally represents between 2 and 3 % of the total sugars. [279]. At the resulting low concentrations of L-arabinose in the industrial processes, Gal2 operates far from substrate saturation and is, moreover, strongly inhibited by D-glucose. Based on its kinetic characteristics, as analysed in transport assays and growing cultures, *Pc*AraT represents an interesting candidate transporter for evaluation of L-arabinose co-consumption under industrial conditions. If the characteristics of *Pc*AraT determined in the present study can be reproduced in industrial strains and under industrial conditions, this transporter can contribute to a timely and efficient conversion of L-arabinose and, thereby to the overall process economics.

Conclusion

Transcriptome analyses of L-arabinose-limited *Penicillium chrysogenum* chemostat cultures proved valuable for identification of the high-affinity L-arabinose transporter *Pc*AraT. Functional expression and characterization in *Saccharomyces cerevisiae* revealed a high affinity and specificity of this transporter for L-arabinose (K_m = 0.13 mmol L^{-1}), combined with a limited sensitivity to inhibition by D-glucose and D-xylose, which are present at high concentrations in lignocellulosic hydrolysates. These characteristics differentiate *Pc*AraT from the endogenous *S. cerevisiae* transporter capable of L-arabinose transport (Gal2) and qualify it as a potentially valuable additional element in metabolic engineering strategies towards efficient and complete conversion of L-arabinose present in second generation feedstocks for yeast-based production of fuels and chemicals.

Acknowledgements

Supplementary Material
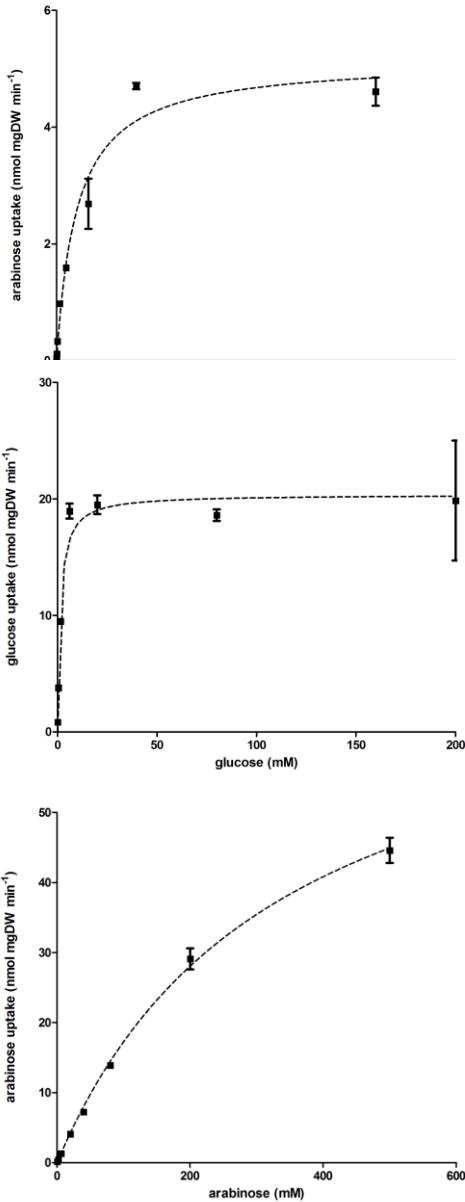
Additional File 1 | Specific rate of ʟ-arabinose uptake by *Pc*AraT. Uptake experiments were performed with increasing concentrations of [¹⁴C-] ʟ-arabinose with the Hxt1-7 and Gal2 deletion strain *S. cerevisiae* DS68625-*PcaraT* expressing *PcaraT* on a centromeric plasmid. No [¹⁴C-] ᴅ-glucose uptake was observed for this strain. Data are derived from duplicate experiments and shown as the average ± mean deviation.

Additional File 2 | Specific rate of ᴅ-glucose uptake by Gal2. Uptake experiments were performed with increasing concentrations of [¹⁴C-] ᴅ-glucose with the Hxt1-7 and Gal2 deletion strain *S. cerevisiae* DS68625-*GAL2* expressing *GAL2* on a centromeric plasmid. Data are derived from duplicate experiments and shown as the average ± mean deviation.

Additional File 3 | Specific rate of ʟ-arabinose uptake by Gal2. Uptake experiments were performed with increasing concentrations of [¹⁴C-] ʟ-arabinose with the Hxt1-7 and Gal2 deletion strain *S. cerevisiae* DS68625-*GAL2* expressing *GAL2* on a centromeric plasmid. Data are derived from duplicate experiments and shown as the average ± mean deviation.

Additional File 4 | Effect of D-glucose (**A.**) and D-xylose (**B.**) on the specific rate of L-arabinose uptake by *Pc*AraT (filled triangles) and Gal2 (filled squares). Uptake experiments were performed with 50 mmol L^{-1} [^{14}C-] L-arabinose in the presence of increasing concentrations of D-glucose. Symbols indicate uptake rates observed with the Hxt1-7 and Gal2 deletion strain *S. cerevisiae* DS68625-*PcaraT* (closed triangles) and DS68625-*GAL2*, expressing either *Pc*AraT or Gal2, respectively. Data are derived from duplicate experiments and shown as the average ± mean deviation.
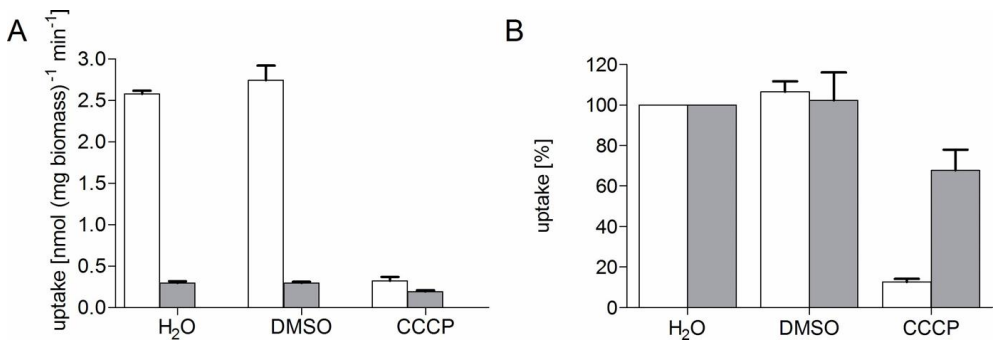
Additional File 5 | Impact of proton-gradient uncoupling on transport activity. Transport rates of [^{14}C]-L-arabinose of the Hxt1-7 and Gal2 deletion strains DS68625-*PcaraT* and DS68625-*GAL2* expressing either *Pc*AraT (DS68625-*PcaraT*, white bars) or Gal2 (DS68625-*GAL2*, grey bars) on a centromeric plasmid. Transport rates were determined in 200 μl synthetic medium at a [^{14}C]-L-arabinose concentration of 2 mmol L^{-1} upon addition of either 0.5 μL water, 0.5 μL DMSO, or 10 μM CCCP (0.5 μl of a stock solution dissolved in 100 % DMSO)(**A**). Panel (**B**) shows the uptake capacity in % relative to the control (H$_2$O). Data are derived from duplicate experiments and shown as the average ± mean deviation.

3

Additional File 6 | Primers used in this study.

Primers used for amplification of integration fragments:

Primer nr.:	Purpose:	Template:	Sequence 5' -> 3':
4653	flGal1-*cas9-A* fragment	p414-TEF1p-cas9-CYC1t	GTGCCTATTGATGATCTGGCG-GAATGTCTGCCGTGCCATAGCCATGCCTTCACATATAGTCCGCAAATTAAAGCCTTCGAG
5981	flGal1-*cas9-A* fragment	p414-TEF1p-cas9-CYC1t	TTCACCGGTCGCGTTCCTGAAAC-GCAGATGTGCCTCGCGCCGCACACCGTATTACCGCCTTTG
3093	A-AmdSYM-flGal80 fragment	pUG-amdSYM	ACTATATGTGAAGGCATGGCTATGGCACGGCAGA-CATTCCGCCAGATCATCAATAGGCACCTTCGTACGCTGCAGGTCGAC
1678	A-AmdSYM-flGal80 fragment	pUG-amdSYM	AATGAGAAGTTGTTCTGAACAAAGTAAAAAAAA-GAAGTATACTTACATAGGCCACTAGTGGATCTG
5910	flGRE3_G fragment	CEN.PK113-7D	CCACCTGGTGGAACATCCTAGAAC
5911	flGRE3_G fragment	CEN.PK113-7D	AAGGGCCATGACCACCTGATGCACCAATT-AGGTAGGTCTGGCTATGTCTATACCTCTGGCCTACCAGCAACAATTGGGAAAC
7133	fl_*RPE1*_H fragment	pUD347	TATAATATTTCATTATCGGAACTCTAGATTC-TATACTTGTTTCCCAATTGTTGCTGGTAGGGCCCTTCCGGGAGTTTATC
3290	fl_*RPE1*_H fragment	pUD347	GTCACGGGTTCTCAGCAATTCG
3291	H_*TKL1*_I fragment	pUD348	CTCTAACGCCTCAGCCATCATCG
4068	H_*TKL1*_I fragment	pUD348	GCCTACGGTTCCCGAAGTATGC
3274	I_*TAL1*_A fragment	pUD349	TATTCACGTAGACGGATAGGTATAGC
3275	I_*TAL1*_A fragment	pUD349	GTGCCTATTGATGATCTGGCGGAATG
3847	A_*NQM1*_B fragment	pUD344	ACTATATGTGAAGGCATGGCTATGG
3276	A_*NQM1*_B fragment	pUD344	GTTGAACATTCTTAGGCTGGTCGAATC
4672	B_*RKI1*_C fragment	pUD345	CACCTTTCGAGAGGACGATG
3277	B_*RKI1*_C fragment	pUD345	CTAGCGTGTCCTCGCATAGTTCTTAGATTG
3283	C_*TKL2*_F fragment	pUD346	ACGTCTCACGGATCGTATATGC
3288	C_*TKL2*_F fragment	pUD346	TGCCGAACTTTCCCTGTATGAAGC
5936	F_flGRE3	CEN.PK113-7D	CATACGTTGAAACTACGG-CAAAGGATTGGTCAGATCGCTTCATACAGGGAAAGTTCGGCACCCTCATTCCGATGCTGTATATGTG
5937	F_flGRE3	CEN.PK113-7D	ACTGCTTCGTCTAGGTCTTG
6628	flGal80_*AraA*_G fragment	pUD354	TCCTTGCCGACCAGCGTATACAATCTCGATAGTT-GGTTTCCCGTTCTTTCCACTCCCGTCCGCGCAGATTAGCGAAGC

92

6285	flGal80_*AraA*_G fragment	pUD354	AAGGGCCATGACCACCTGATGCACCAATT-AGGTAGGTCTGGCTATGTCTATACCTCTGGCGCGATACCCTGCGATCTTC
6273	G_*AraA*_A fragment	pUD354	GCCAGAGGTATAGACATAGCCAGACCTAC-CTAATTGGTGCATCAGGTGGTCATGGCCCTTCGCGCAGATTAGCGAAGC
6280	G_*AraA*_A fragment	pUD354	GTGCCTATTGATGATCTGGCG-GAATGTCTGCCGTGCCATAGCCATGCCTTCACATATAGTGCGATACCCTGCGATCTTC
6270	A_*AraA*_B fragment	pUD354	ACTATATGTGAAGGCATGGCTATGGCACGGCAGA-CATTCCGCCAGATCATCAATAGGCACCGCGCAGATTAGCGAAGC
6281	A_*AraA*_B fragment	pUD354	GTTGAACATTCTTAGGCTGGTCGAATCATTTAGA-CACGGGCATCGTCCTCTCGAAAGGTGGCGATACCCTGCGATCTTC
6271	B_*AraA*_C fragment	pUD354	CACCTTTCGAGAGGAC-GATGCCCGTGTCTAAATGATTCGACCAGCCTAAGAATGTTCAACCGCGCAGATTAGCGAAGC
6282	B_*AraA*_C fragment	pUD354	CTAGCGTGTCCTCGCATAGTTCTTAGATTGTCGC-TACGGCATATACGATCCGTGAGACGTGCGATACCCTGCGATCTTC
6272	C_*AraA*_D fragment	pUD354	ACGTCTCACGGATCGTATATGCCG-TAGCGACAATCTAAGAACTATGCGAGGACACGCTAGCGCGCAGATTAGCGAAGC
6284	C_*AraA*_D fragment	pUD354	AATCACTCTCCATACAGGGTTTCATA-CATTTCTCCACGGGACCCACAGTCGTAGATGCGTGCGATACCCTGCGATCTTC
6283	D_*AraA*_M fragment	pUD354	ACGCATCTACGACTGTGGGTCCCGTGGA-GAAATGTATGAAACCCTGTATGGAGAGTGATTGCGATACCCTGCGATCTTC
6275	D_*AraA*_M fragment	pUD354	ACGAGAGATGAAGGCTCACCGATGGACTTAG-TATGATGCCATGCTGGAAGCTCCGGTCATCGCGCAGATTAGCGAAGC
6287	M_*AraA*_N fragment	pUD354	ATGACCGGAGCTTCCAGCATGGCATCATACT-AAGTCCATCGGTGAGCCTTCATCTCTCGTGCGATACCCTGCGATCTTC
6276	M_*AraA*_N fragment	pUD354	TTCTAGGCTTTGATGCAAGGTCCACATA-TCTTCGTTAGGACTCAATCGTGGCTGCTGATCCGCGCAGATTAGCGAAGC
6288	N_*AraA*_O fragment	pUD354	GATCAGCAGCCACGATTGAGTCCTAACGAAGA-TATGTGGACCTTGCATCAAAGCCTAGAAGCGATACCCTGCGATCTTC
6277	N_*AraA*_O fragment	pUD354	ATACTCCCTGCACAGATGAGTCAAGC-TATTGAACACCGAGAACGCGCTGAACGATCATTCCGCGCAGATTAGCGAAGC
6289	O_*AraA*_I fragment	pUD354	GAATGATCGTTCAGCGCGTTCTCGGTGTTCAA-TAGCTTGACTCATCTGTGCAGGGAGTATGCGATACCCTGCGATCTTC

3

6274	O_*AraA*_I fragment	pUD354	GCCTAC-GGTTCCCGAAGTATGCTGCTGATGTCTGGCTATAC CTATCCGTCTACGTGAATACGCG-CAGATTAGCGAAGC
3274	I_*AraB*_K fragment	pUD355	TATTCACGTAGACGGATAGGTATAGC
6636	I_*AraB*_K fragment	pUD355	GCGAGGACTTCCCATCAATTGC
6634	K_*AraD*_flGal80	pUD356	AAGATAGTCGCCGAACTCGC
6635	K_*AraD*_flGal80	pUD356	CTCAGTATTCGTTTTTATAACGTTCGCTGCAC-TGGGGGCCAAGCACAGGGCAAGATGCTTTGCCGAA CTTTCCCTGTATG
7676	*PcaraT* fragment	pPWT118	TTTCTAATGCCTTTTCCATCATGTTACTACGAG-TTTTCTGAACCTCCTCGCACATTGGTATCTTCACG CGTGTTCGAG
7660	*PcaraT* fragment	pPWT118	TATAAATATTTATCGTCACGAA-TAAATCCCGTGAATTTCTAACAAAGTTTATACAAT ATCTAACCTCGGAAGATCGTCGACAAG
2641	Ura3 repair fragment	CEN.PK113-7D	ATTGCCCAGTATTCTTAACC
1522	Ura3 repair fragment	CEN.PK113-7D	CGAGATTCCCGGGTAATAACTG
2788	*HXK2* KO cassette	pUG-72	ATTGTAGGAATATAATTCTCCACACATAA-TAAGTACGTTAATATAAACAGCTGAAGCTTCGTA CGC
2789	*HXK2* KO cassette	pUG-72	TTAAAAAAAGGGCACCTTCTTGTT-GTTCAAACTTAATTTACAAATTAAGTGCATAGGCC ACTAGTGGATCTG
10585	flGal2_*Pc13g04640*_flGal2	pPWT111	ACACAAATAATAGGTTTAGGTAAGGAATTTATA-TAATCGTAAGGATATCATTGATAAGGAGTTTATC ATTATCAATACTGCCATTTCAAAG
10584	flGal2_*Pc13g04640*_flGal2	pPWT111	TTAGTTTTGTAGACATATATAAACAATCAG-TAATTGGATTGAAAATTTGGTGTTGTGAATTAAC CTCGGAAGATCGTCGACAAG
10585	flGal2_*Pc13g08230*_flGal2	pPWT113	ACACAAATAATAGGTTTAGGTAAGGAATTTATA-TAATCGTAAGGATATCATTGATAAGGAGTTTATC ATTATCAATACTGCCATTTCAAAG
10584	flGal2_*Pc13g08230*_flGal2	pPWT113	TTAGTTTTGTAGACATATATAAACAATCAG-TAATTGGATTGAAAATTTGGTGTTGTGAATTAAC CTCGGAAGATCGTCGACAAG
10585	flGal2_*Pc16g05670*_flGal2	pPWT116	ACACAAATAATAGGTTTAGGTAAGGAATTTATA-TAATCGTAAGGATATCATTGATAAGGAGTTTATC ATTATCAATACTGCCATTTCAAAG
10584	flGal2_*Pc16g05670*_flGal2	pPWT116	TTAGTTTTGTAGACATATATAAACAATCAG-TAATTGGATTGAAAATTTGGTGTTGTGAATTAAC CTCGGAAGATCGTCGACAAG
10585	flGal2_*PcaraT*_flGal2_flGal2	pPWT118	ACACAAATAATAGGTTTAGGTAAGGAATTTATA-TAATCGTAAGGATATCATTGATAAGGAGTTTATC ATTATCAATACTGCCATTTCAAAG

10584	flGal2_*PcaraT*_flGal2_flGal2	pPWT118	TTAGTTTTGTAGACATATATAAACAATCAG-TAATTGGATTGAAAATTTGGTGTTGTGAATTAACCTCGGAAGATCGTCGACAAG
10585	flGal2_*Pc22g14520*_flGal2	pPWT123	ACACAAATAATAGGTTTAGGTAAGGAATTTATA-TAATCGTAAGGATATCATTGATAAGGAGTTTATCATTATCAATACTGCCATTTCAAAG
10584	flGal2_*Pc22g14520*_flGal2	pPWT123	TTAGTTTTGTAGACATATATAAACAATCAG-TAATTGGATTGAAAATTTGGTGTTGTGAATTAACCTCGGAAGATCGTCGACAAG
9563	*GAL2* KO cassette	-	GGATTGAAAATTTGGTGTTGTGAATT-GCTCTTCATTATGCACCTTATTCAATTATCATCAGATAACATGCTCTGCCATCCTTTGTTCACCGAG-CAAAATTAAAAACGCAAATGAATTGT
9564	*GAL2* KO cassette	-	ACAATTCATTTTGCGTTTTTAATTTT-GCTCGGTGAACAAAGGATGGCAGAGCATGTTATCTGATGATAATTGAATAAGGTGCATAATGAAGAG-CAATTCACAACACCAAATTTTCAATCC
943	flGal2_*KanMX*_flGal2	pUG6	TAAGTAAACACAAGATTAACATAATAAAAAAAA-TAATTCTTTCATAGCATAGGCCACTAGTGGATCTG
944	flGal2_Kan*MX*_flGal2	pUG6	TAAGAGAGATGATGGAGCGTCTCACTTCAAAC-GCATTATTCCAGCTGAAGCTTCGTACGC

Primers used for the construction of gRNA expression plasmids:

Primer nr.:	Purpose:	Template:	Primer nr.:
5792	pUDE348/335/327 backbone	pMEL10	GTTTTAGAGCTAGAAATAGCAAGTTAAAATAAG
5980	pUDE348/335/327 backbone	pMEL10	CGACCGAGTTGCTCTTG
6631	pUDE348 gRNA	pMEL10	ATTTTAACTTGCTATTTCTAGCTCTAAAACAA-GATCTCTTGTTGTAGTCCGATCATTTATCTTTCACTGCGG
5979	pUDE335 gRNA	pMEL10	TATTGACGCCGGGCAAGAGC
9283	pUDR245 gRNA	pROS10	TGCGCATGTTTCGGCGTTCGAAACTTCTCCGCAG-TGAAAGATAAATGATCGTTGACTACACCAATGACAAGTTTTAGAGCTAGAAATAGCAAGT
9283	pUDR246 gRNA1	pROS10	TGCGCATGTTTCGGCGTTCGAAACTTCTCCGCAG-TGAAAGATAAATGATCGTTGACTACACCAATGACAAGTTTTAGAGCTAGAAATAGCAAGT
10024	pUDR246 gRNA2	pROS10	TGCGCATGTTTCGGCGTTCGAAACTTCTCCGCAG-TGAAAGATAAATGATCTTCATGTTTGGCTGGGATACGTTTTAGAGCTAGAAATAGCAAGTTAAAA-TAAGGCTAGTCCGTTATCAAC
6005	pUDR246/245 backbone	pROS10	GATCATTTATCTTTCACTGCGGAGAAG
2528	PCR verification of gRNA	pUDE335	TCTTTCCTGCGTTATCCC
960	PCR verification of gRNA	pUDE335	GTGGATGATGTGGTCTCTAC

Primers used for verifying integration of fragments:

Primer nr.:	Purpose:	Primer nr.:

970	Checking *AraA* integration	CATTTACCGGCGCACTCTCG
6925	Checking *AraA* integration	GGTGCTTTGGAATGGATG
6924	Checking *AraA* integration	TGTTGAGAACCGGTAACG
4692	Checking *AraA* integration	AAGGGCCATGACCACCTG
3275	Checking *AraA* integration	GTGCCTATTGATGATCTGGCGGAATG
4173	Checking *AraA* integration	GTTGAACATTCTTAGGCTGG
3277	Checking *AraA* integration	CTAGCGTGTCCTCGCATAGTTCTTAGATTG
5231	Checking *AraA* integration	AATCACTCTCCATACAGGG
3354	Checking *AraA* integration	ACGCATCTACGACTGTGGGTC
4184	Checking *AraA* integration	ATGACCGGAGCTTCCAGCATG
3843	Checking *AraA* integration	GATCAGCAGCCACGATTG
3837	Checking *AraA* integration	GAATGATCGTTCAGCGCG
4068	Checking *AraA* integration	GCCTACGGTTCCCGAAGTATGC
6926	Checking *AraB* integration	TGTCTACCGCTGGTGAAGGTG
6636	Checking *AraB* integration	GCGAGGACTTCCCATCAATTGC
6928	Checking *AraD* integration	GAGAAAGCACGGTGCTTCTG
971	Checking *AraD* integration	ATAAGAACACCCGCATGCAC
1977	Checking PPP integration	TACCTTCTGCTCTCTCTG
5164	Checking PPP integration	AAAGGATTCGGGCCCAAATCGG
3225	Checking PPP integration	CTGTGATCTCCAGAGCAAAG
2673	Checking PPP integration	TGAAGTGGTACGGCGATGC
3878	Checking PPP integration	gcgGGTACCCGCCTCGTTTCTTTTTCTTC
2913	Checking PPP integration	AATAGCCGCCAGGAAATGCC
1999	Checking PPP integration	CGCGCTCAACCTGGAATTAC
2374	Checking PPP integration	GCAGAAGTGTCTGAATGTATTAAGG
3515	Checking PPP integration	CTGACAGGTGGTTTGTTACG
5603	Checking PPP integration	CGCAAGTTTATCAATGTCGG
3927	Checking PPP integration	AAGAGAATGGACCTATGAACTGATG
5396	Checking PPP integration	CGAATAAACACACATAAACAAACAAAATGGCACAG-TTCTCCGACATTG
5937	Checking PPP integration	ACTGCTTCGTCTAGGTCTTG
5910	Checking PPP integration	CCACCTGGTGGAACATCCTAGAAC
4657	Check PcAraT integration	TTGCGCTAAGAGAATGGACC
5905	Check PcAraT integration	CTTTTTTTTAGTTTTAAAACACCAAGAACTTAG
4930	Checking Hxk2 deletion	GGCAAGAGTATAGCGTGATACC
3070	Checking Hxk2 deletion	AGTGCTTCCGTTCGTTCCAG
3564	Checking Hxk2 deletion	TTGGTGCTAGAGCTGCTAGATTG
2926	Checking Hxk2 deletion	ATCAATTCCTTTGGCACATCGGC
8883	Checking Gal2 deletion	AGTTAAGCCCTTCCCATCTC
8889	Checking Gal2 deletion	GCGAAACATAGCCCTAATGG
8883	Checking integration of *gal2::PcAraT/ Pc13g04640/ Pc13g08230/ Pc16g05670 Pc22g14520*	AGTTAAGCCCTTCCCATCTC
8889	Checking integration of *gal2::PcAraT/ Pc13g04640/ Pc13g08230/ Pc16g05670 Pc22g14520*	GCGAAACATAGCCCTAATGG

Chapter 4: Laboratory evolution of a glucose-phosphorylation-deficient, arabinose-fermenting *S. cerevisiae* strain reveals mutations in *GAL2* that enable glucose-insensitive L-arabinose uptake

Maarten D. Verhoeven, Jasmine M. Bracher, Jeroen G. Nijland, Jonna Bouwknegt, Jean-Marc G. Daran, Arnold J.M. Driessen, Antonius J.A. van Maris & Jack T. Pronk

Abstract

Cas9-assisted genome editing was used to construct an engineered glucose-phosphorylation-negative *S. cerevisiae* strain, expressing the *Lactobacillus plantarum* L-arabinose pathway and the *Penicillium chrysogenum* transporter *Pc*AraT. This strain, which showed a growth rate of 0.26 h^{-1} on L-arabinose in aerobic batch cultures, was subsequently evolved for anaerobic growth on L-arabinose in the presence of D-glucose and D-xylose. In four strains isolated from two independent evolution experiments the galactose-transporter gene *GAL2* had been duplicated, with all alleles encoding $Gal2^{N376T}$ or $Gal2^{N376I}$ substitutions. In one strain, a single *GAL2* allele additionally encoded a $Gal2^{T89I}$ substitution, which was subsequently also detected in the independently evolved strain IMS0010. In ^{14}C-sugar-transport assays, $Gal2^{N376S}$, $Gal2^{N376T}$ and $Gal2^{N376I}$ substitutions showed a much lower glucose sensitivity of L-arabinose transport and a much higher K_m for D-glucose transport than wild-type Gal2. Introduction of the $Gal2^{N376I}$ substitution in a non-evolved strain enabled growth on L-arabinose in the presence of D-glucose. $Gal2^{N376T, T89I}$ and $Gal2^{T89I}$ variants showed a lower K_m for L-arabinose and a higher K_m for D-glucose than wild-type Gal2, while reverting $Gal2^{N376T, T89I}$ to $Gal2^{N376}$ in an evolved strain negatively affected anaerobic growth on arabinose. This study indicates that optimal conversion of mixed-sugar feedstocks may require complex 'transporter landscapes', consisting of sugar transporters with complementary kinetic and regulatory properties.

Introduction

Saccharomyces cerevisiae is used on a massive scale for industrial production of ethanol from cane sugar and hydrolysed corn starch, in which fermentable sugars predominantly occur as hexoses or hexose dimers [16]. In contrast, hydrolysis of lignocellulosic feedstocks such as the agricultural residues corn stover, corn cobs and wheat straw, yields mixtures of pentose and hexose sugars [40, 206]. Industrial ethanol production from lignocellulosic feedstocks therefore requires efficient conversion of pentose and hexose sugars into ethanol [40]. In most lignocellulosic hydrolysates, D-xylose represents up to 25% of the total sugar monomers while another pentose, L-arabinose, typically accounts for up to 3% of the sugar content. In some industrially relevant hydrolysates, such as those derived from corn-fibre hydrolysates and sugar-beet pulp, L-arabinose can account for up to 26% of the sugar content [41, 42, 206].

Since wild-type *S. cerevisiae* strains cannot ferment pentoses, metabolic engineering is required to enable utilization of these substrates. Strategies to engineer *S. cerevisiae* for D-xylose fermentation are either based on heterologous expression of a fungal D-xylose reductase and xylitol dehydrogenase or on expression of a heterologous D-xylose isomerase [7, 241, 246]. Current L-arabinose-fermenting *S. cerevisiae* strains are based on functional expression of genes encoding L-arabinose isomerase (AraA), L-ribulo-kinase (AraB), and L-ribulose-5-phosphate-4-epimerase (AraD) from bacteria such as *Escherichia coli*, *Bacillus subtilis* or *Lactobacillus plantarum* [46, 84, 85]. Unlike the fungal L-arabinose pathway [320], the bacterial pathway enables conversion of L-arabinose to D-xylulose-5-phosphate via redox-cofactor-independent reactions [84, 85]. As previously shown for engineered D-xylose-consuming strains [7], overexpression of the *S. cerevisiae* genes encoding xylulokinase (Xks1, EC 2.7.1.17), ribulose 5-phosphate epimerase (Rpe1, EC 5.3.1.1), ribulose 5-phosphate isomerase (Rki1, EC 5.3.1.6), transketolase (Tkl1, EC 2.2.1.1) and transaldolase (Tal1, EC 2.2.1.2) enabled efficient coupling of the heterologously expressed L-arabinose pathway to glycolysis and alcoholic fermentation [84]. Subsequent laboratory evolution yielded an efficient L-arabinose fermenting strain, which combined a high ethanol yield (0.43 g g^{-1}) with an ethanol production rate of 0.29 g h^{-1} [g biomass] $^{-1}$ and an arabinose consumption rate of 0.70 g h^{-1} [g biomass]$^{-1}$) [84]. Transcriptome studies identified that increased expression of the genes encoding 'secondary' isoenzymes of transaldolase (*NQM1*) and transketolase (*TKL2*) contributed to improved L-arabinose fermentation of this laboratory-evolved strain [163]. Improvements in L-arabinose fermentation were also achieved by codon optimization of bacterial L-arabinose genes to match the codon preference of highly expressed glycolytic yeast genes [86].

Transport of pentose sugars in *S. cerevisiae* occurs by facilitated diffusion, mediated by native HXT hexose transporters [85, 164]. Transport of L-arabinose predominantly occurs via the hexose transporter Gal2 which, however, exhibits a much lower affinity for L-arabinose than for D-glucose or galactose [85, 88, 161, 162]. Of the other *S. cerevisiae* HXT transporters, only Hxt9p and Hxt10p show low rates of L-arabinose

transport [88]. In practice, expression of *GAL2* has been found to be essential for L-arabinose fermentation by strains that do not express heterologous transporters [85, 88, 163, 321]. Recently, an *in silico* model of the three-dimensional structure of Gal2, based on the crystal structure of the *E. coli* xylose permease XylEp, was used to predict mutations in *GAL2* that improve L-arabinose docking in Gal2. Based on this theoretical analysis, single-amino-acid substitutions were introduced at position 85 of Gal2 and shown to significantly increase L-arabinose transport activity [321].

Since transcription of *GAL2* is both induced by D-galactose and repressed by D-glucose, design of L-arabinose-fermenting *S. cerevisiae* strains often includes expression of *GAL2* behind a strong constitutive promoter [308, 321]. Alternatively, laboratory evolution can result in upregulation of *GAL2* [13, 163]. However, L-arabinose transport by Gal2 is also subject to strong competitive inhibition by D-glucose [162, 184], which precludes simultaneous utilization of L-arabinose and D-glucose in batch cultures grown on sugar mixtures [13, 163].

To improve the kinetics of L-arabinose transport, transporter genes from other yeasts, filamentous fungi and plants have been functionally expressed in L-arabinose-metabolizing *S. cerevisiae* strains [88, 184, 186, 317, 322]. K_m values of these heterologous transporters for L-arabinose ranged from 0.13 to 263 mM, while reported V_{max} values ranged from 0.4 to 171 [nmol L-arabinose (mg biomass)$^{-1}$ min^{-1}]. Several heterologous transporters, including the high-affinity L-arabinose proton symporter PcAraT from *P. chrysogenum* [322] allowed for L-arabinose uptake in the presence of D-glucose [88, 184, 186, 322].

Laboratory evolution of pentose-fermenting *S. cerevisiae* strains in which D-glucose phosphorylation was abolished has been successfully used to select strains in which L-arabinose or D-xylose uptake is less sensitive to D-glucose inhibition [112, 123, 176]. Single-amino-acid substitutions, found at corresponding positions in the hexose transporters Hxt7 (N370) and Gal2 (N376), as well as in a chimera of Hxt3 and Hxt6 (N367), were shown to substantially decrease inhibition of D-xylose transport by D-glucose [112, 123].

The aim of the present study was to identify mutations that enable anaerobic growth of engineered, L-arabinose-fermenting *S. cerevisiae* strains on L-arabinose in the presence of D-glucose and D-xylose, with a focus on mutations that affect uptake of L-arabinose. To this end, we constructed a glucose-phosphorylation-negative, L-arabinose-fermenting *S. cerevisiae* strain by Cas9-assisted genome editing. This strain was then subjected to prolonged laboratory evolution in sequential batch bioreactor cultures, grown on mixtures of L-arabinose, D-xylose and D-glucose. Subsequently, causal mutations for glucose-insensitive growth on L-arabinose were identified by whole-genome sequencing and functional analysis of mutant alleles in non-evolved strain backgrounds.

Materials and Methods

Strains and maintenance. The *S. cerevisiae* strains used and constructed in this study (Table 1) were derived from the CEN.PK lineage [251, 266]. All stock cultures were grown in shake flasks on synthetic medium (SM, see below) or, in case of auxotrophic strains, on yeast-extract/peptone (YP) medium (10 g L^{-1} Bacto yeast extract (Becton Dickinson, Franklin Lakes, NJ) and 20 g L^{-1} Bacto Peptone (Becton Dickinson)) [51]. These media were either supplemented with 20 g L^{-1} D-glucose or, in case of the constructed glucose-phosphorylation-negative strains, 20 g L^{-1} L-arabinose. For storage and in pre-cultures, single-colony isolates obtained after laboratory evolution were grown in medium containing 20 g L^{-1} of each D-glucose, D-xylose and L-arabinose. After adding glycerol (30% vol/vol) to these cultures, 1 mL aliquots were stored at -80 °C.

Table 1 | *Saccharomyces cerevisiae* strains used in this study

Strain	Relevant genotype	Reference
CEN.PK 113-7D	*MATa MAL2-8c SUC2*	[251]
IMX080	*MATa ura3-52 his3-1 leu2-3,112 MAL2-8c SUC2 glk1::Sphis5, hxk1::KlLEU2*	[291]
IMX486	*MATa ura3-52 his3-1 leu2-3,112 MAL2-8c SUC2 glk1::Sphis5, hxk1::KlLEU2 gal1::cas9-amdS*	This study
IMX604	*MATa ura3-52 his3-1 leu2-3,112 MAL2-8c SUC2 glk1::Sphis5, hxk1::KlLEU2 gal1::cas9- amdS gre3::pTDH3_RPE1 pPGK1_TKL1, pTEF1_TAL1 pPGI1_NQM1 pTPI1_RKI1 pPYK1_TKL2*	This study
IMX658	*MATa ura3-52 his3-1 leu2-3,112 MAL2-8c SUC2 glk1::Sphis5, hxk1::KlLEU2 gal1::cas9- amdS gre3::pTDH3_RPE1 pPGK1_TKL1, pTEF1_TAL1 pPGI1_NQM1 pTPI1_RKI1 pPYK1_TKL2 gal80::(pTPI_araA_tCYC)*9 pPYK-araB-tPGI1 pPGK-araD-tTDH3*	This study
IMX660	*MATa ura3-52 his3-1 leu2-3,112 MAL2-8c SUC2 glk1::Sphis5, hxk1::KlLEU2 gal1::cas9- amdS gre3::pTDH3_RPE1 pPGK1_TKL1, pTEF1_TAL1 pPGI1_NQM1 pTPI1_RKI1 pPYK1_TKL2 gal80::(pTPI_araA_tCYC)*9 pPYK-araB-tPGI1 pPGK-araD-tTDH3 hxk2::KlURA3*	This study
IMX728	*MATa ura3-52 his3-1 leu2-3,112 MAL2-8c SUC2 glk1::Sphis5, hxk1::KlLEU2 gal1::cas9- amdS gre3::pTDH3_RPE1 pPGK1_TKL1, pTEF1_TAL1 pPGI1_NQM1 pTPI1_RKI1 pPYK1_TKL2 gal80::(pTPI_araA_tCYC)*9 pPYK-araB-tPGI1 pPGK-araD-tTDH3 hxk2:: PcaraT*	This study
IMX1106	*MATa ura3-52 his3-1 leu2-3,112 MAL2-8c SUC2 glk1::Sphis5, hxk1::KlLEU2 gal1::cas9- amdS gre3::pTDH3_RPE1 pPGK1_TKL1, pTEF1_TAL1 pPGI1_NQM1 pTPI1_RKI1 pPYK1_TKL2 gal80::(pTPI_araA_tCYC)*9 pPYK-araB-tPGI1 pPGK-araD-tTDH3 hxk2::KlURA3 gal2::gal2^{N376I}*	This study
IMX1386	*MATa ura3-52 his3-1 leu2-3,112 MAL2-8c SUC2 glk1::Sphis5, hxk1::KlLEU2 gal1::cas9- amdS gre3::pTDH3_RPE1 pPGK1_TKL1, pTEF1_TAL1 pPGI1_NQM1 pTPI1_RKI1 pPYK1_TKL2 gal80::(pTPI_araA_tCYC)*9 pPYK-araB-tPGI1 pPGK-araD-tTDH3 hxk2::KlURA3 CAN1::pGAL2_GAL2_tGAL2*	This study

IMS0514	IMX728 that has undergone laboratory evolution on a mixture of arabinose and glucose under aerobic conditions	This study
IMS0520	IMX728 that has undergone laboratory evolution on mixture of arabinose, glucose and xylose under anaerobic conditions	This study
IMS0521	IMX728 that has undergone laboratory evolution on mixture of arabinose, glucose and xylose under anaerobic conditions	This study
IMS0522	IMX728 that has undergone laboratory evolution on mixture of arabinose, glucose and xylose under anaerobic conditions	This study
IMS0523	IMX728 that has undergone laboratory evolution on mixture of arabinose, glucose and xylose under anaerobic conditions	This study
IMW088	*As IMS0522; PcAraTΔ*	This study
IMW091	*As IMS0522; gal2^{I89T}*	This study
DS68616	*Mat a, ura3-52, leu2-112, gre3::loxP, loxP-Ptpi:TAL1, loxP-Ptpi::RKI1, loxP-Ptpi-TKL1, loxP-Ptpi-RPE1, delta::Padh1XKS1Tcyc1-LEU2, delta::URA3-Ptpi-xylA-Tcyc1*	DSM, The Netherlands
DS68625	*DS68616, his3::loxP, hxt2::loxP-kanMX-loxP, hxt367::loxP-hphMX-loxP, hxt145::loxP-natMX-loxP, gal2::loxP-zeoMX-loxP*	[112]
DS68625-Gal2	*DS68616, his3::loxP, hxt2::loxP-kanMX-loxP, hxt367::loxP-hphMX-loxP, hxt145::loxP-natMX-loxP, gal2::loxP-zeoMX-loxP*	This study
DS68625-Gal2^{N376I}	*DS68616, his3::loxP, hxt2::loxP-kanMX-loxP, hxt367::loxP-hphMX-loxP, hxt145::loxP-natMX-loxP, gal2::loxP-zeoMX-loxP*	This study
DS68625-Gal2^{N376S}	*DS68616, his3::loxP, hxt2::loxP-kanMX-loxP, hxt367::loxP-hphMX-loxP, hxt145::loxP-natMX-loxP, gal2::loxP-zeoMX-loxP*	This study
DS68625-Gal2^{N376T}	*DS68616, his3::loxP, hxt2::loxP-kanMX-loxP, hxt367::loxP-hphMX-loxP, hxt145::loxP-natMX-loxP, gal2::loxP-zeoMX-loxP*	This study
DS68625-Gal2$^{N376T/T89I}$	*DS68616, his3::loxP, hxt2::loxP-kanMX-loxP, hxt367::loxP-hphMX-loxP, hxt145::loxP-natMX-loxP, gal2::loxP-zeoMX-loxP*	This study
DS68625-Gal2^{T89I}	*DS68616, his3::loxP, hxt2::loxP-kanMX-loxP, hxt367::loxP-hphMX-loxP, hxt145::loxP-natMX-loxP, gal2::loxP-zeoMX-loxP*	This study
DS68625-mcs	*DS68616, his3::loxP, hxt2::loxP-kanMX-loxP, hxt367::loxP-hphMX-loxP, hxt145::loxP-natMX-loxP, gal2::loxP-zeoMX-loxP*	This study

Cultivation and media. All strain characterisation studies were performed in synthetic medium (SM) prepared as described previously [51]. Carbon source and vitamin solutions were added after autoclaving the medium for 20 min at 121 °C. Concentrated solutions (50 % w/w) of D-glucose, D-xylose and L-arabinose were autoclaved separately at 110 °C for 20 min. Prior to inoculation 20 g L^{-1} L-arabinose (SMA), 20 g L^{-1} D-glucose (SMG), 20 g L^{-1} L-arabinose and 20 g L^{-1} D-glucose (SMAG) or 20 g L^{-1} L-arabinose, 20 g L^{-1} D-glucose and 20 g L^{-1} D-xylose (SMAGX) were added to SM as carbon sources. Aerobic shake-flask cultures were grown in an orbital shaker at 200 rpm set at 30 °C, using 500-ml flasks containing 100 ml medium. For plates 20 g L^{-1} agar (BD) was added prior to autoclaving at 121 °C for 20 min. Aerobic shake-flask cultures used as pre-cultures for anaerobic cultures were inoculated with frozen stocks and, in late-exponential phase, a 1 mL sample was used to start a second aerobic pre-culture. Anaerobic batch cultures used for characterization were inoculated from these cultures to obtain an initial OD_{660} of 0.5. Anaerobic shake-flask cultures were incubated at 30 °C in an Innova anaerobic chamber (5% H_2, 6% CO_2, and 89% N_2, New Brunswick Scientific, Edison, NJ) in 50 mL shake flasks

placed on an orbital shaker set at 200 rpm. Bioreactor batch cultures were performed at 30 °C in 2-L laboratory bioreactors (Applikon, Delft, The Netherlands) with a working volume of 1 L. Culture pH was controlled at 5.0 by automatic addition of 2 M KOH and cultures were stirred at 800 rpm. Anaerobic bioreactors were equipped with Viton O-rings and Norprene tubing (Cole Palmer Instrument Company, Vernon Hills, IL) to minimize oxygen diffusion and continuously sparged with nitrogen gas (<10 ppm oxygen) at 0.5 L min^{-1}. After autoclaving, synthetic media were supplemented with 0.2 g L^{-1} antifoam C (Sigma-Aldrich, St. Louis, MO). Furthermore, the anaerobic growth factors Tween 80 (420 mg L^{-1}) and ergosterol (10 mg L^{-1}) were added to the medium as described previously [271]. Laboratory evolution experiments were performed in sequential batch reactors (SBRs). On-line measurement of CO_2 concentrations in the off gas of SBRs was used as input for a control routine programmed in MFCS/win 3.0 (Sartorius AG, Göttingen, Germany). An empty-refill cycle was automatically initiated when the CO_2 concentration in the off gas had first exceeded a threshold value of 0.2 % and subsequently declined below 0.1 % as fermentable sugars were depleted. After the emptying phase, when approximately 7% of the initial culture volume was left in the reactor, the reactor was automatically refilled with fresh medium from a 20-L reservoir, which was continuously sparged with nitrogen gas. After ca. 450 generations of selective growth, single colony isolates were obtained by plating culture samples on SMAGX agar, supplemented with Tween 80 (420mg L^{-1}) and ergosterol (10 mg L^{-1}). Plates were incubated in an anaerobic chamber for 6 days and restreaked three times to obtain single-cell lines.

Plasmid and strain construction. The plasmids constructed and used in this study are shown in Additional File 1. The open reading frames of *AraA* [Genbank: ODO63149.1, encoding L-arabinose isomerase], *AraB* [Genbank: ODO63147.1, encoding L-ribulose kinase] and *AraD* [Genbank: ODO63147.1, encoding L-ribulose-5-phosphate epimerase] were codon optimized based on the codon usage in glycolytic genes in *S. cerevisiae* [86], synthesized behind the promoter of *TPI1*, *PGK1* and *PYK1* originating from CEN.PK113-7D and cloned in pMK-RQ based vectors by GenArt GmbH (Regensburg, Germany). These plasmids were named pUD354-pUD356 and transformed into *E. coli* DH5a cells. Plasmid DNA was isolated from *E. coli* cultures using a GenElute Plasmid kit (Sigma-Aldrich, St. Louis, MO). PCR amplification of expression cassettes and plasmid fragments was performed using Phusion High Fidelity DNA Polymerase (Thermo Scientific, Waltham, MA). *S. cerevisiae* strains were transformed as described by Gietz and Woods [323]. To facilitate CRISPR/Cas9-mediated genome editing in strain *S. cerevisiae* IMX080, a Cas9 expression cassette PCR-amplified from p414-TEF1p-cas9-CYCt using primers 4653-5981 as well as a second fragment containing the amdSYM marker cassette, PCR amplified from pUG-amdSYM with primers 3093-1678 [270], were *in vivo* co-assembled and integrated [249] into the *GAL1* locus through a double cross over mediated by homologous recombination (Additional File 3a). After each transformation round the cells were restreaked thrice and correct integration of all the fragments was confirmed by diagnostic PCR. Transformants

were selected on solid synthetic medium with acetamide [270] as sole nitrogen source and checked by diagnostic PCR using DreamTaq polymerase (Thermo Scientific), according to the manufacturer's protocol. The resulting strain IMX486 was subsequently transformed with 200 pmol each of eight DNA fragments containing expression cassettes for the genes encoding the enzymes of the non-oxidative branch of the pentose phosphate pathway, which were PCR amplified from pUD344-346 and two 500bp fragments containing flanking regions of *GRE3* amplified from CEN.PK113-7D genomic DNA, using oligonucleotide primers shown in Additional File 2. These fragments were co-transformed with 500 ng of plasmid pUDE335 to induce a double strand break in the *GRE3* locus using CRISPR-Cas9 (Additional File 3b). The cells were plated on SMG plates and correct assembly of all six fragments in the *GRE3* locus was verified by diagnostic colony PCR. Plasmid pUDE335 was counter selected on YP with 20 g L^{-1} D-glucose (YPD) agar with 5-fluoroorotic acid (5-FOA) as described previously [137]. The resulting strain IMX604 was then transformed with nine DNA fragments that carried expression cassettes for *araA* and single fragments for *araB* and *araD* amplified from pUD354-356. The primers used for PCR amplification of these fragments added homologous regions required for *in-vivo* assembly and integration into the *GAL80* locus (Additional File 3c). The fragments were co-transformed with gRNA-plasmid pUDE348, which was constructed as described previously [295]. After verification of the correct assembly and integration of the fragments by diagnostic PCR, plasmid pUDE348 was counter selected with 5-FOA, yielding strain IMX658. *HXK2* was deleted by inducing a double strand break using the gRNA plasmid pUDE327, and using an expression cassette for the *PcaraT* gene, obtained by PCR amplification from plasmid Pwt118, as the repair fragment (Additional File 3d). After counter selection of pUDE327 with 5-FOA, a DNA fragment carrying the *URA3* gene from CEN.PK113-7D was amplified using primers 2641-1522 and transformed to restore a wild-type *URA3* gene, yielding strain IMX728. Strain IMX660 was constructed from IMX658 by transforming a KlURA3 based knock-out cassette targeting the *HXK2* locus.

Strain IMX1386 was obtained by co-transforming IMX728 with plasmid pROS13 and a fragment containing the promoter region, ORF and terminator of *GAL2*, PCR amplified from genomic DNA of strain CEN.PK113-7D with primer pair 7285-7286. Transformants were selected on YP with 20 g L^{-1} L-arabinose (YPA) supplemented with G418. After verifying correct integration of the *GAL2* expression cassette in the *CAN1* locus, the gRNA plasmid was counter selected by serial plating on YPA as described previously [137]. The gRNA plasmids pUDR172 and pUDR187 were constructed using pROS13 as template by Gibson assembly according to the method described by Mans *et al.* [137]. The single nucleotide polymorphism (SNP) at position 1127 in *GAL2* was inserted by co-transforming strain IMX660 with pUDR172 and a repair fragment containing the single nucleotide change resulting in the amino acid substitution from N to I at position 376. Expression cassettes of the *GAL2*, *GAL2*^{N376I} and *GAL2*^{N376S} variants were amplified using genomic DNA from CEN.PK113-7D, IMS0520 and IMS0514 as template using the primers F_Gal2_XbaI and R_Gal2_Cfr9I (Supplemental Table S2) and subsequently cloned

into plasmid pRS313-P7T7. To obtain the $GAL2^{N376T}$, $GAL2^{N376T / T89I}$ and $GAL2^{T89I}$ mutants, fragments were PCR amplified from CEN.PK113-7D genomic DNA using the primers shown in Supplemental Table S2. Subsequently, overlap PCR amplifications were done to obtain the full-length genes encoding for $Gal2^{N376T}$, $Gal2^{N376T / T89I}$ and $Gal2^{T89I}$. All genes were cloned into pRS313-P7T7 and subsequently confirmed by Sanger sequencing (Base-clear).

The Gal2 variants and the pRS313-P7T7-mcs plasmid (as an empty plasmid/control) were transformed to the hexose transporter deletion strain DS68625 and positive colonies were named DS68625-Gal2, DS68625-Gal2 N376I, DS68625-Gal2 N376S, DS68625-Gal2 N376T, DS68625-Gal2 N376T / T89I, DS68625-Gal2 T89I and DS68625-mcs. To revert the altered amino acid position 89 in Gal2 from isoleucine to threonine, pUDR187 and a repair fragment containing the original coding sequence were co-transformed. Inactivation of PcAraT in IMS0522 was achieved by in-vivo assembling of the pROS13 backbone and the gRNA expression cassette, both PCR amplified from pROS13 using the primers shown in Additional File 2 and providing a repair oligo for *HXK2*. After verifying correct transformants the plasmids were removed by counter selection on YPAGX plates and the resulting strains were named IMW091 and IMW088 respectively

Analytical methods. To monitor growth of batch cultures, a Libra S11 spectrometer (Biochrom, Cambridge, United Kingdom) was used for optical density measurements at 660 nm. To calculate specific growth rates, biomass dry weight measurements were performed on at least six samples taken during the exponential growth phase. Dry weight measurements were performed by filtering 10 mL culture samples over pre-weighed nitrocellulose filter (pore size, 0.45 μm; Gelman Laboratory, Ann Arbor, MI). The filter was washed with demineralized water and dried in a microwave oven (Bosch, Stuttgart, Germany) for 20 min at 360 W. The correlation between these CDW measurement and the corresponding OD data was used to estimate CDW in samples for which no direct CDW measurements were done. Metabolite concentrations in culture supernatants, obtained by centrifugation, were determined by high-performance liquid chromatography (HPLC)on an Agilent 1260 HPLC (Agilent Technologies, Santa Clara, CA) equipped with a Bio-Rad HPX 87 H column (Bio-Rad, Hercules, CA). The column was eluted at 60 °C with 0.5 g L^{-1} H_2SO_4 at a flow rate of 0.6 ml min^{-1}. Detection was by means of an Agilent G1362A refractive-index detector and an Agilent G1314F VWD detector. CO_2 and O_2 concentrations were measured in bioreactor off gas using an NGA 2000 analyzer (Rosemount Analytical, Orrville, OH) after it was first cooled by a condenser (2 °C) and dried with a Permapure MD-110-48P-4 dryer (Permapure, Toms River, NJ). Correction for ethanol evaporation was done for all bioreactor experiments as described previously [89].

DNA sequence analysis. Genomic DNA for sequencing was isolated using the QIAGEN Blood & Cell Culture Kit With 100/G Genomic-tips (QIAGEN, Valencia, CA) according to

the manufacturer's protocol. DNA libraries were prepared using the Nextera XT DNA library Preparation Kit (Illumina, San Diego, CA), yielding 300bp fragments. The Libraries were sequenced using the Illumina MiSeq platform (Illumina, San Diego, CA, USA). Data were aligned and mapped to the CEN.PK113-7D genome using the Burrows-Wheeler alignment tool [272]. Variant calling by Pilon [273] was checked with the Integrated Genomics Viewer (IGV) [274]. The Poisson mixture model based algorithm Magnolya [275] was used to detect and quantify chromosomal copy number variations (CNV). Copy numbers of *AraA, AraB, AraD* and PcAraT were estimated as described previously using the average read depth of the chromosomes that did not contain any duplication according to the CNV analysis done with Magnolya [295]. Genome sequence data of strains IMS0520, IMS0521, IMS0522, IMS0523, IMS514 and parental strains IMX728 and IMX660 have been deposited at the NCBI Sequence Read archive (www.ncbi.nlm.nih.gov/sra) with the corresponding BioProject ID PRJNA414371. *GAL2* ORFs from strains IMS0002 and IMS0010 and the nucleotides surrounding position T89 in IMS0003 and IMS0007 were PCR amplified from genomic DNA using primers as listed in Additional File 2 and sanger sequenced (Baseclear).

Sugar transport assays. Strains expressing *GAL2* alleles in the DS68625 strain background were pre-grown in aerobic shake flasks on synthetic medium with 20 g L^{-1} D-xylose, after which cells were collected by centrifugation (3000 g, 3 min), washed and resuspended in SM without sugar. Uptake experiments were initiated by adding [^{14}C] L-arabinose or [^{14}C] D-glucose (ARC St. Louis, MO, USA) to the cell suspension at concentrations ranging from 0.2 to 500 mM. [^{14}C] L-arabinose and [^{14}C] D-glucose (50-60 mCi mmol^{-1}) were added at concentrations of 0.1mCi ml^{-1}. At set time points, uptake was arrested by adding 5 mL of ice-cold 0.1 M LiCl, filtration over 0.45-µm HV membrane filters (Millipore, France) and washing with 5 mL ice-cold 0.1 M LiCl. Radioactivity on the filters was then counted using a Liquid Scintillation Counter (PerkinElmer, Waltham, MA) in Ultima Gold MV Scintillation cocktail (PerkinElmer). D-Glucose inhibition experiments were measured using 50 mM [^{14}C] L-arabinose with [^{14}C] D-glucose added at concentrations between 50 and 500 mM.

Results

Construction of a *S. cerevisiae* L-arabinose specialist strain. To investigate uptake and growth on L-arabinose in the presence of D-glucose, an L-arabinose 'specialist strain' was constructed by Cas9-assisted genome editing. First, a Cas9 expression cassette [136] and the counter-selectable marker cassette AmdSYM [270] were *in vivo* assembled and integrated at the *GAL1* locus in *S. cerevisiae* IMX080 (*hxk1Δ glk1Δ*) (Additional File 3a). In the resulting strain IMX486 (*hxk1Δ glk1Δ gal1Δ::{Spcas9*-AmdSYM}, *HXK2* was the sole remaining functional gene encoding a hexose kinase. Subsequently, six cassettes for constitutive expression of *RPE1, RKI1, TKL1, TKL2, TAL1* and *NQM1*, which encode (iso)enzymes of the non-oxidative pentose-phosphate pathway (NPPP), were *in vivo* assembled and integrated at the *GRE3* locus of strain IMX486, yielding strain IMX658 (*hxk1Δ glk1Δ gal1Δ::{Spcas9*-AmdSYM} *gre3Δ::{NPPP}*) (Additional File 3b). Inactivation of *GRE3* prevents xylitol formation by the Gre3 non-specific aldose reductase [7, 250]. To introduce a functional bacterial L-arabinose pathway (ARAP) [84], the *Lactobacillus plantarum* genes encoding L-arabinose isomerase (*AraA*), ribulokinase (*AraB*) and ribulose-5P epimerase (*AraD*) were codon optimized and placed under the control of the strong constitutive promoters of *TPI1*, *PGI1* and *TDH3*, respectively. For high expression of *AraA*, we used the multi-copy tandem integration strategy previously described for high-level expression of xylose isomerase which, in laboratory evolution experiments, facilitates rapid adaptation of copy number by homologous recombination [295]. Using this approach, nine copies of the *AraA* cassette and single copies of the *AraB* and *AraD* cassettes were then integrated at the *GAL80* locus by *in vivo* assembly and Cas9-mediated integration (Additional File 3c). Inactivation of *GAL80* eliminates the need for galactose induction of *GAL2* expression [307, 308, 324]. Expression of the high-affinity L-arabinose transporter PcAraT from *P. chrysogenum* enables L-arabinose uptake in the presence of glucose [322]. To simultaneously abolish the ability to metabolize D-glucose, an expression cassette for PcAraT [322] was integrated into the *HXK2* locus. Subsequent introduction of a functional *URA3* allele from *S. cerevisiae* CEN.PK113-7D (Additional File 3d) yielded the prototrophic 'arabinose specialist' *S. cerevisiae* strain IMX728 (*hxk1Δ glk1Δ gal1Δ::{Spcas9*-AmdSYM} *gre3Δ::{NPPP} hxk2Δ::PcaraT gal80Δ::{ARAP}*).

In aerobic shake flasks on SMA, strain IMX728 exhibited a specific growth rate of 0.26 h^{-1} (Fig. 1). As anticipated after deletion of all four genes encoding glucose-phosphorylating enzymes [112, 123, 176], no growth was observed on SMG. Consistent with the incomplete inhibition of PcAraT by glucose [322], strain IMX728 grew at a specific growth rate of 0.04 h^{-1} in aerobic batch cultures on SMAGX (Fig. 1).
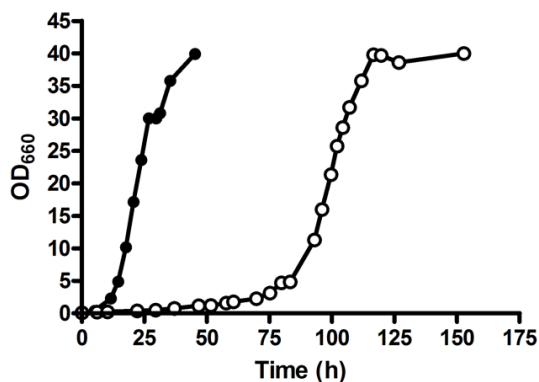
Fig. 1 | Growth curves of *S. cerevisiae* strain IMX728 (engineered, non-evolved arabinose-consuming, glucose-phosphorylation-negative, expressing *PcaraT*) in aerobic batch cultures on synthetic medium containing 20 g L^{-1} L-arabinose (SMA) as sole carbon and energy source (closed circles) and in synthetic medium with 20 g L^{-1} L-arabinose, 20 g L^{-1} D-glucose and 20 g L^{-1} D-xylose added (open circles). Data shown in the figure represent single representative experiments from a set of independent duplicate experiments.
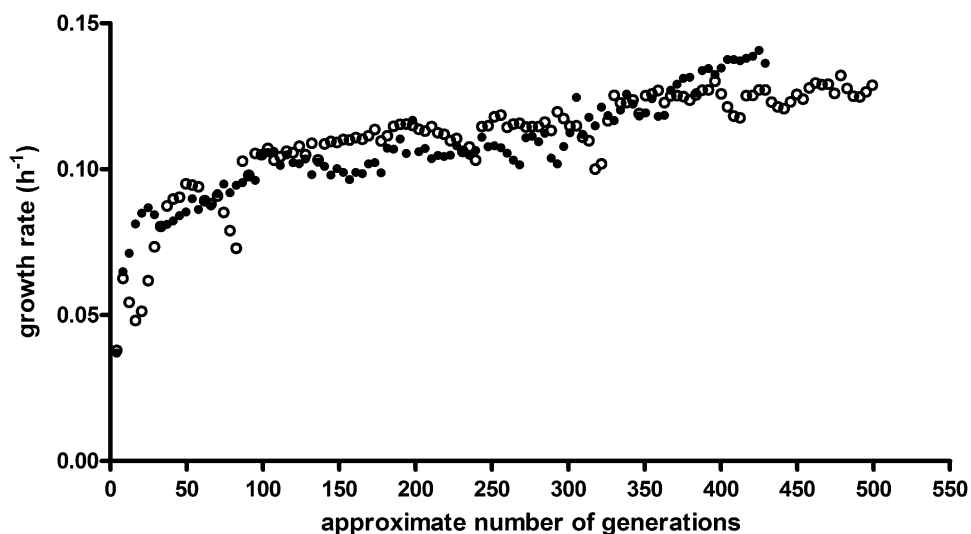
Fig. 2 | Specific growth rate (h^{-1}) estimated from CO_2 production profiles in two parallel laboratory evolution experiments in anaerobic sequential batch reactors SBR 1 (open circles) and SBR 2 (closed circles). Both cultures were inoculated with the L-arabinose consuming, glucose-phosphorylation-negative *S. cerevisiae* strain IMX728 and grown on synthetic medium with 20 g L^{-1} L-arabinose, 20 g L^{-1} D-glucose and 20 g L^{-1} D-xylose. The first data point for each experiment corresponds to the initial aerobic batch cultivation, all subsequent data points represent estimated growth rates in anaerobic SBR cycles.

Anaerobic laboratory evolution of an engineered L-arabinose specialist in the presence of D-glucose. The ability of strain IMX728 to grow anaerobically on L-arabinose as sole carbon source was investigated in anaerobic bioreactors. In contrast to the fast and

instantaneous growth in aerobic shake flasks (Fig. 1), slow anaerobic growth on L-arabinose was only observed after approximately 150 h (Additional File 4). To select for spontaneous mutants that combined an increased anaerobic growth rate on L-arabinose with a decreased sensitivity to growth inhibition by D-glucose and D-xylose, strain IMX728 was grown in duplicate anaerobic sequential batch reactors (SBRs) on SMAGX. Continuous measurements of CO_2 concentrations in the off gas of the SBRs were used to automatically initiate empty-refill cycles and monitor the increase of specific growth rate over time (Additional File 5). After an initial cultivation cycle under aerobic conditions, the first anaerobic cycle required a 17-d period before growth was observed. Only then, within 24 h, both replicate cultures showed an exponential increase in CO_2 production, corresponding to an estimated specific growth rate of 0.07 h^{-1}. Both SBRs were operated for 254 d (Fig. 2), after which specific growth rates had increased to above 0.13 h^{-1}. Specific growth rates on SMAGX of 31 single-colony isolates obtained from the SBR cultures were then measured in anaerobic shake flasks (Additional File 6). Four selected isolates, named IMS0520 to IMS0523, showed specific growth rates of 0.13 to 0.17 h^{-1} in anaerobic bioreactor batch cultures on SMAGX, which corresponded closely to the growth rates estimated from on-line CO_2 analysis of the evolving SBR cultures (Additional File 7).

Evolved strains show mutations, duplication and allelic variation in *GAL2*. To identify the mutations that enabled growth of laboratory-evolved isolates IMS0520-IMS0523 on L-arabinose in the presence of D-glucose and D-xylose, their genomes were sequenced and compared to that of their common parental strain IMX728. Variant screening for nonsynonymous single-nucleotide mutants and insertion/deletions revealed that, together, the four strains carried 9 single-nucleotide mutations in open reading frames (Table 2). All four isolates carried mutations in *GAL2* that changed the asparagine in position 376 of Gal2, into an isoleucine (Gal2^{N376I}) or a threonine (Gal2^{N376T}) in isolates originating from SBR 1 and 2, respectively. Isolate IMS0522 contained an additional single-nucleotide mutation in *GAL2* resulting in a Gal2^{T89I} substitution, which, however, was only observed in 57% of the reads already suggesting a copy number increase of *GAL2* locus.

In addition to mutations in *GAL2*, single-nucleotide changes were identified in *DCK1*, *IPT1 UPC2* and *RPL6B*, which each occurred in only one of the four isolates. *IPT1* encodes an inositol phosphotransferase involved in sphingolipid production [326], while *UPC2* plays a key role in regulation of sterol metabolism and uptake [327]. Both mutations may have affected membrane composition and, thereby, the uptake of L-arabinose. Mutations in *BMH1* were observed in strains IMS0520, IMS0522 and IMS523. In view of the pleiotropic phenotype of *bmh1* mutants [328-331], we decided to not investigate the impact of these mutations on L-arabinose fermentation. Since, *GAL2* was the only transporter gene whose coding region was found to be mutated in strain IMS0521, further analysis was focused on the *GAL2* mutations found in the four strains. [328].

Table 2 | Single-nucleotide mutations in L-arabinose-metabolizing, glucose-phosphorylation-negative *S. cerevisiae* strains IMS0520-IMS0523, evolved for anaerobic growth on L-arabinose in the presence of D-xylose and D-glucose in biological duplicate (reactors 1 and 2). Mutants were identified alignment of the whole-genome sequence data to *S. cerevisiae* IMX728. Read coverage observed for each SNP was higher than 99% unless stated otherwise in the table. Descriptions of gene functions are derived from the *Saccharomyces* Genome Database (as of 19-11-2017).

Gene and strain	Nucleotide change	Amino acid change	Description
GAL2			Galactose permease; required for utilization of galactose and also able to transport glucose.[161]
IMS0520 (reactor 1)	A1127T	N376I	
IMS0521 (reactor 1)	A1127T	N376I	
IMS0522 (reactor 2)	A1127C	N376T	
	C266T (57%)	T89I	
IMS0523 (reactor 2)	A1127C	N376T	
BMH1			14-3-3 protein, major isoform; controls, involved in regulation of exocytosis, vesicle transport, Ras/MAPK and rapamycin-sensitive signalling, aggresome formation, spindle position checkpoint
IMS0520 (reactor 1)	G383T	G128V	
IMS0522 (reactor 2)	G64T	E22*	
IMS0523 (reactor 2)	G64T	E22*	
DCK1			Dock family protein (Dedicator Of CytoKinesis), homolog of human DOCK1; interacts with Ino4p; cytoplasmic protein that relocates to mitochondria under oxidative stress
IMS0522 (reactor 2)	T2890C (42%)	Y964H	
IPT1			Inositolphosphotransferase; involved in synthesis of mannose-(inositol-P)2-ceramide (M(IP)2C) sphingolipid; can mutate to resistance to the antifungals syringomycin E and DmAMP1 and to *K. lactis* zymocin
IMS0522 (reactor 2)	C938T	S313F	
UPC2			Sterol regulatory element binding protein; induces sterol biosynthetic genes, upon sterol depletion; acts as a sterol sensor, binding ergosterol in sterol rich conditions;
IMS0523(reactor 2)	A2648G	Y883C	
RPL6B			Ribosomal 60S subunit protein L6B; binds 5.8S rRNA; homologous to mammalian ribosomal protein L6,
IMS0520 (reactor 1)	T784A	E261G	

As frequently observed in laboratory evolution experiments with *S. cerevisiae* [111, 217], read depth analysis revealed changes in copy number of specific regions in the genomes of the evolved strains (Additional File 8). Notably, regions of Chromosome XII, which harbors *GAL2*, were found to be duplicated in all four isolates, with strain IMS0522 showing a probable duplication of this entire chromosome (Fig. 3). To test the physiological significance of the resulting duplication of *GAL2*, an additional copy of the wild-type *GAL2* allele was integrated in the genome of the parental 'arabinose specialist' IMX728, yielding strain IMS1386. Similar to *S. cerevisiae* IMX728, the strain with two copies of *GAL2* required 120-h before growth on L-arabinose was observed in anaerobic batch cultures (Additional File 9), indicating that duplication of *GAL2* was not, in itself, sufficient to enable instantaneous anaerobic growth on L-arabinose.

4
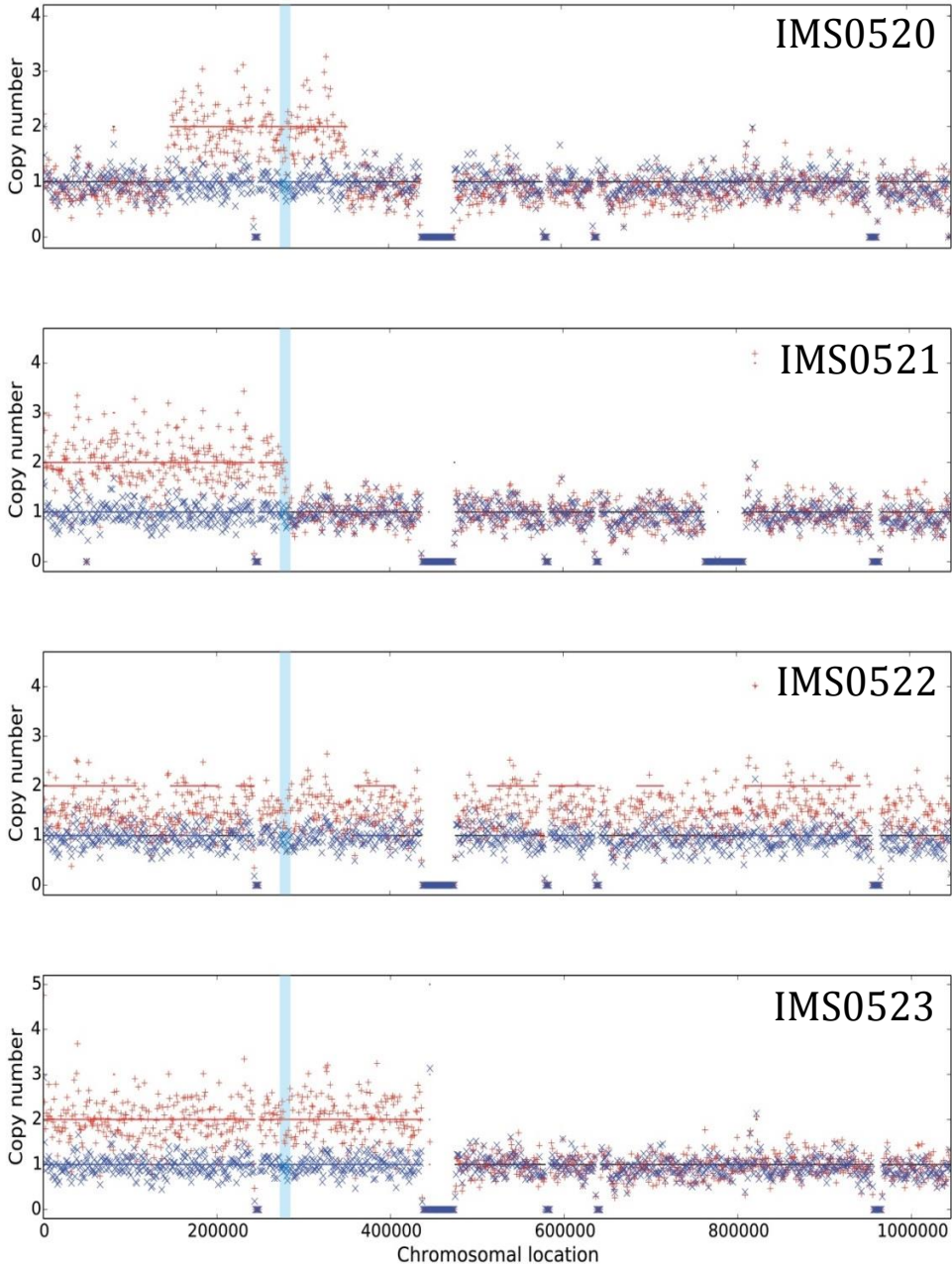
Fig. 3 | Chromosomal copy number estimations for chromosome 12 in the evolved anaerobically ʟ-arabinose-growing, glucose-tolerant *S. cerevisiae* strains IMS0520 to IMS0523. Chromosomal copy numbers were estimated using the Magnolya algorithm[275]. Reads of the four strains (red crosses) show duplications relative to the corresponding chromosome 12 sequences in the common parental strain IMX728 (blue crosses). The light blue region corresponds to the location of *GAL2*.

Table 3 | Estimated copy numbers of the heterologously expressed *Lactobacillus plantarum* genes *AraA*, *AraB* and *AraD* and *Penicillium chrysogenum PcaraT* in the evolved, anaerobically growing and glucose-tolerant 'arabinose specialist' strains *S. cerevisiae* IMS0520-IMS0523, obtained from two independent evolution experiments in sequential batch reactors (1 and 2), and in the parental strain IMX728. Copy numbers were estimated by comparing gene read depths to the average of all chromosomes.

Gene	*reference* IMX728	*Reactor 1* IMS0520	IMS0521	*Reactor 2* IMS0522	IMS0523
araA	17.5	8.7	19.3	19.5	16.4
araB	0.8	0.9	3.1	2.2	1.2
araD	0.9	1.0	1.2	1.0	1.1
PcaraT	0.9	1.1	1.0	1.1	1.2
[1]Excluded chromosomes:		*3, 10, 12, 16*	*2, 8, 12*	*12*	*12, 16*

[1]Chromosomes excluded from the average read depth, based on duplication of chromosomal regions identified with the Magnolya algorithm [38].

Read-depth comparisons of the genes encoding the enzymes of the bacterial L-arabinose pathway (araA, araB, araD) revealed some differences in copy number of *araA* and *araB* between evolved strains and the parental strain (Table 3). However, these differences were not consistent across the four evolved strains. Read-depth analysis of the *PcaraT* transporter gene revealed no copy number changes in any of the four evolved isolates. To examine the contribution of *PcaraT* to the physiology of the evolved strains, it was deleted in evolved strain IMS0522, resulting in strain IMW088. In duplicate anaerobic bioreactor cultures of strains IMS0522 and IMW088 on SMAGX, both completely ferment the L-arabinose in the medium. The strain lacking *PcaraT* (IMW088) did, however, exhibit a lower specific growth rate than strain IMS0522 (0.10 h^{-1} and 0.12h^{-1}, respectively; Table 4) and, consequently, required substantially more time for complete conversion of L-arabinose in the anaerobic batch cultures (Fig. 4).

Table 4 | Specific growth rates, biomass and product yields and carbon recoveries in anaerobic bioreactor batch cultures of *S. cerevisiae* strains IMS0522 (D-glucose-phosphorylation-negative strain evolved for L-arabinose fermentation in presence of D-xylose and D-glucose), IMW088 (IMS0522 with *PcaraTΔ*) and IMW091 (IMS0522 with Gal2^{89I} reverted to Gal2^{89T}) in synthetic medium with 20 g L^{-1} L-arabinose, 20 g L^{-1} D-glucose and 20 g L^{-1} D-xylose. The values are average and mean deviation of data from two independent cultures of each strain.

	μ^{max} (h^{-1})	Yield (g g^{-1} L-arabinose consumed)				Carbon recovery (%)
		Biomass	Ethanol	Glycerol	Acetate	
IMS0522	0.121±0.001	0.075±0.002	0.384±0.004	0.090±0.004	0.018±0.001	96.9±0.1
IMW088	0.102±0.01	0.079±0.005	0.381±0.006	0.094±0.002	0.019±0.002	99.3± 2.1
IMW091	0.069±0.01	0.060±0.005	0.394±0.004	0.088±0.001	0.020±0.001	103.4 ± 1.4

4
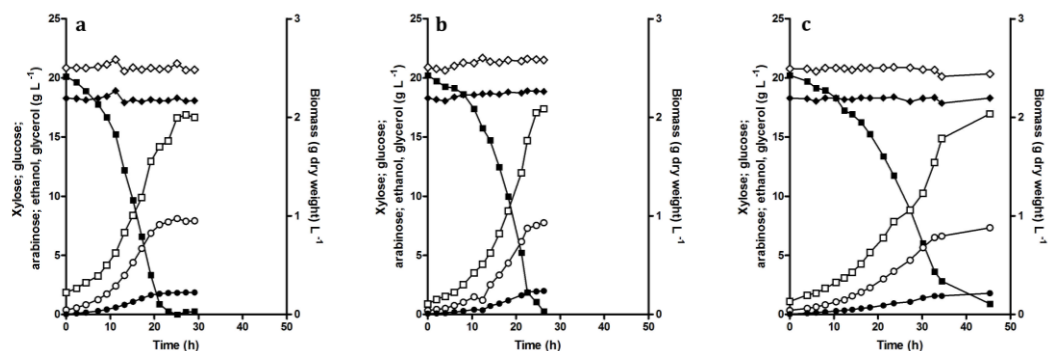
Fig. 4 | Growth and extracellular metabolite concentrations in anaerobic cultures of the evolved L-arabinose consuming, glucose-phosphorylation negative *S. cerevisiae* strain IMS0522 and two derived strains with specific genetic modifications. Cultures were grown in bioreactors containing synthetic medium with 20 g L^{-1} L-arabinose, 20 g L^{-1} D-glucose and 20 g L^{-1} D-xylose. **a.** IMS0522, **b.** IMW088 (*PcaraTΔ*), **c.** IMW091 (Gal2^{89I} restored to Gal2^{89T}). *Closed square* L-arabinose; *open square* biomass dry weight; *closed circle* glycerol; *open circle* ethanol; *closed diamond* D-glucose; *open diamond* D-xylose. Data shown in the figure represent single representative experiments from a set of independent duplicate experiments.

Amino acid substitutions in Gal2 at position N376 enable L-arabinose uptake in the presence of D-glucose and D-xylose. A previous laboratory evolution study with D-xylose-fermenting, glucose-phosphorylation-deficient *S. cerevisiae* strains also identified mutations that led to a single-amino-acid change in Gal2 at position 376, which enabled growth on D-xylose in the presence of D-glucose [123]. In the present study, the parental strain IMX728 could not only import L-arabinose via Gal2, but also via the fungal L-arabinose transporter *Pc*AraT, which is much less sensitive to glucose inhibition than Gal2 [322]. To investigate whether the observed mutations in *GAL2* were also required enable growth on L-arabinose in the presence of D-glucose in a strain background without *PcAraT*, a short laboratory evolution experiment was conducted with the 'arabinose specialist' strain IMX660, which differed from strain IMX728 by the absence of *Pc*AraT. After approximately 100 h incubation in an aerobic shake flask on 20 g L^{-1} L-arabinose and D-glucose, growth was observed and strain IMS0514 was obtained as a single colony isolate and confirmed to have a stable phenotype for growth on SMAG (data not shown). As in strains IMS0520-IMS0523, whole-genome sequencing of strain IMS514 revealed a single mutation in *GAL2* at position 1128, in this case resulting in a Gal2^{N376S} substitution. Additionally, introduction of the Gal2^{N376I} substitution in both *GAL2* alleles of strain IMS0520 enabled immediate growth on SMAG of the arabinose specialist strain lacking *Pc*AraT (IMX1106, Fig. 5).
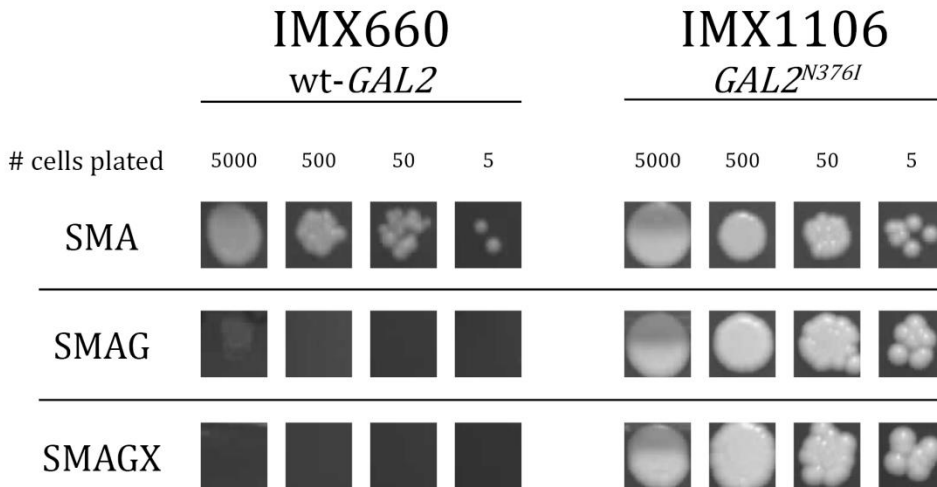
Fig. 5 | Growth of engineered glucose-phosphorylation-negative *S. cerevisiae* strains on L-arabinose in the presence and absence of D-glucose and D-xylose. An approximate set numbers of cells of strain *S. cerevisiae* IMX1106, expressing Gal2 with amino acid substitution N376 and parental strain IMX660 were plated on solid synthetic medium with L-arabinose (SMA), L-arabinose and D-glucose (SMAG) or L-arabinose, D-glucose and D-xylose (SMAGX). Plates were incubated aerobically at 30°C for 4 days .
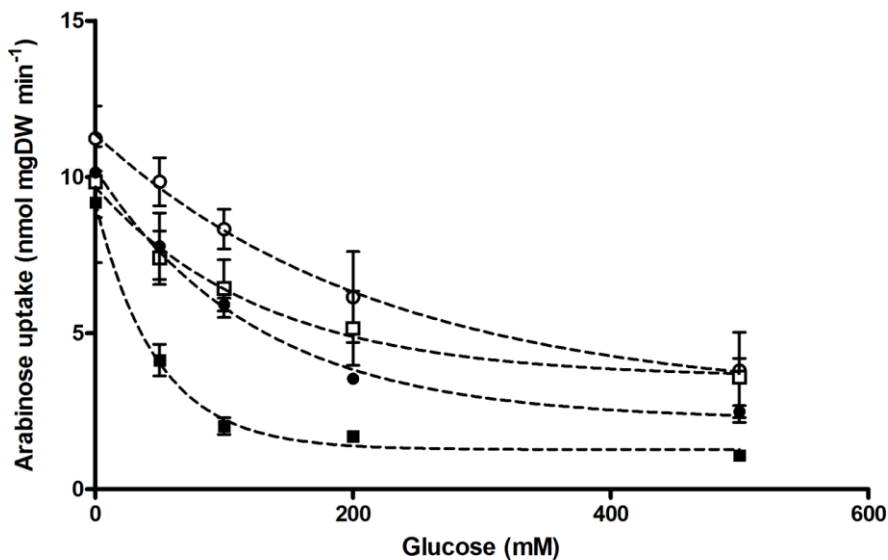
Fig. 6 | Effect of D-glucose on specific rates of L-arabinose uptake by different Gal2 variants. Uptake experiments were performed with 50 mM [^{14}C-] L-arabinose in the presence of different D-glucose concentrations. Symbols indicate uptake rates observed with strain *S. cerevisiae* DS68625 expressing Gal2^{N376T} (*open circles*), Gal2^{N376S} (*closed circles*), Gal2^{N376I} (*open squares*) and wild-type Gal2 (*closed squares*).

Sugar transport kinetics of Gal2 variants obtained by laboratory evolution. To examine inhibition by D-glucose of L-arabinose transport by different Gal2 variants found in evolved strains, the corresponding evolved *GAL2* alleles were expressed in *S. cerevisiae* DS68625. In this strain, which does not express the pathway required for arabinose metabolism, the hexose-transporter genes *HXT1* to *HXT7* and *GAL2* have been disrupted [112]. To examine the extent to which D-glucose inhibited L-arabinose uptake by the different Gal2 variants, [^{14}C]-L-arabinose-uptake experiments were performed at different concentrations of D-glucose (Fig. 6). Consistent with earlier reports [88, 123], uptake of L-arabinose (50 mM) by wild-type Gal2 was inhibited by ca. 80 % in the presence of 100 mM D-glucose (Fig. 6). D-glucose inhibition was not significantly affected by the Gal2^{T89I} substitution but, under the same conditions, L-arabinose uptake by Gal2^{N376I}, Gal2^{N376S} and Gal2^{N376T} was inhibited by only 20-30 % (Fig. 6 and Additional File 10). The Gal2^{N376I}, Gal2^{N376S} and Gal2^{N376T} substitutions yielded 25-60 % lower K_m values for L-arabinose than wild-type Gal2, while their K_m values for D-glucose were one to two orders of magnitude higher than those of wild-type Gal2 (Table 5). As a result, the ratios of the K_m values for L-arabinose vs. D-glucose was 2 orders of magnitude lower for the strains expression Gal2 variants with substitutions at position 376. For Gal2 variants that only carried an amino acid substitution at this position, transport capacities (V_{max}) for L-arabinose and D-glucose differed by less than two-fold from those of wild-type Gal2 (Table 5). These changes in transport kinetics are consistent with a strongly reduced competitive inhibition of L-arabinose transport by D-glucose.

A single Gal2^{T89I} substitution increased the K_m for D-glucose transport from 1.9 to 7mM, while it decreased the K_m for L-arabinose from 335 to 99 mM. For both sugars, the Gal2^{T89I} substitution caused a 2-3 fold reduction of V_{max} (Table 5). These kinetic properties suggest that Gal2^{T89I} may, by itself, confer a selective advantage at low extracellular L-arabinose concentrations. Remarkably, a Gal2 variant that harboured both the Gal2^{N376T} and Gal2^{T89I} substitutions no longer transported D-glucose, while K_m and V_{max} values for L-arabinose were similar to those of Gal2^{T89I} (Table 5).

The Gal2^{T89I} substitution also occurs in a previously evolved pentose-fermenting strain. Strain *S. cerevisiae* IMS0010 is an engineered pentose-fermenting strain that was previously evolved for improved anaerobic fermentation kinetics on mixtures of D-glucose, D-xylose and L-arabinose [13]. Sequence analysis of *GAL2* in IMS0010 showed that this strain contains the same Gal2^{T89I} substitution found in one of the two *GAL2* alleles in the independently evolved glucose-phosphorylation-negative strain IMS0522. Analysis of *GAL2* sequences in two intermediate strains in the construction and laboratory evolution of strain IMS0010 (strains IMS0002 and IMS0007; [13]) showed that this mutation was acquired during the evolution for improved kinetics of mixed-substrate utilisation.

Table 5 | K_m and V_{max} values for L-arabinose and D-glucose for Gal2 variants with amino acid substitutions at positions N376 and T89. Transport kinetics were measured by uptake studies with radioactive sugars

after expression of *GAL2* alleles in *S. cerevisiae* DS68625. Values are average and mean deviation of two independent sets of uptake experiments. The detection limit for D-glucose uptake (V_{max}) was 1.8 nmol^{-1} (mg biomass)$^{-1}$ min^{-1}. Data used to calculate K_m and V_{max} values are shown in Additional File 11.

	K_m (mM)		K_m ratio	V_{max} (nmol (mg biomass)$^{-1}$ min^{-1})	
Gal2 variant	L-arabinose	D-glucose	Ara/Glc	L-arabinose	D-glucose
Gal2[1]	335 ± 21	1.9 ± 0.2	176	75 ± 5	26 ± 1
Gal2[N376I]	117 ± 16	101 ± 47	1	39 ± 3	32 ± 18
Gal2[N376S]	186 ± 33	38 ± 1	5	64 ± 2	28 ± 1
Gal2[N376T]	171 ± 17	57 ± 1	3	65 ± 2	17 ± 4
Gal2[T89I + N376T]	103 ± 40	-	-	30 ± 2	< 1.8
Gal2[T89I]	99 ± 18	7 ± 0.2	15	22 ± 3	13 ± 0.1

Reverting the Gal[T89I] substitution negatively affects L-arabinose consumption. CO_2 production profiles of anaerobic bioreactor batch cultures (Additional File 7) indicated that strain IMS0522, in which one of the two *GAL2* alleles encodes both the Gal2[N376T] and Gal2[T89I] substitutions, grew faster on L-arabinose in the presence of D-glucose and D-xylose than strain IMS0523, in which both copies of *GAL2* only encode the Gal2[N376T] substitution. To investigate whether the additional Gal2[T89I] substitution contributed to this phenotype, the allele encoding this substitution was restored to 'Gal2[N376T] only'. Anaerobic batch cultures of the resulting strain IMW091 on SMAGX showed a substantially reduced specific growth rate relative to its parental strain IMS0522 (0.069 h^{-1} and 0.12 h^{-1}, respectively, Table 4). As a consequence, the time needed to completely ferment L-arabinose in the presence of D-glucose and D-xylose was much shorter for the parental strain IMS0522 (Gal2[N376T]/Gal2[N376T T89I]) than for the strain IMW091 (Gal2[N376T]/Gal2[N376T T]); 25 and 45 h, respectively) (Fig. 4).

Discussion

The *S. cerevisiae* strain used for this evolutionary engineering study combined genetic modifications that were previously shown to enable or stimulate growth on L-arabinose. Combined expression of a bacterial L-arabinose pathway [46, 84, 85], overexpression of native non-oxidative pentose-phosphate-pathway enzymes [7, 84], deletion of the non-specific aldose reductase gene *GRE3* [250], deregulated expression of the Gal2 galactose/L-arabinose transporter [308, 321], here accomplished by deletion of *GAL80* [307, 308, 324], and expression of the fungal L-arabinose transporter *Pc*AraT [322] yielded a strain that, in aerobic shake-flask cultures, exhibited a specific growth rate on L-arabinose of 0.26 h^{-1}. Moreover, deletion of all four genes encoding enzymes with glucose-phosphorylating activity rendered this 'arabinose-specialist' strain *S. cerevisiae* IMX728 unable to

grow on glucose. Construction of this strain was completed within 3 months, which illustrates the power of Cas9-assisted genome editing combined with *in vivo* and *in vitro* DNA assembly methods [136-138, 249].

The specific growth rate of strain IMX728 on L-arabinose in aerobic batch cultures, which was achieved without evolutionary engineering or random mutagenesis, corresponded to ca. 65 % of the specific growth rate on glucose of the parental CEN.PK113-7D strain [291] and is the highest growth rate on L-arabinose hitherto reported for an engineered *S. cerevisiae* strain[84, 86, 332]. However, the targeted genetic modifications in this strain were not sufficient to enable anaerobic growth on L-arabinose. Anaerobic growth on L-arabinose requires that the biomass-specific L-arabinose consumption rate ($q_{arabinose}$) is sufficiently high to meet the ATP requirement for cellular maintenance (ca. 1 mmol ATP (g biomass)$^{-1}$ h^{-1}, [333]). If L-arabinose uptake occurs via Gal2-mediated facilitated diffusion, anaerobic, fermentative metabolism of L-arabinose yields 1.67 ATP, while transport of L-arabinose exclusively via *Pc*AraT-mediated -proton symport would result in a 60 % lower ATP yield [334]. Even if L-arabinose metabolism in the aerobic batch cultures of strain IMX728 would occur exclusively via the energetically much more favorable process of respiratory dissimilation [257, 295], its specific growth rate of 0.26 h^{-1} would still correspond to a $q_{arabinose}$ of at least 3 mmol g^{-1} h^{-1}. This rate of L-arabinose metabolism should be sufficient to meet anaerobic maintenance requirements via fermentative metabolism. The inability of strain IMX728 to instantaneously grow on L-arabinose in anaerobic cultures therefore suggests that it cannot achieve the same $q_{arabinose}$ under those conditions, which might reflect suboptimal expression, folding, membrane environment and/or stability of wild-type Gal2 in anaerobic cultures.

The observation that the two *GAL2* copies in individual strains evolved for anaerobic growth in L-arabinose in the presence of D-glucose and D-xylose encoded the same Gal^{N376} substitution, indicated that these substitutions most probably preceded gene duplication. The importance of these substitutions is further underlined by the observation that introduction of a single copy of the *GAL*^{N376I} allele enabled growth of an 'arabinose specialist' strain on L-arabinose in the presence of glucose and/or L-arabinose under aerobic conditions (Fig. 5). *GAL* genes are transcriptionally regulated via pathways involving Mig1 and Gal80 [324]. In the present study, Gal80-mediated repression was eliminated by deletion of its encoding gene. The observed growth of glucose-phosphorylation-negative strains expressing an evolved *GAL*^{N376} allele on L-arabinose in glucose-containing media indicates that any Mig1-mediated glucose repression of *GAL2* was incomplete. In the glucose-phosphorylation-negative strains, absence of Hxk2, which is involved in Mig1-dependent glucose repression [335] is likely to have glucose derepression of *GAL* genes. Indeed, deletion of *HXK2* has been reported to stimulate co-consumption of glucose and galactose [336]. Additionally, in the same *S. cerevisiae* genetic background, combined deletion of *MIG1*, *GAL6* and *GAL80* was shown not to significantly affect *GAL2* transcript levels [337].

Two previous studies used D-glucose-phosphorylation-negative D-xylose-fermenting strains to evolve for D-glucose tolerance of D-xylose utilization [112, 123]. These studies identified mutations in hexose transporters that reduced D-glucose sensitivity of D-xylose transport. In Gal2, which also transports D-xylose [123] and in a chimera of Hxt3 and Hxt6 (Hxt36) [112], these mutations caused amino acid substitutions at the corresponding positions N376 and N367, respectively. Using in silico models of the three-dimensional structure of Gal2 and Hxt36, based on the crystal structure of the *E. coli* XylE D-xylose/H$^+$ symporter, changes of the amino acid at these positions were predicted to confine the space in the substrate binding pocket for the hydroxymethyl group of D-glucose [112, 123, 338]. Both studies showed that size, charge, polarity and presence of hydrophobic side chains for the substituted amino acid strongly influenced relative transport activities with D-glucose and D-xylose. The present study shows that modifications of Gal2 at this position also enable transport of L-arabinose in the presence of D-glucose. Of the Gal2^{N376} substitutions identified and kinetically analyzed in our study, Gal2^{N376T} showed the highest K_m and lowest V_{max} for D-glucose. Moreover, this substitution decreased the K_m for L-arabinose without affecting V_{max} for uptake of this pentose.

Of the four d-glucose-tolerant evolved strains isolated from the evolution experiments, strain IMS0522 showed significantly better L-arabinose fermentation performance than the other strains. Its L-arabinose consumption rate of 1.6 ± 0.08 g (g biomass)$^{-1}$ h^{-1} and ethanol production rate of 0.61 ± 0.01 g (g biomass)$^{-1}$ h^{-1} in anaerobic cultures are the highest reported to date for an engineered *S. cerevisiae* strain [84, 86, 332]. In addition to a Gal2^{N376T} substitution, one of the *GAL2* copies in this strain encoded an additional Gal2^{T89I} substitution, whose restoration to wild type resulted in a fermentation performance similar to that of the other strains. The physiological relevance of the mutation was further supported by its identification in a strain that was previously evolved for mixed-sugar fermentation [13]. By itself, the Gal2^{T89I} showed a reduced K_m for L-arabinose and an increased K_m for D-glucose, while the V_{max} for both sugars was decreased relative to that of wild-type Gal2. The Gal2^{T89I} variant was also investigated in a recent study that systematically investigated amino acid substitutions at positions within or close to the predicted L-arabinose binding pocket of Gal2 [321]. Subsequent expression of the Gal2^{T89I} substitution did not show a significant effect on the growth rate on L-arabinose [321]. However, our results suggest that, by itself, this substitution is advantageous for L-arabinose uptake in the presence of glucose and/or at low L-arabinose concentrations. Additionally, in the evolved strain IMS0010, in which Gal2 contained only this substitution, the mutations may have contributed to anaerobic co-consumption of L-arabinose and D-xylose [13].

Transport assays with the Gal2^{N376T,T89I} variant showed complete loss of D-glucose transport capacity, combined with a reduced K_m and V_{max} for L-arabinose. In the context of the SBR protocol in which this variant evolved, these kinetic properties are particularly relevant during the growth phase in which the L-arabinose concentration declined, while D-glucose in still present at 20 g L^{-1}. The complete loss of glucose transport

4

activity of the Gal2^{N376T,T89I}, which was encoded by only one of two copies of *GAL2* in the laboratory-evolved strain originating from a duplication of Chromosome XII, underline the importance of chromosomal copy number variations in laboratory evolution and neofunctionalization of duplicated genes [217]. These results from a 500-generation laboratory evolution experiment illustrate how, during evolution in dynamic natural environments, similar duplication and neofunctionalization events, may have contributed to the diverse kinetic characteristics and substrate specificities of the Hxt transporter family in *S. cerevisiae* [167, 339, 340].

In addition to Gal2, the parental strain used in the evolution experiments expressed the fungal L-arabinose transporter *Pc*AraT, which upon expression in *S. cerevisiae* mediates high-affinity, L-arabinose-proton symport (K_m = 0.13 mM) and is much less sensitive to glucose inhibition than wild-type Gal2 [322]. During the evolution experiments, no loss of function mutations were observed in *Pc*AraT. This observation indicates that its presence did not confer a strong selective disadvantage, for example as a result of the activity of a futile cycle caused by simultaneous facilitated diffusion and proton symport of L-arabinose. Moreover, the observations that deletion of *Pc*AraT resulted in decreased specific growth rate on L-arabinose and that presence of *Pc*AraT coincided with a faster consumption of L-arabinose towards the end of anaerobic batch cultures (Fig. 4b), are in line with its reported low V_{max} and low K_m for L-arabinose upon expression in *S. cerevisiae* [322]. These results demonstrate the potential of high-affinity L-arabinose transporters to efficiently convert low concentrations of L-arabinose towards the end of fermentation processes, thereby preventing prolonged 'tailing' of industrial fermentation processes.

Conclusion

Laboratory evolution of engineered, L-arabinose-metabolizing and glucose-phosphorylation-negative *S. cerevisiae* yielded evolved strains that anaerobically fermented L-arabinose in the presence of D-glucose and D-xylose. Amino acid substitutions in Gal2 that affected the kinetics of L-arabinose and D-glucose transport played a key role in this evolution. The best performing evolved strain contained two different mutated alleles of *GAL2*, encoding Gal2 variants with distinct kinetic properties. This result demonstrates the importance of engineering 'transporter landscapes' for uptake of individual sugars, consisting of transporters with complementary kinetic and/or regulatory properties, for efficient sugar conversion in dynamic, mixed-sugar fermentation processes.

Acknowledgements

Renzo Rozenbroek (TUD), Paul de Waal (DSM), Hans de Bruijn (DSM) and Paul Klaassen (DSM) for their input in this project.

Supplementary Material

Additional File 1 | Plasmids used in this study

Plasmid	Characteristic	Source
p414-TEF1p-cas9-CYC1t	*CEN6/ARS4* ampR *pTEF1-cas9-tCYC1*	[136]
pPWT118	KanMX, amdSYM, pADH1_PcAraT_tPMA1	Bracher et al. 2017
pUG-amdSYM	Template for amdS marker	[270]
pUG-72	Template for KlURA3 marker	[292]
pUDE327	2 μm ori, KlURA3, pSNR52-gRNA.HXK2.Y	[294]
pUDE335	2 μm ori, KlURA3, pSNR52-gRNA.GRE3.Y	[295]
pMEL10	pSNR52-gRNA.CAN1.Y-tSUP4	[137]
pROS10	2 μm ori, KlURA3, pSNR52-gRNA.CAN1.Y pSNR52-gRNA.ADE2.Y	[137]
pROS10	2 μm ori, kanMX, pSNR52-gRNA.CAN1.Y pSNR52-gRNA.ADE2.Y	[137]
pUD344	pJET1.2Blunt + TagA_pPGI1_NQM1_TagB	[295]
pUD345	pJET1.2Blunt + TagB_pTPI1_RKI1_Tagc	[295]
pUD346	pJET1.2Blunt + TagC_pPYK1_TKL2_TagF	[295]
pUD347	pJET1.2Blunt + TagG_pTDH3_RPE1_TagH	[295]
pUD348	pJET1.2Blunt + TagH_pPGK1_TKL1_TagI	[295]
pUD349	pJET1.2Blunt + TagI_pTEF1_TAL1_TagA	[295]
pUD354	pMK-RQ_pTPI1_AraA_tADH3	This study
pUD355	pMK-RQ_pPYK1_AraB_tPGI1	This study
pUD356	pMK-RQ_pPGK1_AraD_tTDH3	This study
pUDE348	2 μm ori, KlURA3, pSNR52-gRNA.GAL80.Y	This study
pUDR172	2 μm ori, KlURA3, pSNR52-gRNA.GAL2^{N376}.Y pSNR52-gRNA.GAL2^{N376}.Y	This study
pUDR187	2 μm ori, kanMX, pSNR52-gRNA.GAL2^{I89}.Y pSNR52-gRNA.GAL2^{I89}.Y	This study
pRS313-Gal2	*CEN6/ARS4* ampR *pHXT7-Gal2-tHXT7*	This study
pRS313-Gal2-T	CEN6/ARS4 ampR pHXT7-Gal2-N376T-tHXT7	This study
pRS313-Gal2-S	CEN6/ARS4 ampR pHXT7-Gal2-N376S-tHXT7	This study
pRS313-Gal2-I	CEN6/ARS4 ampR pHXT7-Gal2-N376I-tHXT7	This study
pRS313-Gal2-TI	CEN6/ARS4 ampR pHXT7-Gal2-N376T-T89I-tHXT7	This study
pRS313-PcAraT	CEN6/ARS4 ampR pHXT7-PcAraT-tHXT7	Bracher et al. 2017
pRS313-mcs	CEN6/ARS4 ampR pHXT7-mcs-tHXT7	[112]

Additional File 2 | List of primers used in this study

Primers used for amplification of integration fragments:			
Primer nr.:	Purpose:	Template:	Sequence 5' -> 3':
4653	flGal1-*cas9-A* fragment	p414-TEF1p-cas9-CYC1t	GTGCCTATTGATGATCTGGCGGAATGTCTGCCGTG CCATAGCCATGCCTTCACATATAGTCCGCAAATTA AAGCCTTCGAG
5981	flGal1-*cas9-A* fragment	p414-TEF1p-cas9-CYC1t	TTCACCGGTCGCGTTCCTGAAACGCAGATGTGCCT CGCGCCGCACACCGTATTACCGCCTTTG
3093	A-AmdSYM-flGal80 fragment	pUG-amdSYM	ACTATATGTGAAGGCATGGCTATGGCACGGCAGA CATTCCGCCAGATCATCAATAGGCACCTTCGTACG CTGCAGGTCGAC
1678	A-AmdSYM-flGal80 fragment	pUG-amdSYM	AATGAGAAGTTGTTCTGAACAAAGTAAAAAAAAG AAGTATACTTACATAGGCCACTAGTGGATCTG
5910	flGRE3_G fragment	CEN.PK113-7D	CCACCTGGTGGAACATCCTAGAAC
5911	flGRE3_G fragment	CEN.PK113-7D	AAGGGCCATGACCACCTGATGCACCAATTAGGTAG GTCTGGCTATGTCTATACCTCTGGCCTACCAGCAA CAATTGGGAAAC
7133	fl_*RPE1*_H fragment	pUD347	TATAATATTTCATTATCGGAACTCTAGATTCTATA CTTGTTTCCCAATTGTTGCTGGTAGGGCCCTTCCG GGAGTTTATC
3290	fl_*RPE1*_H fragment	pUD347	GTCACGGGTTCTCAGCAATTCG
3291	H_*TKL1*_I fragment	pUD348	CTCTAACGCCTCAGCCATCATCG
4068	H_*TKL1*_I fragment	pUD348	GCCTACGGTTCCCGAAGTATGC
3274	I_*TAL1*_A fragment	pUD349	TATTCACGTAGACGGATAGGTATAGC
3275	I_*TAL1*_A fragment	pUD349	GTGCCTATTGATGATCTGGCGGAATG
3847	A_*NQM1*_B fragment	pUD344	ACTATATGTGAAGGCATGGCTATGG
3276	A_*NQM1*_B fragment	pUD344	GTTGAACATTCTTAGGCTGGTCGAATC
4672	B_*RKI1*_C fragment	pUD345	CACCTTTCGAGAGGACGATG
3277	B_*RKI1*_C fragment	pUD345	CTAGCGTGTCCTCGCATAGTTCTTAGATTG
3283	C_*TKL2*_F fragment	pUD346	ACGTCTCACGGATCGTATATGC
3288	C_*TKL2*_F fragment	pUD346	TGCCGAACTTTCCCTGTATGAAGC
5936	F_flGRE3	CEN.PK113-7D	CATACGTTGAAACTACGGCAAAGGATTGGTCAGA TCGCTTCATACAGGGAAAGTTCGGCACCCTCATTC CGATGCTGTATATGTG
5937	F_flGRE3	CEN.PK113-7D	ACTGCTTCGTCTAGGTCTTG
6628	flGal80_*AraA*_G fragment	pUD354	TCCTTGCCGACCAGCGTATACAATCTCGATAGTTG GTTTCCCGTTCTTTCCACTCCCGTCCGCGCAGATT AGCGAAGC
6285	flGal80_*AraA*_G fragment	pUD354	AAGGGCCATGACCACCTGATGCACCAATTAGGTAG GTCTGGCTATGTCTATACCTCTGGCGCGATACCCT GCGATCTTC
6273	G_*AraA*_A fragment	pUD354	GCCAGAGGTATAGACATAGCCAGACCTACCTAATT GGTGCATCAGGTGGTCATGGCCCTTCGCGCAGATT AGCGAAGC
6280	G_*AraA*_A fragment	pUD354	GTGCCTATTGATGATCTGGCGGAATGTCTGCCGTG CCATAGCCATGCCTTCACATATAGTGCGATACCCT GCGATCTTC
6270	A_*AraA*_B fragment	pUD354	ACTATATGTGAAGGCATGGCTATGGCACGGCAGA CATTCCGCCAGATCATCAATAGGCACCGCGCAGAT TAGCGAAGC
6281	A_*AraA*_B fragment	pUD354	GTTGAACATTCTTAGGCTGGTCGAATCATTTAGAC ACGGGCATCGTCCTCTCGAAAGGTGGCGATACCCT GCGATCTTC

6271	B_*AraA*_C fragment	pUD354	CACCTTTCGAGAGGACGATGCCCGTGTCTAAATGATTCGACCAGCCTAAGAATGTTCAACCGCGCAGATTAGCGAAGC
6282	B_*AraA*_C fragment	pUD354	CTAGCGTGTCCTCGCATAGTTCTTAGATTGTCGCTACGGCATATACGATCCGTGAGACGTGCGATACCCTGCGATCTTC
6272	C_*AraA*_D fragment	pUD354	ACGTCTCACGGATCGTATATGCCGTAGCGACAATCTAAGAACTATGCGAGGACACGCTAGCGCGCAGATTAGCGAAGC
6284	C_*AraA*_D fragment	pUD354	AATCACTCTCCATACAGGGTTTCATACATTTCTCCACGGGACCCACAGTCGTAGATGCGTGCGATACCCTGCGATCTTC
6283	D_*AraA*_M fragment	pUD354	ACGCATCTACGACTGTGGGTCCCGTGGAGAAATGTATGAAACCCTGTATGGAGAGTGATTGCGATACCCTGCGATCTTC
6275	D_*AraA*_M fragment	pUD354	ACGAGAGATGAAGGCTCACCGATGGACTTAGTATGATGCCATGCTGGAAGCTCCGGTCATCGCGCGAGATTAGCGAAGC
6287	M_*AraA*_N fragment	pUD354	ATGACCGGAGCTTCCAGCATGGCATCATACTAAGTCCATCGGTGAGCCTTCATCTCTCGTGCGATACCCTGCGATCTTC
6276	M_*AraA*_N fragment	pUD354	TTCTAGGCTTTGATGCAAGGTCCACATATCTTCGTTAGGACTCAATCGTGGCTGCTGATCCGCGCAGATTAGCGAAGC
6288	N_*AraA*_O fragment	pUD354	GATCAGCAGCCACGATTGAGTCCTAACGAAGATATGTGGACCTTGCATCAAAGCCTAGAAGCGATACCCTGCGATCTTC
6277	N_*AraA*_O fragment	pUD354	ATACTCCCTGCACAGATGAGTCAAGCTATTGAACACCGAGAACGCGCTGAACGATCATTCCGCGCAGATTAGCGAAGC
6289	O_*AraA*_I fragment	pUD354	GAATGATCGTTCAGCGCGTTCTCGGTGTTCAATAGCTTGACTCATCTGTGCAGGGAGTATGCGATACCCTGCGATCTTC
6274	O_*AraA*_I fragment	pUD354	GCCTACGGTTCCCGAAGTATGCTGCTGATGTCTGGCTATACCTATCCGTCTACGTGAATACGCGCAGATTAGCGAAGC
3274	I_*AraB*_K fragment	pUD355	TATTCACGTAGACGGATAGGTATAGC
6636	I_*AraB*_K fragment	pUD355	GCGAGGACTTCCCATCAATTGC
6634	K_*AraD*_flGal80	pUD356	AAGATAGTCGCCGAACTCGC
6635	K_*AraD*_flGal80	pUD356	CTCAGTATTCGTTTTTATAACGTTCGCTGCACTGGGGGCCAAGCACAGGGCAAGATGCTTTGCCGAACTTTCCCTGTATG
7676	PcAraT fragment	pPWT118	TTTCTAATGCCTTTTCCATCATGTTACTACGAGTTTTCTGAACCTCCTCGCACATTGGTATCTTCACGCGTGTTCGAG
7660	PcAraT fragment	pPWT118	TATAAATATTTATCGTCACGAATAAATCCCGTGAATTTCTAACAAAGTTTATACAATATCTAACCTCGGAAGATCGTCGACAAG
2641	Ura3 repair fragment	CEN.PK113-7D	ATTGCCCAGTATTCTTAACC
1522	Ura3 repair fragment	CEN.PK113-7D	CGAGATTCCCGGGTAATAACTG
2788	*HXK2* KO cassette	pUG-72	ATTGTAGGAATATAATTCTCCACACATAATAAGTACGTTAATATAAACAGCTGAAGCTTCGTACGC
2789	*HXK2* KO cassette	pUG-72	TTAAAAAAAGGGCACCTTCTTGTTGTTCAAACTTAATTTACAAATTAAGTGCATAGGCCACTAGTGGATCTG

10867	*Gal2* expression cassette	CEN.PK113-7D	TTTCAATCTGTCGTCAATCGAAAGTTTATTTCAGA GTTCTTCAGACTTCTTAACTCCTGTACCAGTTTCG CTGCAGAAG
10868	*Gal2* expression cassette	CEN.PK113-7D	TATGAGGGTGAGAATGCGAAATGGCGTGGGAATG TGATTAAAGGTAATAAAACGTCATATGAGATAAC CTCGTCGCTTGG

Primers used for the construction of Gal2 expression plasmids:

Primer name	Purpose:	Template:	Sequence 5' -> 3':
F Gal2 XbaI	Gal2 expression	various	ACTCGTCTAGAATGGCAGTTGAGGAGAACAATATG
R Gal2 Cfr9I	Gal2 expression	various	GCAGCCCGGGTTATACGACTTCTTCGTGAGTGGC

Primers used for the construction of gRNA expression plasmids:

Primer nr.:	Purpose:	Template:	Sequence 5' -> 3':
5792	pUDE348 backbone	pMEL10	GTTTTAGAGCTAGAAATAGCAAGTTAAAATAAG
5980	pUDE348 backbone	pMEL10	CGACCGGTTGCTCTTG
6631	pUDE348 gRNA	pMEL10	ATTTTAACTTGCTATTTCTAGCTCTAAAACAAG ATCTCTTGTTGTAGTCCGATCATTTATCTTTCA CTGCGG
5979	pUDE335 gRNA	pMEL10	TATTGACGCCGGGCAAGAGC
2528	PCR verification of gRNA	pUDE335	tctttcctgcgttatccc
960	PCR verification of gRNA	pUDE335	GTGGATGATGTGGTCTCTAC
6005	pROS13 Backbone	pROS13	GATCATTTATCTTTCACTGCGGAGAAG
9213	PcAraT gRNA	pROS13	TGCGCATGTTTCGGCGTTCGAAACTTCTCCGCA GTGAAAGATAAATGATCagaatcagaggtagaattgtG TTTTAGAGCTAGAAATAGCAAGTTAAAATAAG
9283	Gal2^{N376I} gRNA	pROS13	TGCGCATGTTTCGGCGTTCGAAACTTCTCCGCA GTGAAAGATAAATGATCgttgactacaccaatgacaaG TTTTAGAGCTAGAAATAGCAAGTTAAAATAAGG CTAGTCCGTTATCAAC
9384	Gal2^{I89T} gRNA	pROS13	TGCGCATGTTTCGGCGTTCGAAACTTCTCCGCA GTGAAAGATAAATGATCTGGGATATCGGTACTA TTTCGTTTTAGAGCTAGAAATAGCAAGTTAAAA TAAG

Primers used for verifying integration of fragments:

Primer nr.:	Purpose:	Sequence 5' -> 3':
970	Checking *AraA* integration	CATTTACCGGCGCACTCTCG
6925	Checking *AraA* integration	GGTGCTTTGGAATGGATG
6924	Checking *AraA* integration	TGTTGAGAACCGGTAACG
4692	Checking *AraA* integration	AAGGGCCATGACCACCTG
3275	Checking *AraA* integration	GTGCCTATTGATGATCTGGCGGAATG
4173	Checking *AraA* integration	GTTGAACATTCTTAGGCTGG
3277	Checking *AraA* integration	CTAGCGTGTCCTCGCATAGTTCTTAGATTG
5231	Checking *AraA* integration	AATCACTCTCCATACAGGG
3354	Checking *AraA* integration	ACGCATCTACGACTGTGGGTC
4184	Checking *AraA* integration	ATGACCGGAGCTTCCAGCATG
3843	Checking *AraA* integration	GATCAGCAGCCACGATTG
3837	Checking *AraA* integration	GAATGATCGTTCAGCGCG
4068	Checking *AraA* integration	GCCTACGGTTCCCGAAGTATGC
6926	Checking *AraB* integration	TGTCTACCGCTGGTGAAGGTG
6636	Checking *AraB* integration	GCGAGGACTTCCCATCAATTGC
6928	Checking *AraD* integration	GAGAAAGCACGGTGCTTCTG
971	Checking *AraD* integration	ATAAGAACACCCGCATGCAC
1977	Checking PPP integration	TACCTTCTGCTCTCTCTG

5164	Checking PPP integration	AAAGGATTCGGGCCCAAATCGG
3225	Checking PPP integration	CTGTGATCTCCAGAGCAAAG
2673	Checking PPP integration	TGAAGTGGTACGGCGATGC
3878	Checking PPP integration	gcgGGTACCCGCCTCGTTTCTTTTTCTTC
2913	Checking PPP integration	AATAGCCGCCAGGAAATGCC
1999	Checking PPP integration	CGCGCTCAACCTGGAATTAC
2374	Checking PPP integration	GCAGAAGTGTCTGAATGTATTAAGG
3515	Checking PPP integration	CTGACAGGTGGTTTGTTACG
5603	Checking PPP integration	CGCAAGTTTATCAATGTCGG
3927	Checking PPP integration	AAGAGAATGGACCTATGAACTGATG
5396	Checking PPP integration	CGAATAAACACACATAAACAAACAAAATGGCACAGT TCTCCGACATTG
5937	Checking PPP integration	ACTGCTTCGTCTAGGTCTTG
5910	Checking PPP integration	CCACCTGGTGGAACATCCTAGAAC
4657	Checking PcAraT integration	TTGCGCTAAGAGAATGGACC
5905	Checking PcAraT integration	CTTTTTTTTAGTTTTAAAACACCAAGAACTTAG
4930	Checking Hxk2 deletion	GGCAAGAGTATAGCGTGATACC
3070	Checking Hxk2 deletion	AGTGCTTCCGTTCGTTCCAG
3564	Checking Hxk2 deletion	TTGGTGCTAGAGCTGCTAGATTG
2926	Checking Hxk2 deletion	ATCAATTCCTTTGGCACATCGGC
1638	Checking PcAraT KO	AACCAGCTTCGGTGTGT
5000	Checking PcAraT KO	CTGGGACAAGCAGTAGTGAAAG

Primers used for Sanger sequencing and resctriction analysis of Gal2:

Primer nr.:	Sequence 5' -> 3':
8883	AGTTAAGCCCTTCCCATCTC
909	ATGGCAGTTGAGGAGAACAATATG
8884	TCATGTTTGGCTGGGATACC
8885	TAGGGCTATGTTTCGCTTGG
8886	CAAGTCAGTTGGCCTGGATG
8887	GTCTTCATGGGCTGTTTG
8892	TGCTCGGTGAACAAAGGATG
8891	CACGGTTTGTCGTCATGTTG
8890	GGCGTAGATGACCATACAAG
8889	GCGAAACATAGCCCTAATGG
8888	GGCGACGATTAAACCTGTTC
8381	CTCTACCGCTGTCACTAATGG
8382	GGGCTGTACTAATCCAAGGAG
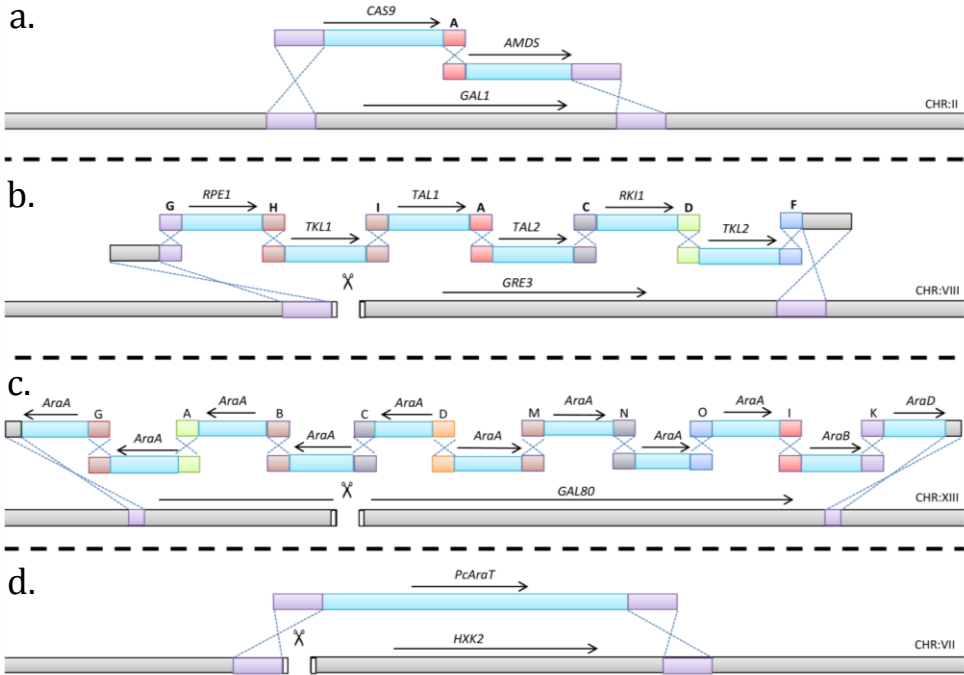
Additional File 3 | Schematic overview of the integrated constructs that result in strain IMX728 (*hxk1Δ glk1Δ gal1Δ::*{Cas9_AmdSYM} *gre3Δ::*{NPPP} *hxk2Δ::PcaraT gal80Δ::*{ARAP}). **a.** fragments with expression cassettes for Cas9 and AmdSYM were cotrasnformed in IMX080. **b.** the fragments with six expression cassettes for genes in the non-oxidative PPP were transformed with pUDE335 allowing for a Cas9-induced double-strand break in *GRE3*. **c.** 11 fragments with 9 times an expression cassette for *AraA* and single fragments for *AraB* and *AraD* were transformed with plasmid pUDE348. **d.** *PcaraT* was integrated in the HXK2 locus using plasmid pUDE327. Correct integration of all the fragments was verified by diagnostic PCR.
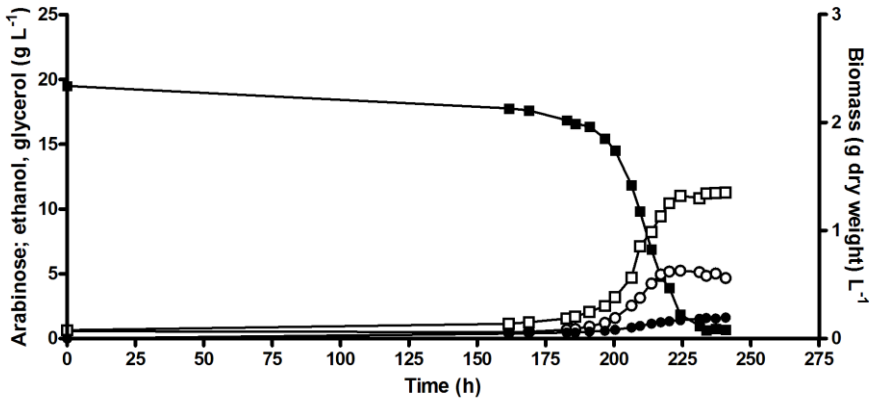
Additional File 4 | Growth and extracellular metabolite concentrations for an anaerobic culture of engineered L-arabinose consuming glucose-phosphorylation negative strain IMX728. The culture was grown in bioreactors containing synthetic medium containing 20 g L^{-1} L-arabinose. *Closed square* L-arabinose; *open square* biomass dry weight; *closed circle* glycerol; *open circle* ethanol. Data obtained from independent duplicate experiments differed less than 5%. Only one of the duplicates is shown in the figure.
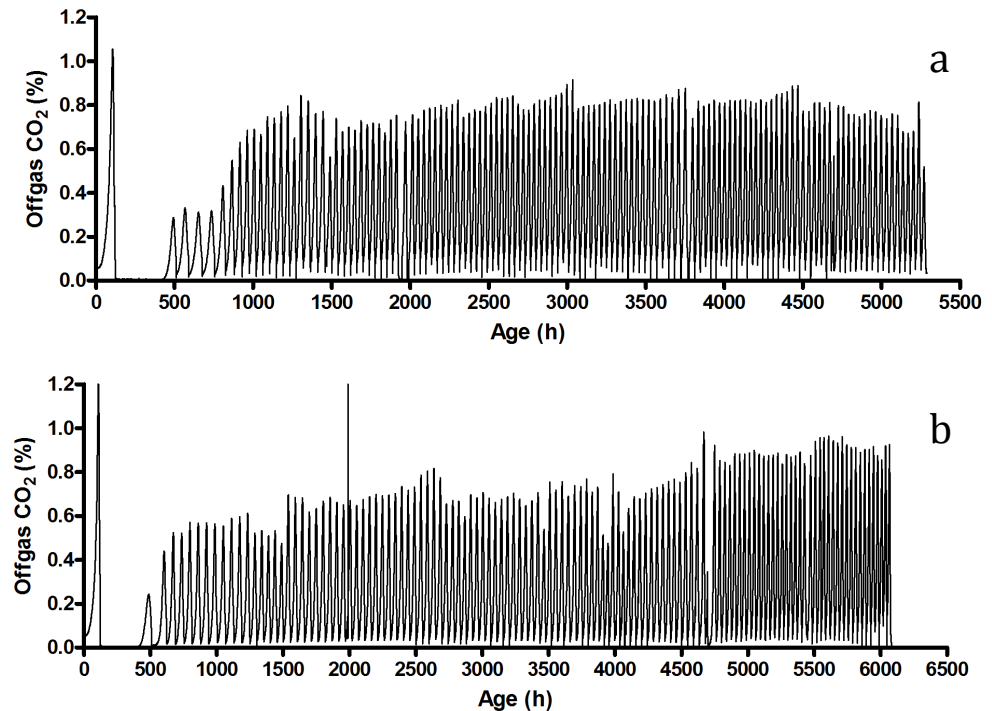
Additional File 5 | CO_2 offgas measurements (%) for both anaerobic sequential batch **a.** reactor 1 and **b.** reactor 2 during laboratory evolution of strain IMX728 (L-arabinose consuming, glucose-phosphorylation-negative) on synthetic medium with 20 g L^{-1} L-arabinose, 20 g L^{-1} D-glucose and 20 g L^{-1} D-xylose. The first CO_2 curve corresponds to the initial aerobic batch prior to switching sparging from air to nitrogen.
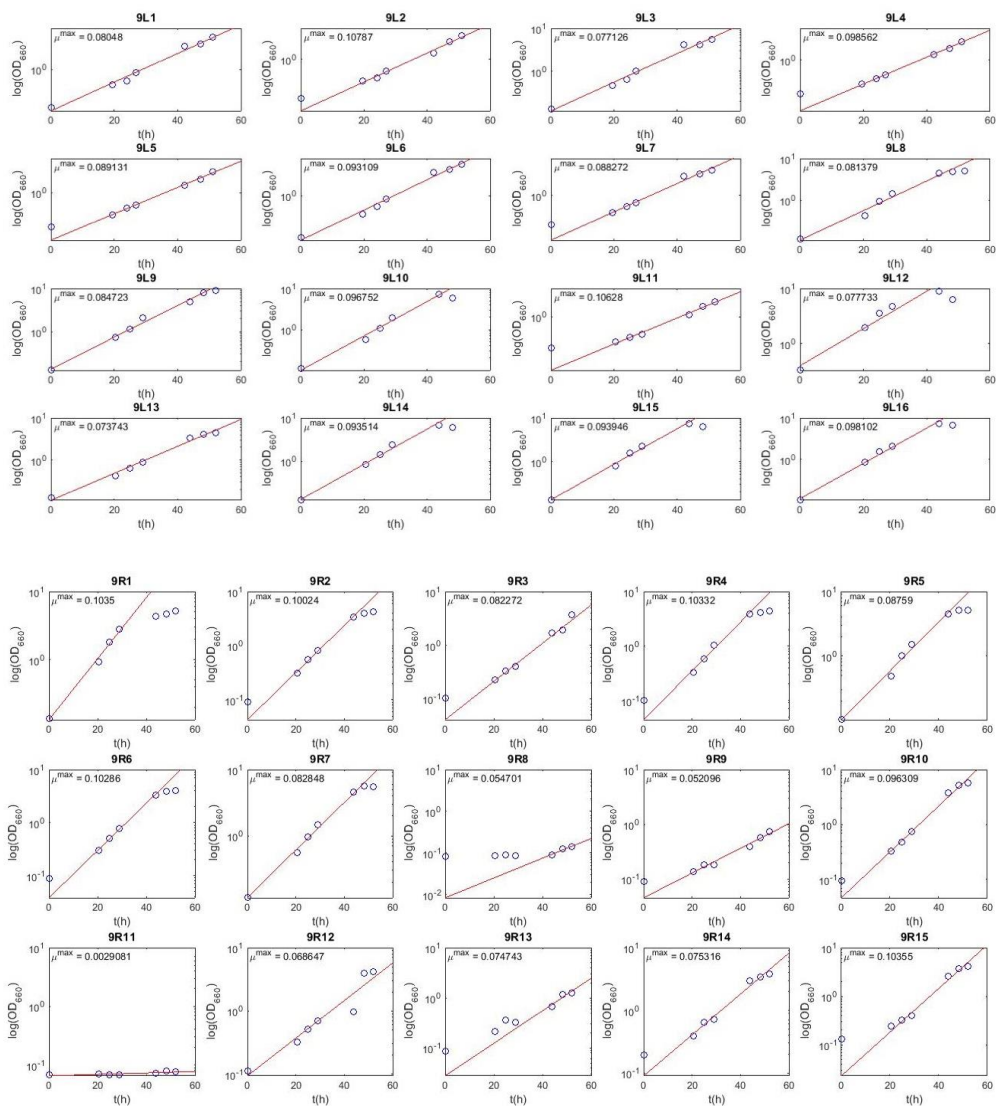
Additional File 6 | Logarithmic plots of OD_{660} measurements for anaerobic shake flask cultures using single colony isolates obtained after laboratory evolution of strain IMX728. Shake flasks were incubated at 30°C in an anaerobic chamber. 9L1-9L16 and 9R1-9R15 correspond to isolates originating from laboratory evolution reactor 1 or 2 respectively. Values shown are averaged from two independent duplicates.

4
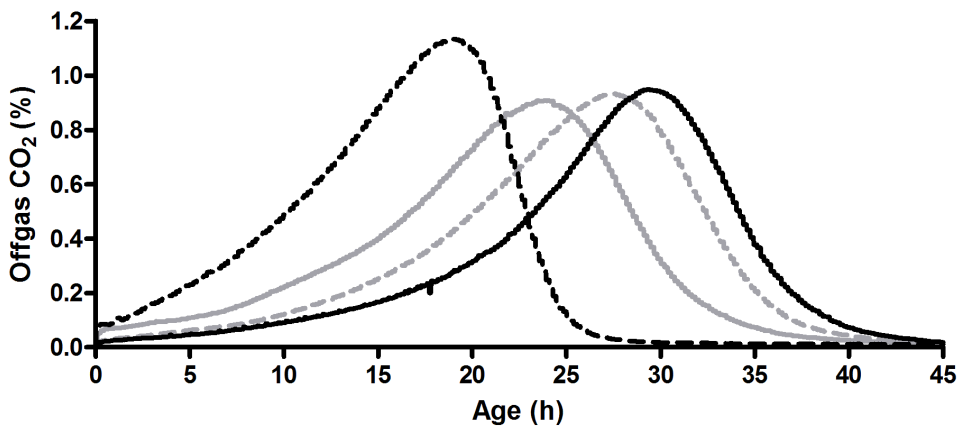
Additional File 7 | CO_2 offgas measurements (%) for four isolates selected after laboratory evolution of IMX728 (L-arabinose consuming, glucose-phosphorylation-negative) on synthetic medium with 20 g L^{-1} L-arabinose, 20 g L^{-1} D-glucose and 20 g L^{-1} D-xylose (SMAGX). Single anaerobic bioreactor cultures of IMS0520 (solid grey), IMS0521 (dashed grey), IMS0522 (dashed black) and IMS523 (solid black) were conducted and monitored on SMAGX at 30°C and pH5.0.
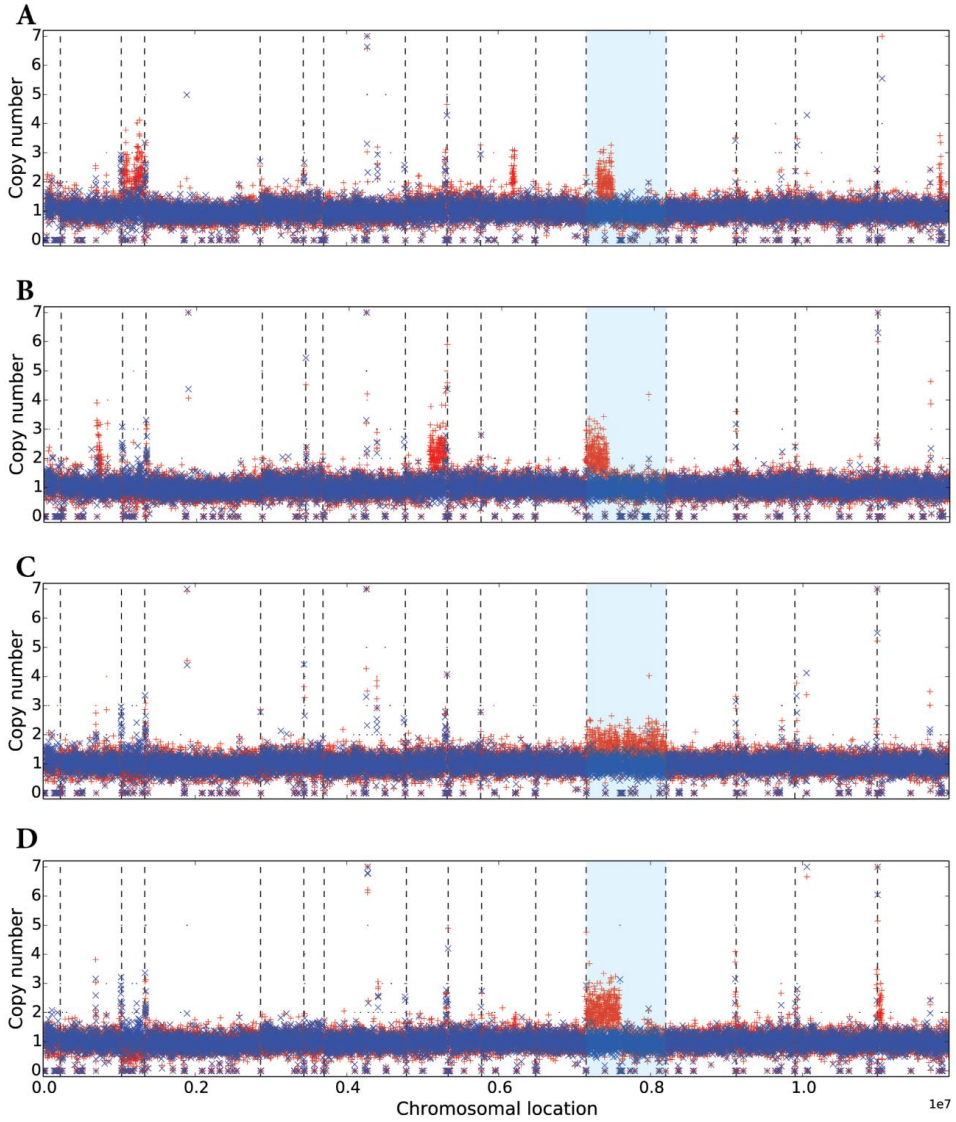
Additional File 8 | Chromosomal copy number prediction of the full *S. cerevisiae* genome estimated using the Magnolya algorithm. Graphs A to D correspond to single colony isolated IMS0520 to IMS0523 respectively. Reads from each isolate (red crosses) show duplications in chromosome 12 compared to parental strain IMX728 (blue crosses). The light blue region corresponds to chromosome 12.
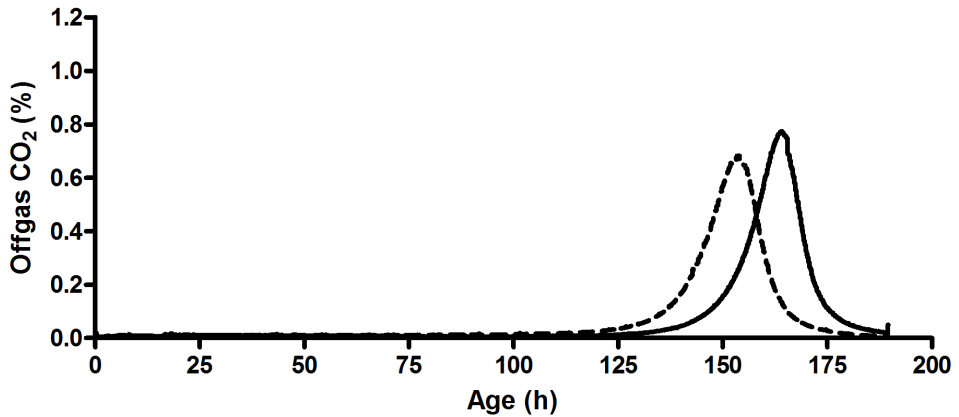
Additional File 9 | CO$_2$ offgas measurements (%) for strain IMX1286 (L-arabinose consuming, glucose-phosphorylation-negative, with an additional copy of Gal2 integrated in the SGA1 locus) on synthetic medium with 20 g L^{-1} L-arabinose. The two curves represent the measurement data of two independent replicate experiments.
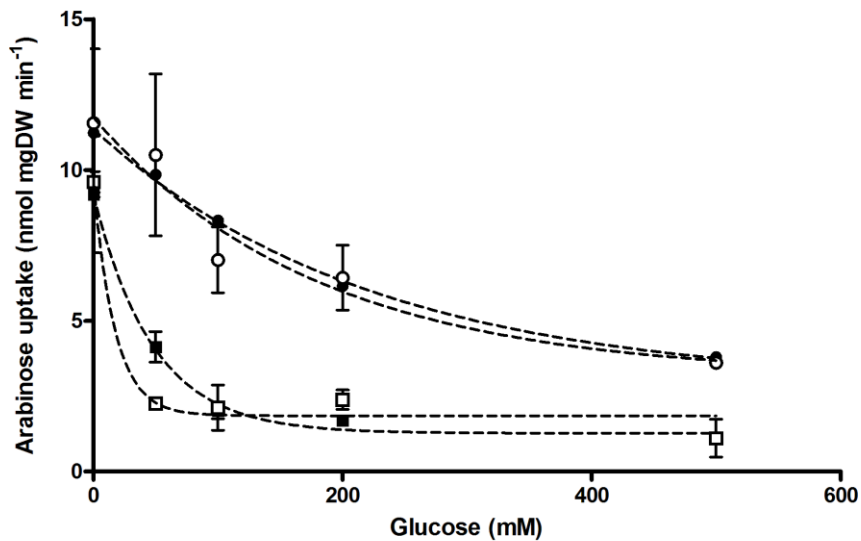
Additional File 10 | Uptake experiments using 50 mM [^{14}C-] L-arabinose in the presence of a range of D-glucose concentrations using strain DS68625 expressing Gal2 variants: N376T+T89I (*open circles*), N376T (*closed circles*), T89I (*open squares*) and Gal2 wild-type (*closed squares*).

4
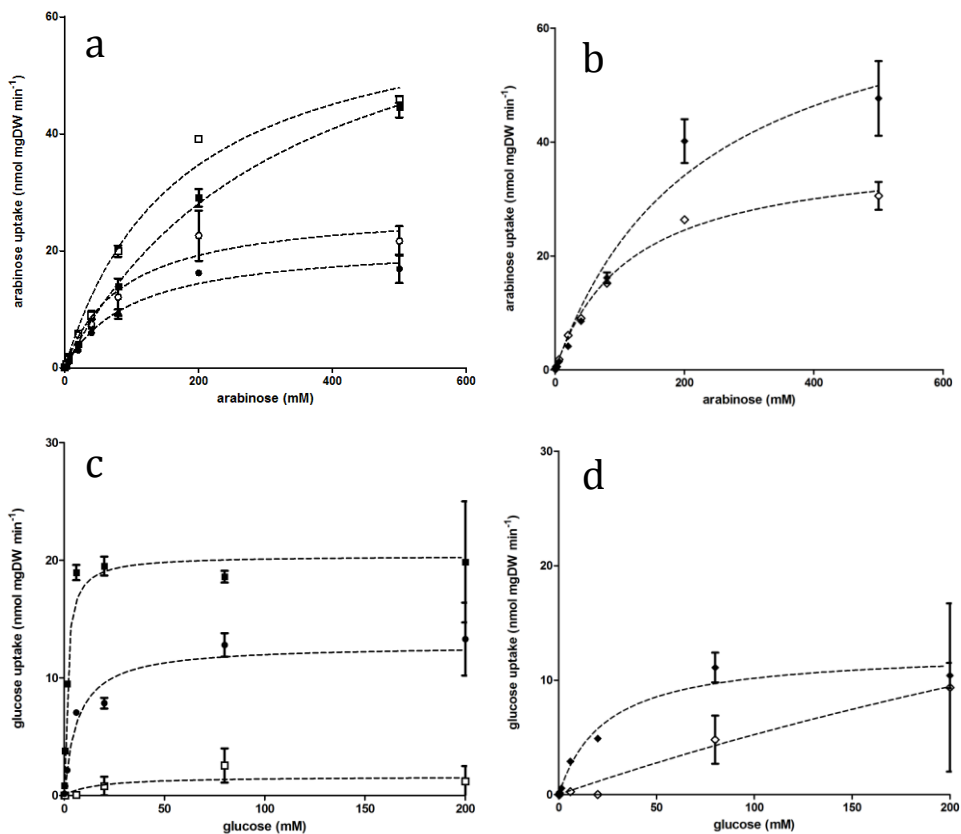
Additional File 11 | Uptake experiments using various concentrations of [^{14}C-] L-arabinose (graph **a.** and **b.**) or [^{14}C-] D-glucose (graph **c.** and **d.**) to determine K_m and V_{max} of strain DS68625 expressing Gal2 variants: T89I (*open circles*), N376T+T89I (*closed circles*), N376T (*open squares*), Gal2 wild-type (*closed squares*), N376S (*closed diamonds*) and N376I (*open diamonds*).

Chapter 5: Laboratory evolution for forced glucose-xylose co-consumption enables identification of mutations that improve mixed-sugar fermentation by xylose-fermenting *Saccharomyces cerevisiae*

Ioannis Papapetridis*, Maarten D. Verhoeven*, Sanne J. Wiersma, Maaike Goudriaan, Antonius J.A. van Maris[a] and Jack T. Pronk[b]
*These authors contributed equally to the presented work

Abstract

Simultaneous fermentation of glucose and xylose can contribute to improved productivity and robustness of yeast-based processes for bioethanol production from lignocellulosic hydrolysates. This study explores a novel laboratory evolution strategy for identifying mutations that contribute to simultaneous utilization of these sugars in batch cultures of *Saccharomyces cerevisiae*. To force simultaneous utilization of xylose and glucose, the genes encoding glucose-6-phosphate isomerase (*PGI1*) and ribulose-5-phosphate epimerase (*RPE1*) were deleted in a xylose-isomerase-based xylose-fermenting strain with a modified oxidative pentose-phosphate pathway. Laboratory evolution of this strain in serial batch cultures on glucose-xylose mixtures yielded mutants that rapidly co-consumed the two sugars. Whole-genome sequencing of evolved strains identified mutations in *HKX2*, *RSP5* and *GAL83*, whose introduction into a non-evolved xylose-fermenting *S. cerevisiae* strain improved co-consumption of xylose and glucose under aerobic and anaerobic conditions. Combined deletion of *HXK2* and introduction of a *GAL83^{G673T}* allele yielded a strain with a 2.5-fold higher xylose and glucose co-consumption ratio than its xylose-fermenting parental strain. These two modifications decreased the time required for full sugar conversion in anaerobic bioreactor batch cultures, grown on 20 g L^{-1} glucose and 10 g L^{-1} xylose, by over 24 h. This study demonstrates that laboratory evolution and genome resequencing of microbial strains engineered for forced co-consumption is a powerful approach for studying and improving simultaneous conversion of mixed substrates.

Introduction

Industrial biotechnology can contribute to reconciliating global demands for liquid transport fuels with the almost universally accepted need to limit anthropogenic CO_2 emissions [341]. Bioethanol, the biofuel with the largest annual global production volume, is still predominantly produced by fermentation of sucrose or glucose, derived from sugar cane or corn starch, respectively [342]. These 'first-generation' bioethanol processes exploit the natural high fermentation rates and ethanol yield of the yeast *Saccharomyces cerevisiae*. Optimization of yeast strains and production processes enables many industrial processes to operate at >90% of the theoretical ethanol yield on sugar [17, 342, 343]. However, the massive scaling up of production volumes that would be required to replace a substantial fraction of petroleum-based transport fuels cannot be sustainably achieved with corn starch and cane sugar as only feedstocks. Instead, a large fraction of the feedstock will have to be derived from lignocellulosic plant biomass, such as agricultural residues and energy crops [344].

In comparison with first-generation feedstocks, lignocellulosic hydrolysates pose additional challenges for yeasts and yeast researchers. In addition to containing mixtures of hexose and pentose (mainly D-xylose and L-arabinose) sugars, the deconstruction of lignocellulosic biomass that precedes yeast-based fermentation releases fermentation inhibitors [52, 206, 279]. Intensive metabolic engineering studies, encompassing functional expression of heterologous pathways for xylose and arabinose catabolism, improvements in inhibitor tolerance and minimization of by-product formation have yielded *Saccharomyces cerevisiae* strains that are now applied in the first full-scale 'second-generation' industrial bioethanol plants [175, 279]. However, further improvements in ethanol titers, yields and productivities are important to increase the economic viability of this nascent technology.

Current strain engineering strategies for enabling pentose fermentation by *S. cerevisiae* typically yield strains that, in anaerobic batch cultures grown on sugar mixtures, preferentially ferment glucose, while xylose and/or arabinose are predominantly converted in a second, slower fermentation phase [279]. This strong preference for glucose over pentoses persists even after extensive laboratory evolution on sugar mixtures [9, 11, 13, 103, 345]. Achieving efficient co-fermentation of glucose and pentoses, while maintaining a high overall rate of sugar conversion, could increase volumetric productivity of industrial processes. Moreover, since several inhibitors of yeast performance are more harmful during the slower pentose fermentation phase [172-174, 279], simultaneous fermentation of glucose and pentose sugars can also contribute to robustness under industrial process conditions.

Random mutagenesis, laboratory evolution and protein engineering of xylose transporters has yielded transporter variants with improved xylose affinity and reduced glucose inhibition, which enabled the construction of yeast strains with improved xylose consumption in the presence of glucose [112, 123, 125, 126]. In an alternative approach,

expression of a heterologous cellodextrin transporter and an intracellular *β*-glucosidase, along with a heterologous xylose reductase/xylitol dehydrogenase pathway, enabled simultaneous consumption of cellobiose and xylose in *S. cerevisiae* by reducing the impact of glucose repression [346]. However, despite progress in this area, engineering of yeast strains showing simultaneous, fast fermentation of glucose and xylose remains a key challenge.

Deletion of *RPE1*, which encodes the pentose-phosphate-pathway (PPP) enzyme ribulose-5-phosphate epimerase, was recently shown to result in coupling of glucose and xylose catabolism, at a ratio of 10:1, in an engineered xylose-utilizing *S. cerevisiae* strain [347]. Despite a low xylose-to-glucose consumption ratio, this strategy indicated the potential of forced stoichiometric coupling of glucose and pentose metabolism in *S. cerevisiae*. In *S. cerevisiae*, phosphoglucose isomerase (Pgi1) catalyses interconversion of glucose-6-phosphate to fructose-6-phosphate in upper glycolysis [348]. Since deletion of *PGI1* blocks glycolysis, *pgi1Δ* strains cannot grow on glucose as the sole carbon source unless all glucose-6-phosphate is rerouted through the pentose-phosphate pathway. Deletion of *eda*, *rpe* and *pgi* in *E. coli* was previously shown to enable co-consumption of xylose and glucose [349]. As conversion of 1 mol glucose-6-phosphate to 1 mol ribulose-5-phosphate via the oxidative branch of the PPP results in a net generation of 2 mol NADPH, the absence of a redox imbalance relied on conversion of excess NADPH to NADH by the native *E. coli* transhydrogenases.

Wild-type *S. cerevisiae* strains cannot reoxidize all NADPH generated by such a redirection of metabolism and, consequently, *pgi1*-null mutants cannot grow on glucose as sole carbon source [350, 351]. Overexpression of *GDH2*, which encodes NAD$^+$-dependent glutamate dehydrogenase, can restore growth of *pgi1Δ* strains by enabling a transhydrogenase-like cycle that couples the interconversion of 2-oxoglutarate and glutamate to the conversion of NADPH and NAD$^+$ to NADP$^+$ and NADH [350]. Based on the impact of a *pgi1Δ* mutation on glucose metabolism, we reasoned that inactivation of *PGI1* might be used to construct strains with a stringent requirement for co-utilization of xylose and glucose, at much higher ratios than hitherto demonstrated.

The goal of this study was to explore a new strategy for identifying mutations that stimulate glucose-xylose co-consumption by *S. cerevisiae*. The strategy was based on enforcing a strict stoichiometric coupling of glucose and xylose fermentation by the combined deletion of *RPE1* and *PGI1* in an engineered, xylose-isomerase-based *S. cerevisiae* strain [7, 295]. Furthermore, to reduce the impact of these modifications on NADP$^+$/NADPH redox cofactor balancing, the native NADP$^+$-dependent 6-phosphogluconate dehydrogenases (Gnd1 and Gnd2) were replaced by a heterologous NAD$^+$-dependent enzyme [91]. After laboratory evolution for improved growth on glucose-xylose mixtures, the physiology of evolved strains was analysed in aerobic shake-flask and bioreactor batch cultures. Potential causal mutations identified by whole-genome sequencing were introduced into a non-evolved (*PGI1 RPE1 GND1 GND2*) xylose-fermenting

strain background. The resulting reverse engineered strains were then analysed in shake-flask and anaerobic bioreactor batch cultures, grown on mixtures of glucose and xylose.

Materials and Methods

Maintenance of strains. The CEN.PK lineage of *S. cerevisiae* laboratory strains [251] was used to construct and evolve all strains used in this study (Table 1). Depending on strain auxotrophies, cultures were grown in YP (10 g L^{-1} yeast extract, 20 g L^{-1} peptone) (BD, Franklin Lakes, NJ) or synthetic medium (SM) [51], supplemented with glucose (20 g L^{-1}), xylose (20 g L^{-1}), a glucose/xylose mixture (10 g L^{-1} of each sugar) or a xylose/fructose/glucose mixture (20, 10 and 1 g L^{-1} respectively). Propagation of *E. coli XL-1* Blue cultures was performed in LB medium (5 g L^{-1} Bacto yeast extract, 10 g L^{-1} Bacto tryptone, 5 g L^{-1} NaCl, 100 µg mL^{-1} ampicillin). Frozen stock cultures were stored at -80 °C, after addition of glycerol (30% v/v final concentration).

Table 1 | Strains used in this study.

Strain name	Relevant Genotype	Origin
CEN.PK113-7D	*MATa MAL2-8c SUC2 CAN1*	[251]
IMX581	*MATa ura3-52 MAL2-8c SUC2 can1::cas9-natN2*	[137]
IMX705	*MATa MAL2-8c SUC2 can1::cas9-natNT2 gnd2Δ gnd1::gndA*	[91]
IMX963	*MATa MAL2-8c SUC2 can1::cas9-natNT2 gnd2Δ gnd1::gndA gre3::ZWF1, SOL3, TKL1, TAL1, NQM1, RKI1, TKL2*	This work
IMX990	*MATa MAL2-8c SUC2 can1::cas9-natNT2 gnd2Δ gnd1:: gndA gre3::ZWF1, SOL3, TKL1, TAL1, NQM1, RKI1, TKL2 sga1::9*xylA,XKS1*	This work
IMX1046	*MATa MAL2-8c SUC2 can1::cas9-natNT2 gnd2Δ gnd1::gndA gre3::ZWF1, SOL3, TKL1, TAL1, NQM1, RKI1, TKL2 sga1::9*xylA, XKS1 rpe1Δ pgi1Δ*	This work
IMS0628	*MATa MAL2-8c SUC2 can1::cas9-natNT2 gnd2Δ gnd1::gndA gre3::ZWF1, SOL3, TKL1, TAL1, NQM1, RKI1, TKL2 sga1::9*xylA, XKS rpe1Δ pgi1Δ* Evolved isolate 1	This work
IMS0629	*MATa MAL2-8c SUC2 can1::cas9-natNT2 gnd2Δ gnd1::gndA gre3::ZWF1, SOL3, TKL1, TAL1, NQM1, RKI1, TKL2 sga1::9*xylA, XKS rpe1Δ pgi1Δ* Evolved isolate 2	This work
IMS0630	*MATa MAL2-8c SUC2 can1::cas9-natNT2 gnd2Δ gnd1::gndA gre3::ZWF1, SOL3, TKL1, TAL1, NQM1, RKI1, TKL2 sga1::9*xylA, XKS rpe1Δ pgi1Δ* Evolved isolate 3	This work
IMS0634	*MATa MAL2-8c SUC2 can1::cas9-natNT2 gnd2Δ gnd1::gndA gre3::ZWF1, SOL3, TKL1, TAL1, NQM1, RKI1, TKL2 sga1::9*xylA, XKS rpe1Δ pgi1Δ* Evolved isolate 4	This work
IMS0635	*MATa MAL2-8c SUC2 can1::cas9-natNT2 gnd2Δ gnd1::gndA gre3::ZWF1, SOL3, TKL1, TAL1, NQM1, RKI1, TKL2 sga1::9*xylA, XKS rpe1Δ pgi1Δ* Evolved isolate 5	This work
IMS0636	*MATa MAL2-8c SUC2 can1::cas9-natNT2 gnd2Δ gnd1::gndA gre3::ZWF1, SOL3, TKL1, TAL1, NQM1, RKI1, TKL2 sga1::9*xylA, XKS rpe1Δ pgi1Δ* Evolved isolate 6	This work

IMX994	*MATa ura3-52 MAL2-8c SUC2 can1::cas9-natN2, gre3::RPE1, TKL1, TAL1, RKI1, XKS1*	This work
IMU079	*MATa ura3-52 MAL2-8c SUC2 can1::cas9-natN2, gre3::RPE1, TKL1, TAL1, RKI1, XKS1* pAKX002	This work
IMX1384	*MATa ura3-52 MAL2-8c SUC2 can1::cas9-natNT2 gre3::RPE1, TKL1, TAL1, RKI1, XKS1 hxk2Δ* pUDE327	This work
IMX1385	*MATa ura3-52 MAL2-8c SUC2 can1::cas9-natNT2 gre3::RPE1, TKL1, TAL1, RKI1, XKS1 gal83Δ* pMEL10.*GAL83*	This work
IMX1442	*MATa ura3-52 MAL2-8c SUC2 can1::cas9-natNT2 gre3::RPE1, TKL1, TAL1, RKI1, XKS1 rsp5Δ* pMEL10.*RSP5*	This work
IMX1408	*MATa ura3-52 MAL2-8c SUC2 can1::cas9-natNT2 gre3::RPE1, TKL1, TAL1, RKI1, XKS1 hxk2Δ*	This work
IMX1409	*MATa ura3-52 MAL2-8c SUC2 can1::cas9-natNT2 gre3::RPE1, TKL1, TAL1, RKI1, XKS1 gal83Δ*	This work
IMX1451	*MATa ura3-52 MAL2-8c SUC2 can1::cas9-natNT2 gre3::RPE1, TKL1, TAL1, RKI1, XKS1 rsp5Δ*	This work
IMX1453	*MATa ura3-52 MAL2-8c SUC2 gre3::RPE1, TKL1, TAL1, RKI1, XKS1 gal83::GAL83[G673T]*	This work
IMX1484	*MATa ura3-52 MAL2-8c SUC2 gre3::RPE1, TKL1, TAL1, RKI1, XKS1 rsp5Δ hxk2Δ* pUDE327	This work
IMX1485	*MATa ura3-52 MAL2-8c SUC2 gre3::RPE1, TKL1, TAL1, RRKI1, XKS1 hxk2Δ* pAKX002	This work
IMX1486	*MATa ura3-52 MAL2-8c SUC2 gre3::RPE1, TKL1, TAL1, RKI1, XKS1 gal83Δ* pAKX002	This work
IMX1487	*MATa ura3-52 MAL2-8c SUC2 gre3::RPE1, TKL1, TAL1, RKI1, XKS1 rsp5Δ* pAKX002	This work
IMX1488	*MATa ura3-52 MAL2-8c SUC2 gre3::RPE1, TKL1, TAL1, RKI1, XKS1 gal83::GAL83[G673T]* pAKX002	This work
IMX1510	*MATa ura3-52 MAL2-8c SUC2 gre3::RPE1, TKL1, TAL1, RKI1, XKS1 rsp5Δ hxk2Δ*	This work
IMX1515	*MATa ura3-52 MAL2-8c SUC2 gre3::RPE1, TKL1, TAL1, RKI1, XKS1 rsp5Δ hxk2Δ* pAKX002	This work
IMX1563	*MATa ura3-52 MAL2-8c SUC2 gre3::RPE1, TKL1, TAL1, RKI1, XKS1 gal83::GAL83[G673T] hxk2Δ* pUDE327	This work
IMX1571	*MATa ura3-52 MAL2-8c SUC2 gre3::RPE1, TKL1, TAL1, RKI1, XKS1 gal83::GAL83[G673T] hxk2Δ*	This work
IMX1583	*MATa ura3-52 MAL2-8c SUC2 gre3::RPE1, TKL1, TAL1, RKI1, XKS1 gal83::GAL83[G673T] hxk2Δ* pAKX002	This work

Construction of plasmids and cassettes PCR amplification for construction of plasmid fragments and yeast integration cassettes was performed with Phusion High Fidelity DNA Polymerase (Thermo-Scientific, Waltham, MA), according to the manufacturer's guidelines. Plasmid assembly was performed *in vitro* with a Gibson Assembly Cloning kit (New England Biolabs, Ipswich, MA), following the supplier's guidelines, or *in vivo* by transformation of plasmid fragments into yeast cells [249]. For all constructs, correct assembly was confirmed by diagnostic PCR with DreamTaq polymerase (Thermo-Scientific), following the manufacturer's protocol. Plasmids used and constructed in this work are described

in Table 2. All yeast genetic modifications were performed using CRISPR/Cas9-based ge-
nome editing [137]. Unique guide-RNA (gRNA) sequences targeting *GRE3*, *GAL83* and
RSP5 were selected from a publicly available list [136] and synthesized (Baseclear, Leiden,
The Netherlands). Primers and oligonucleotides used in this work are listed in Additional
File 1.

Table 2 | Plasmids used in this study.

Plasmid	Characteristics	Origin
pMEL10	2 μm, *KlURA3*, p*SNR52*-gRNA.*CAN1-tSUP4*	[137]
pMEL11	2 μm, *amdS*, p*SNR52*-gRNA.*CAN1-tSUP4*	[137]
pROS11	*amdS*, gRNA.*CAN1*-2 μm ori-gRNA.*ADE2*	[137]
pUDE335	2 μm, *KlURA3*, p*SNR52*-gRNA.*GRE3-tSUP4*	[295]
pUD344	p*PGI1-NQM1*-t*NQM1* PCR template vector	[295]
pUD345	p*TPI1-RKI1*-t*RKI1* PCR template vector	[295]
pUD346	p*PYK1-TKL2*-t*TKL2* PCR template vector	[295]
pUD347	p*TDH3-RPE1*-t*RPE1* PCR template vector	[295]
pUD348	p*PGK1-TKL1*-t*TKL1* PCR template vector	[295]
pUD349	p*TEF1-TAL1*-t*TAL1* PCR template vector	[295]
pUD350	p*TPI1-xylA*-t*CYC1* PCR template vector	[295]
pUD353	p*TEF1-XKS1*-t*XKS1* PCR template vector	[295]
pUD426	p*ADH1-ZWF1*-t*ZWF1* PCR template vector	This work
pUD427	p*ENO1-SOL3*-t*SOL3* PCR template vector	This work
pUDR119	2 μm ori, *amdS*, p*SNR52*-gRNA.*SGA1-tSUP4*	[352]
pUDR202	*amdS*, gRNA.*RPE1*-2 μm ori-gRNA.*PGI1*	This work
pUDR204	2 μm ori, *amdS*, p*SNR52*-gRNA.*GRE3-tSUP4*	This work
pUDR105	*hphNT*, gRNA.*SynthSite*-2 μm ori-gRNA.*SynthSite*	[141]
pUDE327	URA3, p*SNR52*-gRNA.*HXK2*-t*SUP4*	[294]
pAKX002	2 μm ori, *URA3*, p*TPI1-xylA*-t*CYC1*	[353]

To construct the *GRE3*-targeting CRISPR-plasmid pUDR204, the plasmid back-
bone of pMEL11 was PCR amplified using primer combination 5980/5792. The insert
fragment, expressing the *GRE3*-targeting gRNA, was amplified using primer combination
5979/5978 and pMEL11 as template. To construct the *RPE1*/*PGI1* double-targeting
CRISPR-plasmid pUDR202, the plasmid backbone and the insert fragment were PCR am-
plified using primer combinations 5941/6005 and 9269/9401, respectively, using
pROS11 as template. Both plasmids were assembled *in vitro* in yeast and cloned in *E. coli*.
To construct CRISPR-plasmids for single deletion of *GAL83* and *RSP5*, the plasmid back-
bone, the *GAL83*-gRNA insert and the *RSP5*-gRNA insert were amplified using primer
combination 5792/5980, 5979/11270 and 5979/11373, respectively, using pMEL10 as
template and assembled *in vivo*.

To generate *ZWF1* and *SOL3* overexpression cassettes, promoter regions of *ADH1*
and *ENO1* and the coding regions of *ZWF1* and *SOL3* (including their terminator regions)
were PCR amplified using primer combinations 8956/8960, 8958/8961, 8953/8964 and
8984/8986, respectively, using CEN.PK113-7D genomic DNA as a template. The resulting

products were used as templates for fusion-PCR assembly of the p*ADH1-ZWF1*-t*ZWF1* and p*ENO1-SOL3*-t*SOL3* overexpression cassettes with primer combinations 8956/8964 and 8958/8986 respectively, which yielded plasmids pUD426 and pUD427 after ligation to pJET-blunt vectors (Thermo-Scientific) and cloning in *E. coli*.

　　To generate yeast-integration cassettes for overexpression of the major genes of the complete PPP, p*ADH1-ZWF1*-t*ZWF1*, p*ENO1-SOL3*-t*SOL3*, p*PGK1-TKL1*-t*TKL1*, p*TEF1-TAL1*-t*TAL1*, p*PGI1-NQM1*-t*NQM1*, p*TPI1-RKI1*-t*RKI1* and p*PYK1-TKL2*-t*TKL2* cassettes were PCR amplified using primer combinations 4870/7369, 8958/3290, 3291/4068, 3274/3275, 3847/3276, 4691/3277, 3283/3288, respectively, using plasmids pUD426, pUD427, pUD348, pUD349, pUD344, pUD345 and pUD346, respectively, as templates. To generate yeast-integration cassettes of the genes of the non-oxidative PPP, the p*TDH3-RPE1*-t*RPE1*, p*PGK1-TKL1*-t*TKL1*, p*TEF1-TAL1*-t*TAL1*, p*TPI1-RKI1*-t*RKI1* overexpression cassettes were PCR-amplified using primer pairs 7133/3290, 3291/4068, 3724/3725, 10460/10461, respectively and plasmids pUD347, pUD348, pUD34 and pUD345 as templates.

　　Yeast-integration cassettes for overexpression of *Piromyces sp.* xylose isomerase (*pTPI1-xylA-tCYC1*) were PCR-amplified using primer combinations 6285/7548, 6280/6273, 6281/6270, 6282/6271, 6284/6272, 6283/6275, 6287/6276, 6288/6277 or 6289/6274, using pUD350 as template. Yeast xylulokinase overexpression cassettes (*pTEF1-XKS1*-t*XKS1*) were PCR-amplified from plasmid pUD353, using primer combination 5920/9029 or 7135/7222. A yeast-integration cassette of p*GAL83-gal83::GAL83^{G673T}*-t*GAL83* was PCR-amplified from genomic DNA of IMS0629, using primer combination 11273/11274.

Strain construction. Yeast transformation was performed as previously described [269]. Transformation mixtures were plated on SM or YP agar plates (2% Bacto Agar, BD), supplemented with the appropriate carbon sources. For transformations with the *amdS* marker cassette, agar plates were prepared and counter selection was performed as previously described [270]. For transformations with the *URA3* selection marker counter-selection was performed using 5-fluoro-orotic acid (Zymo Research, Irvine, CA), following the supplier's protocol. For transformations with the *hphNT* marker, agar plates were additionally supplemented with 200 mg L^{-1} hygromycin B (Invivogen, San Diego, CA) and plasmid loss was induced by cultivation in non-selective medium. After each transformation, correct genotypes were confirmed by diagnostic PCR using DreamTaq polymerase (Thermo-Scientific, see Additional File 1 for primer sequences).

　　Co-transformation of pUDR204 along with the p*ADH1-ZWF1*-t*ZWF1*, p*ENO1-SOL3*-t*SOL3*, p*PGK1-TKL1*-t*TKL1*, p*TEF1-TAL1*-t*TAL1*, p*PGI1-NQM1*-t*NQM1*, p*TPI1-RKI1*-t*RKI1* and p*PYK1-TKL2*-t*TKL2* integration cassettes to IMX705 [91] and subsequent plasmid counter-selection, yielded strain IMX963, which overexpresses the major enzymes of the PPP. Co-transformation of pUDR119, 9 copies of the *pTPI1-xylA-tCYC1* integration cassette, along with a single copy of the *pTEF1-XKS1-tXKS1* cassette, to IMX963, followed by

plasmid counterselection yielded the xylose-fermenting strain IMX990. In IMX990, the *pTPI1-xylA-tCYC1* cassettes recombined *in vivo* to form a multi-copy construct of xylose isomerase overexpression [295]. To construct IMX1046, in which *RPE1* and *PGI1* were deleted, plasmid pUDR202 and the repair oligonucleotides 9279/9280/9281/9282 were co-transformed to IMX990. Transformation mixes of IMX1046 were plated on SM agar supplemented with a xylose/fructose/glucose mixture (20, 10 and 1 g L^{-1} final concentrations respectively), to avoid potential glucose toxicity [350].

To construct strain IMX994, plasmid pUDE335 was co-transformed to IMX581, along with the p*TDH3-RPE1*-t*RPE1*, p*PGK1-TKL1*-t*TKL1*, p*TEF1-TAL1*-t*TAL1*, p*TPI1-RKI1*-t*RKI1* and *pTEF1-XKS1-tXKS1* integration cassettes, after which the CRISPR plasmid was recycled. Transformation of pAKX002 to IMX994 yielded the xylose-fermenting strain IMU079. Co-transformation of pUDE327 along with the repair oligonucleotides 5888/5889 to IMX994 yielded strain IMX1384, in which *HXK2* was deleted. Co-transformation of the pMEL10 backbone fragment, along with the *GAL83*-gRNA insert or the *RSP5*-gRNA insert and repair oligonucleotides 11271/11272 or 11374/11375, respectively, yielded strains IMX1385 (*GAL83* deletion) and IMX1442 (*RSP5* deletion). Counterselection of the CRISPR plasmids from IMX1384, IMX1385 and IMX1442 yielded, respectively, strains IMX1408, IMX1409 and IMX1451. Transformation of pAKX002 to IMX1408, IMX1409 and IMX1451 yielded, respectively, the xylose-fermenting strains IMX1485, IMX1486 and IMX1487. To construct strain IMX1453, in which the mutated *GAL83*^{G673T} gene replaced the wild-type *GAL83* allele, plasmid pUDR105 was co-transformed to IMX1409 with the p*GAL83-gal83::GAL83*^{G673T}-t*GAL83* cassette. Transformation of pAKX002 to IMX1453 yielded the xylose-fermenting strain IMX1488. To construct the *hxk2Δ rsp5Δ* strain IMX1484, plasmid pUDE327 was co-transformed to IMX1451, along with the repair oligonucleotides 5888/5889. Counterselection of pUDE327 from IMX1484 yielded strain IMX1510. Transformation of pAKX002 to IMX1510 yielded the xylose-fermenting strain IMX1515. To construct the *hxk2Δ gal83::GAL83*^{G673T} strain IMX1563, plasmid pUDE327 along with the repair-oligonucleotides 5888/5889 was co-transformed to IMX1453. Counterselection of pUDE327 from IMX1563 yielded IMX1571. The xylose-fermenting strain IMX1583 was obtained by transformation of pAKX002 to IMX1571.

Cultivation and media. Shake-flask growth experiments were performed in 500-mL conical shake flasks containing 100 mL of SM with urea as nitrogen source (2.3 g L^{-1} urea, 6.6 g L^{-1} K$_2$SO$_4$, 3 g L^{-1} KH$_2$PO$_4$, 1 mL L^{-1} trace elements solution (Verduyn *et al.* 1992) and 1 mL L^{-1} vitamin solution [51] to prevent medium acidification. The initial pH of the medium was set to 6.0 by titration with 2 mol L^{-1} KOH. Depending on the strains grown, different mixtures of carbon sources (glucose/xylose/fructose) were added and media were filter-sterilized (0.2 μm, Merck, Darmstadt, Germany). The temperature was set to 30 °C and the shaking speed to 200 rpm in an Innova incubator (New Brunswick Scientific, Edison, NJ). In each case, pre-culture shake-flasks were inoculated from frozen stocks. After 8-12 h of growth, exponentially growing cells from the initial shake-flasks were used to inoculate

fresh cultures that, after 12-18 h of growth, were used as inoculum for the growth experiments, to a starting OD_{660} of 0.4-0.5 in the case of shake-flask growth experiments and of 0.2-0.3 in the case of bioreactor cultivation.

Bioreactor cultures were grown on SM [51], supplemented with a glucose/xylose mixture (10 g L^{-1}/20 g L^{-1} for aerobic cultivation or 20 g L^{-1}/10 g L^{-1} for anaerobic cultivation). Sterilization of the salt solution was performed by autoclaving at 121 °C for 20 min. Sugar solutions were sterilized separately by autoclaving at 110 °C for 20 min and added to the sterile salt media along with filter-sterilized vitamin solution. In the case of anaerobic cultivation, media were additionally supplemented with ergosterol (10 mg L^{-1}) and Tween 80 (420 mg L^{-1}). Sterile antifoam C (0.2 g L^{-1}; Sigma-Aldrich, St. Louis, MO) was added to all media used for bioreactor cultivation. Batch cultures were grown in 2-L bioreactors (Applikon, Delft, The Netherlands) with a 1-L working volume, stirred at 800 rpm. Culture pH was maintained at 5.0 by automatic titration with 2 mol L^{-1} KOH. Temperature was maintained at 30 °C. Bioreactors were sparged at 0.5 L min^{-1} with either pressurized air (aerobic cultivation) or nitrogen gas (<10 ppm oxygen, anaerobic cultivation). All reactors were equipped with Viton O-rings and Norprene tubing to minimize oxygen diffusion. Evaporation in bioreactor cultures was minimized by cooling the offgas outlet to 4 °C.

Laboratory evolution. Laboratory evolution of strain IMX1046 was performed via serial shake-flask cultivation on SM [51]. Cultures were grown in 500-mL shake-flasks with 100 mL working volume. Growth conditions were the same as described above. Initially, the cultures were grown on a glucose/xylose concentration ratio of (1.0 g L^{-1}/20 g L^{-1}). After growth was observed, exponentially growing cells (0.05 mL of culture) were transferred to SM with a glucose/xylose concentration ratio of 2.0 g L^{-1}/20 g L^{-1}. During subsequent serial transfers, the glucose content was progressively increased as high growth rates were established at each sugar composition, reaching a final glucose/xylose ratio of 20 g L^{-1}/20 g L^{-1}, , to increase the selective pressure for alleviation of glucose repression and/or inhibition of xylose conversion. At that point three single colonies were isolated from two replicate evolution experiments (IMS0628-630 and IMS0634-636, respectively) by plating on SM with 10 g L^{-1} glucose and 20 g L^{-1} xylose. This medium composition supported fast growth on plates during three consecutive restreaks.

Analytical methods. Off-gas analysis, biomass dry weight measurements, HPLC analysis of culture supernatants and correction for ethanol evaporation in bioreactor experiments were performed as previously described [91]. Determination of optical density was performed at 660 nm using a Jenway 7200 spectrophotometer (Cole-Palmer, Staffordshire, UK). Yields of products and biomass-specific sugar uptake rates in bioreactor batch cultures were determined as previously described [13, 91]. All values are represented as averages ± mean deviation of independent biological duplicate cultures.

***In silico* determination of sugar uptake.** The Yeast v7.6 consensus metabolic model [354] was used for *in silico* prediction of relative xylose and glucose consumption rates in aerobic bioreactor batch cultures of strain IMS0629. The COBRA v2 toolbox [355] was used to read the model in MATLAB vR2017b (Mathworks, Natick, MA), supported by the SBML Toolbox v4.1 and the libSBML v5.12 [356]. The Gurobi v6.5 linear programming solver (Gurobi Optimization Inc, Houston, TX) was installed and used according to the manual provided. The MATLAB script is provided in Additional File 2.

Genome sequencing

Genomic DNA of strains IMS0629 and IMS0634 was isolated from exponentially growing shake-flask cultures on SM (10 g L^{-1} glucose/20 g L^{-1} xylose) with a Qiagen Blood & Cell culture DNA kit (Qiagen, Germantown, MD), according to the manufacturer's specifications. Whole-genome sequencing was performed on an Illumina HiSeq PE150 sequencer (Novogene Company Limited, Hong Kong), as previously described [352]. Sequence data were mapped to the reference CEN.PK113-7D genome [266], to which the sequences of the p*TPI1*-*gndA*-t*CYC1* and p*TPI1*-xylA-t*CYC1* cassettes were manually added. Data processing and chromosome copy number analysis were carried as previously described [352].

Results

Design of an *S. cerevisiae* strain with a forced, high stoichiometry of xylose and glucose co-consumption. Design of an *S. cerevisiae* strain whose growth depended on extensive co-consumption of xylose and glucose was based on the observation that inactivation of *PGI1* blocks entry of glucose-6-phosphate into glycolysis, while inactivation of *RPE1* prevents entry of ribulose-5-phosphate into the non-oxidative PPP (Figure 1). As a consequence, a *pgi1Δ rpe1Δ* strain is unable to grow on glucose. If conversion of xylose into xylulose-5-phosphate in such a strain is enabled by expression of a heterologous xylose isomerase and overexpression of the native xylulose kinase Xks1 [7], co-consumption of xylose and glucose should enable growth (Figure 1). Overexpression of native genes encoding the enzymes of the non-oxidative PPP has previously been shown to stimulate the required conversion of xylulose-5-phosphate into the glycolytic intermediates fructose-6-phosphate and glyceraldehyde-3-phosphate (Figure 1) [7, 357]. The predicted stoichiometry for conversion of glucose and xylose into pyruvate in a yeast strain that combines these genetic modifications is summarized in Equation 1:

$$C_6H_{12}O_6 + 2\ C_5H_{10}O_5 + 5\ ADP + 5\ P_i + 2\ NADP^+ + 5\ NAD^+ \rightarrow 5\ C_3H_4O_3 + 5\ ATP + 4\ H_2O + 2\ NADPH + 5\ NADH + 7\ H^+ + CO_2\ \ (1)$$
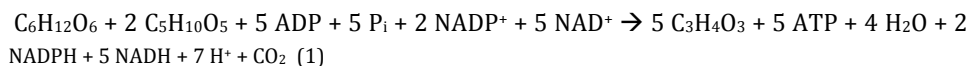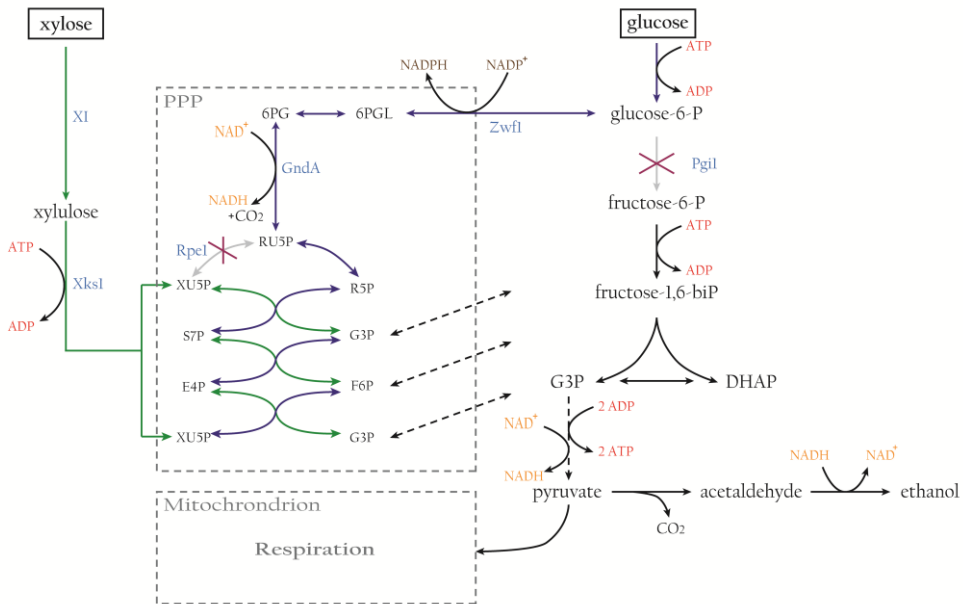
Figure 1 | Schematic representation of central carbon metabolism in yeast strain engineered for forced co-consumption of glucose and xylose. In a *pgi1Δ rpe1Δ Saccharomyces cerevisiae* expressing a heterologous xylose isomerase (XI, Kuyper *et al.* 2003), the native 6-phosphogluconate dehydrogenases (Gnd1 and Gnd2) were replaced by a bacterial NAD$^+$-dependent enzyme (GndA, Papapetridis *et al.* 2016). Additionally, xylulokinase (Xks1) and enzymes of the pentose phosphate pathway (PPP) were overexpressed. F6P fructose-6-phosphate; G3P glyceraldehyde-3-phosphate; DHAP dihydroxyacetone phosphate; 6PGL 6-phosphogluconolactone; 6PG 6-phosphogluconate; RU5P ribulose-5-phosphate; XU5P xylulose-5-phosphate; R5P ribose-5-phosphate; S7P sedoheptulose-7-phosphate; E4P erythrose-4-phosphate.

To prevent a potential excessive formation of NADPH [350, 351], the strain design further included replacement of the native *S. cerevisiae* NADP$^+$-dependent 6-phosphogluconate dehydrogenases (Gnd1 and Gnd2) by the NAD$^+$-dependent bacterial enzyme GndA [91], leading to the stoichiometry shown in Equation 2:

$$C_6H_{12}O_6 + 2\ C_5H_{10}O_5 + 5\ ADP + 5\ P_i + 1\ NADP^+ + 6\ NAD^+ \rightarrow 5\ C_3H_4O_3 + 5\ ATP + 4\ H_2O + NADPH + 6\ NADH + 7\ H^+ + CO_2 \qquad (2)$$

As indicated by Equation 2, this strain design forces co-consumption of 2 mol xylose and 1 mol glucose for the production of 5 mol pyruvate, with a concomitant formation of 1 mol NADPH, 6 mol NADH and 5 mol ATP. NADPH generated in this process can be reoxidized in biosynthetic reactions [358] or via an L-glutamate-2-oxoglutarate transhydrogenase cycle catalysed by Gdh1 and Gdh2 [350]. Actual *in vivo* stoichiometries of mixed-sugar consumption will depend on the relative contribution of precursors derived from glucose and xylose to biomass synthesis and on the biomass yield [271]. In

aerobic cultures, the latter strongly depends on the mode of NADH reoxidation (mitochondrial respiration, alcoholic fermentation and/or glycerol production; Bakker *et al.* 2001). While quantitation of precise co-consumption stoichiometries will therefore require experimental analysis, this strain design clearly has the potential to force xylose and glucose co-consumption at much higher stoichiometries than previously reported [112, 126, 183,

Sugar composition:	20 g L^{-1} xylose 1 g L^{-1} glucose	20 g L^{-1} xylose 2 g L^{-1} glucose	20 g L^{-1} xylose 5 g L^{-1} glucose	20 g L^{-1} xylose 10 g L^{-1} glucose	20 g L^{-1} xylose 10 g L^{-1} glucose	20 g L^{-1} xylose 20 g L^{-1} glucose
Growth after first transfer:	Immediate	Immediate	Observed after 18 or 11 days, respectively	Observed after 9 or 7 days, respectively	Observed after 5 or 3 days, respectively	Observed after 4 days
# of transfers in same medium:	1	1	1	5	2	3

345, 347, 359, 360].

Figure 2 | Laboratory evolution of *S. cerevisiae* IMX1046 (*pgi1Δ rpe1Δ gnd1Δ gnd2Δ gndA XylA XKS1↑* PPP↑) for improved co-consumption of xylose at high glucose concentrations. Cultures were grown in shake flasks containing 100 mL SM (pH 6) supplemented with 20 g L^{-1} xylose and progressively increasing glucose concentrations. In every transfer, 0.05 mL of an exponentially growing culture was used to inoculate the next shake flask.

Construction, laboratory evolution and growth stoichiometry of glucose-xylose co-consuming *S. cerevisiae* strains. To implement the proposed strain design for forced co-consumption of xylose and glucose, multiple copies of a codon-optimized expression cassette for *Piromyces xylA* [295] were integrated into the genome of *S. cerevisiae* IMX705 (*gnd1Δ gnd2Δ gndA*; Papapetridis *et al.* 2016), along with overexpression cassettes for *S. cerevisiae XKS1* and for structural genes encoding PPP enzymes. Deletion of *RPE1* and *PGI1* in the resulting xylose-consuming strain IMX990, yielded strain IMX1046, which grew instantaneously in aerobic shake-flask cultures on SM with 1 g L^{-1} glucose and 20 g L^{-1} xylose as sole carbon sources without a requirement for laboratory evolution. However, this strain did not grow at the same xylose concentration when the glucose concentration was increased to 10 g L^{-1}. Kinetic and/or regulatory constraints in glucose-xylose co-consumption at higher glucose concentrations could, for example, reflect interference of glucose with expression or activity of Hxt transporters involved in xylose uptake.

To select for co-consumption of xylose at higher glucose concentrations, duplicate serial-transfer experiments were performed in aerobic shake-flask cultures on SM with 20 g L^{-1} xylose. During serial transfer, the glucose concentration in the medium was

gradually increased from 1 g L^{-1} to 20 g L^{-1} (Figure 2). Samples of the evolving cultures were regularly inoculated in SM containing either 20 g L^{-1} glucose or 20 g L^{-1} xylose as sole carbon source. Absence of growth on these single sugars showed that laboratory evolution did not result in an escape from their forced co-consumption. When, after 13 transfers, vigorous growth was observed on a mixture of 20 g L^{-1} glucose and 20 g L^{-1} xylose, three single-colony isolates were obtained from each laboratory evolution experiment by streaking on SM agar (10 g L^{-1} glucose/20 g L^{-1} xylose).
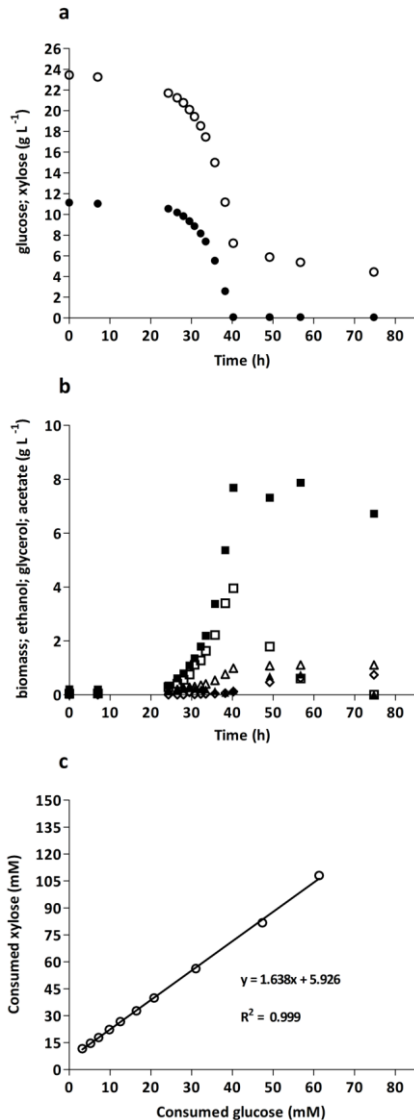
Figure 3 | Sugar consumption, biomass and metabolite production profiles of the evolved *S. cerevisiae* strain IMS0629 (*pgi1Δ rpe1Δ gnd1Δ gnd2Δ gndA XylA XKS1*↑ PPP↑), grown on SM with 10 g L^{-1} glucose and 20 g L^{-1} xylose in aerobic bioreactor batch cultures (pH 5, 30 °C). Cultures were grown in duplicate, the data shown are from a single representative culture. **a**: ● glucose, ○ xylose; **b**: ■ biomass □ ethanol ▲ acetate △ glycerol ◇ xylitol; **c**: ratio of xylose and glucose consumption during exponential growth phase.

147

Growth studies with the six evolved isolates in shake-flask cultures on SM with 10 g L^{-1} glucose and 20 g L^{-1} xylose (Additional File 3) identified isolate IMS0629 (Evolution Line 1) as the fastest growing isolate (μ = 0.21 h^{-1}). The physiology of this strain was further characterized in aerobic bioreactor batch cultures on SM containing 10 g L^{-1} glucose and 20 g L^{-1} xylose. After a ca 10 h lag phase (Figure 3, Additional File 4) exponential growth was observed at a specific growth rate of 0.18 h^{-1}. Biomass, ethanol and CO_2 were the main products, with additional minor formation of glycerol and acetate (Table 3, Figure 3, Additional File 4). During the exponential growth phase, xylose and glucose were co-consumed at a fixed molar ratio of 1.64 mol mol^{-1} (Table 3, Figure 3). Growth ceased after glucose depletion, at which point xylose consumption rates drastically decreased and corresponded to a simultaneous low rate of xylitol formation (Figure 3, Additional File 4). As previously reported for XylA-expressing, xylose-fermenting *S. cerevisiae* strains [7, 295], no production of xylitol was observed during the exponential growth phase. The biomass and ethanol yields on total sugars consumed were 0.28 g biomass (g sugar)$^{-1}$ and 0.18 g ethanol (g sugar)$^{-1}$, respectively. Together with a respiratory quotient of 1.5, these observations indicated a respiro-fermentative sugar dissimilation. In line with the inability of *pgi1Δ S. cerevisiae* to generate glucose-6-phosphate from ethanol and acetate, reconsumption of these fermentation products after glucose depletion was not coupled to growth (Figure 3, Additional File 4). However, their oxidation may have provided redox equivalents for the observed slow production of xylitol from xylose (Figure 3).

The quantitative data on biomass and product formation obtained from the bioreactor batch cultures enabled a comparison of the observed molar ratio of xylose and glucose consumption with a model-based prediction. To this end, the engineered metabolic network of strain IMX1046 was re-created *in silico*, using the Yeast v7.6 consensus metabolic model as a basis (Aung *et al.* 2013; Additional File 2). Consistent with the experimental observations on forced co-consumption, inactivation of either xylose or glucose uptake in the model network did not result in any feasible growth solutions. Using the experimentally determined average specific growth rates and oxygen consumption rates from the aerobic bioreactor batch cultures of strain IMS0629 as constraints on the model resulted in predicted xylose and glucose uptake rates of 2.68 and 1.93 mmol (g biomass)$^{-1}$ h^{-1}, respectively, corresponding to a molar ratio of the xylose and glucose consumption rates of 1.4. In view of the complexity of the model and the potential impact of differences in biomass composition, this number corresponded well with the experimentally measured value of 1.64 (Table 3).

Whole genome sequencing of evolved glucose-xylose co-consuming *S. cerevisiae*. To identify causal mutations for the improved growth of the evolved glucose-xylose co-consuming *S. cerevisiae* strains at high glucose concentrations, the genomes of strains IMS0629 and IMS0634 (fastest growing isolates from evolution line 1 and 2, respectively, Additional File 3) were sequenced and compared to that of their common parental strain. Despite the well documented role of *S. cerevisiae* hexose transporters in xylose uptake

[123, 164, 165, 167], no mutations were found in the coding region of any of the 18 genes encoding these transporters (HXT1-17 and GAL2), or in other known transporter genes. Both evolved strains harboured mutations in HXK2 (Table 4). This gene encodes the major S. cerevisiae hexokinase which, in addition to its catalytic role, is involved in glucose repression [336, 361]. The mutation in IMS0629 caused a premature stop codon at position 309 of Hxk2. Both strains also harboured mutations in RSP5, which encodes an E3-ubiquitin ligase linked to ubiquitination and endocytosis of membrane proteins [362]. In strain IMS0629, a substitution at position 686 caused a glycine to aspartic acid change at position 229 of Rsp5 (Table 4). Strain IMS0634 carried a 41 bp internal deletion in RSP5, which included the location of the mutation in strain IMS0629 and probably caused loss of function.

Table 3 | Product yields, biomass specific sugar uptake and production rates in aerobic bioreactor batch cultures of evolved strain *S. cerevisiae* IMS0629 (*pgi1Δ rpe1Δ gnd1Δ gnd2Δ gndA XylA XKS1↑* PPP↑) on SM supplemented with 10 g L^{-1} glucose and 20 g L^{-1} xylose (pH 5, 30 °C). Biomass-specific rates, yields and ratios were calculated from samples taken during the mid-exponential growth phase and represent averages ± mean deviation of independent duplicate cultures. Ethanol yield was corrected for evaporation.

Growth rate (h^{-1})	0.18 ± 0.00
Glucose-xylose consumption ratio mol mol^{-1}	1.64 ± 0.00
Spec. xylose uptake rate mmol (g biomass)$^{-1}$ h^{-1}	2.52 ± 0.00
Spec. glucose uptake rate mmol (g biomass)$^{-1}$ h^{-1}	1.54 ± 0.07
Spec. glycerol production rate mmol (g biomass)$^{-1}$ h^{-1}	0.23 ± 0.01
Spec. ethanol production rate mmol (g biomass)$^{-1}$ h^{-1}	2.25 ± 0.37
Spec. CO$_2$ production rate mmol (g biomass)$^{-1}$ h^{-1}	10.43 ± 0.98
Spec. O$_2$ uptake rate mmol (g biomass)$^{-1}$ h^{-1}	6.87 ± 0.56
Respiratory quotient	1.52 ± 0.03
Biomass yield g biomass (g sugars)$^{-1}$	0.28 ± 0.00
Ethanol yield g (g sugars)$^{-1}$	0.18 ± 0.00

Compared to strain IMS0634, strain IMS0629 harboured 4 additional nucleotide changes in protein-coding regions (Table 4). A G-A change at position 896 of the transcriptional regulator gene *CYC8* introduced a stop codon at position 299 of the protein. Deletion of *CYC8* was previously shown to enhance xylose uptake in the presence of glucose, albeit at the expense of growth rate [363]. A G-T change at position 673 of the transcriptional regulator gene *GAL83* caused an amino acid change from aspartic acid to tyrosine at position 225 of the protein. Gal83 plays a vital role in the function of the Snf1-kinase complex of *S. cerevisiae*, which is involved in activation of glucose-repressed genes in the absence of the sugar [364-367].

Analysis of chromosomal copy number variations showed no chromosomal rearrangements in strain IMS0629 (Additional File 5). In contrast, strain IMS0634 carried a duplication of the right arm of chromosome 3, a duplication of the middle part of chromosome 8 and a duplication of chromosome 9 (Additional File 5).

Table 4 | Mutations identified by whole-genome sequencing of glucose-xylose co-consuming *S. cerevisiae* strains evolved for fast growth at high glucose concentrations. Gene descriptions were taken from the Saccharomyces Genome Database (https://www.yeastgenome.org/, Accessed 14-12-2017).

Strain and gene	Nucleotide change	Amino acid change	Description
IMS0629			
CYC8	G896A	W299→Stop	General transcriptional co-repressor; acts together with Tup1; also acts as part of a transcriptional co-activator complex that recruits the SWI/SNF and SAGA complexes to promoters; can form the prion [OCT+]
GAL83	G673T	D225Y	One of three possible beta-subunits of the Snf1 kinase complex; allows nuclear localization of the Snf1 kinase complex in the presence of a non-fermentable carbon source
RSP5	G686A	G229D	NEDD4 family E3 ubiquitin ligase; regulates processes including: MVB sorting, the heat shock response, transcription, endocytosis and ribosome stability; ubiquitinates Sec23, Sna3, Ste4, Nfi1, Rpo21 and Sem1; autoubiquitinates; deubiquitinated by Ubp2; regulated by SUMO ligase Siz1, in turn regulates Siz1p SUMO ligase activity; required for efficient Golgi-to-ER trafficking in COPI mutants
HXK2	C927G	Y309→Stop	Hexokinase isoenzyme 2; phosphorylates glucose in cytosol; predominant hexokinase during growth on glucose; represses expression of *HXK1*, *GLK1*
RBH1	C190A	Q64K	Putative protein of unknown function; expression is cell-cycle regulated as shown by microarray analysis; potential regulatory target of Mbp1, which binds to the YJL181W promoter region; contains a PH-like domain
DCS1	C636G	Y212→Stop	Non-essential hydrolase involved in mRNA decapping; activates Xrn1; may function in a feedback mechanism to regulate deadenylation, contains pyrophosphatase activity and a HIT (histidine triad) motif; acts as inhibitor of neutral trehalase Nth1; required for growth on glycerol medium
IMS0634			
RSP5	Internal Deletion, 41 nucleotides	Frameshift	NEDD4 family E3 ubiquitin ligase; regulates processes including: MVB sorting, the heat shock response, transcription, endocytosis and ribosome stability; ubiquitinates Sec23, Sna3, Ste4, Nfi1, Rpo21 and Sem1; autoubiquitinates; deubiquitinated by Ubp2; regulated by SUMO ligase Siz1, in turn regulates Siz1p SUMO ligase activity; required for efficient Golgi-to-ER trafficking in COPI mutants
HXK2	G1027C	D343H	Hexokinase isoenzyme 2; phosphorylates glucose in cytosol; predominant hexokinase during growth on glucose; represses expression of *HXK1*, *GLK1*

The duplications in chromosomes 8 and 9 in IMS0634 spanned the *GND1*, *GRE3* and *SGA1* loci at which the expressing cassettes for heterologous genes were integrated (Table 1). In the evolved strains IMS0629 and IMS0634, *xylA* copy numbers had increased to ca. 27 and 20, respectively. This observation is consistent with previous research that showed a requirement for high copy numbers of *xylA* expression cassettes to support fast xylose consumption [239, 295]. The duplication in of a segment of chromosome 8 in strain IMS0634 also spanned the locations of the low-to-moderate affinity hexose transporter genes *HXT1* and *HXT5* and the high-affinity hexose transporter gene *HXT4*.

Mutations in *HXK2*, *RSP5* and *GAL83* stimulate co-consumption of xylose and glucose in aerobic cultures of xylose-consuming *S. cerevisiae.* To investigate whether mutations acquired during evolution for forced co-consumption of glucose and xylose were relevant for mixed-sugar utilization in a strain without forced glucose-xylose co-consumption, we focused on mutations in *HXK2* and *RSP5* (which were present in both IMS0629 and IMS0634) and/or *GAL83*. Mutations in these genes were introduced into an engineered, non-evolved xylose-consuming *S. cerevisiae* strain background (IMX994,Table 1). Overexpression of *xylA* was accomplished by transforming strains with the multi-copy *xylA* expression vector pAKX002 [353]. In aerobic shake-flask cultures grown on 10 g L^{-1} glucose and 10 g L^{-1} xylose, the reference strain IMU079 (*XKS1*↑ PPP↑ pAKX002) displayed a pronounced biphasic growth profile and only a minor co-consumption of the two sugars (0.13 mol xylose (mol glucose)$^{-1}$; Table 5, Figure 4, Additional File 6). Co-consumption was strongly enhanced in the congenic *hxk2Δ* strain IMX1485, which showed a 3-fold higher molar ratio of xylose and glucose consumption (0.41 mol mol^{-1}). However, its specific growth rate before glucose depletion (0.28 h^{-1}) was 13% lower than that of the reference strain (Table 5). Strain IMX1487 (*rsp5Δ*), which showed a 20% lower specific growth rate than the reference strain, showed a slight improvement in co-consumption (Table 5). Deletion of *GAL83* (strain IMX1486) affected neither sugar co-consumption nor growth rate. In contrast, replacement of *GAL83* by *GAL83^G673T^* (strain IMX1488) resulted in a 40% higher co-consumption of glucose and xylose than observed in the reference strain IMU079, without affecting growth rate (Table 5).

Since independently evolved glucose-xylose co-consuming strains both contained putative loss-of-function mutations in *HXK2* and *RSP5*, both genes were deleted in strain IMX1515 (*hxk2Δ rsp5Δ XKS1*↑ PPP↑ pAKX002). Similarly, deletion of *HXK2* and introduction of *GAL83^G673T^* were combined in strain IMX1583 (*hxk2Δ gal83::GAL83^G673T^ XKS1*↑ PPP↑ pAKX002). Co-consumption ratios in the two strains (0.60 and 0.49 mol xylose (mol glucose)$^{-1}$, respectively) were 4- to 5-fold higher than in the reference strain IMU079 (Table 5, Figure 4, Additional File 6). However, strain IMX1515 exhibited a 40% lower specific growth rate (0.19 h^{-1}) than the reference strain, resulting in a 9 h extension of the fermentation experiments (Figure 4, Additional File 6). In contrast, strain IMX1583

combined a high co-consumption ratio with the same specific growth rate as that of the reference strain.
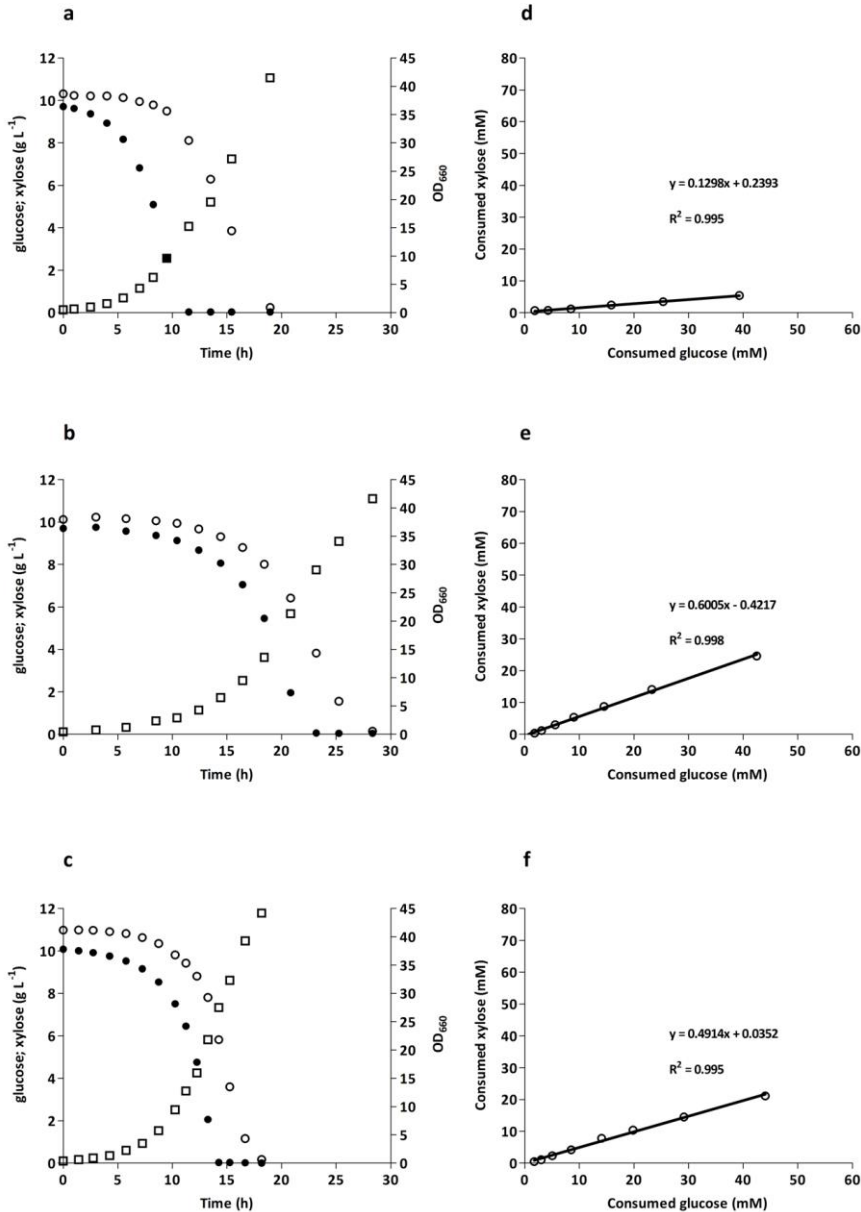
Figure 4 | Consumption of glucose and xylose and growth of strains IMU079 (*XKS1*↑ PPP↑ pAKX002; **a, d**), IMX1515 (*hxk2Δ rsp5Δ XKS1*↑ PPP↑ pAKX002; **b, e**) and IMX1583 (*hxk2Δ gal83::GAL83^{G673T} XKS1*↑ PPP↑ pAKX002; **c, f**) in batch cultures. The three strains were grown on SM (urea as nitrogen source) with 10 g L^{-1} glucose and 10 g L^{-1} xylose in aerobic shake-flask cultures (pH 6, 30 °C). **a, b, c**: ● glucose, ○ xylose, □ OD$_{660}$; **d, e, f**: ratio of xylose and glucose consumption during exponential growth phase.

Combined mutations in *HXK2* and *GAL83* significantly accelerate conversion of glucose-xylose mixtures by anaerobic cultures of xylose-consuming *S. cerevisiae*. To investigate the impact of the identified mutations under more industrially relevant conditions, anaerobic growth of the reference xylose-fermenting strain IMU079 (*XKS1*↑ PPP↑ pAKX002) in bioreactor batch experiments was compared with that of the two congenic double mutants IMX1515 (*hxk2Δ rsp5Δ*) and IMX1583 (*hxk2Δ gal83::GAL83^G673T*), that showed the highest glucose-xylose co-consumption in the aerobic shake-flask experiments. The anaerobic cultures were grown on 20 g L^{-1} glucose and 10 g L^{-1} xylose to simulate the relative concentrations of these sugars typically found in corn stover and wheat straw lignocellulosic hydrolysates [206].

Table 5 | Specific growth rates (μ) and ratio of xylose and glucose consumption in aerobic shake-flask cultures of strains IMU079 (*XKS1*↑ PPP↑ pAKX002), IMX1485 (*hkx2Δ XKS1*↑ PPP↑ pAKX002), IMX1486 (*gal83Δ XKS1*↑ PPP↑ pAKX002), IMX1487 (*rsp5Δ XKS1*↑ PPP↑ pAKX002), IMX1488 (*gal83::GAL83^G673T XKS1*↑ PPP↑ pAKX002), IMX1515 (*hxk2Δ rsp5Δ XKS1*↑ PPP↑ pAKX002) and IMX1583 (*hxk2Δ gal83::GAL83^G673T XKS1*↑ PPP↑ pAKX002) grown on SM (urea as nitrogen source) with 10 g L^{-1} glucose and 10 g L^{-1} xylose (pH 6, 30 °C). Growth rates and ratios were calculated from samples taken during the mid-exponential growth phase and represent averages ± mean deviation of independent duplicate cultures.

Strain	Relevant Genotype	μ (h^{-1})	Xylose-Glucose consumption ratio (mol mol^{-1})
IMU079	*HXK2 RSP5 GAL83*	0.32 ± 0.01	0.13 ± 0.00
IMX1485	*hxk2Δ*	0.28 ± 0.00	0.41 ± 0.01
IMX1486	*gal83Δ*	0.31 ± 0.00	0.14 ± 0.01
IMX1487	*rsp5Δ*	0.26 ± 0.00	0.15 ± 0.00
IMX1488	*gal83::GAL83^G673T*	0.31 ± 0.00	0.18 ± 0.01
IMX1515	*hxk2Δ rsp5Δ*	0.19 ± 0.00	0.60 ± 0.00
IMX1583	*hxk2Δ gal83::GAL83^G673T*	0.31 ± 0.00	0.49 ± 0.00

In the anaerobic batch cultures, strains IMU079, IMX1515 and IMX1583 all produced CO_2, biomass, ethanol and glycerol as main products, with a minor production of acetate (Table 6, Figure 5, Additional File 7). The strains did not produce xylitol during exponential growth and low concentrations of xylitol in cultures of strain IMU079 (2.2 ± 0.1 mmol L^{-1}) were only observed at the end of fermentation. As observed in aerobic cultures (Figure 4), strain IMU079 showed a clear biphasic growth profile in the anaerobic bioreactors (Figure 5, Additional File 7), during which a fast glucose phase (ca. 16 h) was followed by a much slower and decelerating xylose consumption phase. During the glucose phase, this reference strain maintained a specific growth rate of 0.29 h^{-1} and a glucose-xylose co-consumption ratio of 0.14 mol mol^{-1} (Table 6). After a ca. 30 h lag phase (Figure 5, Additional File 7), strain IMX1515 exhibited an exponential growth rate of 0.07 ± 0.00 h^{-1}, with a high glucose-xylose co-consumption ratio (0.45 ± 0.03 mol mol^{-1}). Mainly as a result of its lag phase, strain IMX1515 took longer to consume all sugars than the reference strain IMU079, but its xylose-consumption phase was ca. 65% shorter (ca. 14 h and 43 h, respectively; Figure 5, Additional File 7).

5
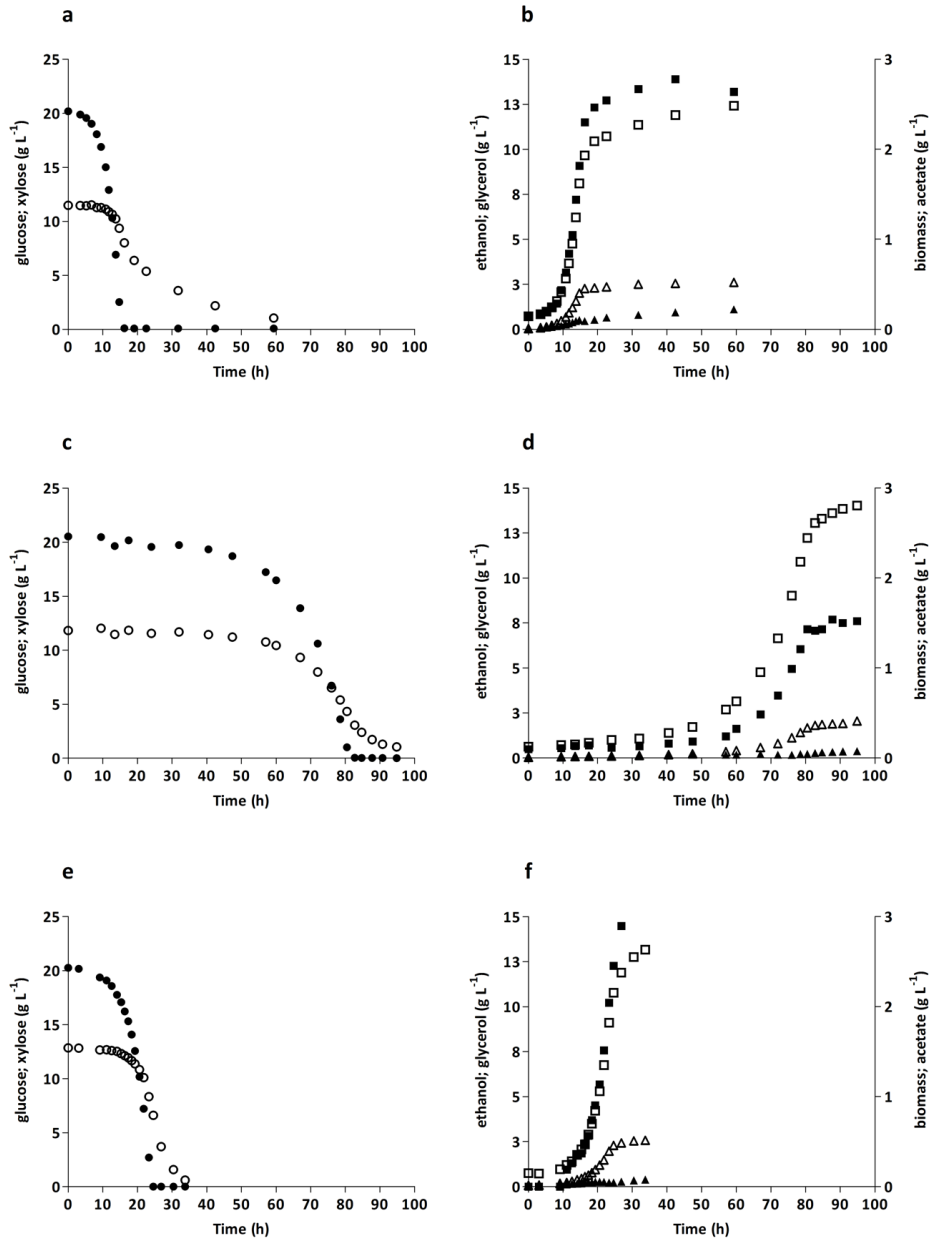
Figure 5 | Sugar consumption, biomass and metabolite production profiles of *S. cerevisiae* strains IMU079 (*XKS1*↑ PPP↑ pAKX002; **a, b**), IMX1515 (*hxk2Δ rsp5Δ XKS1*↑ PPP↑ pAKX002; **c, d**) and IMX1583 (*hxk2Δ gal83::GAL83^G673T XKS1*↑ PPP↑ pAKX002; **e, f**), grown on SM with 20 g L⁻¹ glucose and 10 g L⁻¹ xylose in anaerobic bioreactor batch cultures (pH 5, 30 °C). Cultures were grown in duplicate, the data shown are from a single representative culture. **a, c, e**: ● glucose, ○ xylose; **b, d, f**: ■ biomass □ ethanol ▲ acetate △ glycerol. Data on ethanol corrected for evaporation.

154

In contrast to strain IMX1515, strain IMX1583 (*hxk2Δ gal83::GAL83^G673T^ XKS1↑* PPP↑ pAKX002) did not exhibit a lag phase but immediately started exponential growth at 0.21 h⁻¹ (Figure 5). A comparison of biomass-specific uptake rates of xylose and glucose in the anaerobic batch experiments showed that strain IMX1583 maintained a 44% higher xylose uptake rate than strain IMU079 before glucose exhaustion (Table 6). Moreover, both strains IMX1515 and IMX1583 did not show the pronounced decline of xylose consumption after glucose exhaustion that was observed in the reference strain (Figure 5, Additional File 7). As a result, the xylose consumption phase in anaerobic cultures of strain IMX1583 was 80% shorter than that strain IMU079 (ca. 9 h compared to 43 h), thereby reducing the time required for complete sugar conversion by over 24 h (Figure 5).

Table 6 | Product yields, biomass specific rates and sugar uptake ratios in anaerobic bioreactor batch cultures of strains IMU079 (*XKS1↑* PPP↑ pAKX002), IMX1515 (*hxk2Δ rsp5Δ XKS1↑* PPP↑ pAKX002) and IMX1583 (*hxk2Δ gal83::GAL83^G673T^ XKS1↑* PPP↑ pAKX002) grown on SM supplemented with 20 g L⁻¹ glucose and 10 g L⁻¹ xylose (pH 5, 30 °C). Rates, yields and ratios were calculated from samples taken during the mid-exponential growth phase and represent averages ± mean deviation of independent duplicate cultures. Ethanol yields were corrected for evaporation.

Strain	IMU079	IMX1515	IMX1583
Relevant genotype	*HXK2 RSP5 GAL83*	*hxk2Δ rsp5Δ*	*hxk2Δ gal83::GAL83^G673T^*
μ (h⁻¹)	0.29 ± 0.01	0.07 ± 0.00	0.21 ± 0.00
Spec. xylose uptake rate mmol (g biomass)⁻¹ h⁻¹	2.22 ± 0.14	2.50 ± 0.12	3.19 ± 0.02
Spec. glucose uptake rate mmol (g biomass)⁻¹ h⁻¹	15.65 ± 0.52	5.58 ± 0.08	10.09 ± 0.08
Glucose-xylose consumption ratio (mol mol⁻¹)	0.14 ± 0.00	0.45 ± 0.03	0.32 ± 0.01
Biomass yield on sugars (g biomass g⁻¹)	0.09 ± 0.01	0.05 ± 0.00	0.09 ± 0.00
Ethanol yield on sugars (g g⁻¹)	0.37 ± 0.00	0.43 ± 0.00	0.38 ± 0.01
Glycerol yield on sugars (g g⁻¹)	0.10 ± 0.00	0.06 ± 0.00	0.08 ± 0.00
Ratio glycerol production on biomass production (mmol (g biomass)⁻¹)	11.5 ± 0.60	12.0 ± 0.50	9.9 ± 0.10
Xylitol production (mmol L⁻¹)	2.22 ± 0.06	0.90 ± 0.04	0.35 ± 0.04

5

Discussion

Engineering *S. cerevisiae* for forced co-consumption of xylose and glucose. In previous studies, laboratory evolution of glucose-phosphorylation-negative, pentose-fermenting strains in the presence of glucose yielded valuable leads for improving utilization of glucose-xylose mixtures, including mutations in *HXT* genes that improved pentose uptake in the presence of glucose [112, 123, 176, 363]. The strategy described in this study not only enabled selection for xylose utilization in the presence of glucose, but also for simultaneous metabolism of the two sugars. The molar ratio of xylose and glucose co-consumption (1.64 mol xylose (mol glucose)$^{-1}$) by the evolved strain IMS0629 is the highest reported to date for batch cultures of *S. cerevisiae* [112, 126, 183, 345, 347, 359, 360].

Inactivation of *PGI1* played a key role in the presented strategy for forcing simultaneous utilization of xylose and glucose (Figure 1). The growth defect of *S. cerevisiae* *pgi1Δ* mutants on media that contain glucose as sole carbon source is related to their inability to reoxidize the NADPH that is generated when metabolism of glucose-6-phosphate is rerouted through the oxidative PPP [350, 368]. Since such a rerouting was a key element in our strain design (Figure 1), the NADPH yield from conversion of glucose-6-phosphate through the oxidative PPP was reduced from 2 to 1 mol mol^{-1} by replacing Gnd1 and Gnd2 with the NAD^{+}-linked bacterial 6-phosphogluconate dehydrogenase GndA [91]. Together with the co-consumption of xylose, via an engineered pathway that did not involve NAD(P)H generation (Figure 1), these modifications enabled the engineered strain IMX1046 to grow on mixtures of xylose and 1 g L^{-1} glucose, without the fructose supplementation that is normally required for growth of *pgi1*-null mutants on glucose [348, 350]. The evolved strain IMS0629 consumed 8.6 mmol glucose (g biomass)$^{-1}$ in aerobic batch cultures (Table 3), which is close to the requirement of 9.3 mmol NADPH (g biomass)$^{-1}$ for aerobic growth on glucose of wild-type *S. cerevisiae* [358]. However, since glucose-6-phosphate is a key biosynthetic precursor, not all glucose consumed by the cultures can be converted through the oxidative PPP. Additional enzymes, such as NADP^{+}-dependent acetaldehyde dehydrogenase Ald6 [91, 369, 370] are therefore likely to have supplemented NADPH generation via the oxidative PPP in the 'forced co-consumption' strains.

The key objective of this study was to develop and test a strain platform that, via laboratory evolution and subsequent genome resequencing, can be used to identify mutations that support co-metabolism of xylose and glucose. However, the reported strategy for forced co-consumption of xylose and glucose may also be used in optimizing the yeast metabolic network for aerobic production of economically relevant compounds from lignocellulosic hydrolysates. In particular, imposing fixed stoichiometries of glycolytic and (non-oxidative) PPP reactions may offer interesting options for high-yield production of compounds whose synthesis requires a large net input of PPP intermediates and/or NADPH, such as aromatic compounds derived from the shikimate pathway and lipids [371-373].

Improvement of mixed-sugar fermentation in aerobic and anaerobic cultures of xylose-fermenting *S. cerevisiae*. Mutations in *HXK2*, *RSP5* and *GAL83* were selected to investigate whether genetic changes that occurred during evolution of strain IMX1046 (*pgi1Δ rpe1Δ gnd1Δ gnd2Δ gndA XylA XKS1↑* PPP↑) on glucose-xylose mixtures would also stimulate mixed-substrate utilization in a genetic background that does not impose forced co-utilization. To this end, these mutations were reverse engineered into a non-evolved strain (*XKS1↑* PPP↑). During growth on glucose-xylose mixtures, the reference strain IMU079 (*XKS1↑* PPP↑ pAKX002) displayed the typical biphasic growth profile seen in non-evolved, xylose-consuming strains that express a basic, functional xylose-isomerase (XI) based xylose fermentation pathway [7, 353]. Biphasic growth was especially pronounced in anaerobic cultures, in which the xylose consumption rate collapsed upon glucose depletion (Figure 5). Deletion of *HXK2*, either combined with the deletion of *RSP5* or with the introduction of a *GAL83^{G673T}* mutation, strongly improved mixed sugar fermentation kinetics, both by increased co-utilization and by faster conversion of xylose after glucose had been depleted (Figures 4 and 5). While analysis of the molecular mechanisms by which the mutations in *HXK2*, *RSP5* and *GAL83* affected mixed substrate utilization is beyond the scope of this study, the scientific literature enables a first interpretation.

Hxk2, the major hexokinase in *S. cerevisiae*, plays an additional key role in transcriptional repression of a large set of yeast genes [374-376] by glucose. Deletion of *HXK2* has been shown to enhance co-consumption of combinations of natural substrates (glucose-galactose, glucose-sucrose and glucose-ethanol) in batch cultures [336]. During exponential growth on glucose in batch cultures, *hxk2Δ* mutants show increased transcription of the high-affinity hexose transporter genes *HXT2* and *HXT7* and decreased transcription of the low-affinity hexose transporter genes *HXT1* and *HXT3* [377]. The high-affinity Hxt transporters, which in wild-type strains are only expressed at low glucose concentrations [168], have a much lower K_m for xylose than their low-affinity counterparts [164, 165]. Several studies have demonstrated that overexpression of high-affinity hexose transporters stimulates xylose uptake [112, 123, 125, 126, 128, 162, 279, 359]. The observed improved co-utilization of glucose and xylose upon inactivation of *HXK2* may therefore reflect an increased abundance of high-affinity hexose transporters in the yeast plasma membrane during growth on glucose-xylose mixtures. A recent *in silico* study also identified *HXK2* as potential target for improving xylose uptake rates in *S. cerevisiae* [378]. However, when this prediction was verified by deleting *HXK2* in a strain expressing a xylose reductase/xylitol dehydrogenase-based (XR/XDH) pathway, faster xylose uptake was accompanied by increased production of by-products and reduced ethanol productivity [378]. The absence of such negative effects in the present study is in line with previous reports that xylose-isomerase-based strains are less prone to by-product formation than XR/XDH-based strains (for reviews see Moysés *et al.* 2016; Jansen *et al.* 2017).

Rsp5, the only representative of the NEDD4 family of E3-ubiquitin ligases in *S. cerevisiae*, is involved in regulation of a multitude of cellular processes, including intracellular protein trafficking, regulation of the large subunit of RNA polymerase II, ribosome stability, regulation of fatty acid synthesis and stress response [362, 379-381]. This multitude of roles may explain the reduced growth rate of the *rsp5Δ* strains (Tables 5 and 6) in this study. Involvement of Rsp5 in ubiquitination and subsequent endocytosis of the high-affinity hexose transporters Hxt6 and Hxt7 [382, 383] could explain the strong synergistic effect of the *hxk2Δ* and *rsp5Δ* deletions: while deletion of *HXK2* prevents glucose repression of the synthesis of these transporters, deletion of *RSP5* could prevent their ubiquitination and removal from the membrane. Removal of ubiquitination sites in the hexose transporters Hxt1 and Hxt36 was previously shown to enhance xylose uptake by *S. cerevisiae* [128]. Our results suggest that a similar modification of Hxt6 and Hxt7 could also be beneficial.

Gal83 is one of three possible β-subunits of the Snf1-kinase complex, which enables transcription of glucose-repressed genes at low glucose concentrations (for reviews see Gancedo 1998; Schüller 2003). At non-repressing glucose concentrations, Gal83 directs the Snf1-Gal83 complex to the cell nucleus [384], where it mediates transcriptional upregulation of genes involved in utilization of alternative carbon sources [366]. Targets of the Snf1-Gal83 complex include the *GAL* regulon [385, 386] and the high-affinity hexose transporter genes *HXT2* and *HXT4* [283]. The D225Y substitution, which stimulated glucose-xylose co-consumption in the present study, is located in the glycogen-binding domain (GBD) of Gal83 (residues 161-243 [387]). Other mutations in this domain have been shown to cause transcription of Snf1-Gal83 targets in the presence of glucose [325, 387, 388]. In contrast to deletion of the transcriptional regulator *CYC8* [363], which also stimulated co-utilization but caused severe reductions of the specific growth rate of engineered strains, the *GAL83^{G673T}* mutation did not have a strong impact on growth rate (Tables 5 and 6). The synergistic effect of the *hxk2Δ* and *GAL83^{G673T}* mutations may be related to the involvement of Hxk2 in deactivation of Snf1 in the presence of glucose, causing constitutive activity of the Snf1-Gal83 complex in *hxk2*-null mutants [389, 390].

The reverse engineered mutations in *HXK2* and *GAL83* or *RSP5* not only stimulated simultaneous utilization of xylose and glucose when both sugars were present, but also prevented the sharp decline in xylose uptake rates that occurred in the reference strain IMU079 (*XKS1*↑ PPP↑ pAKX002). In the reference strain, the biomass-specific rate of xylose consumption, probably mediated by low- or moderate-affinity Hxt transporters, declined to values below 0.5 mmol (g biomass)$^{-1}$ h^{-1} after glucose depletion (Figure 5, Additional File 7). Under anaerobic conditions, this low rate of xylose fermentation would correspond to a biomass-specific rate of ATP production of 0.8 mmol (g biomass)$^{-1}$ h^{-1}. This value is lower than the estimated ATP requirement for cellular maintenance of *S. cerevisiae* (ca. 1 mmol ATP (g biomass)$^{-1}$ h^{-1} [333]). Since protein synthesis is a highly ATP-intensive process [391], an inability of the reference strain to functionally express high-affinity hexose transporters upon glucose depletion may therefore reflect an energy

shortage. A similar effect was observed during transitions between glucose and galactose growth in anaerobic *S. cerevisiae* cultures [259]. By already expressing functional high-affinity transporters before glucose was depleted, the *hxk2Δ rsp5Δ* and *hxk2Δ GAL83^G673T* may have enabled cells to avoid such a bioenergetic 'valley of death' upon the transition to xylose fermentation. In industrial processes using lignocellulosic feedstocks, this energetic challenge is likely to be even more stringent due to the presence of compounds such as acetic acid that increase maintenance energy requirements [51, 173, 196].

While reverse engineering of *HXK2*, *RSP5* and *GAL83* mutations demonstrated the relevance of the forced co-utilization strategy demonstrated in this study, they do not exhaust its possibilities. Prolongation of the evolution experiments, combined with anaerobic conditions and/or a further increase of the glucose to xylose ratio in the medium, may allow for selection of additional relevant mutations. The IMS0629 strain can, for example, be used to select mutations that enable efficient co-utilization of glucose and xylose at different concentrations or in lignocellulosic hydrolysates that, in addition to fermentable sugars, contain inhibitors of yeast performance [52, 64, 67]. Alternatively, the strain design can be adapted to enable selection for co-metabolism of other sugars, for example by replacing the xylose pathway by a bacterial pathway for conversion of L-arabinose into xylulose-5-phosphate [84, 85].

Conclusion

Engineering of carbon and redox metabolism yielded an *S. cerevisiae* strain whose growth was strictly dependent on the simultaneous uptake and metabolism of xylose and glucose. Laboratory evolution improved growth of the resulting strains on mixtures of xylose and glucose at elevated glucose concentrations. Mutations in *HXK2*, *RSP5* and *GAL83* were identified by genome sequencing of the evolved strains. Upon their combined introduction into an engineered xylose-fermenting yeast strain, these mutations strongly stimulated simultaneous utilization of xylose and glucose and, after depletion of glucose, fast conversion of the remaining xylose. The developed strain platform and modified versions thereof can be used for identification of further metabolic engineering targets for improving the performance of yeast strains in industrial processes based on lignocellulosic feedstocks.

Acknowledgements

Supplementary Material

Additional File 1 | Primers used in this study.

Primer code	Sequence 5'-3'	Purpose
5980	CGACCGAGTTGCTCTTG	plasmid backbone amplification
5792	GTTTTAGAGCTAGAAATAGCAAGTTAAAATAAG	plasmid backbone amplification
5979	TATTGACGCCGGGCAAGAGC	plasmid insert amplification
5978	ATTTTAACTTGCTATTTCTAGCTCTAAAACTTTATGAC-GTATACGTTTACGATCATTTATCTTTCACTGCGG	plasmid insert amplification
5941	GCTGGCCTTTTGCTCACATG	plasmid backbone amplification
6005	GATCATTTATCTTTCACTGCGGAGAAG	plasmid backbone amplification
9269	TGCGCATGTTTCGGCGTTCGAAACTTCTCCGCAGTGAAAGA-TAAATGATCATTGACACCAAAAACATGTTGTTTTAGAGCTAGAAATAGCAAGTTAAAATAAG	plasmid insert amplification
9401	TGCGCATGTTTCGGCGTTCGAAACTTCTCCGCAGTGAAAGA-TAAATGATCTTTTGTTCCAAACATTACTCGTTTTAGAGCTAGAAATAGCAAGTTAAAATAAGGCTAGTCCGTTATCAAC	plasmid insert amplification
11270	GTTGATAACGGACTAGCCTTATTTTAACTTGC-TATTTCTAGCTCTAAAACAGTAACGTACACTTTATTACGATCATTTATCTTTCACTGCGGAGAAGTTTCGAAC-GCCGAAACATGCGCA	plasmid insert amplification
11373	GTTGATAACGGACTAGCCTTATTTTAACTTGC-TATTTCTAGCTCTAAAACCTTATATAATGACTCTGCAGGATCATTTATCTTTCACTGCGGAGAAGTTTCGAAC-GCCGAAACATGCGCA	plasmid insert amplification
8956	GCCAGAGGTATAGACATAGCCAGACCTACCTAATTGGTG-CATCAGGTGGTCATGGCCCTTGACGCGCATAACCGCTAGAG	cassette construction
8960	TGTATATGAGATAGTTGATT	cassette construction
8958	TGAGCTACACTGTCCGCAAGATTGCGACCTCGTCATGGC-TATACGGTCTCGCAGATCGCTCCACTAGTCAGATGCCGCGG	cassette construction
8961	TTTGATTTAGTGTTTGTGTG	cassette construction
8953	CCAAGCATACAATCAACTATCTCATATACAATGAG-TGAAGGCCCCGTCAA	cassette construction
8964	AGCGATCTGCGAGACCGTATAGCCATGACGAGGTCG-CAATCTTGCGGACAGTGTAGCTCAGGGCAAAGGGACAGATGAAG	cassette construction
8984	TGCTTATCAACACACAAACACTAAATCAAAATGGTGACAG-TCGGTGTGTT	cassette construction
8986	GTCACGGGTTCTCAGCAATTCGAGCTATTAC-CGATGATGGCTGAGGCGTTAGAGTAATCTCGGGCTAGAGATCTTGACTG	cassette construction
4870	GCCAGAGGTATAGACATAGCC	cassette construction
7369	AGCGATCTGCGAGACCGTATAG	cassette construction

3290	GTCACGGGTTCTCAGCAATTCG	cassette construction
3291	CTCTAACGCCTCAGCCATCATCG	cassette construction
4068	GCCTACGGTTCCCGAAGTATGC	cassette construction
3274	TATTCACGTAGACGGATAGGTATAGC	cassette construction
3275	GTGCCTATTGATGATCTGGCGGAATG	cassette construction
3847	ACTATATGTGAAGGCATGGCTATGG	cassette construction
3276	GTTGAACATTCTTAGGCTGGTCGAATC	cassette construction
4691	CACCTTTCGAGAGGACGATG	cassette construction
3277	CTAGCGTGTCCTCGCATAGTTCTTAGATTG	cassette construction
3283	ACGTCTCACGGATCGTATATGC	cassette construction
3288	TGCCGAACTTTCCCTGTATGAAGC	cassette construction
7133	TATAATATTTCATTATCGGAACTCTAGATTCTATACTT-GTTTCCCAATTGTTGCTGGTAGGGCCCTTCCGGGAGTTTATC	cassette construction
10460	ACTATATGTGAAGGCATGGCTATGGCACGGCAGA-CATTCCGCCAGATCATCAATAGGCACCGGCCGTGTTTAAAGATTAC	cassette construction
10461	GCCGTAGCTTCCGCAAGTATGCCGTAGTTGAAGAGCATTT-GCCGTCGGTTCAGGTCATATTCATAGGTGAGAAAGAGATGGAGAATGTAG	cassette construction
6285	AAGGGCCATGACCACCTGATGCACCAATT-AGGTAGGTCTGGCTATGTCTATACCTCTGGCGCGATACCCTGCGATCTTC	cassette construction
7548	GCATAGAACATTATCCGCGGAAACGGG-TATTAGGGGTGAGGGTGAATAAGGAAAGTCAGGGAAATCGGGCCGCGCAGATTAGCGAAGC	cassette construction
6280	GTGCCTATTGATGATCTGGCGGAATGTCTGCCGTGCCA-TAGCCATGCCTTCACATATAGTGCGATACCCTGCGATCTTC	cassette construction
6273	GCCAGAGGTATAGACATAGCCAGACCTACCTAATTGGTG-CATCAGGTGGTCATGGCCCTTCGCGCAGATTAGCGAAGC	cassette construction
6281	GTTGAACATTCTTAGGCTGGTCGAATCATTTAGACACGGG-CATCGTCCTCTCGAAAGGTGGCGATACCCTGCGATCTTC	cassette construction
6270	ACTATATGTGAAGGCATGGCTATGGCACGGCAGA-CATTCCGCCAGATCATCAATAGGCACCGCGCAGATTAGCGAAGC	cassette construction
6282	CTAGCGTGTCCTCGCATAGTTCTTAGATTGTCGCTACGG-CATATACGATCCGTGAGACGTGCGATACCCTGCGATCTTC	cassette construction
6271	CACCTTTCGAGAGGACGATGCCCGTGTCTAAATGATTCGAC-CAGCCTAAGAATGTTCAACCGCGCAGATTAGCGAAGC	cassette construction
6284	AATCACTCTCCATACAGGGTTTCATACATTTCTCCACGG-GACCCACAGTCGTAGATGCGTGCGATACCCTGCGATCTTC	cassette construction
6272	ACGTCTCACGGATCGTATATGCCGTAGCGACAATCTAA-GAACTATGCGAGGACACGCTAGCGCGCAGATTAGCGAAGC	cassette construction
6283	ACGCATCTACGACTGTGGGTCCCGTGGA-GAAATGTATGAAACCCTGTATGGAGAGTGATTGCGATACCCTGCGATCTTC	cassette construction
6275	ACGAGAGATGAAGGCTCACCGATGGACTTAG-TATGATGCCATGCTGGAAGCTCCGGTCATCGCGCAGATTAGCGAAGC	cassette construction

161

6287	ATGACCGGAGCTTCCAGCATGGCATCATACT-AAGTCCATCGGTGAGCCTTCATCTCTCGTGCGATACCCTGCGATCTTC	cassette construction
6276	TTCTAGGCTTTGATGCAAGGTCCACATATCTTCGTTAG-GACTCAATCGTGGCTGCTGATCCGCGCAGATTAGCGAAGC	cassette construction
6288	GATCAGCAGCCACGATTGAGTCCTAACGAAGATATGTGGAC-CTTGCATCAAAGCCTAGAAGCGATACCCTGCGATCTTC	cassette construction
6277	ATACTCCCTGCACAGATGAGTCAAGCTATTGAACACCGA-GAACGCGCTGAACGATCATTCCGCGCAGATTAGCGAAGC	cassette construction
6289	GAATGATCGTTCAGCGCGTTCTCGGTGTTCAATAGCTT-GACTCATCTGTGCAGGGAGTATGCGATACCCTGCGATCTTC	cassette construction
6274	GCCTACGGTTCCCGAAGTATGCTGCTGATGTCTGGCTATAC-CTATCCGTCTACGTGAATACGCGCAGATTAGCGAAGC	cassette construction
5920	TATTCACGTAGACGGATAGGTATAGCCAGACATCAGCAG-CATACTTCGGGAACCGTAGGCAGCTCATAGCTTCAAAATGTTTCTACTCC	cassette construction
9029	TATATTTGATGTAAATATCTAGGAAATACACTTGTG-TATACTTCTCGCTTTTCTTTTATTGTCCAGTGCTTCCACATC	cassette construction
7135	ATATGACCTGAACCGACGGCAAATGCTCTTCAACTACGG-CATACTTGCGGAAGCTACGGCCATAGCTTCAAAATGTTTCTACTCC	cassette construction
7222	CAGACAGCAAACTTTGTTCCATGGTCGCCATTGAC-TATGGTGCAATCGCTGACATGAGCCGTCCAGTGCTTCCACATC	cassette construction
11273	CCGTTAAAACACAGGCCACG	cassette construction
11274	TGCCGTGTGAACGTTCAAAG	cassette construction
3275	GTGCCTATTGATGATCTGGCGGAATG	diagnostic
3276	GTTGAACATTCTTAGGCTGGTCGAATC	diagnostic
5971	AGAGCCGGCATGCAAGGAAC	diagnostic
6637	GGCTGCTGTTAAGGATGATG	diagnostic
6640	CTAGATGTGGTCAGCCATTC	diagnostic
7869	CTTTGGGCAATCCTTTGGAG	diagnostic
7870	CTTCATCAGCACCGTCAAAC	diagnostic
7871	GGTGATTTCGGCTCTATTGC	diagnostic
7872	TCGGCTTCACCCTTGTAATC	diagnostic
7873	ACCCATGTGGTTGCTGATTC	diagnostic
7874	AAATCTGGGTGCCGAATTCC	diagnostic
7875	TTGATAAGCTAGCCGTCTCC	diagnostic
7877	CAACCATATGCCTCGTATCG	diagnostic
7923	GAAGCAGCGTATTGCAAAGC	diagnostic
8969	TCAGAGACGTGATGCAGAAC	diagnostic
8987	ATCGTGGCACCAAGCAACTC	diagnostic
8988	TTGGGCTGTGGTCCTGATGG	diagnostic
533	CATGGCATGTAATGGAAAGCA	diagnostic
3354	ACGCATCTACGACTGTGGGTC	diagnostic
3837	GAATGATCGTTCAGCGCG	diagnostic
3843	GATCAGCAGCCACGATTG	diagnostic
4173	GTTGAACATTCTTAGGCTGG	diagnostic

4184	ATGACCGGAGCTTCCAGCATG	diagnostic
4692	AAGGGCCATGACCACCTG	diagnostic
5231	AATCACTCTCCATACAGGG	diagnostic
6632	AGCGTCGTAGTAGTGGAAAGC	diagnostic
6633	ATGGACGCTATGGCTAGAGCTTTGG	diagnostic
7056	AGAGGTGGTGGTTTCGTTAC	diagnostic
7298	TTGTTCAATGGATGCGGTTC	diagnostic
7479	GGACGTTCCGACATAGTATC	diagnostic
9010	CCTCTCCCTTGCCAAAGAACC	diagnostic
1814	CAAACTGGCCACTGAATTGC	diagnostic
1815	TCCAATTCCTTGCCGATGAC	diagnostic
5004	GTAGATTGCACCATCTGAAGAGGC	diagnostic
5007	GAGGATGCTAAAAGTCCCGTC	diagnostic
7868	CAACTTGGGTTGCGAATGTC	diagnostic
7922	CGCAATTCCTTCGAGACTTC	diagnostic
9271	ATGAGGCAAGAACCGGGATG	diagnostic
9272	CCTTCGCGCACTGATTCATC	diagnostic
9275	AGTTGCACTCTGATGGGCTC	diagnostic
9276	GACGATACTGCATCCCAGGG	diagnostic
4930	GGCAAGAGTATAGCGTGATACC	diagnostic
4931	CGCAAGCTATCTAGAGGAAGTG	diagnostic
11273	CCGTTAAAACACAGGCCACG	diagnostic
11274	TGCCGTGTGAACGTTCAAAG	diagnostic
11376	AGCACCCACCCAGCTATGTC	diagnostic
11377	GTACGCTCGTTTCAGGTATG	diagnostic
9279	TTTAATACATATTCCTCTAGTCTTGCAAAATCGATTTA-GAATCAAGATACCAGCCTAAAAACAAATCGCTCTTAAATATATACCTAAAGAACATTAAAGCTATATTATAAGCAAAGATAC	*PGI1* knockout repair fragment
9280	GTATCTTTGCTTATAA-TATAGCTTTAATGTTCTTTAGGTATATATTTAAGAGCGATTTGTTTTTAGGCTGGTATCTTGATTCTAAATCGATTTTGCAA-GACTAGAGGAATATGTATTAAA	*PGI1* knockout repair fragment
9281	CAATTTCATGCAAGAAGGCCATTTGCTAATTCCAA-GAGCGAGGTAAACACACAAGAAAAATTGTACATATGCGGCATTTCTTATATTTATACTCTCTATACTATACGATATGG-TATTTTT	*RPE1* knockout repair fragment
9282	AAAAATACCATATCGTATAGTATAGAGAGTATAAATATAA-GAAATGCCGCATATGTACAATTTTTCTTGTGTGTTTACCTCGCTCTTGGAATTAGCAAATGGCCTTCTTGCATGAAATTG	*RPE1* knockout repair fragment
5888	TTTCTAATGCCTTTTCCATCATGTTACTACGAG-TTTTCTGAACCTCCTCGCACATTGGTAGCTTAATTTTAAATTTTTTTGGTAGTAAAAGATGCTTATATAAGGATTTCG-TATTTATTG	*HXK2* knockout repair fragment
5889	CAATAAATACGAAATCCTTATATAAGCATCTTTTACTAC-CAAAAAAATTTAAAATTAAGCTACCAATGTGCGAGGAGGTTCAGAAAACTCGTAGTAACATGATGGAAAAGGCATTAGAAA	*HXK2* knockout repair fragment

11271	GGTCGTTTCCTGCACAATAATAAATTATCTACACTGAAATT-GTAGAATTTCACCTAGACGTGGATATGATTATAGAGCTTATAGCTACATCTTTTTAGATAAA	*GAL83* knockout repair fragment + synthetic PAM sequence addition
11272	TTTATCTAAAAAGATGTAGCTATAAGCTCTATAATCATA-TCCACGTCTAGGTGAAATTCTACAATTTCAGTGTAGATAATTTATTATTGTGCAGGAAACGACC	*GAL83* knockout repair fragment + synthetic PAM sequence addition
11374	TTTCTTTGTTAGCTTGGGTATTA-TATTTAAAGTAACAGAAAGGAAAGAAAAAAGAAAAAATTATTCCGCAC-CAATTTTTTTTTTTATTTATGGTGTCCGTTTTCCCAACATTCTTTCTGC	*RSP5* knockout repair fragment
11375	GCAGAAAGAATGTTGGGAAAACGGACACCATAAA-TAAAAAAAAAAATTGGTGCGGAATAATTTTTTCTTTTTTCTTTCCTTTCTGTTACTTTAAATATAATACCCAAGCTAACAAA-GAAA	*RSP5* knockout repair fragment

Additional File 2 | MATLAB script for modification of the Yeast v7.6 consensus metabolic model [354] according to the glucose-xylose forced co-consumption strategy. The COBRA v2 toolbox [355] was used to read the model in MATLAB vR2017b (Mathworks, Natick, MA).

```
function [model,solution,ratio] = coconsumption(model,mu,qO2)
```

Adapting model to strategy

```
%remove GRE3, GND1/GND2, RPE1, PGI1 ad BNA5
removeList = [{'r_1093'},{'r_0889'},{'r_0984'},{'r_0467'},{'r_0670'}];
model_strat = changeRxnBounds(model,removeList,0,'b');
removed = ['The following reactions have been disabled in the
stoichiometric model: ', strjoin(removeList)]; disp(removed)
%add XI and gndA
disp('The following reactions have been added to the stoichiometric model:
')
model_strat =
addReaction(model_strat,'r_5001',{'s_0578[c_03]','s_0580[c_03]'},[-1 1]);
model_strat = addReaction(model_strat,'r_5002','s_0340[c_03] +
s_1198[c_03] <=> s_0456[c_03] + s_0577[c_03] + s_1203[c_03]');
%Unlimited boundaries for glucose and xylose uptake
model_strat = changeRxnBounds(model_strat,[{'r_1714'},{'r_1718'}],-
1000,[{'l'},{'l'}]);
model_strat =
changeRxnBounds(model_strat,[{'r_1714'},{'r_1718'}],1000,[{'u'},{'u'}]);
```

Add experimental data

```
%Add experimentally measured growth rate and O2 uptake rate
model_strat = changeRxnBounds(model_strat,'r_2111',mu,'u');
model_strat = changeRxnBounds(model_strat,'r_1992',qO2,'b');
%Change objective function to growth
model_strat = changeObjective(model_strat,'r_2111');
```

Retrieve glucose and xylose uptake rates

```
solution = optimizeCbModel(model_strat);
glucose_rate = solution.x(findRxnIDs(model_strat,'r_1714'));
xylose_rate = solution.x(findRxnIDs(model_strat,'r_1718'));
rates = [glucose_rate; xylose_rate];
rates_disp = ['At a growth rate of ',num2str(mu), '/h and a qO2 of
',num2str(qO2),' mmol/gDW.h, the glucose- and xylose uptake rates are
',num2str(glucose_rate), ' and ',num2str(xylose_rate), ' mmol/gDW.h,
respectively'];
ratio = xylose_rate/glucose_rate; ratio_disp = ['The ratio of xylose over
glucose uptake is ',num2str(ratio)];
```

Check for requirement of co-consumption

```
model_check = changeRxnBounds(model_strat,'r_1714',0,'b');
solution_check = optimizeCbModel(model_check); no_glucose =
solution_check.origStat;
model_check = changeRxnBounds(model_strat,'r_1718',0,'b');
solution_check = optimizeCbModel(model_check); no_xylose =
solution_check.origStat;
check1 = ['Without glucose, solving the model is ', no_glucose];
check2 = ['Without xylose, solving the model is ', no_xylose];
```

Displaying output

```
disp(rates_disp); disp(ratio_disp); disp(check1); disp(check2)

end
```

Additional File 3 | Specific growth rates (μ) in aerobic shake-flask cultures of evolved strains grown on SM (parental IMX1046, *pgi1Δ rpe1Δ gnd1Δ gnd2Δ gndA XylA XKS1*↑ PPP↑) with 10 g L^{-1} glucose and 20 g L^{-1} xylose (pH 6, 30 °C). Growth rates were calculated from samples taken during the mid-exponential growth phase and represent averages ± mean deviation of independent duplicate cultures.

Strain		μ (h^{-1})
Evolution Line 1	IMS0628	0.18 ± 0.00
	IMS0629	0.21 ± 0.00
	IMS0630	0.19 ± 0.01
Evolution Line 2	IMS0634	0.16 ± 0.00
	IMS0635	0.14 ± 0.01
	IMS0636	0.15 ± 0.01
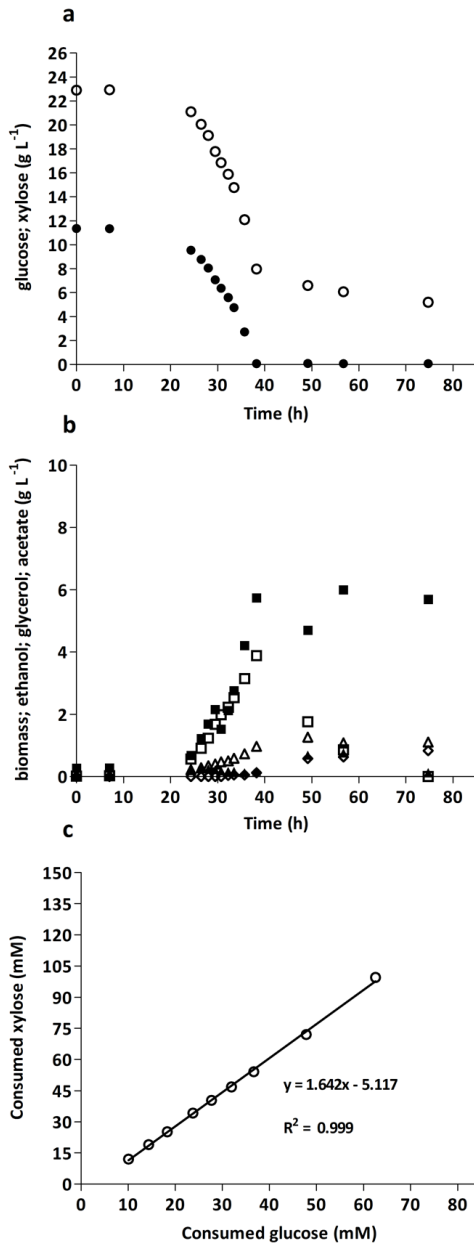
Additional File 4 | Sugar consumption, biomass and metabolite production profiles of the evolved *S. cerevisiae* strain IMS0629 (*pgi1Δ rpe1Δ gnd1Δ gnd2Δ gndA XylA XKS1↑* PPP↑), grown on SM with 10 g L⁻¹ glucose and 20 g L⁻¹ xylose in aerobic bioreactor batch cultures (pH 5, 30 °C). Cultures were grown in duplicate, the data shown are from a single representative culture. **a**: ● glucose, ○ xylose; **b**: ■ biomass □ ethanol ▲ acetate △ glycerol ◇ xylitol; **c**: ratio of xylose and glucose consumption during exponential growth phase.

a

b
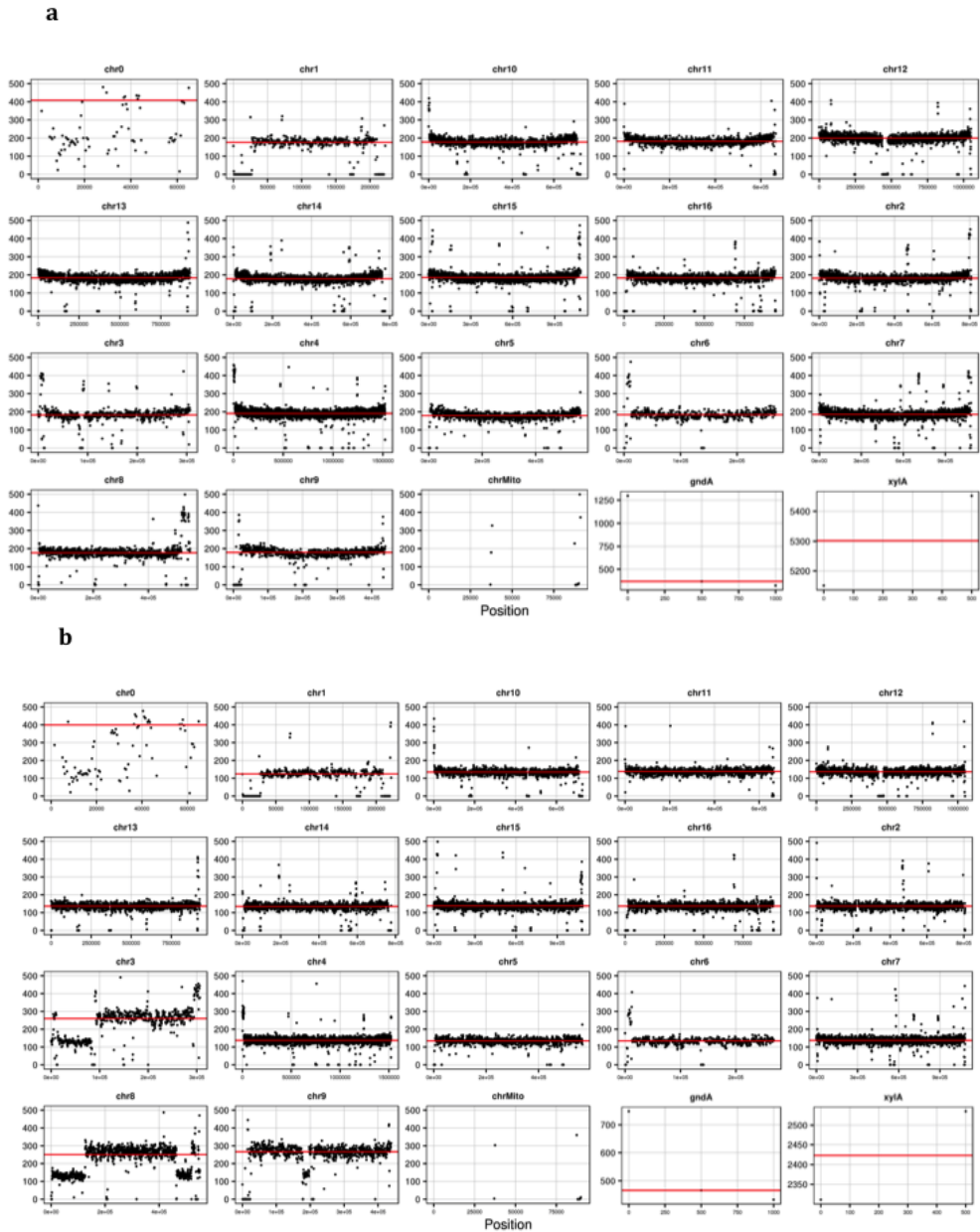
Additional File 5 | Sequence coverage plots comparing the genome of IMS0629 (a) and IMS0634 (b) to a published genome of CEN.PK113-7D (Nijkamp *et al.* 2012), generated using BWA to map the sequence reads from IMS0629 and IMS0634 to the CEN.PK113-7D reference. Further processed by SAMtools to extract the per base sequence depth and an in-house script to calculate the average coverage for 500 bp non-overlapping windows. R script was used to plot the 500 bp windows (black dots) and median coverage (red line).
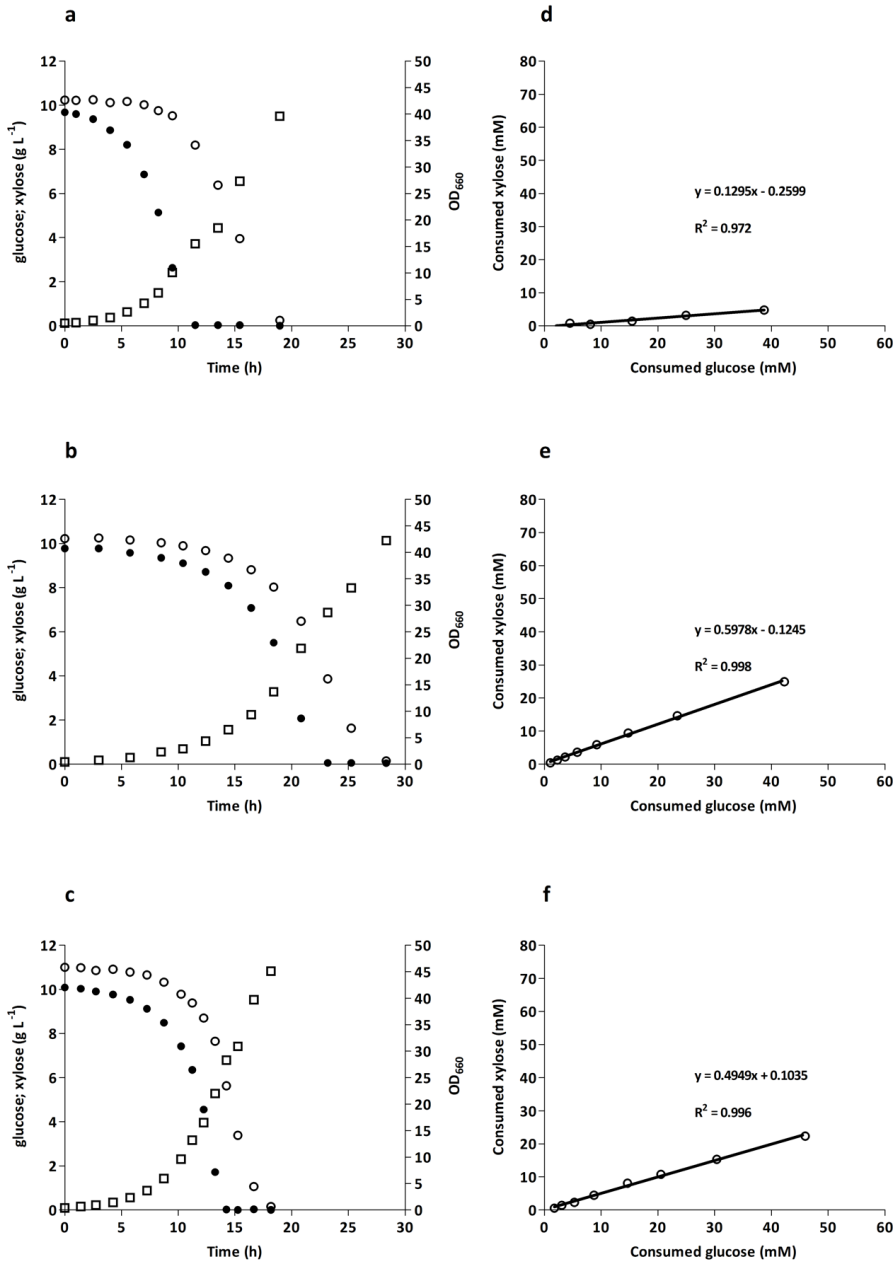
Additional File 6 | Consumption of glucose and xylose and growth of strains IMU079 (*XKS1*↑ PPP↑ pAKX002; a, d), IMX1515 (*hxk2Δ rsp5Δ XKS1*↑ PPP↑ pAKX002; b, e) and IMX1583 *(hxk2Δ gal83::GAL83*[G673T] *XKS1*↑ PPP↑ pAKX002; c, f) in batch cultures. The three strains were grown on SM (urea as nitrogen source) with 10 g L^{-1} glucose and 10 g L^{-1} xylose in aerobic shake-flask cultures (pH 6, 30 °C). a, b, c: ● glucose, ○ xylose, □ OD660; d, e, f: ratio of xylose and glucose consumption during exponential growth phase.
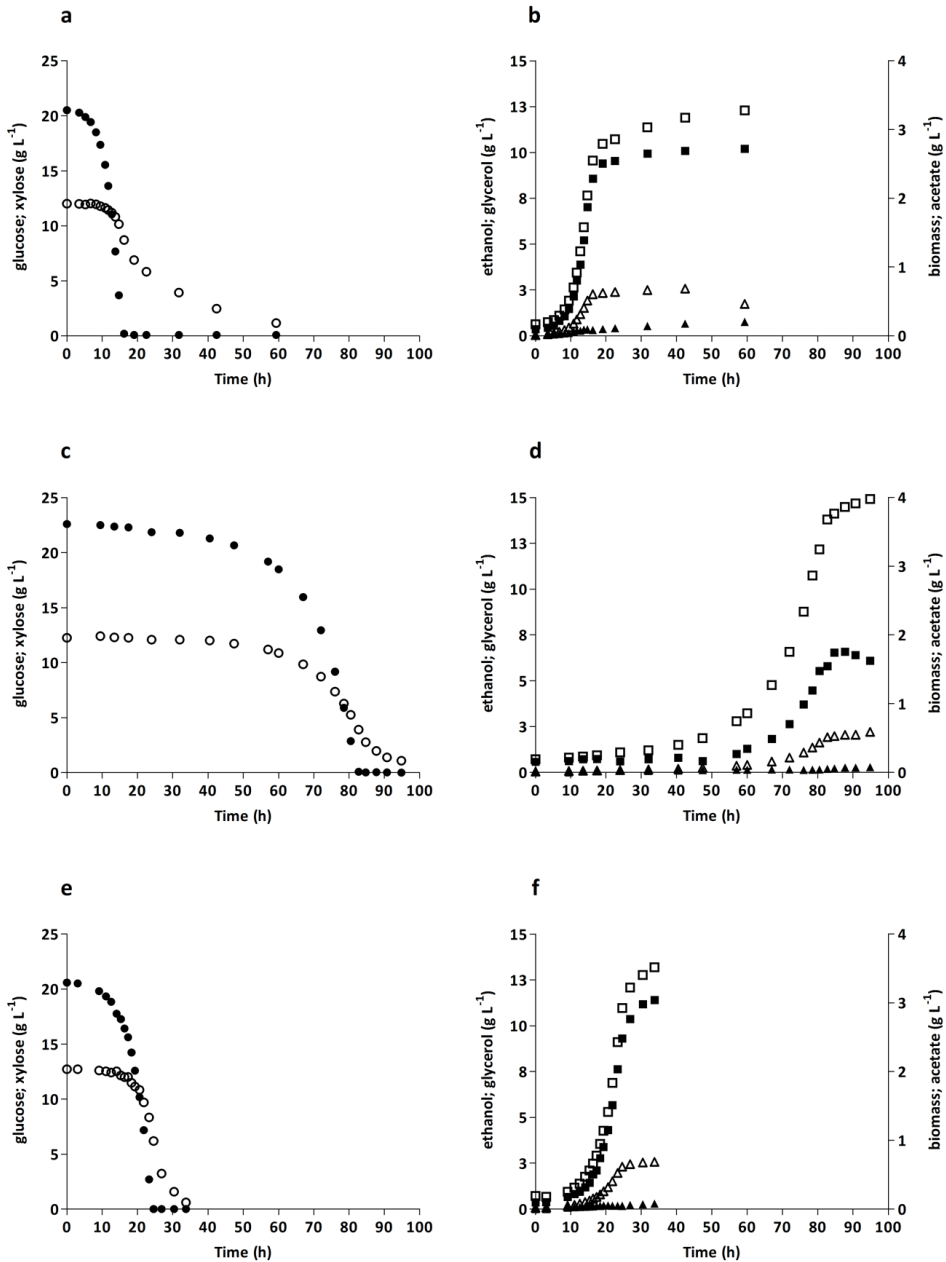
Additional File 7 | Sugar consumption, biomass and metabolite production profiles of S. cerevisiae strains IMU079 (*XKS1*↑ PPP↑ pAKX002; a, b), IMX1515 (*hxk2Δ rsp5Δ XKS1*↑ PPP↑ pAKX002; c, d) and IMX1583 (*hxk2Δ gal83::GAL83^{G673T} XKS1*↑ PPP↑ pAKX002; e, f), grown on SM with 20 g L-1 glucose and 10 g L-1 xylose in anaerobic bioreactor batch cultures (pH 5, 30 °C). Cultures were grown in duplicate, the data shown are from a single representative culture. a: ● glucose, ○ xylose; b: ■ biomass □ ethanol ▲ acetate △ glycerol. Data on ethanol corrected for evaporation.

Chapter 6: Fermentation of glucose-xylose-arabinose mixtures in repeated batch cultures by a synthetic consortium of single-sugar- fermenting *Saccharomyces cerevisiae* strains

Maarten D. Verhoeven, Sophie C. de Valk, Jean-Marc G. Daran, Antonius J.A. van Maris & Jack T. Pronk

Abstract

D-Glucose, D-xylose and L-arabinose are major sugars in lignocellulosic hydrolysates. This study explores fermentation of glucose-xylose-arabinose mixtures by a consortium of three 'specialist' *Saccharomyces cerevisiae* strains. A D-glucose- and L-arabinose-tolerant xylose specialist was constructed by eliminating hexose phosphorylation in an engineered xylose-fermenting strain and subsequent laboratory evolution. A resulting strain anaerobically grew and fermented D-xylose in the presence of 20 g L^{-1} of D-glucose and L-arabinose. A synthetic consortium that additionally comprised a similarly obtained arabinose specialist and a pentose-non-fermenting laboratory strain, rapidly and simultaneously converted D-glucose and L-arabinose in anaerobic batch cultures on three-sugar mixtures. However, performance of the xylose specialist was strongly impaired in these mixed cultures. After prolonged cultivation of the consortium on three-sugar mixtures, the time required for complete sugar conversion approached that of a previously constructed and evolved 'generalist' strain. In contrast to the generalist strain, whose fermentation kinetics deteriorated during prolonged repeated-batch cultivation on a mixture of 20 g L^{-1} D-glucose, 10 g L^{-1} D-xylose and 5 g L^{-1} L-arabinose, the evolved consortium showed stable fermentation kinetics. Understanding the interactions between specialist strains is a key challenge in further exploring the applicability of this synthetic consortium approach for industrial fermentation of lignocellulosic hydrolysates.

Introduction

Industrial production of fuel ethanol by *Saccharomyces cerevisiae* still predominantly relies on hydrolysed cane sugar and corn starch as carbon sources [16]. Alternatively, fermentable sugar mixtures can be generated by hydrolysis of agricultural residues such as corn stover, wheat straw, corn fiber or corn cobs [40, 206]. Cost-effective operation of such lignocellulose-based processes, for which the first full-scale plants have recently come on line [279], requires complete conversion of all sugars in lignocellulosic hydrolysates. In addition to D-glucose, these hydrolysates contain substantial amounts of the pentoses D-xylose (10-25% of dry biomass) and L-arabinose (usually 2-3%, although some hydrolysates contain up to 20% L-arabinose) [41, 42, 206].

Intensive metabolic engineering of *S. cerevisiae*, which cannot naturally ferment pentoses, has enabled efficient anaerobic fermentation of D-xylose and L-arabinose [206, 279]. In engineered strains, pentoses enter the yeast metabolic network as D-xylulose-5-phosphate, whose entry into glycolysis is facilitated by overexpression of the enzymes of the non-oxidative pentose-phosphate pathway (PPP) [7, 98, 148-151, 392]. Conversion of D-xylose into D-xylulose-5-phosphate in these strains relies on overexpression of xylulokinase (Xks1), along with heterologous expression of a xylose isomerase [98, 148-151, 246] or combined heterologous expression a xylose reductase and xylitol dehydrogenase [5, 44, 81, 132, 142]. Conversion of L-arabinose into D-xylulose-5-phosphate has been achieved by expression of bacterial genes encoding L-arabinose isomerase (AraA), L-ribulokinase (AraB), and L-ribulose-5-phosphate-4-epimerase (AraD) [46, 84, 85], combined with deregulation of the Gal2 galactose permease, which also transports L-arabinose [46, 88, 163, 321]. Further knowledge-based engineering, random mutagenesis and evolutionary engineering has yielded *S. cerevisiae* strains that are now applied at industrial scale for conversion of lignocellulosic hydrolysates (for a recent review see [279]).

Anaerobic fermentation of sugar mixtures by pentose-fermenting *S. cerevisiae* strains is typically characterized by a fast phase of glucose fermentation, followed by slower utilization of the two pentoses [13, 393, 394]. Maximizing fermentation rates throughout mixed-sugar conversion processes will not only benefit volumetric productivity of industrial processes, but also increase tolerance to inhibitors present in lignocellulosic hydrolysates [110, 173, 279]. Poor kinetics of Hxt- and Gal2-mediated pentose transport, reflected by low affinity for these pentoses and strong competitive inhibition by glucose play a key role in the preferential use of glucose and 'tailing' of pentose concentrations towards the end of fermentation processes [7, 13, 93, 103]. Intensive research is therefore directed at improving pentose-uptake kinetics by expressing variants of native Hxt transporters and/or heterologous transporters that enable high-affinity pentose uptake in the presence of glucose [88, 123, 162, 164, 171, 177, 184, 186, 322] as well as by improvement of the kinetics of pentose isomerases [105, 133, 153]. While progress has been made in optimizing pentose fermentation kinetics, engineered *S. cerevisiae*

strains described in the public domain still exhibit lower fermentation rates on pentoses than on D-glucose [279].

So far, research on fermentation of lignocellulosic hydrolysates by *S. cerevisiae* has focused on the development of 'generalist' yeast strains, capable of fermenting mixtures of D-glucose, D-xylose and L-arabinose. However, from a theoretical perspective, the maximum conversion rate under substrate-excess conditions can only be reached when, through evolutionary adaptation or strain engineering, a microbe preferentially allocates its cellular resources (e.g. ribosomal capacity, ATP, amino acids) to fast conversion of a single substrate [395]. This principle, which explains evolution of sequential (diauxic) substrate utilization during mixed-substrate utilization by wild-type micro-organisms, suggests that use of consortia of yeast strains specialized in the fermentation of either D-glucose, D-xylose or L-arabinose might enable better mixed-sugar fermentation kinetics than application of a single generalist strain.

An additional potential advantage of mixed-sugar conversion by consortia of specialist strains relates to process stability. To optimize volumetric productivity, industrial processes should ideally recycle yeast biomass, rather than to initiate each new batch cycle with a new, freshly propagated inoculum of yeast biomass. Such yeast biomass recycling requires stability of fermentation kinetics through a large number of cultivation cycles. However, laboratory evolution experiments with engineered pentose-fermenting generalist yeast strains have shown progressive degeneration of their pentose fermentation kinetics during prolonged growth in repeated batch cultures [13, 396]. This observation has also been attributed to a strong selective pressure for resource allocation to a preferred substrate, at the expense of the utilization of less preferred substrates [13, 396].

The trade-offs imposed by resource allocation and/or metabolic interference between different substrate-conversion pathways should, in theory, not apply during conversion of substrate mixtures by consortia of 'specialist' microbes that can each only convert a single substrate [239, 397]. Several previous studies have investigated conversion of glucose-xylose mixtures by defined microbial consortia. A binary consortium of recombinant *E. coli* single-sugar specialists strains was shown to efficiently produce lactate from a mixture of xylose and glucose [398, 399]. Studies on the use of defined microbial consortia for ethanol production from sugar mixtures focused on co-cultivation of non-engineered glucose-fermenting microbes such as *S. cerevisiae* with naturally D-xylose consuming organisms such as *Scheffersomyces stipitis, E. coli* or *Zymomonas mobilis* in which glucose metabolism was inactivated [239, 400]. Biosynthetic oxygen requirements [401], byproduct formation [397], sensitivity to phages and/or lower ethanol tolerance [206, 400, 402] represent challenges in the industrial application of such non-*Saccharomyces* ethanologens. Additionally, previous studies on ethanol production from sugar mixtures by synthetic microbial consortia have not compared the long-term stability of mixed-sugar fermentation in cultures of single generalist strains and consortia of specialists.

175

The goal of the present study was to explore conversion of mixtures of D-glucose, D-xylose and L-arabinose by a synthetic consortium of a glucose-fermenting laboratory strain of *S. cerevisiae* and two glucose-phosphorylation-deficient *S. cerevisiae* strains engineered and evolved for efficient fermentation of either D-xylose or L-arabinose in the presence of the other two sugars. After studying fermentation of sugar mixtures by the individual specialist strains, fermentation kinetics of the consortium were improved by laboratory evolution. Performance and stability of fermentation kinetics by the consortium during prolonged, anaerobic repeated batch cultivation were compared with that of a previously described 'generalist' strain engineered and evolved for fermentation of glucose-pentose mixtures [13].

Materials and Methods

Strains and maintenance. The *S. cerevisiae* strains used in this study were derived from the CEN.PK lineage [251, 266] (Table 1). For storage, strains were grown on synthetic medium [51] containing 20 g L^{-1} D-glucose or, in the case of glucose-phosphorylation-negative, xylose- or arabinose-fermenting strains, 20 g L^{-1} D-xylose or 20 g L^{-1} L-arabinose respectively. Auxotrophic strains were grown on yeast-extract/peptone (YP) medium (10 g L^{-1} Bacto yeast extract (Becton Dickinson, Franklin Lakes, NJ) and 20 g L^{-1} Bacto Peptone (Becton Dickinson). Single-colony isolates obtained after laboratory evolution were grown in synthetic medium containing 20 g L^{-1} of each D-glucose, D-xylose and L-arabinose. After strains were grown in shake flasks [295], glycerol (30% vol/vol) was added and 1 mL aliquots were stored at -80 °C.

Media and shake flask cultivation. Synthetic medium (SM) and sugar solutions were prepared as described previously [51]. After autoclaving the mineral salts medium for 20 min at 121 °C, filter-sterilized vitamin solution [51] and 50 % (w/w) sterile solutions of D-glucose, D-xylose and L-arabinose were added. Prior to inoculation, 20 g L^{-1} L-arabinose (SMA), 20 g L^{-1} D-glucose (SMD), 20 g L^{-1} D-xylose (SMX), 20 g L^{-1} L-arabinose and 20 g L^{-1} D-glucose (SMAG), 20 g L^{-1} D-xylose and 20 g L^{-1} D-glucose (SMXG), or 20 g L^{-1} L-arabinose, 20 g L^{-1} D-glucose and 20 g L^{-1} D-xylose (SMAGX) were added to SM as carbon sources. Solid media were prepared by adding 20 g L^{-1} agar (Becton Dickinson) to SM or YP medium prior to autoclaving at 121 °C for 20 min. Shake-flask cultures were conducted in 500-ml flasks containing 100 ml of medium and were incubated in an orbital shaker at 200 rpm set at 30 °C. Physiological characterization of aerobic growth was performed in shake flasks containing SMX or SMXG with urea as sole nitrogen source [403] to prevent acidification. Cultures were prepared by inoculating frozen stocks (1 ml aliquots in 30% glycerol) directly into pre-culture shake flasks. In late exponential phase an aliquot was transferred to a second pre-culture to obtain an initial OD_{660} of 0.1. All cultures used for physiological characterization were inoculated from such secondary pre-cultures, growing in late exponential phase. Shake-flask cultures grown under anaerobic conditions were incubated at 30 °C in an Innova anaerobic chamber (5% H_2, 6% CO_2, and 89% N_2,

New Brunswick Scientific, Edison, NJ) in 50 mL shake flasks placed on an orbital shaker set at 200 rpm. Synthetic media used for anaerobic cultivations were supplemented with the anaerobic growth factors Tween 80 (420 mg L^{-1}) and ergosterol (10 mg L^{-1}), dissolved in ethanol [271]. To avoid growth limitation by anaerobic growth factors at biomass concentrations above 2.5 g L^{-1} [271]. Tween 80 and ergosterol concentrations in culture stability experiments were increased to 504 mg L^{-1} and 12 mg L^{-1} respectively.

Table 1 | *Saccharomyces cerevisiae* strains used in this study

Strain	Relevant genotype	Reference
CEN.PK 113-7D	*MATa MAL2-8c SUC2*	[251]
IMS0010	*MATa ura3-52 leu2-112 loxP-pTPI::(266, 1)TAL1 gre3::hphMX pUGPTPI-TKL1 pUGPTPI-RPE1 loxP-PTPI::(40, 1)RKI1 {pRW231, pRW243};* strain harboring *Piromyces* sp. E2 *xylA* and *L. plantarum araA* and *araD* on 2μ-based plasmid pRW231 and *XKS1* and *L. plantarum araB* on integration plasmid pRW243; selected for anaerobic growth on L-arabinose, and mixtures of D-xylose, D-glucose and L-arabinose	[13]
IMS0522	*MATa ura3-52 his3-1 leu2-3,112 MAL2-8c SUC2 glk1::Sphis5, hxk1::KlLEU2 gal1::cas9- amdS gre3::pTDH3_RPE1 pPGK1_TKL1, pTEF1_TAL1 pPGI1_NQM1 pTPI1_RKI1 pPYK1_TKL2 gal80::(pTPI_araA_tCYC)*9 pPYK-araB-tPGI1 pPGK-araD-tTDH3 hxk2:: PcaraT* that has undergone laboratory evolution on mixture of arabinose, glucose and xylose under anaerobic conditions	[404]
IMX604	*MATa ura3-52 his3-1 leu2-3,112 MAL2-8c SUC2 glk1::Sphis5, hxk1::KlLEU2 gal1::cas9- amdS gre3::pTDH3_RPE1 pPGK1_TKL1, pTEF1_TAL1 pPGI1_NQM1 pTPI1_RKI1 pPYK1_TKL2*	[404]
IMX659	*MATa ura3-52 his3-1 leu2-3,112 MAL2-8c SUC2 glk1::Sphis5, hxk1::KlLEU2 gal1::cas9- amdS gre3::pTDH3_RPE1 pPGK1_TKL1, pTEF1_TAL1 pPGI1_NQM1 pTPI1_RKI1 pPYK1_TKL2 can1::(pTPI_xylA_tCYC)*9 pTEF1-XKS1*	This study
IMX730	*MATa ura3-52 his3-1 leu2-3,112 MAL2-8c SUC2 glk1::Sphis5, hxk1::KlLEU2 gal1::cas9- amdS gre3::pTDH3_RPE1 pPGK1_TKL1, pTEF1_TAL1 pPGI1_NQM1 pTPI1_RKI1 pPYK1_TKL2 can1::(pTPI_xylA_tCYC)*9 pTEF1-XKS1 hxk2:: PcaraT*	This study
IMS0524	IMX730 subjected to evolutionary engineering on a mixture of D-xylose, D-glucose and L-arabinose under anaerobic conditions	This study
IMS0533	IMX730 subjected to evolutionary engineering on a mixture of D-xylose, D-glucose and L-arabinose under anaerobic conditions	This study
IMS0535	IMX730 subjected to evolutionary engineering on a mixture of D-xylose, D-glucose and L-arabinose under anaerobic conditions	This study
IMS0537	IMX730 subjected to evolutionary engineering on a mixture of D-xylose, D-glucose and L-arabinose under anaerobic conditions	This study

Strain construction. *S. cerevisiae* strains were transformed following the protocol of Gietz and Woods [323]. The plasmids used in this study are listed in Supplemental Table 1. Plasmid DNA was isolated from *E. coli* cultures using a GenElute Plasmid kit (Sigma-

Aldrich, St. Louis, MO). Nine DNA fragments carrying the expression cassettes of the *Piromyces* SP E2. *xylA* and a single overexpression cassette of *xks1* were PCR amplified from pUD350 and pUD353 [295] using the primers as listed in Supplemental Table 2 The PCR amplifications added homologous flanks that facilitated *in vivo* assembly and integration into the *CAN1* locus. Strain IMX604 was co-transformed with all ten fragments and the *CAN1*-gRNA plasmid pMEL10 [137]. Transformed cells were incubated for one hour in SMD after which they were plated on SMX. Colonies were restreaked thrice on SMX plates and correct assembly of all ten fragments in the *CAN1* locus was confirmed by diagnostic PCR (Dreamtaq, Thermo Scientific). Plasmid pMEL10 was counter selected on YP with 20 g L^{-1} D-xylose (YPX) agar with 5-fluoroorotic acid (5-FOA) as described previously [137]. *HXK2* was deleted in the resulting strain IMX659 by co-transforming plasmid pUDE327 and the *Pc*araT expression cassette obtained from pPWT118 as the repair fragment. After counter selection of pUDE327 with 5-FOA, the wild-type *URA3* gene was restored as described previously [137], yielding strain IMX730.

Batch cultivation and laboratory evolution. Anaerobic batch cultivation was performed in 2-L laboratory bioreactors (Applikon, Delft, The Netherlands) with a working volume of 1 L, which were stirred at 800 rpm and continuously sparged with nitrogen gas (<10 ppm oxygen) at 0.5 L min^{-1}. Temperature was set at 30 °C and culture pH was controlled at 5.0 by automated addition of 2 M KOH. To minimize oxygen diffusion, anaerobic bioreactors were equipped with Viton O-rings and Norprene tubing (Cole Palmer Instrument Company, Vernon Hills, IL). Excessive foaming was prevented by adding 0.2 g L^{-1} antifoam C (Sigma-Aldrich, St. Louis, MO) to synthetic media used for bioreactor cultivation. Precultures were pelleted by centrifugation and resuspended in demi water prior to inoculation. Laboratory evolution experiments for improving D-xylose fermentation in the presence of D-glucose and L-arabinose, as well as culture stability experiments were performed in sequential batch reactors (SBRs). On-line measurement of CO_2 concentrations in the off gas of SBRs was used as input for a control routine programmed in MFCS/win 3.0 (Sartorius AG, Göttingen, Germany). During each cycle, an empty-refill cycle was automatically initiated when the CO_2 concentration in the exhaust gas had first increased above a threshold value of 0.2% (indicating growth) and subsequently decreased below a second threshold of 0.1 % (indicating sugar depletion). For culture stability experiments, the latter threshold was set at 0.05% as this value approximately corresponded to the CO_2 output of a non-growing culture. After the emptying phase, when approximately 7% of the initial culture volume was left in the reactor, the reactor was automatically refilled with fresh medium from a 20-L glass vessel, which was continuously sparged with nitrogen gas. Single colony isolates were obtained by three consecutive restreaks using samples of the single strain laboratory evolution cultures on SMAGX agar plates, incubated anaerobically at 30 °C. Laboratory evolution of the consortia was initiated in 50 mL shake-flasks containing SMAGX with urea to prevent acidification. Synthetic medium used for IMS0010 fermentations, consortium cultivation

and culture stability experiments in SBRs were supplemented with twice the amount of vitamins solution to avoid nutrient limitations. Moreover, additional Tween-80 and ergosterol (504 mg L^{-1} and 12 mg L^{-1} respectively) were added when the biomass concentration in these cultures reached 2.5 g dw L^{-1}. The initial concentrations of these anaerobic growth factors were not altered, in order to avoid growth inhibition [271].

Analytical methods. Biomass optical density measurements at 660nm were performed with a Libra S11 spectrometer (Biochrom, Cambridge, United Kingdom). Specific growth rates were calculated based on biomass dry weight measurements performed on at least six samples taken during the exponential growth phase. Culture dry weight (CDW) was analysed by filtering 10 mL culture samples over pre-weighed nitrocellulose filters (pore size, 0.45 μm; Gelman Laboratory, Ann Arbor, MI). Filters were washed with demineralized water and dried in a microwave oven (Bosch, Stuttgart, Germany) for 20 min at 360 W. Bioreactor exhaust gas was cooled by a condenser (2 °C) and dried with a Permapure MD-110-48P-4 dryer (Permapure, Toms River, NJ). CO_2 concentrations in the dried gas were measured using an NGA 2000 analyser (Rosemount Analytical, Orrville, OH). Metabolite concentrations in culture samples were determined by centrifugation and subsequent analysis of the supernatant by high-performance liquid chromatography (HPLC) on an Agilent 1260 HPLC (Agilent Technologies, Santa Clara, CA) equipped with a Bio-Rad HPX 87 H column (Bio-Rad, Hercules, CA) eluted at 60 °C with 0.5 g L^{-1} H_2SO_4 at a flow rate of 0.6 ml min^{-1}. Metabolite levels were quantified using an Agilent G1362A refractive-index detector and an Agilent G1314F VWD detector. D-xylitol concentrations in the presence of L-arabinose were measured using a D-sorbitol/xylitol assay kit (Megazyme International Ireland, Wicklow, Ireland). Correction for ethanol evaporation was done for all bioreactor experiments as described previously [89][492].

Results

Repeated batch cultivation of a pentose-fermenting *S. cerevisiae* strain on sugar mixtures leads to deterioration of fermentation kinetics. The D-glucose, D-xylose and L-arabinose fermenting *S. cerevisiae* strain IMS0010 was previously generated by a combination of metabolic and evolutionary engineering [13]. Evolutionary engineering of this strain involved prolonged cultivation in sequential batch reactors (SBRs) that were alternatingly grown on SMA, SMAG and SMAGX. This dynamic cultivation regime was designed to avoid selection for faster fermentation of glucose at the expense of pentose fermentation kinetics [13]. In anaerobic batch cultures, strain IMS0010 first consumed D-glucose and only then the two pentose sugars (Figure 1A, [13]).

To investigate stability of the mixed-sugar fermentation kinetics of *S. cerevisiae* IMS0010 during repeated batch cultivation on a mixture of three sugars, duplicate anaerobic SBR cultures were performed. To resemble sugar concentrations in common lignocellulosic hydrolysates [206], these cultures were grown on SM supplemented with

20 g L^{-1} D-glucose, 10 g L^{-1} D-xylose and 5 g L^{-1} L-arabinose. Over the first 6 cycles (ca. 200 h of cultivation), carbon dioxide production profiles revealed stable fermentation kinetics (Figure 1A, Supplemental Figure 1A). After this time, the length of the SBR cycles progressively increased (Figure 1B). In one of the reactors, a mechanical failure, which occurred after 600 h, resulted in premature execution of the empty-refill routine during the glucose consumption phase. This incident coincided with a sharp increase of the cycle length in the next cycle, from which the culture did not recover (Supplemental Fig 1B). After 38 days of operation, the cycle time of both reactors had increased from 25 ± 0.6 h in the fifth cycle to 51 ± 1.2 h in the final cycle (24th and 27th cycle for reactor 1 and 2, respectively). Biomass and extracellular metabolite measurements, analysed during the fifth and final SBR cycles, indicated that slower conversion of the sugar mixture was primarily due to deterioration of L-arabinose fermentation kinetics (Figures 1A and 1C).
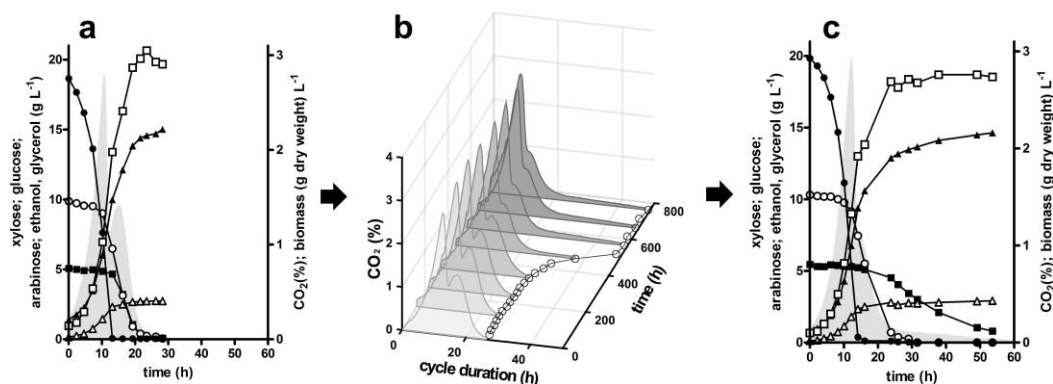
Figure 1 | Metabolite concentrations, CO_2 production curves and cycle length (h) of an anaerobic sequential batch reactor experiment of the glucose-xylose-arabinose consuming generalist strain *S. cerevisiae* IMS0010 on synthetic medium containing 20 g L^{-1} D-glucose, 10 g L^{-1} D-xylose and 5 g L^{-1} L-arabinose. Metabolite and CO_2 production profiles *(solid grey areas)* shown in **a.** and **c.** correspond to the fifth and 24th cycle of the SBR experiment. Symbols List of symbols: ● D-glucose, ○, D-xylose, ■, L-arabinose, □, biomass dry weight, ▲, ethanol, △, glycerol. **b.** 3-axis plot showing cycle length (○) and off-gas CO_2 profiles during prolonged SBR cultivation. To facilitate interpretation, this panel shows data for every fifth cycle 1, 5, 10, 15, etc. Complete off-gas CO_2 profiles for this experiment and an independent duplicate SBR experiment are provided in Supplemental Figure 1.

Construction of a *S. cerevisiae* D-xylose fermenting specialist strain. Glucose-phosphorylation-negative, D-xylose-metabolizing *S. cerevisiae* strains have previously been constructed and applied for *in vivo* evolution of Hxt transporter variants that enable D-xylose uptake in the presence of high glucose concentrations [112, 123, 176]. However, anaerobic growth of such glucose-phosphorylation-negative strains on xylose has not previously been studied. To construct a 'xylose-specialist' S. cerevisiae strain, multiple copies of an expression cassette for Piromyces xylA and a single copy of a XKS1 overexpression cassette were introduced in strain IMX604 (hxk1Δ glk1Δ gal1Δ::{Spcas9-AmdSYM} gre3Δ::{NPPP}), yielding strain IMX659 (hxk1Δ glk1Δ gal1Δ::{Spcas9-AmdSYM} gre3Δ::{NPPP} can1Δ::{xylA*9-XKS1}). After disrupting the remaining hexokinase gene HXK2 by integration of an expression cassette for the high-affinity PcAraT transporter [322, 404] a functional URA3 gene from S. cerevisiae CEN.PK113-7D was introduced, yielding the prototrophic xylose specialist strain IMX730 (hxk1Δ glk1Δ gal1Δ::{Spcas9-AmdSYM} gre3Δ::{NPPP} can1Δ::{*xylA**9-XKS1} hxk2Δ::*Pc*araT). In aerobic shake-flask cultures on SMX, strain IMX730 exhibited a specific growth rate of 0.22 h-1 (Figure 2A) while no growth was observed on SMD or SMA. In agreement with previous reports on inhibition of d-xylose by glucose [112, 123], a lower specific growth rate was observed on SMXG (0.16 h-1).
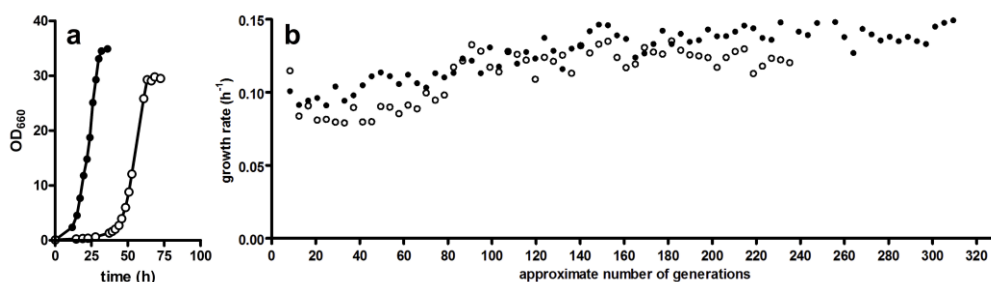
Figure 2 | Growth and laboratory evolution of the xylose specialist strain *S. cerevisiae* IMX730 (*hxk1Δ glk1Δ gal1Δ::{Spcas9*-AmdSYM} *gre3Δ::*{NPPP} *hxk2Δ::PcaraT can1Δ::*{*xylA**9-*XKS1*}). **a.** Growth curves in aerobic shake flask cultures on synthetic medium with 20 g L-1 D-xylose (●) or D-glucose and D-xylose (20 g L-1 each, ○). Data shown are derived from one of two duplicate growth experiments, of which kinetic parameters differed by less than 5%. **b.** Specific growth rate on D-xylose (h-1) during two independent laboratory evolution experiments estimated from CO_2 production profiles in SBR reactors: SBR 1 (○) and SBR 2 (●), in synthetic medium with 20 g L-1 L-arabinose, 20 g L-1 D-xylose and an increasing concentration of D-glucose (up to 20 g L-1) in independent biological replicates. The first data point for each experiment corresponds to the initial aerobic batch culture, all subsequent values were obtained under anaerobic conditions. CO_2 off-gas profiles and measured d-glucose glucose concentrations for both SBR experiments are shown in Additional File 5.

Despite the ability of strain IMX730 to grow aerobically on D-xylose in the presence of D-glucose, 2000 h of incubation in duplicate anaerobic bioreactors containing SMAGX did not result in observable growth (Supplemental Figure 3). After this long incubation period, a limiting oxygen feed (headspace aeration with 0.5 L min-1 of air while stirring the bioreactor at 300 rpm) was applied to generate active biomass. Subsequently,

the two reactors were partially emptied, refilled with fresh medium containing only xylose and switched back to fully anaerobic conditions. When growth was observed after 16 days, the culture was switched to SBR mode. During the first four cycles, the initial concentrations of D-xylose and L-arabinose were kept at 20 g L^{-1}, while the concentration of D-glucose was incrementally increased from 0 g L^{-1} to 20 g L^{-1}. Subsequently, over 150 days of SBR cultivation on SMAGX, the specific growth rate, as estimated from CO_2 production profile, progressively increased to ca. 0.14 h^{-1} and then stabilized (Figure 2b). After 254 and 284 days (Reactors 1 and 2, respectively), single colony isolates were obtained by plating and anaerobic incubation on SMAGX agar. The specific growth rates of 8 isolates from each reactor were analysed in anaerobic shake-flask cultures on SMAGX (Supplemental Figure 4). Based on these experiments, xylose specialist strains IMS0535 and IMS0537, which were selected from different SBR experiments, were grown on SMAGX in anaerobic batch reactors (Supplemental figure 5). Their estimated specific growth rates (0.13 h^{-1} and 0.12 h^{-1}, respectively) in these anaerobic cultures closely resembled those of the evolved populations at the end of the SBR evolution experiments from which they originated (Supplemental Figure 3).

Anaerobic fermentation of mixtures of D-glucose, D-xylose and L-arabinose by individual 'specialist strains'. To provide a baseline for interpretation of experiments with consortia of specialist strains, the D-xylose specialist strain IMS0535 described above and the 'glucose specialist' laboratory reference strain CEN.PK113-7D [251] were characterized in separate anaerobic batch reactors containing synthetic medium with 20 g L^{-1} D-glucose, 20 g L^{-1} D-xylose and 20 g L^{-1} L-arabinose (Figure 3A and 3C). Data from a published study on the hexose-phosphorylation-deficient L-arabinose specialist strain IMS0522 [404] are shown in Figure 3B. Sugar consumption profiles confirmed that each of the specialist strains only consumed a single sugar (Figure 3). The glucose and arabinose specialists reached complete sugar conversion after 12 and 24 h, respectively. Conversion of D-xylose by strain IMS0535 was slower and, when the D-xylose concentration decreased below ca. 5 g L^{-1}, its conversion rate decelerated, leaving ca. 1 g L^{-1} of residual D-xylose after 50 h (corresponding to 95 % conversion). The D-xylose consumption rate of strain IMS0535 in anaerobic cultures on SMAGX (Table 2) was approximately 50% lower than the highest reported rates of xylose consumption reported for engineered *S. cerevisiae* strains grown in synthetic medium with D-xylose as the only sugar [11, 279]. When biomass-specific conversion rates of each of the three sugars during anaerobic growth of the specialist strains on SMAGX were compared with those of the generalist strain IMS0010 (Table 2), the specialist strains consistently showed higher conversion rates. However, based solely on the single-strain experiments of the current xylose-specialist IMS0535 (Figure 3A), a consortium of these three specialists inoculated at similar cell densities would not be expected to reduce the total fermentation time for anaerobic growth on SMAGX relative to strain IMS0010.
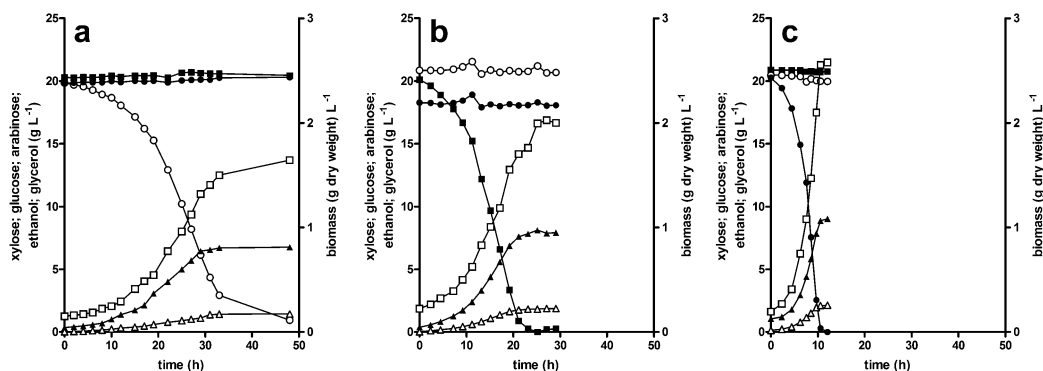
Figure 3 | Growth and extracellular metabolite concentrations in anaerobic batch cultures of the evolved pentose consuming, glucose-phosphorylation negative *S. cerevisiae* strains **a.** IMS0535 (D-xylose fermenting,), **b.** IMS0522 (L-arabinose fermenting, data previously obtained [404]) and **c.** of the D-glucose fermenting laboratory strain CEN.PK113-7D. All cultures were inoculated to a concentration of 0.12 g biomass dry weight L^{-1} in anaerobic bioreactors containing synthetic medium with 20 g L^{-1} D-glucose, 20 g L^{-1} D-xylose and 20 g L^{-1} L-arabinose. List of symbols: ● D-glucose, ○ D-xylose, ■, L-arabinose, □, biomass dry weight, ▲, ethanol, △, glycerol. Data shown in the figure represent data from one of two independent duplicate experiments for which kinetic parameters differed by less than 5% (Table 3).

Table 2 | Biomass-specific sugar consumption rate (q_s), maximum specific growth rate (μ_{max}) and yields of biomass and ethanol on sugars in anaerobic bioreactor batch cultures of *S. cerevisiae* strains IMS0535 (D-glucose-phosphorylation-negative strain evolved for D-xylose fermentation in presence of L-arabinose and D-glucose), IMS0522 (D-glucose-phosphorylation-negative strain evolved for L-arabinose fermentation in presence of D-xylose and D-glucose), CEN.PK113-7D and IMS0010 (D-glucose, D-xylose and L-arabinose fermenting strain) in synthetic medium containing 20 g L^{-1} L-arabinose, 20 g L^{-1} D-glucose and 20 g L^{-1} D-xylose. Data represent average and mean deviation of measurements on two independent cultures of each strain.

	q_s (g g^{-1} h^{-1})			μ^{max}	Yield (g g^{-1} sugar consumed)	
	D-glucose	D-xylose	L-arabinose	(h^{-1})	Biomass	Ethanol
IMS0535	-	0.90 ± 0.13	-	0.09 ± 0.003	0.08 ± 0.002	0.39 ± 0.05
IMS0522	-	-	1.6 ± 0.08	0.12 ± 0.001	0.075 ± 0.002	0.38 ± 0.01
CEN.PK113-7D	2.82 ± 0.05	-	-	0.29 ± 0.01	0.1 ± 0.005	0.40 ± 0.05
IMS0010	1.73 ± 0.07	0.40 ± 0.02	0.57 ± 0.05	0.18 ± 0.004	0.09 ± 0.002	0.41 ± 0.08

Suboptimal conversion of sugar mixtures by a consortium of specialist strains. To investigate the impact of co-cultivation of the three specialist strains on fermentation kinetics, two anaerobic bioreactor batch cultures, inoculated with 0.36 g biomass consisting of equal amounts of biomass of strains IMS0535, IMS0522 and CEN.PK113-7D were grown on SMAGX (Figure 4A). For comparison, growth and fermentation kinetics of the 'generalist' strain IMS0010 were characterised under the same conditions (Figure 4C).

During anaerobic co-cultivation of the consortium on SMAGX, D-glucose and L-arabinose were consumed simultaneously and completely (Figure 4A). Sugar consumption kinetics and, consequently, the time required for full conversion of these sugars resembled those observed in the corresponding single-culture experiments (Figure 3). In contrast, D-xylose fermentation kinetics of the consortium strongly differed from those observed in the single-strain experiment with the xylose specialist IMS0535 (Figure 2B). In the mixed culture, only 15% of the available D-xylose was consumed within 50 h, indicating that growth and/or fermentation kinetics of IMS0535 were severally inhibited by the presence of the D-glucose and/or L-arabinose specialists. Similar mixed-culture fermentation kinetics were observed when strain IMS0535 was replaced by the independently evolved xylose-specialist strain IMS0537 (Supplemental Figure 6).
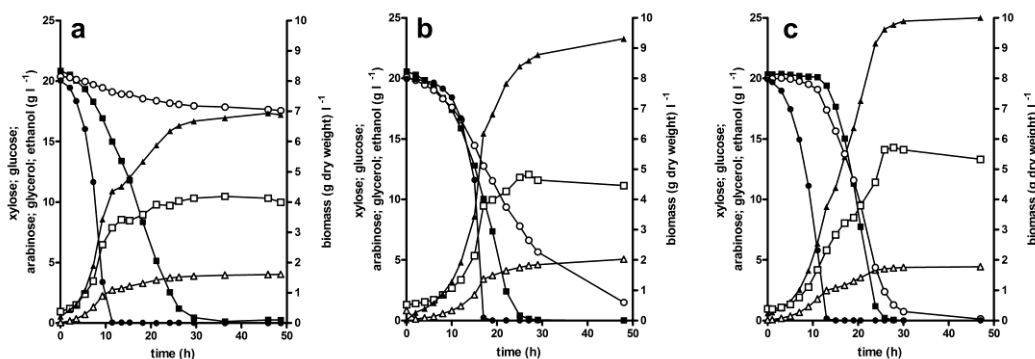
Figure 4 | Growth and extracellular metabolite concentrations in anaerobic batch cultures of (**a.** and **b.**) synthetic consortia consisting of the evolved glucose-phosphorylation-negative *S. cerevisiae* strains IMS0535 (D-xylose fermenting) and IMS0522 (L-arabinose fermenting [404]), together with the D-glucose fermenting laboratory strain CEN.PK113-7D and **c.** pure culture of *S. cerevisiae* IMS0010 (generalist glucose-xylose-arabinose fermenting strain [13]). Cultures were growth with different inoculum ratios; **a.** 33% of each strain; **b.** 59% IMS0535, 38.6% IMS0522 and 2.4% CEN.PK113-7D. All cultures were inoculated to a total initial concentration of 0.36 g biomass dry weight L^{-1} in bioreactors containing synthetic medium with 20 g L^{-1} L-arabinose, 20 g L^{-1} D-glucose and 20 g L^{-1} D-xylose. List of symbols: ● D-glucose, ○, D-xylose, ■, L-arabinose, □, biomass dry weight, ▲, ethanol, △, glycerol. All three growth experiments were performed in duplicate, data shown are from a single experiment. Kinetic parameters calculated from duplicate cultures differed by less than 5%.

Extracellular metabolite measurements showed higher concentrations of D-xylitol (up to 0.6 g L^{-1}) in cultures of consortia containing the xylose specialist strain IMS0535

than in pure cultures of this strain grown on SMAGX (Supplemental Table 3). *In vitro* experiments have shown that D-xylitol is a competitive inhibitor of the *Piromyces* xylose isomerase [98, 405]. However, anaerobic shake-flask cultivation of strain IMS0535 on SMAGX supplemented with 1.5 g L^{-1} of D-xylitol, which is 2.5-fold higher than the concentration observed in the mixed cultures, showed a growth rate decrease of less than 10%, while 80% consumption of D-xylose was reached within 50 h (Supplemental Figure 7). Acetate concentrations were slightly higher than in cultures of the pentose fermenting strain IMS0010 (Supplemental Table 3). Increasing the inoculum size of the xylose-specialist strain IMS0535 relative to that of the other specialists resulted in a slight improvement of D-xylose fermentation kinetics, but D-xylose conversion still strongly decelerated as fermentation of D-glucose and L-arabinose progressed (Figure 4B).

Laboratory evolution of a consortium of specialist strains for improved fermentation of sugar mixtures. To improve kinetics of mixed-sugar fermentation by the consortium, and especially its D-xylose fermentation kinetics, anaerobic laboratory evolution experiments were performed (Figure 5a). These experiments were started in anaerobic shake-flask cultures of the consortium (strains IMS0535, IMS0522 and CEN.PK113-7D) on SMAGX. The initial shake-flask cultures showed the same slow D-xylose fermentation previously observed in anaerobic bioreactors (Figure 4B). When 2 mL samples from stationary-phase shake-flask cultures on SMAGX were used to inoculate fresh shake flasks on the same medium, D-glucose and L-arabinose were completely consumed within 2 days, whereas complete conversion of D-xylose took 3 weeks. Subsequent transfer to fresh SMAGX showed full conversion of D-glucose and D-xylose within 4 days. However, L-arabinose was not converted within this time span, possibly because cells of the arabinose specialist did not survive prolonged starvation. Therefore, at the fourth transfer, the arabinose specialist IMS0522 was reintroduced by supplementing 1 mL of stationairy-phase cultures of this strain on SMAGX, after which the consortium converted all three sugars within 4 days. Subsequently, repeated batch cultivation was continued in duplicate anaerobic SBR cultures on SM + 10 g L^{-1} each of L-arabinose, D-glucose and D-xylose (Figure 5a). Already during the fifth cycle, all three sugars were fully consumed within 31 h (Figure 5c).

After 21 cycles of SBR cultivation (680 h and 750 h for the two reactors), the composition of the sugar mixture was changed to 20 g L^{-1} D-glucose, 10 g L^{-1} D-xylose and 5 g L^{-1} L-arabinose, which resembles the relative concentrations of the three sugars in lignocellulosic hydrolysates [206]. Off-gas CO_2 profiles indicated that for cultures of the consortium, this change strongly affected fermentation kinetics, especially after the initial fast consumption of D-glucose (Supplemental Figure 8). As a result, the SBR cycle time increased from 33 ± 2 h to 47 ± 2 h. When SBR cultivation on the adapted sugar mixture was continued for a further 1200 h, the cycle length progressively decreased until all three

sugars were consumed within 35 ± 1 h (Figure 5D and Supplemental Figure 8). Subsequently, fermentation kinetics of both SBR cultures remained stable for an additional 1000 h (Figure 5E).
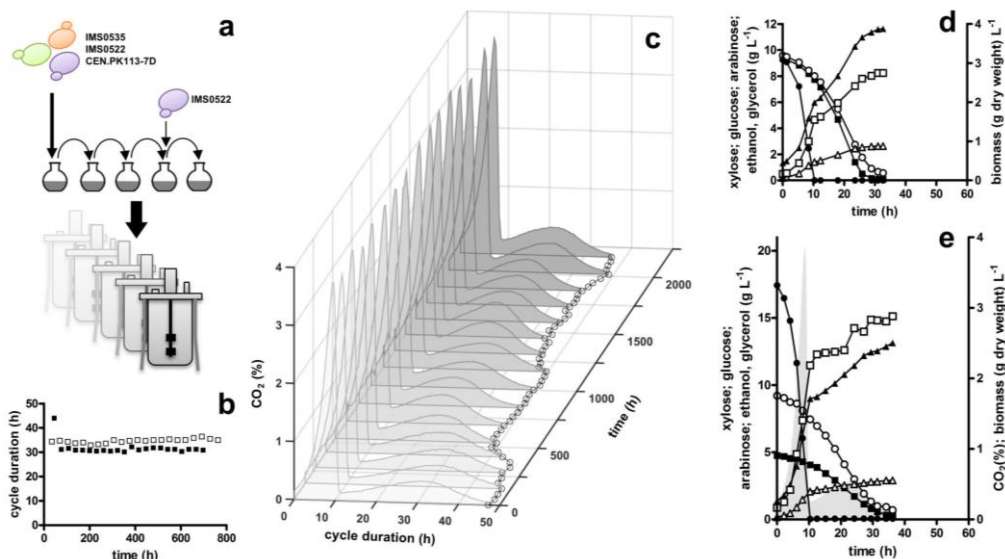
Figure 5 | a. Schematic overview of laboratory evolution experiment with a consortium consisting of the glucose-phosphorylation-negative *S. cerevisiae* strains IMS0535 (D-xylose fermenting) and IMS0522 (L-arabinose fermenting [404]) together with the D-glucose fermenting strain CEN.PK113-7D). Laboratory evolution was initiated in anaerobic shake flasks with synthetic medium containing 20 g L^{-1} D-glucose, 20 g L^{-1} D-xylose and 20 g L^{-1} L-arabinose by inoculating with equal amounts of biomass of each of three strains, giving a total initial concentration of 0.36 g biomass dry weight L^{-1}. After 3 transfers, strain IMS0522 was re-inoculated and cultivation was continued on SM containing 10 g L^{-1} of each sugar. The final shake flask was transferred to anaerobic SBR cultures. **b.** Length of fermentation cycles during the first 21 cycles of SBR cultivation in duplicate (□, reactor 1, ■, reactor 2). **c.** Length of fermentation cycles (○) and off-gas CO_2 profiles for selected cycles during a subsequent series of SBR cycles in the same reactors, in which the sugar composition of the medium contained 20 g L^{-1} D-glucose, 10 g L^{-1} D-xylose and 5 g L^{-1} L-arabinose. The metabolite concentration and CO_2 measured *(solid grey)* shown in panels **d.** and **e.** correspond to the fifth cycle shown in **b.** and the final cycle of the culture stability experiments shown in **c.**, respectively. List of symbols: ● D-glucose, ○, D-xylose, ■, L-arabinose, □, biomass dry weight, ▲, ethanol, △, glycerol. Data shown in the figure corresponds to one reactor of two replicates. Complete off-gas CO_2 profiles for both reactors are shown in Supplemental Fig. 9.

The improvement of the fermentation performance and subsequent stable fermentation kinetics of the consortium (Figure 5) provided a marked contrast with the deteriorating pentose fermentation kinetics of the generalist strain IMS0010 during prolonged SBR cultivation on SMAGX (Figure 1). However, the sugar compositions for the first 20 cycles of the SBR experiments with the consortium (Figure 5) were different from those in the SBR experiments with strain IMS0010 (Figure 1). Therefore, additional duplicate SBR experiments were performed in which the generalist strain IMS0010 was first grown for 21 cycles on 10 g L^{-1} D-glucose, 10 g L^{-1} D-xylose and 10 g L^{-1} L-arabinose. During this phase, no marked deterioration of its fermentation kinetics was observed (Supplemental Figure 10A and B). When both SBRs were subsequently switched to a medium

containing 20 g L^{-1} D-glucose, 10 g L^{-1} D-xylose and 5 g L^{-1} L-arabinose, the overall fermentation cycle duration initially stayed the same. However, already after the fifth cycle of repeated batch cultivation, fermentation kinetics started to deteriorate (Additional File 13C). Metabolite analyses showed that these deteriorated sugar consumption kinetics were due to a slower consumption of both D-xylose and L-arabinose (Supplemental Figure 10D). In the second reactor, a sharper deterioration of sugar fermentation kinetics occurred upon an interruption of the automated pH control. Although growth and sugar consumption resumed after this discontinuity, fermentation kinetics remained slower than before the perturbation (Supplemental Figure 11).

Discussion

Instability of a generalist pentose-fermenting yeast strain during repeated batch cultivation. Prolonged SBR cultivation of the previously described 'generalist' pentose-fermenting strain *S. cerevisiae* IMS0010 [13] on sugar mixtures whose relative concentrations of D-glucose, D-xylose and L-arabinose resembled those in lignocellulosic hydrolysates, led to progressive deterioration of fermentation kinetics (Figure 1). This observation indicates that repeated batch cultivation of this generalist strain on sugar mixtures favoured specialization towards fast utilization of glucose, at the expense of pentose fermentation. Selection for such specialization could reflect competition for limited cellular resources [13], for example due to the need for high-level expression of heterologous isomerases for efficient pentose fermentation [11, 152, 295]. Alternatively or additionally, negative interactions between proteins, metabolites, cofactors and effectors of the catabolic pathways for the three sugars may generate a selective pressure for specialization towards the fast use of a single sugar.

During repeated batch cultivation on mixed substrate, the cumulative selective pressure for fast utilization of each individual substrate is proportional to the number of generations of selective growth on that substrate. When, in such mixed substrate cultures, sugars are consumed sequentially, this number of generations is strongly influenced by their order of consumption as well as by their relative concentrations in the growth medium. In line with the latter factor, deterioration of fermentation kinetics was much more pronounced during prolonged SBR cultivation of strain IMS0010 on a medium in which the concentration of glucose was higher than that of the two pentoses (Figure 1) than in similar experiments in which the concentrations of the three sugars were equal (Supplemental Figure 8A).

In two independent, long-running SBR experiments on sugar mixtures, a rapid deterioration of pentose fermentation kinetics of the generalist strain coincided with perturbations resulting from technical malfunctions (Supplemental Figure 1 and 9). In both instances the negative selective pressure was already evident from an increasing cycle duration prior to the perturbation (Supplemental Figure 1), but was greatly augmented afterwards. This observation suggested that cellular stress associated with these events

enriched for mutations that were already present in the population. The fast deterioration of the generalist strain IMS0010 after perturbations may have been partially caused by changes in copy number of the plasmids that, in this strain, were used for expression of genes involved in xylose- and arabinose metabolism. For the experiment in which pH control was temporarily interrupted, this enhanced deterioration may be related to the observation that a combination of low pH and presence of acetate more strongly affects anaerobic growth of engineered *S. cerevisiae* on D-xylose than on D-glucose [173]. Evolution towards a more specialized phenotype, augmented by occasional process perturbations, as observed here during prolonged SBR cultivation of *S. cerevisiae* IMS0010, is likely to represent a major challenge for development of industrial 'generalist' strains that retain optimal fermentation kinetics through a large number of biomass recycling steps on lignocellulosic hydrolysates.

Fermentation of sugar mixtures by a consortium of engineered, specialist yeast strains. In anaerobic batch cultures grown on SMAGX (Figure 3), specific sugar consumption rates of pure cultures of a hexose-phosphorylation-deficient D-xylose-specialist strain, a similar L-arabinose specialist strain [404] and a pentose-non-fermenting 'glucose-specialist' laboratory strain were 60 to 280 % higher than the corresponding sugar-conversion rates of the generalist strain IMS0010 (Table 2). This difference, which was observed despite the constant presence of potentially inhibiting concentrations of non-fermentable sugars [112, 123, 176, 404] in batch cultures of the specialist strains, underlines the potential benefit of synthetic consortia for mixed substrate conversion. However, in contrast to the specialist strains, the generalist strain could use the biomass formed during glucose consumption for subsequent conversion of the pentoses (Figure 4C), thereby improving volumetric sugar consumption rates. In cultures on sugar mixtures, this benefit of the generalist strain offset the higher biomass-specific conversion rates of the xylose specialist strain, which was the slowest growing of the three specialists (Figures 3).

Co-cultivation of the three specialist strains (IMS0522, IMS0535 and CEN.PK113-7D) on a mixture of L-arabinose, D-glucose and D-xylose showed that mixed-culture performance could not be accurately predicted from the growth and fermentation kinetics of the individual strains in pure cultures (Figure 4A). In particular, fermentation kinetics of the xylose specialist strain were severely impaired when grown together with the other two specialist strains. A possible explanation for this inhibition is that (by-)products of the arabinose and glucose specialists inhibited D-xylose fermentation. Acetate and D-xylitol have been shown to inhibit fermentation rates of xylose-fermenting *S. cerevisiae* strains and *in vitro* xylose isomerase activity, respectively [98, 173, 405]. While both compounds were present at the end of the mixed-culture experiments, their concentrations remained well below 1 g L^{-1} (Supplemental Table 3). At a pH of 5.0 this concentration of acetate is unlikely to strongly affect xylose fermentation rates [107, 173]. Impaired D-xylose consumption can likewise not solely be attributed to D-xylitol accumulation, as shake-

flask cultivations of IMS0535 with even higher D-xylitol concentrations (1.5 g L^{-1}) only showed a minor impact on D-xylose fermentation kinetics (Supplemental Figure 7). This is in line with the previously observed discrepancy between the small impact of D-xylitol on D-xylose fermentation by a *xylA*-based *S. cerevisiae* strain and the strong inhibition of xylose isomerase measured *in vitro* [247]. The increased D-xylitol concentrations may, however, reflect a cellular stress response as its production from D-xylose is catalyzed by the stress-induced NADPH-dependent aldo-keto reductases encoded by *GCY1*, *YPR1*, *GRE3* *ARA1*, *YJR096W* and *YDL124W* [406, 407].

Although growth media were designed to prevent nutrient limitations, the sluggish D-xylose fermentation kinetics of the mixed cultures might still reflect competition of the three strains for one or more essential nutrients. In pure cultures, intracellular stores formed by excessive 'luxury uptake' [408, 409] at the start of a batch culture will be distributed over the growing population as cells divide. In contrast, in consortia, rapid uptake of key nutrients by faster growing partners could constrain the ability of slower growing strains to completely convert their substrate. This hypothesis is consistent with the positive impact of a larger inoculum of the slower growing xylose specialist on overall D-xylose conversion (Figure 4B).

Laboratory evolution of mixed cultures of the D-glucose, D-xylose and L-arabinose fermenting specialist yeast strains eventually yielded a consortium that stably converted mixtures of the three sugars (Figure 5D). In contrast to prolonged SBR cultivation of strain IMS0010, long-term cultivation of the evolved consortia in SBR cultures resulted in stable fermentation kinetics (Figure 5E). This result was entirely consistent with the key hypothesis tested in this study that the fermentation kinetics of consortia of specialist strains are more robust during long-term cultivation on sugar mixtures in long-term cultures than a generalist strain.

Conclusion

This study represents a first exploration of the conversion of mixtures of glucose, xylose and arabinose by a consortium of three 'specialist' *S. cerevisiae* strains. The conclusion that generalist pentose-fermenting strains are likely to be inherently unstable in terms of mixed-sugar fermentation kinetics during repeated batch cultures has important implications for strain optimization and industrial process design. The potential benefit of re-using biomass through multiple cycles of cultivation is illustrated by its large-scale use in Brazilian 'first-generation' bioethanol processes grown on sucrose as the carbon source, where it has even been shown to lead to selection for better performing strains [342]. Our results show that, in terms of strain stability, use of consortia of specialist yeast strains for second-generation bioethanol could confer similar benefits, including an ability to adapt to fluctuations in feedstock composition. Moreover, unlike repeated batch cultivation of generalist strains such as strain IMS0010, repeated batch cultivation of consortia of specialist strains on actual industrial hydrolysates may be used to select for tolerance to

fermentation inhibitors, without the inherent risk of selecting for faster glucose fermentation at the expense of pentose fermentation kinetics. However, before industrial implementation can be contemplated, a deeper insight into the interaction between specialist strains and a further improvement of their sugar fermentation kinetics in mixed-culture processes is essential. Additionally, the consortium of glucose- and pentose-fermenting specialist yeast strains described in this study provides an interesting model to study the molecular ecology of synthetic consortia of industrial microbes. While outside the scope of the present study, resequencing of the genomes of the evolved strains, including those evolved as part of three-partner consortia and evaluation of the impact of the observed mutations by their reverse engineering into non-evolved strains [111, 396], represents a logical next step in such research.

Acknowledgements

Supplementary Material

Supplemental Table 1 | Plasmids used in this study

Plasmid	Characteristic	Source
pUD350	pMK-RQ_p*TPI1*_*xylA*_t*CYC*	[295]
pUD353	pJET_Blunt_p*TEF1*_*XKS1*_t*XKS1*	[295]
pPWT118	KanMX, AmdSYM, pADH1_*Pc*araT_t*PMA1*	[322]
pUDE327	2 µm ori, *KlURA3*, p*SNR52*-gRNA.*HXK2*.Y-t*SUP4*	[294]
pMEL10	2 µm ori, *KlURA3*, p*SNR52*-gRNA.*CAN1*.Y-t*SUP4*	[137]

Supplemental Table 2 | Oligonucleotide primers used in this study

Primers used for amplification of integration fragments:

Primer nr.:	Purpose:	Template:	Sequence 5' -> 3':
6269	fl_*xylA*_G fragment	pUD350	ATCTATGCTACAACATTCCAAAATTTGTCCCAAAAAGTCTTT-GGTTCATGATCTTCCCATCGCGCAGATTAGCGAAGC
6285	fl_*xylA*_G fragment	pUD350	AAGGGCCATGACCACCTGATGCACCAATTAGGTAGGTCTGGC-TATGTCTATACCTCTGGCGCGATACCCTGCGATCTTC
6273	G_*xylA*_A fragment	pUD350	GCCAGAGGTATAGACATAGCCAGACCTACCTAATTGGTG-CATCAGGTGGTCATGGCCCTTCGCGCAGATTAGCGAAGC
6280	G_*xylA*_A fragment	pUD350	GTGCCTATTGATGATCTGGCGGAATGTCTGCCGTGCCA-TAGCCATGCCTTCACATATAGTGCGATACCCTGCGATCTTC
6270	A_*xylA*_B fragment	pUD350	ACTATATGTGAAGGCATGGCTATGGCACGGCAGA-CATTCCGCCAGATCATCAATAGGCACCGCGCAGATTAGCGAAGC
6281	A_*xylA*_B fragment	pUD350	GTTGAACATTCTTAGGCTGGTCGAATCATTTAGACACGGG-CATCGTCCTCTCGAAAGGTGGCGATACCCTGCGATCTTC
6271	B_*xylA*_C fragment	pUD350	CACCTTTCGAGAGGACGATGCCCGTGTCTAAATGATTCGAC-CAGCCTAAGAATGTTCAACCGCGCAGATTAGCGAAGC
6282	B_*xylA*_C fragment	pUD350	CTAGCGTGTCCTCGCATAGTTCTTAGATTGTCGCTACGGCATATAC-GATCCGTGAGACGTGCGATACCCTGCGATCTTC
6272	C_*xylA*_D fragment	pUD350	ACGTCTCACGGATCGTATATGCCGTAGCGACAATCTAAGAAC-TATGCGAGGACACGCTAGCGCGCAGATTAGCGAAGC
6284	C_*xylA*_D fragment	pUD350	AATCACTCTCCATACAGGGTTTCATACATTTCTCCACGG-GACCCACAGTCGTAGATGCGTGCGATACCCTGCGATCTTC
6283	D_*xylA*_M fragment	pUD350	ACGCATCTACGACTGTGGGTCCCGTGGAGAAATGTATGAAACCCTG-TATGGAGAGTGATTGCGATACCCTGCGATCTTC
6275	D_*xylA*_M fragment	pUD350	ACGAGAGATGAAGGCTCACCGATGGACTTAGTATGATGCCATGCTG-GAAGCTCCGGTCATCGCGCAGATTAGCGAAGC
6287	M_*xylA*_N fragment	pUD350	ATGACCGGAGCTTCCAGCATGGCATCATACT-AAGTCCATCGGTGAGCCTTCATCTCTCGTGCGATACCCTGCGATCTTC
6276	M_*xylA*_N fragment	pUD350	TTCTAGGCTTTGATGCAAGGTCCACATATCTTCGTTAG-GACTCAATCGTGGCTGCTGATCCGCGCAGATTAGCGAAGC
6288	N_*xylA*_O fragment	pUD350	GATCAGCAGCCACGATTGAGTCCTAACGAAGATATGTGGACCTT-GCATCAAAGCCTAGAAGCGATACCCTGCGATCTTC

6277	N_*xylA*_O fragment	pUD350	ATACTCCCTGCACAGATGAGTCAAGCTATTGAACACCGAGAAC-GCGCTGAACGATCATTCCGCGCAGATTAGCGAAGC
6289	O_*xylA*_I fragment	pUD350	GAATGATCGTTCAGCGCGTTCTCGGTGTTCAATAGCTT-GACTCATCTGTGCAGGGAGTATGCGATACCCTGCGATCTTC
6274	O_*xylA*_I fragment	pUD350	GCCTACGGTTCCCGAAGTATGCTGCTGATGTCTGGCTATAC-CTATCCGTCTACGTGAATACGCGCAGATTAGCGAAGC
6279	I_*XKS1*_fl fragment	pUD353	GCTCATTAGAAAGAAAGCATAGCAATCTAATCTAAGTTTTATGTT-GTGTTCAGTAATTCAGAGACAG
6278	I_*XKS1*_fl fragment	pUD353	GCAATGACAAATTCAAAAGAAGACGCCGACATAGAGGAGAAGCAT-ATGTACAATGAGCCGGTCCAGTGCTTCCACATC
7676	PcAraT fragment	pPWT118	TTTCTAATGCCTTTTCCATCATGTTACTACGAGTTTTCTGAAC-CTCCTCGCACATTGGTATCTTCACGCGTGTTCGAG
7660	PcAraT fragment	pPWT118	TATAAATATTTATCGTCACGAA-TAAATCCCGTGAATTTCTAACAAAGTTTATACAATATCTAACCTCG GAAGATCGTCGACAAG
2641	Ura3 repair fragment	CEN.PK11 3-7D	ATTGCCCAGTATTCTTAACC
1522	Ura3 repair fragment	CEN.PK11 3-7D	CGAGATTCCCGGGTAATAACTG

Primers used for verifying integration of fragments:

Primer nr.:	Purpose:	Sequence 5' -> 3':
6632	checking *xylA* integration	AGCGTCGTAGTAGTGGAAAGC
2615	checking *xylA* integration	GAAATGGCGTGGGAATGTGA
6921	checking *xylA* integration	AGAGGTGGTGGTTTCGTTAC
4692	checking *xylA* integration	AAGGGCCATGACCACCTG
3275	checking *xylA* integration	GTGCCTATTGATGATCTGGCGGAATG
4173	checking *xylA* integration	GTTGAACATTCTTAGGCTGG
3277	checking *xylA* integration	CTAGCGTGTCCTCGCATAGTTCTTAGATTG
5231	checking *xylA* integration	AATCACTCTCCATACAGGG
3354	checking *xylA* integration	ACGCATCTACGACTGTGGGTC
4184	checking *xylA* integration	ATGACCGGAGCTTCCAGCATG
3843	checking *xylA* integration	GATCAGCAGCCACGATTG
3837	checking *xylA* integration	GAATGATCGTTCAGCGCG
6921	checking *xylA* integration	AGAGGTGGTGGTTTCGTTAC
6922	checking *XKS1* integration	ACTCATGTGCCCTTGGTG
2614	checking *XKS1* integration	CCGAATCAGGGAATCCCTTT
4657	Checking *Pc*AraT integration	TTGCGCTAAGAGAATGGACC
5905	Checking *Pc*AraT integration	CTTTTTTTTAGTTTTAAAACACCAAGAACTTAG
4930	Checking Hxk2 deletion	GGCAAGAGTATAGCGTGATACC
3070	Checking Hxk2 deletion	AGTGCTTCCGTTCGTTCCAG
3564	Checking Hxk2 deletion	TTGGTGCTAGAGCTGCTAGATTG
2926	Checking Hxk2 deletion	ATCAATTCCTTTGGCACATCGGC

Supplemental Table 3 | Extracellular metabolite concentrations measured taken at the end of anaerobic batch cultures shown in Figure 3 of *S. cerevisiae* strains IMS0535 and IMS0537 (D-glucose-phosphorylation-negative strain evolved for D-xylose fermentation in presence of L-arabinose and D-glucose), IMS0522 (D-glucose-phosphorylation-negative strain evolved for L-arabinose fermentation in presence of D-xylose and D-glucose), CEN.PK113-7D and IMS0010 (D-glucose, D-xylose and L-arabinose fermenting strain) and the consortia (Figure 4) with these strains in synthetic medium with 20 g L^{-1} L-arabinose, 20 g L^{-1} D-glucose and 20 g L^{-1} D-xylose. Values shown in the table are averages and mean deviations of measurements on two independent cultures of each strain.

	Final concentration (mg L^{-1})				
	D-xylitol	acetate	lactate	succinate	pyruvate
CEN.PK113-7D	54 ± 1	182 ± 5	176 ± 1	87 ± 9	60 ± 2
IMS0535	22 ± 5	136 ± 25	251 ± 170	95 ± 22	21 ± 2
IMS0522	304 ± 10	136 ± 25	251 ± 170	95 ± 22	21 ± 2
IMS0010	244 ± 10	181 ± 4	417 ± 3	312 ± 3	50 ± 1
(33%) IMS0535, (33%) IMS0522, (33%) CEN.PK113-7D	620 ± 106	591 ± 19	259 ± 25	269 ± 4	36 ± 0
(33%) IMS0537, (33%) IMS0522, (33%) CEN.PK113-7D	880 ± 23	756 ± 9	280 ± 21	279 ± 11	50 ± 1
(59%) IMS0535, (39%) IMS0522, (2%) CEN.PK113-7D	572 ± 31	679 ± 35	324 ± 3	367 ± 26	57 ± 6

6
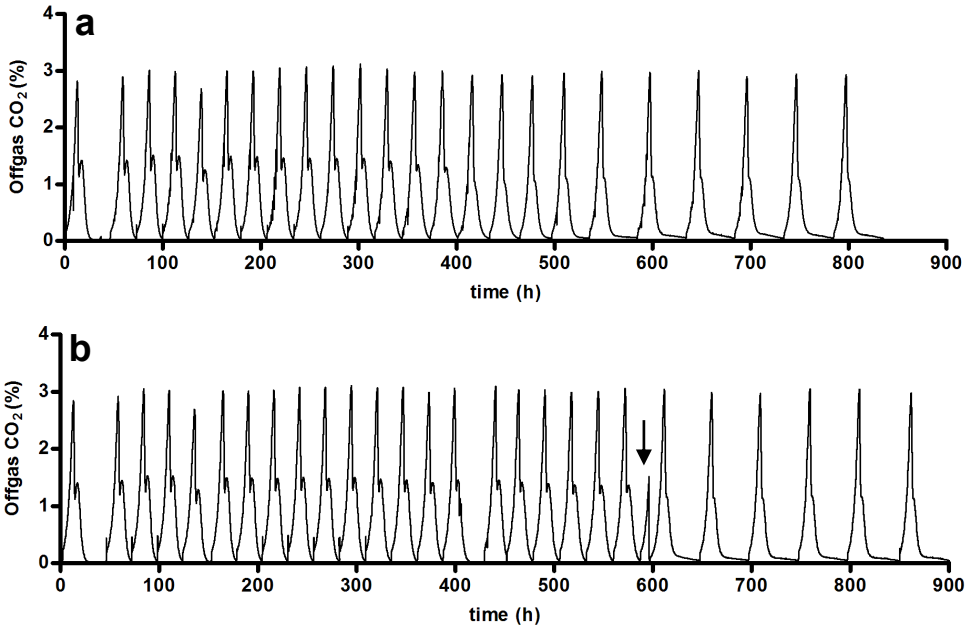
Supplemental Figure 1 | CO₂ offgas measurements (%) for both anaerobic sequential batch **a.** reactor 1 and **b.** reactor 2 during prolonged cultivation of strain IMS0010 on synthetic medium with 20 g L^{-1} D-glucose, 10 g L^{-1} D-xylose and 5 g L^{-1} L-arabinose. Arrow indicates an empty-refill cycle malfunction that occurred after approximately 600 hours for reactor 2.
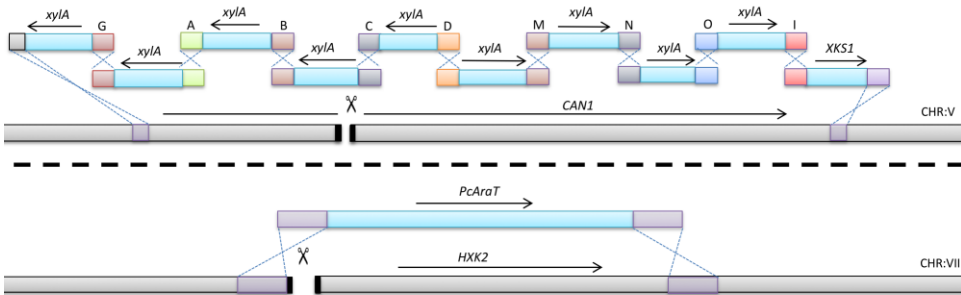
Supplemental Figure 2 | Schematic overview of the integration of multiple DNA fragments during construction of strain *S. cerevisiae* IMX730 (*hxk1Δ glk1Δ gal1Δ::*{cas9_AmdSYM} *gre3Δ::*{NPPP} *hxk2Δ::PcaraT can1Δ::*{*xylAP*}). **a.** Cas9-assisted integration of 10 fragments, comprising 9 copies of a *xylA* expression cassette and a single *XKS1* expression cassette at the *CAN1* locus, using plasmid pMEL10 expressing a gRNA targeting *CAN1*. **b.** Inactivation of *HXK2* by Cas9-assisted integration of a *PcaraT* expression cassette using plasmid gRNA expressing plasmid pUDE327. Correct integration of all the fragments was verified by diagnostic PCR.
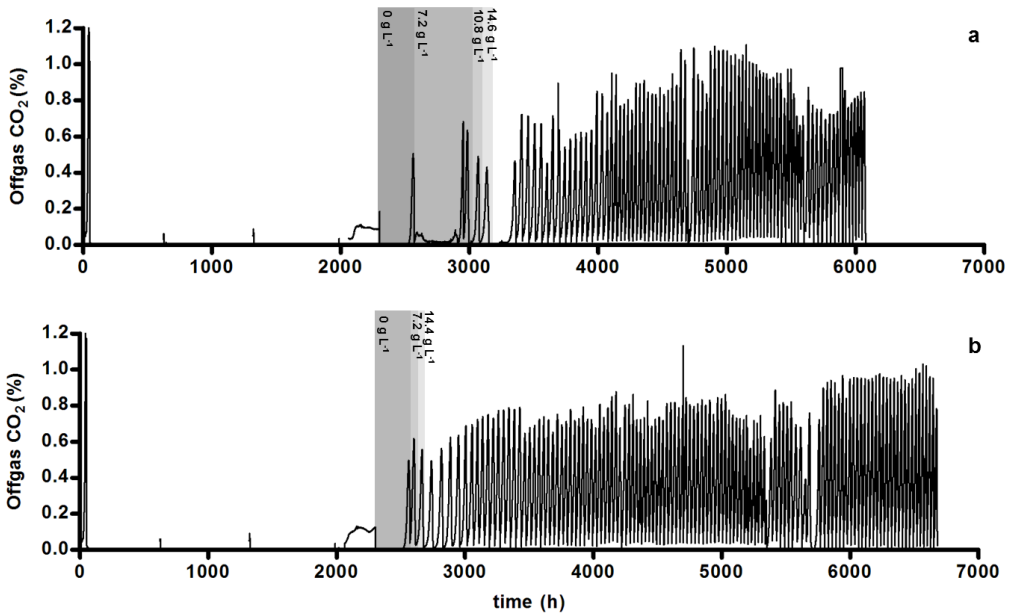
Supplemental Figure 3 | Off-gas CO_2 profiles during laboratory evolution of strain *S. cerevisiae* IMX730 (*hxk1Δ glk1Δ gal1Δ::{cas9*-AmdSYM} *gre3Δ::*{NPPP} *hxk2Δ::PcaraT can1Δ::{xylA*9-XKS1}*) in anaerobic SBR cultures **a.** reactor 1 and **b.** reactor 2. The first CO_2 curve corresponds to the initial aerobic batch prior to switching sparging from air to nitrogen. Cultures were grown on synthetic medium (SM) with 20 g L^{-1} D-xylose, 20 g L^{-1} D-glucose and20 g L^{-1} L-arabinose. After 2250 h, the reactors were emptied and refilled with SM + 20 g L^{-1} D-xylose and 20 g L^{-1} L-arabinose (dark grey). In subsequent cycles. the concentration of D-glucose in the medium was incrementally increased as indicated in grey font.
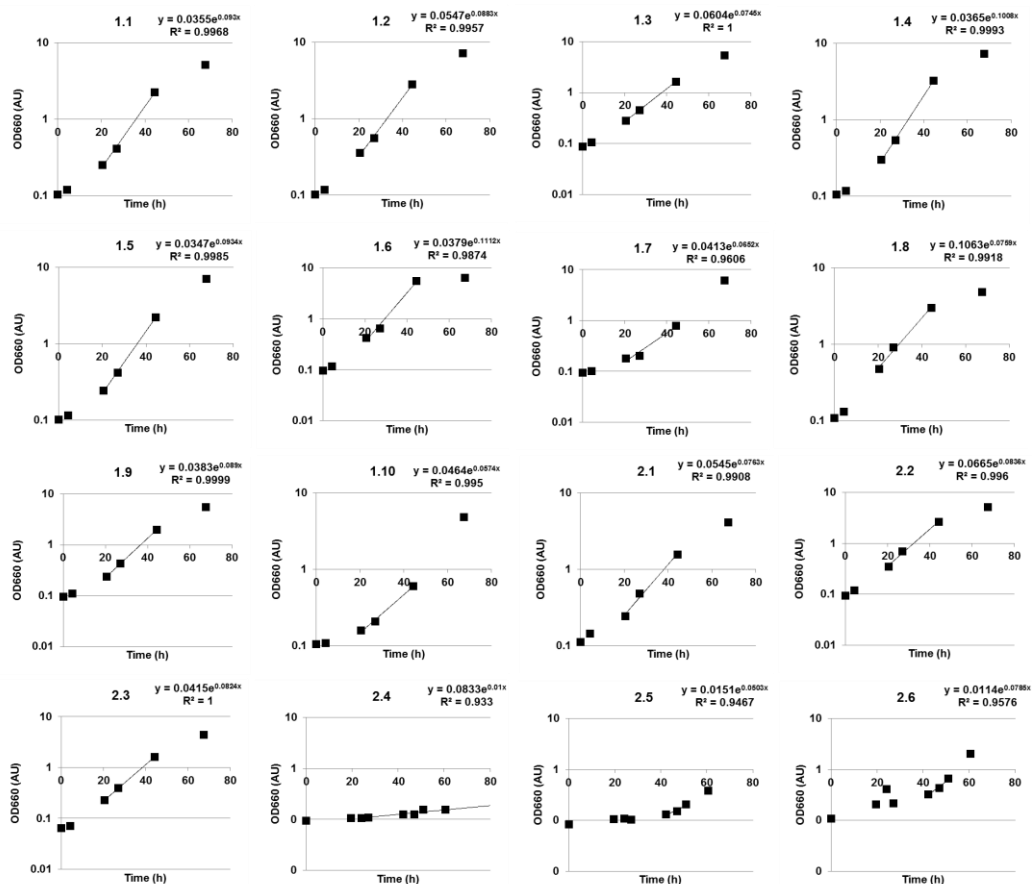
Supplemental Figure 4 | Logarithmic plots OD_{660}-based growth curves of anaerobic shake flask cultures of single-colony isolates obtained after laboratory evolution of strain IMX730 (*hxk1Δ glk1Δ gal1Δ::*{Cas9_AmdSYM} *gre3Δ::*{NPPP} *hxk2Δ::PcaraT can1Δ::*{*xylAP*}). Shake flasks were incubated at 30°C in an anaerobic chamber. 1.1-1.10 and 2.1-2.5 correspond to isolates originating from laboratory evolution reactor 1 and 2, respectively. Values shown are averages of two independent duplicate cultures for each strain.
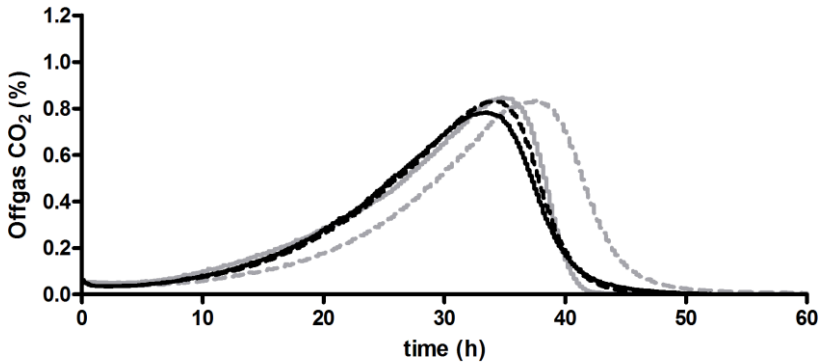
Supplemental Figure 5 | Off-gas CO_2 measurements (%) for four isolates selected after laboratory evolution of *S. cerevisiae* IMX730 (*hxk1Δ glk1Δ gal1Δ::*{Cas9_AmdSYM} *gre3Δ::*{NPPP} *hxk2Δ::PcaraT can1Δ::*{*xylAP*}) on synthetic medium with 20 g L^{-1} L-arabinose, 20 g L^{-1} D-glucose and 20 g L^{-1} D-xylose (SMAGX). Single anaerobic bioreactor cultures on SMAGX at 30°C and pH 5.0 of strains IMS0533 (solid grey line), IMS0537 (dashed grey line), IMS0535 (dashed black line) and IMS524 (solid black line) were conducted and monitored.
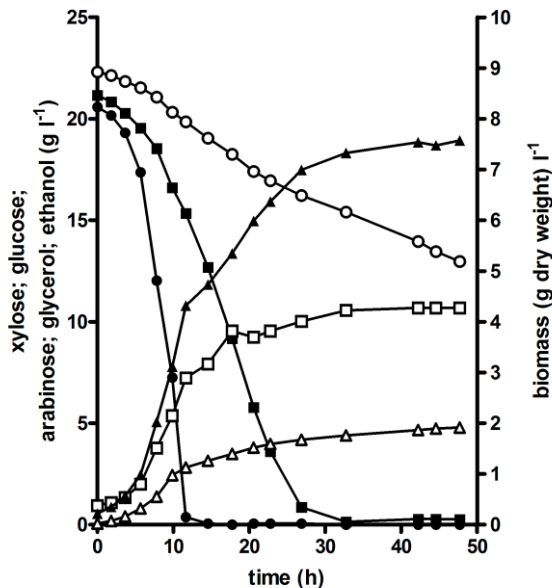
Supplemental Figure 6 | Growth and extracellular metabolite concentrations in anaerobic batch cultures of consortia with evolved glucose-phosphorylation-negative *S. cerevisiae* strains IMS0537 (D-xylose fermenting) and IMS0522 (L-arabinose fermenting) together with D-glucose fermenting strain CEN.PK113-7D, which relative inoculum ratio of 33% for each strain, inoculated to a concentration of 0.36 g dry biomass L^{-1} in bioreactors containing synthetic medium with 20 g L^{-1} D-glucose, 20 g L^{-1} D-xylose and 20 g L^{-1} L-arabinose. List of symbols: ● D-glucose, ○, D-xylose, ■, L-arabinose, □, biomass dry weight, ▲, ethanol, △, glycerol. Data shown in the figure represent data from a single culture from a set of two independent duplicate experiments. Kinetic parameters calculated from duplicate experiments differed by less than 5%.
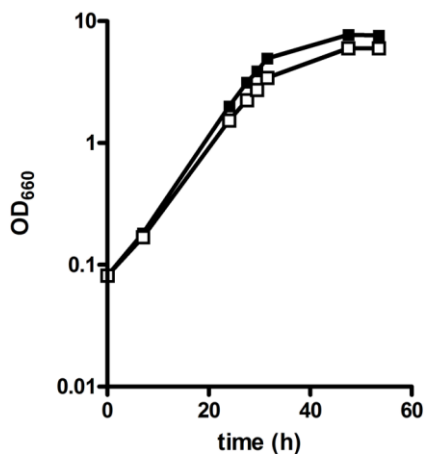
Supplemental Figure 7 | Impact of D-xylitol on anaerobic growth of *S. cerevisiae* strain IMS0535 (D-xylose fermenting). The strain was grown in anaerobic shake-flask cultures on synthetic medium with 20 g L^{-1} D-glucose, 20 g L^{-1} D-xylose and 20 g L^{-1} L-arabinose (■) and on the same medium supplemented with 1.5 g L^{-1} of D-xylitol (□). Extracellular D-xylose concentrations at the end of the experiments were 3.8 ± 0.15 g L^{-1} and 0.69 ± 0.1 g L^{-1} for the cultures with and without D-xylitol addition, respectively. The data shown are from a single shake flask experiment for each strain, data from independent duplicate experiments
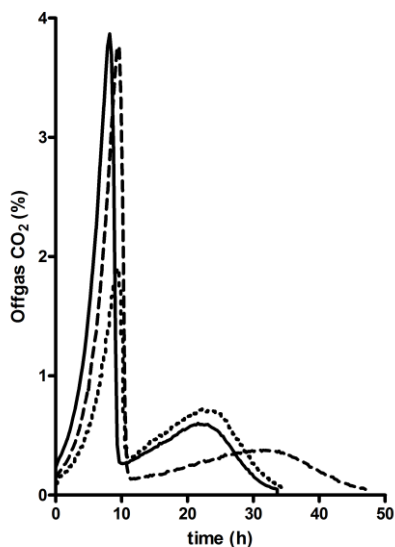
differed by less than 5%.
Supplemental Figure 8 | Off-gas CO_2 profiles for one of two anaerobic SBR experiments (reactor 1) at the end of prolonged cultivation of strains IMS0535 and IMS0522 and CEN.PK113-7D with 10 g L^{-1} D-glucose, 10 g L^{-1} D-xylose and 10 g L^{-1} L-arabinose present (dotted line). Transfer to medium with 20 g L^{-1} D-glucose, 10 g L^{-1} D-xylose and 5 g L^{-1} L-arabinose significantly impacted pentose fermentation (dashed line). Overall growth kinetics improved significantly after 1200 h of cultivation (solid line).

6
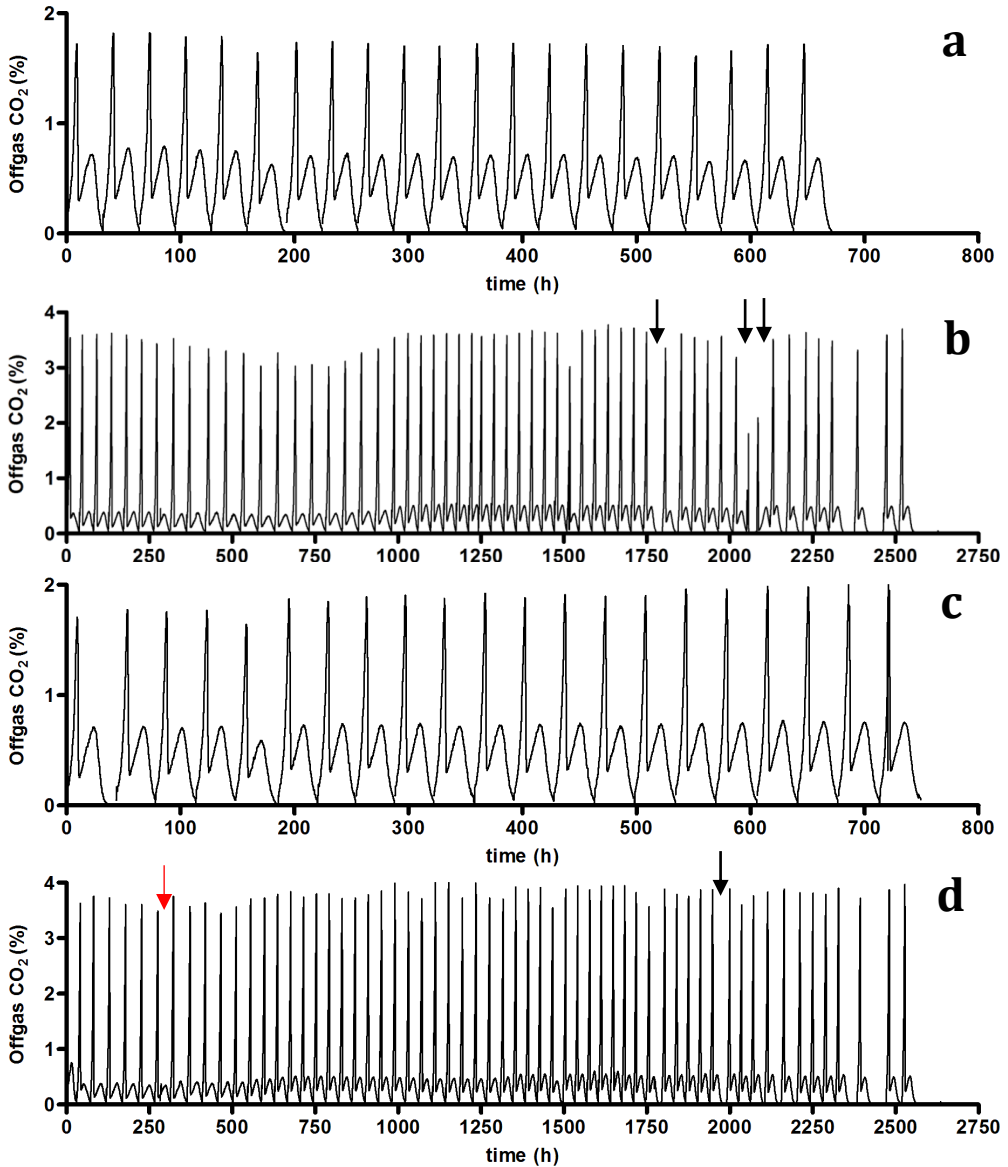
Supplemental Figure 9 | Off-gas CO_2 profiles for two anaerobic SBR experiments. **a.** reactor 1 and **c.** reactor 2 during prolonged cultivation of strains IMS0535 and IMS0522 and CEN.PK113-7D on synthetic medium with 10 g L^{-1} D-glucose, 10 g L^{-1} D-xylose and 10 g L^{-1} L-arabinose. **b.** and **d.** Off-gas CO_2 profiles observed when, after 21 cycles, both reactors were switched to SM + 10 g L^{-1} D-glucose, 10 g L^{-1} D-xylose and 10 g L^{-1} L-arabinose. Black and red arrow(s) indicate malfunctions in empty-refill cycles in which the empty-refill cycle was initiated prematurely and a pH control malfunction led to transient culture acidification, respectively.
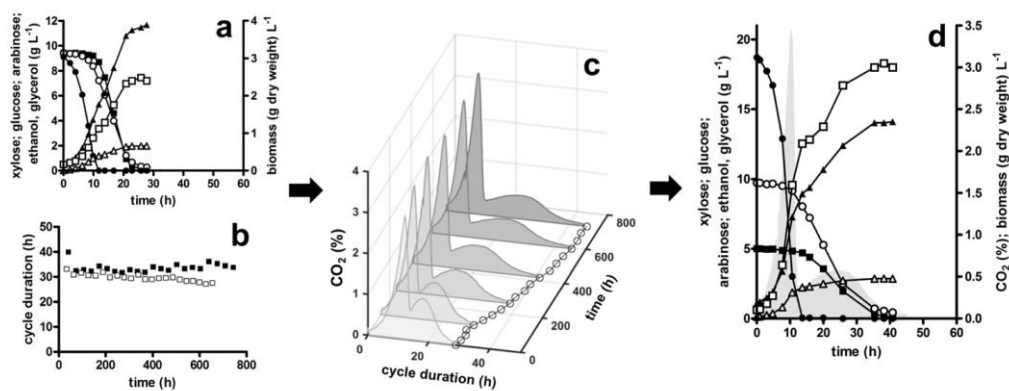
Supplemental Figure 10 | Metabolite concentrations, CO_2 production curves and **b.** cycle duration of anaerobic sequential batch reactor 1 (*closed squares*) and reactor 2 (*open squares*) with glucose-xylose-arabinose consuming strain IMS0010 on synthetic medium containing 10 g L^{-1} D-glucose, 10 g L^{-1} D-xylose and 10 g L^{-1} L-arabinose. After 21 cycles the medium used was changed to 20 g L^{-1} D-glucose, 10 g L^{-1} D-xylose and 5 g L^{-1} L-arabinose and in **c.** the 3-axis plot shows the cycle duration (*open circles*) and CO_2 (%) measured for selected cycles of reactor 1. The metabolite concentration and CO_2 production profiles *(solid grey)* shown in **a.** and **d.** correspond to the fifth and final cycle of the culture stability experiment in reactor 1. List of symbols: ● D-glucose, ○, D-xylose, ■, L-arabinose, □, biomass dry weight, ▲, ethanol, △, glycerol. Data shown in the figure represent single representative experiments from a set of independent duplicate experiments. The data shown in this figure is from one of the biological duplicates shown in supplemental figure 11.
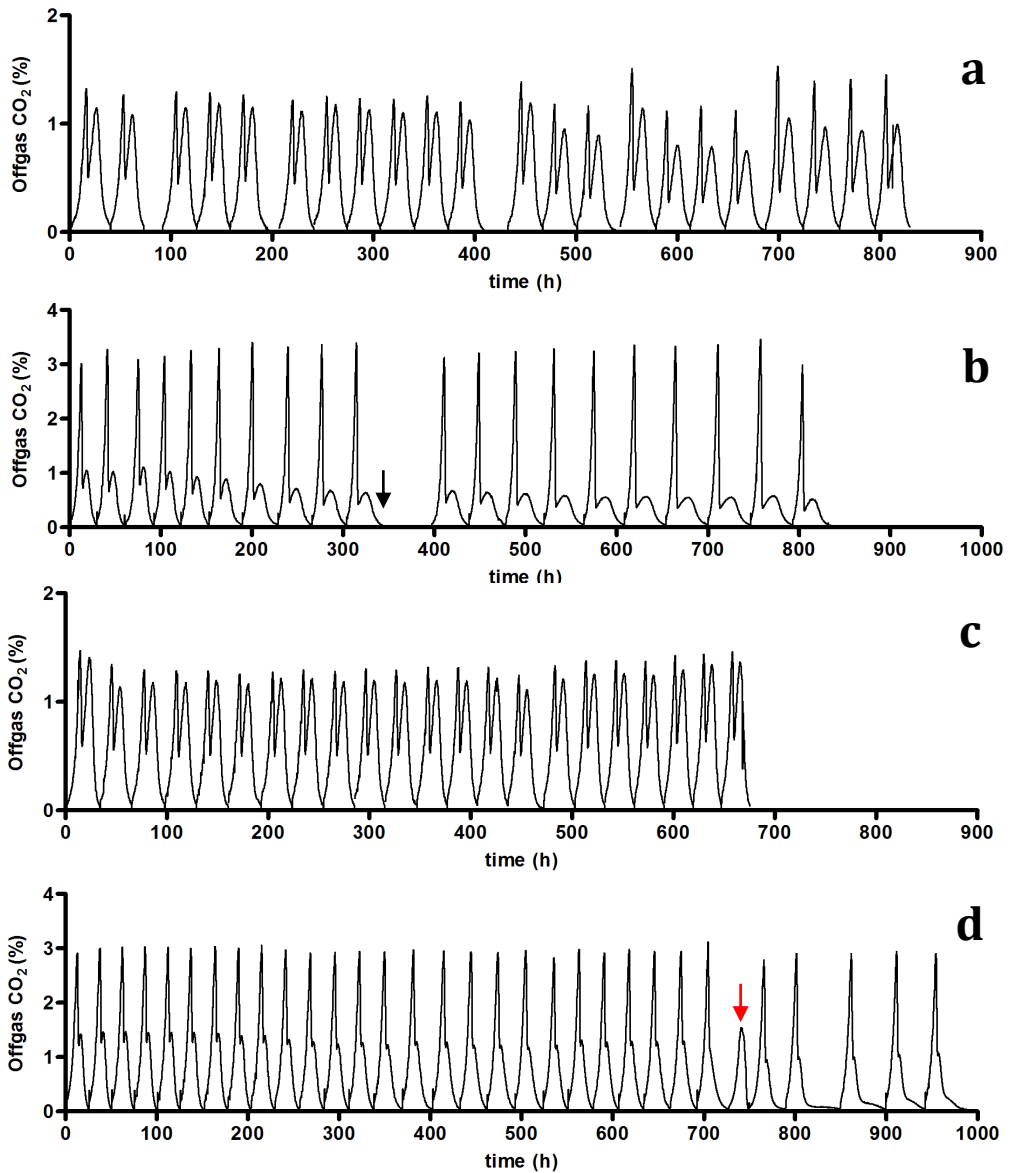
Supplemental Figure 11 | Off-gas CO_2 profiles for anaerobic SBR cultures. **a.** reactor 1 and **c.** reactor 2 during prolonged cultivation of the generalist strain *S. cerevisiae* IMS0010 on synthetic medium containing 10 g L^{-1} D-glucose, 10 g L^{-1} D-xylose and 10 g L^{-1} L-arabinose. **b.** and **d.** CO_2 offgas measurements (%) when after 21 cycles both reactors were switched to SM + 10 g L^{-1} D-glucose, 10 g L^{-1} D-xylose and 10 g L^{-1} L-arabinose. Black and red arrow indicate a malfunction in a single empty-refill cycle and a pH control malfunction that led to transient acidification of the culture, respectively.

Outlook

The first full-scale factories for production of 'second-generation bioethanol' from agricultural residues, which are now coming on line, are complex, multi-step biorefineries for conversion of crude and variable feedstocks. Just as high-efficiency petrochemical refineries did not appear overnight, optimizing the performance of the current frontrunner plants requires substantial efforts in process engineering. As remaining challenges in biomass processing and deconstruction are addressed, yeast-based processes for second-generation biofuels should soon leave the demonstration phase, become fully economically viable, and thus enable an expansion of the global production volume. As described in **Chapter 1**, several decades of intensive research in academia and industry have paved the way for economically viable bioethanol production from lignocellulosic feedstocks. In one of these studies, the functional expression of the *Piromyces* SP2 xylose isomerase, *xylA,* in *Saccharomyces cerevisiae* enabled redox-cofactor-free isomerisation of D-xylose to D-xylulose that allowed for fast growth on this pentose sugar in hydrolysates.

The study in **Chapter 2** demonstrates the importance of metal homeostasis and enzyme loading in xylose isomerase (XI)-based yeast metabolic engineering strategies for anaerobic conversion of xylose-containing lignocellulosic feedstocks into fuels and chemicals. Despite the pivotal role of the functional expression of a heterologous XI in *S. cerevisiae* [8] and the well documented role of metal ions in the active sites of XIs from taxonomically diverse organisms [263], the impact of metal loading on the performance of heterologously expressed XIs in *S. cerevisiae* had previously not been investigated. Similar to bacterial XIs [256], apo-XylA isolated from yeast could be activated with different metals. Inactivation of *PMR1*, combined with overexpression of PPP enzymes, xylulokinase and *xylA* was shown to be sufficient to enable anaerobic growth of *S. cerevisiae* on D-xylose. Beyond xylose utilization, engineering of metal homeostasis has the potential to improve *in vivo* performance of other metal-dependent heterologous enzymes or pathways. The results of this study suggest that metal loading can have a large effect on the *in vivo* catalytic performance of the enzyme.

Besides D-xylose, the other pentose sugar, L-arabinose generally represents between 2 and 3% of the total sugars [206] in lignocellulosic hydrolysates now used in the first industrial-scale plants for second-generation bioethanol production. At the resulting concentrations, the uptake of L-arabinose by *S. cerevisiae* by the Gal2 transporter is far from the optimal due to its low affinity. As L-arabinose is not a carbon source for wild-type *S. cerevisiae* strains, multiple studies have explored the possibility to express heterologous transporters to improve uptake of this pentose sugar [88, 184, 186]. The transcriptome analyses of L-arabinose-limited *Penicillium chrysogenum* chemostat cultures described in **Chapter 3** proved valuable for identification of the high-affinity L-arabinose transporter *Pc*AraT. Functional expression and characterization in *S. cerevisiae* revealed a low K_m

(0.13 mmol L^{-1}) and specificity of this transporter for L-arabinose. Moreover, L-arabinose uptake by *Pc*AraT was much less sensitive to inhibition by D-glucose and D-xylose, which are present at high concentrations in lignocellulosic hydrolysates, than L-arabinose transport via the native *S. cerevisiae* galactose transporter (Gal2). These characteristics qualify *Pc*AraT as a potentially valuable additional element in metabolic engineering strategies towards efficient and complete conversion of L-arabinose present in second generation feedstocks for yeast-based production of fuels and chemicals. In **Chapter 4,** sequential batch cultures on sugar mixtures of a glucose-phosphorylation-negative yeast strain, expressing both *PcAraT* and *GAL2*, were successfully used to select for xylose- and glucose-insensitive growth on L-arabinose. Inactivation, in this strain background, of *PcAraT* significantly impacted L-arabinose uptake towards the end of mixed-sugar fermentation experiments. These results demonstrate the potential of *Pc*AraT to efficiently convert low concentrations of L-arabinose towards the end of fermentation processes, thereby preventing prolonged 'tailing' of industrial fermentation processes. The mutations that were found in the glucose-phosphorylation-negative strain, and specifically the single nucleotide polymorphisms found in the galactose transporter encoded by *GAL2*, provide novel genetic parts that can be used to stimulate co-consumption of L-arabinose and D-glucose in consolidated pentose-hexose fermenting *S. cerevisiae* strains, thereby increasing overall process robustness.

In **Chapter 5** a novel strategy was explored for identifying mutations that stimulate glucose-xylose co-consumption by *S. cerevisiae*. This strategy was based on enforcing a strict stoichiometric coupling of D-glucose and D-xylose fermentation by the combined deletion of *RPE1* and *PGI1* in an engineered, xylose-isomerase-based *S. cerevisiae* strain [7]. After evolutionary engineering for improved growth on glucose-xylose mixtures, potential causal mutations identified by whole-genome sequencing were introduced into a non-evolved xylose-fermenting strain background. In contrast to the method described in **Chapter 4**, the forced stochiometric coupling of hexose and pentose sugar consumption allowed for the selection of mutation that were specifically improving co-consumption. This strategy can be expanded to include L-arabinose and with additional laboratory evolution regimes using more industrially relevant sugar ratios and medium compositions to identify additional mutations stimulate sugar co-consumption under industrial process conditions.

The study in **Chapter 6** represents a first exploration of the conversion of mixtures of D-glucose, D-xylose and L-arabinose by a consortium of three 'specialist' *S. cerevisiae* strains. The observation, in this Chapter, that a generalist pentose-fermenting strain was inherently less stable in terms of mixed-sugar fermentation kinetics during repeated batch cultivation has important implications for industrial strain optimization and process design. The potential benefit of biomass recycling is illustrated by its large-scale use in Brazilian 'first-generation' bioethanol processes, leading to spontaneous selection of better performing strains [342]. Our results show that, in terms of strain stability, use

of consortia of specialist yeast strains for second-generation bioethanol could confer similar benefits, including an ability to adapt to fluctuations in feedstock composition. Moreover, repeated batch cultivation of consortia of specialist strains on actual industrial hydrolysates may be used to select for tolerance to fermentation inhibitors, without the inherent risk of deteriorating pentose fermentation kinetics. However, before industrial implementation can be contemplated, a deeper insight into the interaction between specialist strains and a further improvement of their sugar fermentation kinetics in mixed-culture processes is essential. Additionally, the consortium of glucose- and pentose-fermenting specialist yeast strains described in this study provides an interesting model to study the molecular ecology of synthetic consortia of industrial microbes. Resequencing of the genomes of the evolved strains, including those evolved as part of three-partner consortia and evaluation of the impact of the observed mutations by their reverse engineering into non-evolved strains [111, 396], represents a logical next step in such research.

Even at the current global production volume of ethanol, a 1 % increase in product yield on raw material would amount to ca 1 million tonnes of ethanol. As production volumes, the economic relevance of the conversion of minor, potentially fermentable substrates such as uronic acids and deoxysugars into ethanol [206] will become relevant engineering targets. The metabolic and evolutionary engineering strategies presented in **Chapters 2-6** can, in principle, also be applied to improving efficiency and kinetics of the fermentation these underexplored substrates by engineered yeast strains.

Beyond the studies described in this thesis, consolidated bio-processing (CBP), i.e., the full integration of pretreatment, hydrolysis and fermentation towards ethanol in a single microbial process step, remains a 'holy grail' in lignocellulosic ethanol production. Engineered starch-hydrolysing *S. cerevisiae* strains are already applied in first-generation processes [410]. The first important steps towards efficient cellulose and xylan hydrolysis by *S. cerevisiae* have been made by functional expression of heterologous polysaccharide hydrolases [32, 33]. The resulting engineered strains often produce significant amounts of di- and/or trisaccharides [411-413]. The ability to ferment cellobiose has been successfully introduced into *S. cerevisiae* by combined expression of a heterologous cellobiose transporter and β-glucosidase [414, 415].

Looking beyond *S. cerevisiae*, the use of non-*Saccharomyces* yeasts with industrially interesting properties, such as high-temperature and low-pH tolerance strains is gaining increasing interest [416-418]. Additionally, fast progress is being made in engineering thermophilic and cellulolytic bacteria for efficient ethanol production. High-temperature fermentation processes require less cooling and reduce contamination risks [419]. If, moreover, thermophilic CBP can integrate a simple mechanical pretreatment with biomass deconstruction and fermentation by a single organism [33, 420], while matching the robustness of yeasts under industrial conditions, it could develop into a highly interesting approach for second-generation ethanol production. Even though these developments would mean stepping away from *S. cerevisiae*, many of the academic and

industrial efforts that are described for *S. cerevisiae* in **Chapter 1** and further expanded in **Chapters 2-6** can also be applied for enhancing fermentation robustness and performance of other microbial cell factories.

Bibliography

1.   Karhumaa K, Sanchez RG, Hahn-Hägerdal B, Gorwa-Grauslund M-F: **Comparison of the xylose reductase-xylitol dehydrogenase and the xylose isomerase pathways for xylose fermentation by recombinant** *Saccharomyces cerevisiae*. *Microb Cell Fact* 2007, **6**(1):5.

2.   Londesborough J, Richard P, Valkonen M, Viljanen K: **Effect of C-terminal protein tags on pentitol and L-arabinose transport by** *Ambrosiozyma monospora Lat1* **and** *Lat2* **transporters in** *Saccharomyces cerevisiae*. *Appl Environ Microbiol* 2014, **80**(9):2737-2745.

3.   Sato TK, Tremaine M, Parreiras LS, Hebert AS, Myers KS, Higbee AJ, Sardi M, McIlwain SJ, Ong IM, Breuer RJ: **Directed evolution reveals unexpected epistatic interactions that alter metabolic regulation and enable anaerobic xylose use by** *Saccharomyces cerevisiae*. *PLoS Genet* 2016, **12**(10):e1006372.

4.   Wei N, Quarterman J, Kim SR, Cate JHD, Jin YS: **Enhanced biofuel production through coupled acetic acid and xylose consumption by engineered yeast**. *Nat Comm* 2013, **4**.

5.   Runquist D, Hahn-Hagerdal B, Bettiga M: **Increased ethanol productivity in xylose-utilizing** *Saccharomyces cerevisiae* **via a randomly mutagenized xylose reductase**. *Appl Environ Microbiol* 2010, **76**.

6.   Costa CE, Romaní A, Cunha JT, Johansson B, Domingues L: **Integrated approach for selecting efficient** *Saccharomyces cerevisiae* **for industrial lignocellulosic fermentations: Importance of yeast chassis linked to process conditions**. *Bioresour Technol* 2017, **227**:24-34.

7.   Kuyper M, Hartog MM, Toirkens MJ, Almering MJ, Winkler AA, Dijken JP, Pronk JT: **Metabolic engineering of a xylose-isomerase-expressing** *Saccharomyces cerevisiae* **strain for rapid anaerobic xylose fermentation**. *FEMS Yeast Res* 2005, **5**(4-5):399-409.

8.   van Maris AJA, Winkler AA, Kuyper M, De Laat WT, Van Dijken JP, Pronk JT: **Development of efficient xylose fermentation in** *Saccharomyces cerevisiae***: xylose isomerase as a key component**. In: *Biofuels.* Springer; 2007: 179-204.

9.   Kuyper M, Toirkens MJ, Diderich JA, Winkler AA, Dijken JP, Pronk JT: **Evolutionary engineering of mixed-sugar utilization by a xylose-fermenting** *Saccharomyces cerevisiae* **strain**. *FEMS Yeast Res* 2005, **5**(10):925-934.

10.   Demeke MM, Dumortier F, Li Y, Broeckx T, Foulquié-Moreno MR, Thevelein JM: **Combining inhibitor tolerance and D-xylose fermentation in industrial** *Saccharomyces cerevisiae* **for efficient lignocellulose-based bioethanol production**. *Biotechnol Biofuels* 2013, **6**(1):120.

11.   Zhou H, Cheng JS, Wang BL, Fink GR, Stephanopoulos G: **Xylose isomerase overexpression along with engineering of the pentose phosphate pathway and evolutionary engineering enable rapid xylose utilization and ethanol production by** *Saccharomyces cerevisiae*. *Metab Eng* 2012, **14**.

12.   Li H, Shen Y, Wu M, Hou J, Jiao C, Li Z, Liu X, Bao X: **Engineering a wild-type diploid** *Saccharomyces cerevisiae* **strain for second-generation bioethanol production**. *Bioresour Bioprocess* 2016, **3**(1):51.

13.   Wisselink HW, Toirkens MJ, Wu Q, Pronk JT, van Maris AJA: **Novel evolutionary engineering approach for accelerated utilization of glucose, xylose, and arabinose mixtures by engineered** *Saccharomyces cerevisiae* **strains**. *Appl Environ Microbiol* 2009, **75**.

14.   Demeke MM, Dietz H, Li Y, Foulquié-Moreno MR, Mutturi S, Deprez S, Den Abt T, Bonini BM, Liden G, Dumortier F *et al*: **Development of a D-xylose fermenting and inhibitor tolerant industrial** *Saccharomyces cerevisiae* **strain with high performance in lignocellulose hydrolysates using metabolic and evolutionary engineering**. *Biotechnol Biofuels* 2013, **6**(1):89.

15.   Bernton H, Kovarik B, Sklar S: **The forbidden fuel: Power alcohol in the twentieth century**. New York: Caroline House Pubns; 1982.

16.   **World fuel ethanol production** [http://ethanolrfa.org/resources/industry/statistics/]

17.   Lopes ML, de Lima Paulillo SC, Godoy A, Cherubin RA, Lorenzi MS, Giometti FHC, Bernardino CD, Amorim Neto HBd, Amorim HVd: **Ethanol production in Brazil: a bridge between science and industry**. *Braz J Microbiol* 2016, **47**(Suppl 1):64-76.

18. Della-Bianca BE, Basso TO, Stambuk BU, Basso LC, Gombert AK: **What do we know about the yeast strains from the Brazilian fuel ethanol industry?** *Appl Microbiol Biotechnol* 2013, **97**(3):979-991.
19. Thomas K, Ingledew W: **Production of 21%(v/v) ethanol by fermentation of very high gravity (VHG) wheat mashes**. *J Ind Microbiol Biotechnol* 1992, **10**(1):61-68.
20. Rude MA, Schirmer A: **New microbial fuels: a biotech perspective**. *Curr Opin Biotechnol* 2009, **12**(3):274-281.
21. Otero JM, Panagiotou G, Olsson L: **Fueling industrial biotechnology growth with bioethanol**. In: *Biofuels.* Edited by Olsson L. Berlin, Heidelberg: Springer Berlin Heidelberg; 2007: 1-40.
22. Nordhoff S: **Editorial: Food vs fuel – the role of biotechnology**. *Biotechnol J* 2007, **2**(12):1451.
23. Tenenbaum DJ: **Food vs. fuel: Diversion of crops could cause more hunger**. *Environ Health Perspect* 2008, **116**(6):A254-A257.
24. Farrell AE, Plevin RJ, Turner BT, Jones AD, Hare M, Kammen DM: **Ethanol can contribute to energy and environmental goals**. *Science* 2006, **311**(5760):506.
25. Kleinschmidt J: **Biofueling rural development: making the case for linking biofuel production to rural revitalization**. In: *The Carsey School of Public Policy at the Scholars' Repository.* Edited by Durham NHTCI, University of New Hampshire; 2007.
26. Yan X, Inderwildi OR, King DA: **Biofuels and synthetic fuels in the US and China: A review of Well-to-Wheel energy use and greenhouse gas emissions with the impact of land-use change**. *Energy Environ Sci* 2010, **3**(2):190-197.
27. Pereira LG, Dias MOS, Mariano AP, Maciel Filho R, Bonomi A: **Economic and environmental assessment of n-butanol production in an integrated first and second generation sugarcane biorefinery: Fermentative versus catalytic routes**. *Appl Energy* 2015, **160**:120-131.
28. Hahn-Hägerdal B, Galbe M, Gorwa-Grauslund M-F, Lidén G, Zacchi G: **Bio-ethanol–the fuel of tomorrow from the residues of today**. *Trends Biotechnol* 2006, **24**(12):549-556.
29. Van den Brink J, de Vries RP: **Fungal enzyme sets for plant polysaccharide degradation**. *Appl Microbiol Biotechnol* 2011, **91**(6):1477.
30. Lynd LR, Weimer PJ, van Zyl WH, Pretorius IS: **Microbial cellulose utilization: fundamentals and biotechnology**. *Microbiol Mol Biol Rev* 2002, **66**(3):506-577.
31. Sims-Borre P: **The economics of enzyme production**. In: *Ethanol Producer Magazine.* 2010: 68-69.
32. Den Haan R, Van Rensburg E, Rose SH, Görgens JF, van Zyl WH: **Progress and challenges in the engineering of non-cellulolytic microorganisms for consolidated bioprocessing**. *Curr Opin Biotechnol* 2015, **33**:32-38.
33. Olson DG, McBride JE, Joe Shaw A, Lynd LR: **Recent progress in consolidated bioprocessing**. *Curr Opin Biotechnol* 2012, **23**(3):396-405.
34. Vohra M, Manwar J, Manmode R, Padgilwar S, Patil S: **Bioethanol production: Feedstock and current technologies**. *J Environ Chem Eng* 2014, **2**(1):573-584.
35. **U.S. Ethanol Plants** [http://www.ethanolproducer.com/plants/listplants/US/All/Cellulosic]
36. UNCTAD: **Second generation biofuel markets: state of play, trade and developing country perspectives**. *United Nations Conference on Trade and Development* 2016.
37. Khoo HH: **Review of bio-conversion pathways of lignocellulose-to-ethanol: Sustainability assessment based on land footprint projections**. *Renew Sust Energ Rev* 2015, **46**:100-119.
38. Kenney KL, Smith WA, Gresham GL, Westover TL: **Understanding biomass feedstock variability**. *Biofuels* 2013, **4**(1):111-127.
39. Lin Y, Tanaka S: **Ethanol fermentation from biomass resources: current state and prospects**. *Appl Microbiol Biotechnol* 2006, **69**(6):627-642.
40. Lynd LR: **Overview and evaluation of fuel ethanol from cellulosic biomass: technology, economics, the environment, and policy**. *Annu Rev Energy Env* 1996, **21**(1):403-465.
41. Grohmann K, Bothast R: **Pectin-rich residues generated by processing of citrus fruits, apples, and sugar beets**. In.: ACS Publications; 1994.
42. Grohmann K, Bothast RJ: **Saccharification of corn fibre by combined treatment with dilute sulphuric acid and enzymes**. *Process Biochem* 1997, **32**(5):405-415.
43. Bruinenberg PM, Bot PH, Dijken JP, Scheffers WA: **The role of redox balances in the anaerobic fermentation of xylose by yeasts**. *Appl Microbiol Biotechnol* 1983, **18**(5):287-292.

44. Hahn-Hägerdal B, Wahlbom CF, Gárdonyi M, van Zyl WH, Otero RRC, Jönsson LJ: **Metabolic engineering of *Saccharomyces cerevisiae* for xylose utilization**. In: *Metab Eng.* Springer; 2001: 53-84.

45. Kötter P, Amore R, Hollenberg CP, Ciriacy M: **Isolation and characterization of the *Pichia stipitis* xylitol dehydrogenase gene, *XYL2*, and construction of a xylose-utilizing *Saccharomyces cerevisiae* transformant**. *Curr Genet* 1990, **18**(6):493-500.

46. Sedlak M, Ho NW: **Expression of *E. coli* araBAD operon encoding enzymes for metabolizing L-arabinose in *Saccharomyces cerevisiae***. *Enzyme Microb Technol* 2001, **28**(1):16-24.

47. Van Hazendonk JM, Reinerik EJM, de Waard P, Van Dam JEG: **Structural analysis of acetylated hemicellulose polysaccharides from fibre flax (*Linum usitatissimum*)**. *Carbohydr Res* 1996, **291**:141-154.

48. Beckner M, Ivey ML, Phister TG: **Microbial contamination of fuel ethanol fermentations**. *Lett Appl Microbiol* 2011, **53**(4):387-394.

49. Axe DD, Bailey JE: **Transport of lactate and acetate through the energized cytoplasmic membrane of *Escherichia coli***. *Biotechnol Bioeng* 1995, **47**(1):8-19.

50. Pampulha ME, Loureiro-Dias MC: **Energetics of the effect of acetic acid on growth of *Saccharomyces cerevisiae***. *FEMS Microbiol Lett* 2000, **184**(1):69-72.

51. Verduyn C, Postma E, Scheffers WA, Van Dijken JP: **Effect of benzoic acid on metabolic fluxes in yeasts: A continuous-culture study on the regulation of respiration and alcoholic fermentation**. *Yeast* 1992, **8**(7):501-517.

52. Palmqvist E, Hahn-Hägerdal B: **Fermentation of lignocellulosic hydrolysates. II: inhibitors and mechanisms of inhibition**. *Bioresour Technol* 2000, **74**.

53. Russel JB: **Another explanation for the toxicity of fermentation acids at low pH: anion accumulation versus uncoupling**. *J Appl Microbiol* 1992, **73**(5):363-370.

54. Ullah A, Chandrasekaran G, Brul S, Smits G: **Yeast adaptation to weak acids prevents futile energy expenditure**. *Front Microbiol* 2013, **4**(142).

55. Taherzadeh MJ, Eklund R, Gustafsson L, Niklasson C, Lidén G: **Characterization and fermentation of dilute-acid hydrolyzates from wood**. *Ind Eng Chem Res* 1997, **36**(11):4659-4665.

56. Hendriks ATWM, Zeeman G: **Pretreatments to enhance the digestibility of lignocellulosic biomass**. *Bioresour Technol* 2009, **100**(1):10-18.

57. Narron RH, Kim H, Chang HM, Jameel H, Park S: **Biomass pretreatments capable of enabling lignin valorization in a biorefinery process**. *Curr Opin Biotechnol* 2016, **38**:39-46.

58. Silveira MHL, Morais ARC, Da Costa Lopes AM, Olekszyszen DN, Bogel-Łukasik R, Andreaus J, Pereira Ramos L: **Current pretreatment technologies for the development of cellulosic ethanol and biorefineries**. *ChemSusChem* 2015, **8**(20):3366-3390.

59. Ulbricht R, Northup S, Thomas J: **A review of 5-hydroxymethylfurfural (HMF) in parenteral solutions**. *Fundam Appl Toxicol* 1984, **4**(5):843-853.

60. Dunlop AP: **Furfural Formation and Behavior**. *Ind Eng Chem Res* 1948, **40**(2):204-209.

61. Modig T, Lidén G, Taherzadeh MJ: **Inhibition effects of furfural on alcohol dehydrogenase, aldehyde dehydrogenase and pyruvate dehydrogenase**. *Biochem J* 2002, **363**(Pt 3):769-776.

62. Banerjee N, Bhatnagar R, Viswanathan L: **Inhibition of glycolysis by furfural in *Saccharomyces cerevisiae***. *Appl Microbiol Biotechnol* 1981, **11**(4):226-228.

63. Sárvári Horváth I, Franzén CJ, Taherzadeh MJ, Niklasson C, Lidén G: **Effects of furfural on the respiratory metabolism of *Saccharomyces cerevisiae* in glucose-limited chemostats**. *Appl Environ Microbiol* 2003, **69**(7):4076-4086.

64. Almeida JR, Modig T, Petersson A, Hahn-Hagerdal B, Liden G, Gorwa-Grauslund MF: **Increased tolerance and conversion of inhibitors in lignocellulosic hydrolysates by *Saccharomyces cerevisiae***. *J Chem Technol Biotechnol* 2007, **82**.

65. Kumar R, Mago G, Balan V, Wyman CE: **Physical and chemical characterizations of corn stover and poplar solids resulting from leading pretreatment technologies**. *Bioresour Technol* 2009, **100**(17):3948-3962.

66. Lawther JM, Sun R, Banks WB: **Fractional characterization of alkali-labile lignin and alkali-insoluble lignin from wheat straw**. *Ind Crops Prod* 1996, **5**(4):291-300.

67. Klinke HB, Ahring BK, Schmidt AS, Thomsen AB: **Characterization of degradation products from alkaline wet oxidation of wheat straw**. *Bioresour Technol* 2002, **82**(1):15-26.

68.   Larsson S, Quintana-Sainz A, Reimann A, Nilvebrant NO, Jonsson LJ: **Influence of lignocellulose-derived aromatic compounds on oxygen-limited growth and ethanolic fermentation by** *Saccharomyces cerevisiae*. *Appl Biochem Biotechnol* 2000, **84-86**:617-632.

69.   Adeboye PT, Bettiga M, Olsson L: **The chemical nature of phenolic compounds determines their toxicity and induces distinct physiological responses in** *Saccharomyces cerevisiae* **in lignocellulose hydrolysates**. *AMB Express* 2014, **4**:46.

70.   Klinke HB, Thomsen AB, Ahring BK: **Inhibition of ethanol-producing yeast and bacteria by degradation products produced during pre-treatment of biomass**. *Appl Microbiol Biotechnol* 2004, **66**(1):10-26.

71.   Jönsson LJ, Alriksson B, Nilvebrant NO: **Bioconversion of lignocellulose: inhibitors and detoxification**. *Biotechnol Biofuels* 2013, **6**(1):16.

72.   Casey E, Mosier NS, Adamec J, Stockdale Z, Ho N, Sedlak M: **Effect of salts on the co-fermentation of glucose and xylose by a genetically engineered strain of** *Saccharomyces cerevisiae*. *Biotechnol Biofuels* 2013, **6**(1):83.

73.   Taherzadeh MJ, Gustafsson L, Niklasson C, Lidén G: **Conversion of furfural in aerobic and anaerobic batch fermentation of glucose by** *Saccharomyces cerevisiae*. *J Biosci Bioeng* 1999, **87**(2):169-174.

74.   Liu ZL, Slininger PJ, Dien BS, Berhow MA, Kurtzman CP, Gorsich SW: **Adaptive response of yeasts to furfural and 5-hydroxymethylfurfural and new chemical evidence for HMF conversion to 2,5-bis-hydroxymethylfuran**. *J Ind Microbiol Biotechnol* 2004, **31**(8):345-352.

75.   Koppram R, Mapelli V, Albers E, Olsson L: **The presence of pretreated lignocellulosic solids from birch during** *Saccharomyces cerevisiae* **fermentations leads to increased tolerance to inhibitors – a proteomic study of the effects**. *PLoS One* 2016, **11**(2):e0148635.

76.   Sivers MV, Zacchi G, Olsson L, Hähn-Hägerdal B: **Cost analysis of ethanol production from willow using recombinant** *Escherichia coli*. *Biotechnol Prog* 1994, **10**(5):555-560.

77.   Palmqvist E, Hahn-Hägerdal B: **Fermentation of lignocellulosic hydrolysates. I: inhibition and detoxification**. *Bioresour Technol* 2000, **74**(1):17-24.

78.   Canilha L, Chandel AK, Suzane Dos Santos Milessi T, Antunes FAF, Luiz Da Costa Freitas W, Das Graças Almeida Felipe M, Da Silva SS: **Bioconversion of sugarcane biomass into ethanol: An overview about composition, pretreatment methods, detoxification of hydrolysates, enzymatic saccharification, and ethanol fermentation**. *J Biomed Biotechnol* 2012.

79.   Jeffries TW, Jin Y: **Metabolic engineering for improved fermentation of pentoses by yeasts**. *Appl Microbiol Biotechnol* 2004, **63**(5):495-509.

80.   Bailey J: **Toward a science of metabolic engineering**. *Science* 1991, **252**(5013):1668-1675.

81.   Kötter P, Ciriacy M: **Xylose fermentation by** *Saccharomyces cerevisiae*. *Appl Microbiol Biotechnol* 1993, **38**(6):776-783.

82.   Tantirungkij M, Nakashima N, Seki T, Yoshida T: **Construction of xylose-assimilating** *Saccharomyces cerevisiae*. *J Biosci Bioeng* 1993, **75**(2):83-88.

83.   Kuyper M, Aaron A, van Dijken JP, Pronk JT: **Minimal metabolic engineering of** *Saccharomyces cerevisiae* **for efficient anaerobic xylose fermentation: a proof of principle**. *FEMS Yeast Res* 2004, **4**(6):655-664.

84.   Wisselink HW, Toirkens MJ, Del Rosario Franco Berriel M, Winkler AA, Van Dijken JP, Pronk JT, van Maris AJA: **Engineering of** *Saccharomyces cerevisiae* **for efficient anaerobic alcoholic fermentation of ʟ-arabinose**. *Appl Environ Microbiol* 2007, **73**.

85.   Becker J, Boles E: **A modified** *Saccharomyces cerevisiae* **strain that consumes ʟ-arabinose and produces ethanol**. *Appl Environ Microbiol* 2003, **69**(7):4144-4150.

86.   Wiedemann B, Boles E: **Codon-optimized bacterial genes improve ʟ-arabinose fermentation in recombinant** *Saccharomyces cerevisiae*. *Appl Environ Microbiol* 2008, **74**(7):2043-2050.

87.   Fonseca C, Olofsson K, Ferreira C, Runquist D, Fonseca LL, Hahn-Hägerdal B, Lidén G: **The glucose/xylose facilitator Gxf1 from** *Candida intermedia* **expressed in a xylose-fermenting industrial strain of** *Saccharomyces cerevisiae* **increases xylose uptake in SSCF of wheat straw**. *Enzyme Microb Technol* 2011, **48**(6–7):518-525.

88.   Subtil T, Boles E: **Improving ʟ-arabinose utilization of pentose fermenting** *Saccharomyces cerevisiae* **cells by heterologous expression of ʟ-arabinose transporting sugar transporters**. *Biotechnol Biofuels* 2011, **4**(1):38.

89.   Guadalupe Medina V, Almering MJ, van Maris AJA, Pronk JT: **Elimination of glycerol production in anaerobic cultures of a *Saccharomyces cerevisiae* strain engineered to use acetic acid as an electron acceptor**. *Appl Environ Microbiol* 2010, **76**(1):190-195.

90.   Henningsen BM, Hon S, Covalla SF, Sonu C, Argyros DA, Barrett TF, Wiswall E, Froehlich AC, Zelle RM: **Increasing anaerobic acetate consumption and ethanol yields in *Saccharomyces cerevisiae* with NADPH-specific alcohol dehydrogenase**. *Appl Environ Microbiol* 2015, **81**(23):8108-8117.

91.   Papapetridis I, Dijk M, Dobbe AP, Metz B, Pronk JT, van Maris AJA: **Improving ethanol yield in acetate-reducing *Saccharomyces cerevisiae* by cofactor engineering of 6-phosphogluconate dehydrogenase and deletion of *ALD6***. *Microb Cell Fact* 2016, **15**(1):1.

92.   Roca C, Nielsen J, Olsson L: **Metabolic engineering of ammonium assimilation in xylose-fermenting *Saccharomyces cerevisiae* improves ethanol production**. *Appl Environ Microbiol* 2003, **69**(8):4732-4736.

93.   Sonderegger M, Sauer U: **Evolutionary engineering of *Saccharomyces cerevisiae* for anaerobic growth on xylose**. *Appl Environ Microbiol* 2003, **69**.

94.   Watanabe S, Kodaki T, Makino K: **Complete reversal of coenzyme specificity of xylitol dehydrogenase and increase of thermostability by the introduction of structural zinc**. *J Biol Chem* 2005, **280**(11):10340-10349.

95.   Yu KO, Kim SW, Han SO: **Engineering of glycerol utilization pathway for ethanol production by *Saccharomyces cerevisiae***. *Bioresour Technol* 2010, **101**(11):4157-4161.

96.   Zhang GC, Kong II, Wei N, Peng D, Turner TL, Sung BH, Sohn JH, Jin YS: **Optimization of an acetate reduction pathway for producing cellulosic ethanol by engineered yeast**. *Biotechnol Bioeng* 2016, **113**(12):2587-2596.

97.   Ota M, Sakuragi H, Morisaka H, Kuroda K, Miyake H, Tamaru Y, Ueda M: **Display of *Clostridium cellulovorans* xylose isomerase on the cell surface of *Saccharomyces cerevisiae* and its direct application to xylose fermentation**. *Biotechnol Prog* 2013, **29**(2):346-351.

98.   Brat D, Boles E, Wiedemann B: **Functional expression of a bacterial xylose isomerase in *Saccharomyces cerevisiae***. *Appl Environ Microbiol* 2009, **75**.

99.   Ha S, Galazka JM, Rin Kim S, Choi J, Yang X, Seo J, Louise Glass N, Cate JHD, Jin Y-S: **Engineered *Saccharomyces cerevisiae* capable of simultaneous cellobiose and xylose fermentation**. *Proc Natl Acad Sci* 2011, **108**(2):504-509.

100.   Ilmén M, den Haan R, Brevnova E, McBride J, Wiswall E, Froehlich A, Koivula A, Voutilainen SP, Siika-aho M, la Grange DC *et al*: **High level secretion of cellobiohydrolases by *Saccharomyces cerevisiae***. *Biotechnol Biofuels* 2011, **4**(1):30.

101.   Sadie CJ, Rose SH, den Haan R, van Zyl WH: **Co-expression of a cellobiose phosphorylase and lactose permease enables intracellular cellobiose utilisation by *Saccharomyces cerevisiae***. *Appl Microbiol Biotechnol* 2011, **90**(4):1373-1380.

102.   Sauer U: **Evolutionary engineering of industrially important microbial phenotypes**. In: *Metab Eng.* Springer Berlin Heidelberg; 2001: 129-169.

103.   Sanchez RG, Karhumaa K, Fonseca C, Nogué VS, Almeida JR, Larsson CU, Bengtsson O, Bettiga M, Hahn-Hagerdal B, Gorwa-Grauslund MF: **Improved xylose and arabinose utilization by an industrial recombinant *Saccharomyces cerevisiae* strain using evolutionary engineering**. *Biotechnol Biofuels* 2010, **3**(13).

104.   Kim SR, Skerker JM, Kang W, Lesmana A, Wei N, Arkin AP, Jin Y-S: **Rational and evolutionary engineering approaches uncover a small set of genetic changes efficient for rapid xylose fermentation in *Saccharomyces cerevisiae***. *PLoS One* 2013, **8**(2):e57048.

105.   Lee SM, Jellison T, Alper HS: **Systematic and evolutionary engineering of a xylose isomerase-based pathway in *Saccharomyces cerevisiae* for efficient conversion yields**. *Biotechnol Biofuels* 2014, **7**(1):122.

106.   Almario MP, Reyes LH, Kao KC: **Evolutionary engineering of *Saccharomyces cerevisiae* for enhanced tolerance to hydrolysates of lignocellulosic biomass**. *Biotechnol Bioeng* 2013, **110**(10):2616-2623.

107.   González-Ramos D, de Vries ARG, Grijseels SS, Berkum MC, Swinnen S, Broek M, Nevoigt E, Daran J-MG, Pronk JT, van Maris AJA: **A new laboratory evolution approach to select for constitutive acetic acid tolerance in *Saccharomyces cerevisiae* and identification of causal mutations**. *Biotechnol Biofuels* 2016, **9**(1):173.

108. Koppram R, Albers E, Olsson L: **Evolutionary engineering strategies to enhance tolerance of xylose utilizing recombinant yeast to inhibitors derived from spruce biomass**. *Biotechnol Biofuels* 2012, **5**(1):32.

109. Smith J, van Rensburg E, Görgens JF: **Simultaneously improving xylose fermentation and tolerance to lignocellulosic inhibitors through evolutionary engineering of recombinant *Saccharomyces cerevisiae* harbouring xylose isomerase**. *BMC Biotechnol* 2014, **14**(1):41.

110. Wright J, Bellissimi E, De Hulster E, Wagner A, Pronk JT, van Maris AJA: **Batch and continuous culture-based selection strategies for acetic acid tolerance in xylose-fermenting *Saccharomyces cerevisiae***. *FEMS Yeast Res* 2011, **11**.

111. Oud B, van Maris AJA, Daran J-M, Pronk JT: **Genome-wide analytical approaches for reverse metabolic engineering of industrially relevant phenotypes in yeast**. *FEMS Yeast Res* 2012, **12**(2):183-196.

112. Nijland JG, Shin HY, de Jong RM, de Waal PP, Klaassen P, Driessen AJ: **Engineering of an endogenous hexose transporter into a specific D-xylose transporter facilitates glucose-xylose co-consumption in *Saccharomyces cerevisiae***. *Biotechnol Biofuels* 2014, **7**(1):168.

113. dos Santos LV, Carazzolle MF, Nagamatsu ST, Sampaio NMV, Almeida LD, Pirolla RAS, Borelli G, Corrêa TLR, Argueso JL, Pereira GAG: **Unraveling the genetic basis of xylose consumption in engineered *Saccharomyces cerevisiae* strains**. *Sci Rep* 2016, **6**.

114. Hou J, Jiao C, Peng B, Shen Y, Bao X: **Mutation of a regulator Ask10p improves xylose isomerase activity through up-regulation of molecular chaperones in *Saccharomyces cerevisiae***. *Metab Eng* 2016, **38**:241-250.

115. Pinel D, Colatriano D, Jiang H, Lee H, Martin VJ: **Deconstructing the genetic basis of spent sulphite liquor tolerance using deep sequencing of genome-shuffled yeast**. *Biotechnol Biofuels* 2015, **8**(1):53.

116. Liti G, Louis EJ: **Advances in quantitative trait analysis in yeast**. *PLoS Genet* 2012, **8**(8):e1002912.

117. Wilkening S, Lin G, Fritsch ES, Tekkedil MM, Anders S, Kuehn R, Nguyen M, Aiyar RS, Proctor M, Sakhanenko NA *et al*: **An evaluation of high-throughput approaches to QTL mapping in *Saccharomyces cerevisiae***. *Genetics* 2014, **196**(3):853-865.

118. Swinnen S, Schaerlaekens K, Pais T, Claesen J, Hubmann G, Yang Y, Demeke M, Foulquié-Moreno MR, Goovaerts A, Souvereyns K *et al*: **Identification of novel causative genes determining the complex trait of high ethanol tolerance in yeast using pooled-segregant whole-genome sequence analysis**. *Genome Res* 2012, **22**(5):975-984.

119. Sinha H, Nicholson BP, Steinmetz LM, McCusker JH: **Complex genetic interactions in a quantitative trait locus**. *PLoS Genet* 2006, **2**(2):e13.

120. Hubmann G, Mathé L, Foulquié-Moreno MR, Duitama J, Nevoigt E, Thevelein JM: **Identification of multiple interacting alleles conferring low glycerol and high ethanol yield in *Saccharomyces cerevisiae* ethanolic fermentation**. *Biotechnol Biofuels* 2013, **6**(1):87.

121. Marcheschi RJ, Gronenberg LS, Liao JC: **Protein engineering for metabolic engineering: current and next-generation tools**. *Biotechnol J* 2013, **8**(5):545-555.

122. Li H, Schmitz O, Alper HS: **Enabling glucose/xylose co-transport in yeast through the directed evolution of a sugar transporter**. *Appl Microbiol Biotechnol* 2016, **100**(23):10215-10223.

123. Farwick A, Bruder S, Schadeweg V, Oreb M, Boles E: **Engineering of yeast hexose transporters to transport D-xylose without inhibition by D-glucose**. *Proc Natl Acad Sci* 2014, **111**(14):5159-5164.

124. Wang C, Bao X, Li Y, Jiao C, Hou J, Zhang Q, Zhang W, Liu W, Shen Y: **Cloning and characterization of heterologous transporters in *Saccharomyces cerevisiae* and identification of important amino acids for xylose utilization**. *Metab Eng* 2015, **30**:79-88.

125. Reznicek O, Facey SJ, Waal P, Teunissen AW, Bont J, Nijland JG, Driessen AJ, Hauer B: **Improved xylose uptake in *Saccharomyces cerevisiae* due to directed evolution of galactose permease Gal2 for sugar co-consumption**. *J Appl Microbiol* 2015.

126. Shin HY, Nijland JG, Waal PP, Jong RM, Klaassen P, Driessen AJ: **An engineered cryptic Hxt11 sugar transporter facilitates glucose–xylose co-consumption in *Saccharomyces cerevisiae***. *Biotechnol Biofuels* 2015, **8**(1):176.

127. Young EM, Tong A, Bui H, Spofford C, Alper HS: **Rewiring yeast sugar transporter preference through modifying a conserved protein motif**. *Proc Natl Acad Sci* 2014, **111**(1):131-136.

128. Nijland JG, Vos E, Shin HY, de Waal PP, Klaassen P, Driessen AJM: **Improving pentose fermentation by preventing ubiquitination of hexose transporters in *Saccharomyces cerevisiae***. *Biotechnol Biofuels* 2016, **9**(1):158.

129. Krahulec S, Klimacek M, Nidetzky B: **Engineering of a matched pair of xylose reductase and xylitol dehydrogenase for xylose fermentation by *Saccharomyces cerevisiae***. *Biotechnol J* 2009, **4**(5):684-694.

130. Petschacher B, Leitgeb S, Kavanagh Kathryn L, Wilson David K, Nidetzky B: **The coenzyme specificity of *Candida tenuis* xylose reductase (*AKR2B5*) explored by site-directed mutagenesis and X-ray crystallography**. *Biochem J* 2005, **385**(Pt 1):75-83.

131. Petschacher B, Nidetzky B: **Altering the coenzyme preference of xylose reductase to favor utilization of NADH enhances ethanol yield from xylose in a metabolically engineered strain of *Saccharomyces cerevisiae***. *Microb Cell Fact* 2008, **7**(1):9.

132. Watanabe S, Saleh AA, Pack SP, Annaluru N, Kodaki T, Makino K: **Ethanol production from xylose by recombinant *Saccharomyces cerevisiae* expressing protein-engineered NADH-preferring xylose reductase from *Pichia stipitis***. *Microbiology* 2007, **153**(9):3044-3054.

133. Lee SM, Jellison T, Alper HS: **Directed Evolution of xylose isomerase for improved xylose catabolism and fermentation in the yeast *Saccharomyces cerevisiae***. *Appl Environ Microbiol* 2012, **78**(16):5708-5716.

134. Moon J, Liu ZL: **Engineered NADH-dependent *GRE2* from *Saccharomyces cerevisiae* by directed enzyme evolution enhances HMF reduction using additional cofactor NADPH**. *Enzyme Microb Technol* 2012, **50**(2):115-120.

135. Sander JD, Joung JK: **CRISPR-Cas systems for editing, regulating and targeting genomes**. *Nat Biotechnol* 2014, **32**(4):347-355.

136. DiCarlo JE, Norville JE, Mali P, Rios X, Aach J, Church GM: **Genome engineering in *Saccharomyces cerevisiae* using CRISPR-Cas systems**. *Nucleic Acids Res* 2013, **41**(7):4336-4343.

137. Mans R, van Rossum HM, Wijsman M, Backx A, Kuijpers NG, van den Broek M, Daran-Lapujade P, Pronk JT, van Maris AJA, Daran J-MG: **CRISPR/Cas9: a molecular Swiss army knife for simultaneous introduction of multiple genetic modifications in *Saccharomyces cerevisiae***. *FEMS Yeast Res* 2015, **15**(2):fov004.

138. Tsai C-S, Kong II, Lesmana A, Million G, Zhang G-C, Kim SR, Jin Y-S: **Rapid and marker-free refactoring of xylose-fermenting yeast strains with Cas9/CRISPR**. *Biotechnol Bioeng* 2015, **112**(11):2406-2411.

139. Shi S, Liang Y, Zhang MM, Ang EL, Zhao H: **A highly efficient single-step, markerless strategy for multi-copy chromosomal integration of large biochemical pathways in *Saccharomyces cerevisiae***. *Metab Eng* 2016, **33**:19-27.

140. Stovicek V, Borodina I, Forster J: **CRISPR–Cas system enables fast and simple genome editing of industrial *Saccharomyces cerevisiae* strains**. *Metab Eng Commun* 2015, **2**:13-22.

141. van Rossum HM, Kozak BU, Niemeijer MS, Dykstra JC, Luttik MAH, Daran J-MG, van Maris AJA, Pronk JT: **Requirements for carnitine shuttle-mediated translocation of mitochondrial acetyl moieties to the yeast cytosol**. *mBio* 2016, **7**(3).

142. Jeffries TW: **Engineering yeasts for xylose metabolism**. *Curr Opin Biotechnol* 2006, **17**(3):320-326.

143. Sedlak M, Ho NW: **Production of ethanol from cellulosic biomass hydrolysates using genetically engineered *Saccharomyces* yeast capable of cofermenting glucose and xylose**. In: *Proceedings of the Twenty-Fifth Symposium on Biotechnology for Fuels and Chemicals: 2003; Breckenridge, CO*. Springer: 403-416.

144. Wahlbom CF, Hahn–Hägerdal B: **Furfural, 5-hydroxymethyl furfural, and acetoin act as external electron acceptors during anaerobic fermentation of xylose in recombinant *Saccharomyces cerevisiae***. *Biotechnol Bioeng* 2002, **78**(2):172-178.

145. Moniruzzaman M, Dien B, Skory C, Chen Z, Hespell R, Ho N, Dale B, Bothast R: **Fermentation of corn fibre sugars by an engineered xylose utilizing *Saccharomyces* yeast strain**. *World J Microbiol Biotechnol* 1997, **13**(3):341-346.

146. Katahira S, Mizuike A, Fukuda H, Kondo A: **Ethanol fermentation from lignocellulosic hydrolysate by a recombinant xylose-and cellooligosaccharide-assimilating yeast strain**. *Appl Microbiol Biotechnol* 2006, **72**(6):1136-1143.

147. Harhangi HR, Akhmanova AS, Emmens R, van der Drift C, de Laat WT, van Dijken JP, Jetten MS, Pronk JT, den Camp HJO: **Xylose metabolism in the anaerobic fungus *Piromyces* sp. strain E2 follows the bacterial pathway**. *Arch of Microbiol* 2003, **180**(2):134-141.

148. Dun B, Wang, Z., Ye, K., Zhang, B., Li, G., Lu, M.: **Functional expression of *Arabidopsis thaliana* xylose isomerase in *Saccharomyces cerevisiae***. *Xinjiang Agric Sci* 2012, **49**:681-686.

149. Hector RE, Dien BS, Cotta MA, Mertens JA: **Growth and fermentation of D-xylose by *Saccharomyces cerevisiae* expressing a novel D-xylose isomerase originating from the bacterium *Prevotella ruminicola* TC2-24**. *Biotechnol Biofuels* 2013, **6**(1):1.

150. Hou J, Shen Y, Jiao C, Ge R, Zhang X, Bao X: **Characterization and evolution of xylose isomerase screened from the bovine rumen metagenome in *Saccharomyces cerevisiae***. *J Biosci Bioeng* 2016, **121**(2):160-165.

151. Madhavan A, Tamalampudi S, Ushida K, Kanai D, Katahira S, Srivastava A, Fukuda H, Bisaria VS, Kondo A: **Xylose isomerase from polycentric fungus *Orpinomyces*: gene sequencing, cloning, and expression in *Saccharomyces cerevisiae* for bioconversion of xylose to ethanol**. *Appl Microbiol Biotechnol* 2009, **82**(6):1067-1078.

152. Demeke MM, Foulquié-Moreno MR, Dumortier F, Thevelein JM: **Rapid evolution of recombinant *Saccharomyces cerevisiae* for xylose fermentation through formation of extra-chromosomal circular DNA**. *PLoS Genet* 2015, **11**(3):e1005010.

153. Crook N, Abatemarco J, Sun J, Wagner JM, Schmitz A, Alper HS: **In vivo continuous evolution of genes and pathways in yeast**. *Nat Comm* 2016, **7**.

154. Xia PF, Zhang GC, Liu JJ, Kwak S, Tsai CS, Kong II, Sung BH, Sohn JH, Wang SG, Jin YS: **GroE chaperonins assisted functional expression of bacterial enzymes in *Saccharomyces cerevisiae***. *Biotechnol Bioeng* 2016, **113**(10):2149-2155.

155. Van Vleet JH, Jeffries TW, Olsson L: **Deleting the para-nitrophenyl phosphatase (pNPPase), *PHO13*, in recombinant *Saccharomyces cerevisiae* improves growth and ethanol production on D-xylose**. *Metab Eng* 2008, **10**(6):360-369.

156. Xu H, Kim S, Sorek H, Lee Y, Jeong D, Kim J, Oh EJ, Yun EJ, Wemmer DE, Kim KH: ***PHO13* deletion-induced transcriptional activation prevents sedoheptulose accumulation during xylose metabolism in engineered *Saccharomyces cerevisiae***. *Metab Eng* 2016, **34**:88-96.

157. Ni H, Laplaza JM, Jeffries TW: **Transposon mutagenesis to improve the growth of recombinant *Saccharomyces cerevisiae* on D-xylose**. *Appl Environ Microbiol* 2007, **73**(7):2061-2066.

158. Bamba T, Hasunuma T, Kondo A: **Disruption of *PHO13* improves ethanol production via the xylose isomerase pathway**. *AMB Express* 2016, **6**(1):4.

159. Lee N, Gielow W, Martin R, Hamilton E, Fowler A: **The organization of the *araBAD* operon of *Escherichia coli***. *Gene* 1986, **47**(2):231-244.

160. Bettiga M, Hahn-Hägerdal B, Gorwa-Grauslund MF: **Comparing the xylose reductase/xylitol dehydrogenase and xylose isomerase pathways in arabinose and xylose fermenting *Saccharomyces cerevisiae* strains**. *Biotechnol Biofuels* 2008, **1**(1):1.

161. Kou S-C, Christensen MS, Cirillo VP: **Galactose transport in *Saccharomyces cerevisiae* II. Characteristics of galactose uptake and exchange in galactokinaseless cells**. *J Bacteriol* 1970, **103**(3):671-678.

162. Subtil T, Boles E: **Competition between pentoses and glucose during uptake and catabolism in recombinant *Saccharomyces cerevisiae***. *Biotechnol Biofuels* 2012, **5**.

163. Wisselink HW, Cipollina C, Oud B, Crimi B, Heijnen JJ, Pronk JT, van Maris AJA: **Metabolome, transcriptome and metabolic flux analysis of arabinose fermentation by engineered *Saccharomyces cerevisiae***. *Metab Eng* 2010, **12**(6):537-551.

164. Hamacher T, Becker J, Gárdonyi M, Hahn-Hägerdal B, Boles E: **Characterization of the xylose-transporting properties of yeast hexose transporters and their influence on xylose utilization**. *Microbiology* 2002, **148**(9):2783-2788.

165. Lee W-J, Kim M-D, Ryu Y-W, Bisson L, Seo J-H: **Kinetic studies on glucose and xylose transport in *Saccharomyces cerevisiae***. *Appl Microbiol Biotechnol* 2002, **60**(1):186-191.

166. Saloheimo A, Rauta J, Stasyk V, Sibirny AA, Penttilä M, Ruohonen L: **Xylose transport studies with xylose-utilizing *Saccharomyces cerevisiae* strains expressing heterologous and homologous permeases**. *Appl Microbiol Biotechnol* 2007, **74**(5):1041-1052.

167. Reifenberger E, Boles E, Ciriacy M: **Kinetic characterization of individual hexose transporters of *Saccharomyces cerevisiae* and their relation to the triggering mechanisms of glucose repression**. *FEBS J* 1997, **245**(2):324-333.

168.   Diderich JA, Schepper M, van Hoek P, Luttik MA, van Dijken JP, Pronk JT, Klaassen P, Boelens HF, de Mattos MJT, van Dam K: **Glucose uptake kinetics and transcription of *HXT* genes in chemostat cultures of *Saccharomyces cerevisiae*. *J Biol Chem* 1999, **274**(22):15350-15359.

169.   Horak J, Regelmann J, Wolf DH: **Two distinct proteolytic systems responsible for glucose-induced degradation of fructose-1,6-bisphosphatase and the Gal2p transporter in the yeast *Saccharomyces cerevisiae* share the same protein components of the glucose signaling pathway**. *J Biol Chem* 2002, **277**(10):8248-8254.

170.   Horak J, Wolf DH: **Catabolite inactivation of the galactose transporter in the yeast *Saccharomyces cerevisiae*: ubiquitination, endocytosis, and degradation in the vacuole**. *J Bacteriol* 1997, **179**(5):1541-1549.

171.   Sedlak M, Ho NW: **Characterization of the effectiveness of hexose transporters for transporting xylose during glucose and xylose co-fermentation by a recombinant *Saccharomyces* yeast**. *Yeast* 2004, **21**(8):671-684.

172.   Ask M, Bettiga M, Duraiswamy VR, Olsson L: **Pulsed addition of HMF and furfural to batch-grown xylose-utilizing *Saccharomyces cerevisiae* results in different physiological responses in glucose and xylose consumption phase**. *Biotechnol Biofuels* 2013, **6**(1):181.

173.   Bellissimi E, Van Dijken JP, Pronk JT, van Maris AJA: **Effects of acetic acid on the kinetics of xylose fermentation by an engineered, xylose-isomerase-based *Saccharomyces cerevisiae* strain**. *FEMS Yeast Res* 2009, **9**(3):358-364.

174.   Kim SR, Ha S-J, Wei N, Oh EJ, Jin Y-S: **Simultaneous co-fermentation of mixed sugars: a promising strategy for producing cellulosic ethanol**. *Trends Biotechnol* 2012, **30**(5):274-282.

175.   Moysés D, Reis V, Almeida J, Moraes L, Torres F: **Xylose fermentation by *Saccharomyces cerevisiae*: challenges and prospects**. *Int J Mol Sci* 2016, **17**(3):207.

176.   Wisselink HW, van Maris AJA, Pronk JT, Klaassen P, De Jong RM: **Polypeptides with permease activity**. In., vol. US Patent 9034608 B2; 2015.

177.   Runquist D, Hahn-Hägerdal B, Rådström P: **Comparison of heterologous xylose transporters in recombinant *Saccharomyces cerevisiae*. *Biotechnol Biofuels* 2010, **3**(1):5.

178.   Weierstall T, Hollenberg CP, Boles E: **Cloning and characterization of three genes (*SUT1–3*) encoding glucose transporters of the yeast *Pichia stipitis*. *Mol Microbiol* 1999, **31**(3):871-883.

179.   Young EM, Comer AD, Huang H, Alper HS: **A molecular transporter engineering approach to improving xylose catabolism in *Saccharomyces cerevisiae*. *Metab Eng* 2012, **14**(4):401-411.

180.   Colabardini AC, Ries LNA, Brown NA, Dos Reis TF, Savoldi M, Goldman MHS, Menino JF, Rodrigues F, Goldman GH: **Functional characterization of a xylose transporter in *Aspergillus nidulans*. *Biotechnol Biofuels* 2014, **7**(1):1.

181.   Du J, Li S, Zhao H: **Discovery and characterization of novel D-xylose-specific transporters from *Neurospora crassa* and *Pichia stipitis*. *Mol BioSyst* 2010, **6**(11):2150-2156.

182.   Ferreira D, Nobre A, Silva ML, Faria-Oliveira F, Tulha J, Ferreira C, Lucas C: ***XYLH* encodes a xylose/H+ symporter from the highly related yeast species *Debaryomyces fabryi* and *Debaryomyces hansenii*. *FEMS Yeast Res* 2013, **13**(7):585-596.

183.   Katahira S, Ito M, Takema H, Fujita Y, Tanino T, Tanaka T, Fukuda H, Kondo A: **Improvement of ethanol productivity during xylose and glucose co-fermentation by xylose-assimilating *S. cerevisiae* via expression of glucose transporter Sut1**. *Enzyme Microb Technol* 2008, **43**(2):115-119.

184.   Knoshaug EP, Vidgren V, Magalhães F, Jarvis EE, Franden MA, Zhang M, Singh A: **Novel transporters from *Kluyveromyces marxianus* and *Pichia guilliermondii* expressed in *Saccharomyces cerevisiae* enable growth on L-arabinose and D-xylose**. *Yeast* 2015, **32**(10):615-628.

185.   Leandro MJ, Gonçalves P, Spencer-Martins I: **Two glucose/xylose transporter genes from the yeast *Candida intermedia*: first molecular characterization of a yeast xylose–H+ symporter**. *Biochem J* 2006, **395**(3):543-549.

186.   Li J, Xu J, Cai P, Wang B, Ma Y, Benz JP, Tian C: **Functional analysis of two L-arabinose transporters from filamentous fungi reveals promising characteristics for improved pentose utilization in *Saccharomyces cerevisiae*. *Appl Environ Microbiol* 2015, **81**(12):4062-4070.

187.	Reis TF, Lima PBA, Parachin NS, Mingossi FB, Oliveira JVC, Ries LNA, Goldman GH: **Identification and characterization of putative xylose and cellobiose transporters in *Aspergillus nidulans***. *Biotechnol Biofuels* 2016, **9**(1):204.

188.	Wang M, Yu C, Zhao H: **Directed evolution of xylose specific transporters to facilitate glucose-xylose co-utilization**. *Biotechnol Bioeng* 2016, **113**(3):484-491.

189.	Lewis Liu Z, Moon J, Andersh BJ, Slininger PJ, Weber S: **Multiple gene-mediated NAD(P)H-dependent aldehyde reduction is a mechanism of *in situ* detoxification of furfural and 5-hydroxymethylfurfural by *Saccharomyces cerevisiae***. *Appl Microbiol Biotechnol* 2008, **81**(4):743-753.

190.	Almeida JRM, Bertilsson M, Hahn-Hägerdal B, Lidén G, Gorwa-Grauslund M-F: **Carbon fluxes of xylose-consuming *Saccharomyces cerevisiae* strains are affected differently by NADH and NADPH usage in HMF reduction**. *Appl Microbiol Biotechnol* 2009, **84**(4):751-761.

191.	Jeppsson M, Johansson B, Jensen PR, Hahn-Hägerdal B, Gorwa-Grauslund MF: **The level of glucose-6-phosphate dehydrogenase activity strongly influences xylose fermentation and inhibitor sensitivity in recombinant *Saccharomyces cerevisiae* strains**. *Yeast* 2003, **20**(15):1263-1272.

192.	Adeboye PT, Bettiga M, Olsson L: ***ALD5, PAD1, ATF1* and *ATF2* facilitate the catabolism of coniferyl aldehyde, ferulic acid and p-coumaric acid in *Saccharomyces cerevisiae***. *Sci Rep* 2017, **7**:42635.

193.	Liu ZL: **Molecular mechanisms of yeast tolerance and *in situ* detoxification of lignocellulose hydrolysates**. *Appl Microbiol Biotechnol* 2011, **90**(3):809-825.

194.	Li BZ, Yuan YJ: **Transcriptome shifts in response to furfural and acetic acid in *Saccharomyces cerevisiae***. *Appl Microbiol Biotechnol* 2010, **86**(6):1915-1924.

195.	Mira NP, Palma M, Guerreiro JF, Sá-Correia I: **Genome-wide identification of *Saccharomyces cerevisiae* genes required for tolerance to acetic acid**. *Microb Cell Fact* 2010, **9**:79.

196.	Abbott DA, Knijnenburg TA, De Poorter LMI, Reinders MJT, Pronk JT, van Maris AJA: **Generic and specific transcriptional responses to different weak organic acids in anaerobic chemostat cultures of *Saccharomyces cerevisiae***. *FEMS Yeast Res* 2007, **7**(6):819-833.

197.	Guo Z, Olsson L: **Physiological response of *Saccharomyces cerevisiae* to weak acids present in lignocellulosic hydrolysate**. *FEMS Yeast Res* 2014, **14**(8):1234-1248.

198.	Chen Y, Sheng J, Jiang T, Stevens J, Feng X, Wei N: **Transcriptional profiling reveals molecular basis and novel genetic targets for improved resistance to multiple fermentation inhibitors in *Saccharomyces cerevisiae***. *Biotechnol Biofuels* 2016, **9**(1):1.

199.	Thompson OA, Hawkins GM, Gorsich SW, Doran-Peterson J: **Phenotypic characterization and comparative transcriptomics of evolved *Saccharomyces cerevisiae* strains with improved tolerance to lignocellulosic derived inhibitors**. *Biotechnol Biofuels* 2016, **9**(1).

200.	Swinnen S, Fernández-Niño M, González-Ramos D, van Maris AJA, Nevoigt E: **The fraction of cells that resume growth after acetic acid addition is a strain-dependent parameter of acetic acid tolerance in *Saccharomyces cerevisiae***. *FEMS Yeast Res* 2014, **14**(4):642-653.

201.	Field SJ, Ryden P, Wilson D, James SA, Roberts IN, Richardson DJ, Waldron KW, Clarke TA: **Identification of furfural resistant strains of *Saccharomyces cerevisiae* and *Saccharomyces paradoxus* from a collection of environmental and industrial isolates**. *Biotechnol Biofuels* 2015, **8**(1).

202.	Favaro L, Basaglia M, Trento A, Van Rensburg E, García-Aparicio M, Van Zyl WH, Casella S: **Exploring grape marc as trove for new thermotolerant and inhibitor-tolerant *Saccharomyces cerevisiae* strains for second-generation bioethanol production**. *Biotechnol Biofuels* 2013, **6**(1):168.

203.	Wimalasena TT, Greetham D, Marvin ME, Liti G, Chandelia Y, Hart A, Louis EJ, Phister TG, Tucker GA, Smart KA: **Phenotypic characterisation of *Saccharomyces spp.* yeast for tolerance to stresses encountered during fermentation of lignocellulosic residues to produce bioethanol**. *Microb Cell Fact* 2014, **13**(1):47.

204.	Meijnen J-P, Randazzo P, Foulquié-Moreno MR, van den Brink J, Vandecruys P, Stojiljkovic M, Dumortier F, Zalar P, Boekhout T, Gunde-Cimerman N *et al*: **Polygenic analysis and targeted improvement of the complex trait of high acetic acid tolerance in the yeast *Saccharomyces cerevisiae***. *Biotechnol Biofuels* 2016, **9**:5.

205.	Nielsen J, Larsson C, van Maris AJA, Pronk JT: **Metabolic engineering of yeast for production of fuels and chemicals**. *Curr Opin Biotechnol* 2013, **24**(3):398-404.

206. van Maris AJA, Abbott DA, Bellissimi E, van den Brink J, Kuyper M, Luttik MA, Wisselink HW, Scheffers WA, van Dijken JP, Pronk JT: **Alcoholic fermentation of carbon sources in biomass hydrolysates by *Saccharomyces cerevisiae*: current status**. *Antonie Van Leeuwenhoek* 2006, **90**(4):391-418.

207. Nissen TL, Kielland-Brandt MC, Nielsen J, Villadsen J: **Optimization of ethanol production in *Saccharomyces cerevisiae* by metabolic engineering of the ammonium assimilation**. *Metab Eng* 2000, **2**(1):69-77.

208. Björkqvist S, Ansell R, Adler L, Lidén G: **Physiological response to anaerobicity of glycerol-3-phosphate dehydrogenase mutants of *Saccharomyces cerevisiae***. *Appl Environ Microbiol* 1997, **63**(1):128-132.

209. Van Dijken JP, Scheffers WA: **Redox balances in the metabolism of sugars by yeasts**. *FEMS Microbiol Rev* 1986, **32**(3-4):199-224.

210. Guo Z, Zhang L, Ding Z, Shi G: **Minimization of glycerol synthesis in industrial ethanol yeast without influencing its fermentation performance**. *Metab Eng* 2011, **13**(1):49-59.

211. Hubmann G, Guillouet S, Nevoigt E: **Gpd1 and Gpd2 fine-tuning for sustainable reduction of glycerol formation in *Saccharomyces cerevisiae***. *Appl Environ Microbiol* 2011, **77**(17):5857-5867.

212. Noorman H: **An industrial perspective on bioreactor scale-down: What we can learn from combined large-scale bioprocess and model fluid studies**. *Biotechnol J* 2011, **6**(8):934-943.

213. Li C, Aston JE, Lacey JA, Thompson VS, Thompson DN: **Impact of feedstock quality and variation on biochemical and thermochemical conversion**. *Renew Sust Energ Rev* 2016, **65**:525-536.

214. Knoll JE, Anderson WF, Richard EP, Doran-Peterson J, Baldwin B, Hale AL, Viator RP: **Harvest date effects on biomass quality and ethanol yield of new energycane (*Saccharum* hyb.) genotypes in the Southeast USA**. *Biomass Bioenergy* 2013, **56**:147-156.

215. Basso LC, De Amorim HV, De Oliveira AJ, Lopes ML: **Yeast selection for fuel ethanol production in Brazil**. *FEMS Yeast Res* 2008, **8**(7):1155-1163.

216. Della-Bianca BE, de Hulster E, Pronk JT, van Maris AJA, Gombert AK: **Physiology of the fuel ethanol strain *Saccharomyces cerevisiae* PE-2 at low pH indicates a context-dependent performance relevant for industrial applications**. *FEMS Yeast Res* 2014, **14**(8):1196-1205.

217. de Vries ARG, Pronk JT, Daran J-MG: **Industrial relevance of chromosomal copy number variation in *Saccharomyces* yeasts**. *Appl Environ Microbiol* 2017, **83**(11):e03206-03216.

218. Zhang K, Zhang L-J, Fang Y-H, Jin X-N, Qi L, Wu X-C, Zheng D-Q: **Genomic structural variation contributes to phenotypic change of industrial bioethanol yeast *Saccharomyces cerevisiae***. *FEMS Yeast Res* 2016, **16**(2):fov118.

219. Hahn-Hägerdal B, Karhumaa K, Fonseca C, Spencer-Martins I, Gorwa-Grauslund MF: **Towards industrial pentose-fermenting yeast strains**. *Appl Microbiol Biotechnol* 2007, **74**(5):937-953.

220. Pronk JT: **Auxotrophic yeast strains in fundamental and applied research**. *Appl Environ Microbiol* 2002, **68**(5):2095-2100.

221. Karim AS, Curran KA, Alper HS: **Characterization of plasmid burden and copy number in *Saccharomyces cerevisiae* for optimization of metabolic engineering applications**. *FEMS Yeast Res* 2013, **13**(1):107-116.

222. Wang BL, Ghaderi A, Zhou H, Agresti J, Weitz DA, Fink GR, Stephanopoulos G: **Microfluidic high-throughput culturing of single cells for selection based on extracellular metabolite production or consumption**. *Nat Biotechnol* 2014, **32**(5):473-478.

223. Snoek T, Nicolino MP, Van den Bremt S, Mertens S, Saels V, Verplaetse A, Steensels J, Verstrepen KJ: **Large-scale robot-assisted genome shuffling yields industrial *Saccharomyces cerevisiae* yeasts with increased ethanol tolerance**. *Biotechnol Biofuels* 2015, **8**(1):32.

224. Jacques KA, Lyons TP, Kelsall DR: **The alcohol textbook: a reference for the beverage, fuel and industrial alcohol industries**: Nottingham University Press; 2003.

225. Nielsen F, Tomás-Pejó E, Olsson L, Wallberg O: **Short-term adaptation during propagation improves the performance of xylose-fermenting *Saccharomyces cerevisiae* in simultaneous saccharification and co-fermentation**. *Biotechnol Biofuels* 2015, **8**(1):1.

226. Alkasrawi M, Rudolf A, Lidén G, Zacchi G: **Influence of strain and cultivation procedure on the performance of simultaneous saccharification and fermentation of steam pretreated spruce**. *Enzyme Microb Technol* 2006, **38**(1):279-286.

227. Sànchez i Nogué V, Narayanan V, Gorwa-Grauslund MF: **Short-term adaptation improves the fermentation performance of *Saccharomyces cerevisiae* in the presence of acetic acid at low pH**. *Appl Microbiol Biotechnol* 2013, **97**(16):7517-7525.

228. Narendranath NV, Lewis SM: **Systems and methods for yeast propagation**. In.: US Patent 9034631 B2; 2013.

229. Steiner G: **Use of ethanol plant by-products for yeast propagation**. In., vol. US Patent 8183022 B2; 2008.

230. United States Environmental Protection Agency: **Public data for the Renewable Fuel Standard. https://www.epa.gov/fuels-registration-reporting-and-compliance-help/public-data-renewable-fuel-standard**. *Web, retrieved Jan 4, 2017*

231. BioFuels Digest: **Cellulosic ethanol: Where are the gallons? Answers for your questions. http://www.biofuelsdigest.com/bdigest/2015/07/01/cellulosic-ethanol-where-are-the-gallons-answers-for-your-questions/**.

232. Wang G, Tang W, Xia J, Chu J, Noorman H, van Gulik WM: **Integration of microbial kinetics and fluid dynamics toward model-driven scale-up of industrial bioprocesses**. *Eng Life Sci* 2015, **15**(1):20-29.

233. Villadsen J, Noorman H: **Scale-Up and Scale-Down**. In: *Fundam Bioeng.* 2015.

234. Bischoff KM, Liu S, Leathers TD, Worthington RE, Rich JO: **Modeling bacterial contamination of fuel ethanol fermentation**. *Biotechnol Bioeng* 2009, **103**(1):117-122.

235. Albers E, Johansson E, Franzén CJ, Larsson C: **Selective suppression of bacterial contaminants by process conditions during lignocellulose based yeast fermentations**. *Biotechnol Biofuels* 2011, **4**:59.

236. Muthaiyan A, Limayem A, Ricke S: **Antimicrobial strategies for limiting bacterial contaminants in fuel bioethanol fermentations**. *Prog Energy Combust Sci* 2011, **37**(3):351-370.

237. BioFuels Digest: **Editor's Sketchbook: Beta Renewables cellulosic ethanol project, Crescentino, Italy. http://www.biofuelsdigest.com/bdigest/2014/09/25/editors-sketchbook-beta-renewables-cellulosic-ethanol-project-crescentino-italy/**.

238. Lane J: **Getting it right: The digest's multi-slide guide to Iogen**. *BiofuelsDigest* 2016.

239. Alper H, Stephanopoulos G: **Engineering for biofuels: exploiting innate microbial capacity or importing biosynthetic potential?** *Nat Rev Microbiol* 2009, **7**(10):715-723.

240. Wang PY, Schneider H: **Growth of yeasts on D-xylulose**. *Can J Microbiol* 1980, **26**(9):1165-1168.

241. Jeffries TW: **Utilization of xylose by bacteria, yeasts, and fungi**. In: *Pentoses and Lignin.* Springer; 1983: 1-32.

242. Walfridsson M, Bao X, Anderlund M, Lilius G, Bülow L, Hahn-Hägerdal B: **Ethanolic fermentation of xylose with *Saccharomyces cerevisiae* harboring the *Thermus thermophilus xylA* gene, which expresses an active xylose (glucose) isomerase**. *Appl Environ Microbiol* 1996, **62**(12):4648-4651.

243. Sarthy A, McConaughy B, Lobo Z, Sundstrom J, Furlong CE, Hall B: **Expression of the *Escherichia coli* xylose isomerase gene in *Saccharomyces cerevisiae***. *Appl Environ Microbiol* 1987, **53**(9):1996-2000.

244. Moes CJ, Pretorius IS, van Zyl WH: **Cloning and expression of the *Clostridium thermosulfurogenes* D-xylose isomerase gene (*xylA*) in *Saccharomyces cerevisiae***. *Biotechnol Lett* 1996, **18**(3):269-274.

245. Gárdonyi M, Hahn-Hägerdal B: **The *Streptomyces rubiginosus* xylose isomerase is misfolded when expressed in *Saccharomyces cerevisiae***. *Enzyme Microb Technol* 2003, **32**(2):252-259.

246. Kuyper M, Harhangi HR, Stave AK, Winkler AA, Jetten MS, De Laat WT, Den Ridder JJ, Op Den Camp HJ, Van Dijken JP, Pronk JT: **High-level functional expression of a fungal xylose isomerase: the key to efficient ethanolic fermentation of xylose by *Saccharomyces cerevisiae*** *FEMS Yeast Res* 2003, **4**.

247. Ha S-J, Kim SR, Choi J-H, Park MS, Jin Y-S: **Xylitol does not inhibit xylose fermentation by engineered *Saccharomyces cerevisiae* expressing *xylA* as severely as it inhibits xylose isomerase reaction *in vitro***. *Appl Environ Microbiol* 2011, **92**(1):77-84.

248. Apel AR, Ouellet M, Szmidt-Middleton H, Keasling JD, Mukhopadhyay A: **Evolved hexose transporter enhances xylose uptake and glucose/xylose co-utilization in *Saccharomyces cerevisiae***. *Sci Rep* 2016, **6**:19512.

249. Kuijpers NG, Chroumpi S, Vos T, Solis-Escalante D, Bosman L, Pronk JT, Daran J-M, Daran-Lapujade P: **One-step assembly and targeted integration of multigene constructs assisted by the I-SceI meganuclease in *Saccharomyces cerevisiae***. *FEMS Yeast Res* 2013, **13**(8):769-781.

250. Träff K, Cordero RO, Van Zyl W, Hahn-Hägerdal B: **Deletion of the *GRE3* aldose reductase gene and its influence on xylose metabolism in recombinant strains of *Saccharomyces cerevisiae* expressing the *xylA* and *XKS1* genes**. *Appl Environ Microbiol* 2001, **67**(12):5668-5674.

251. Entian K-D, Kötter P: **25 Yeast genetic strain and plasmid collections**. *Method Microbiol* 2007, **36**:629-666.

252. Lapinskas PJ, Cunningham KW, Liu XF, Fink GR, Culotta VC: **Mutations in *PMR1* suppress oxidative damage in yeast cells lacking superoxide dismutase**. *Mol Cell Biol* 1995, **15**(3):1382-1388.

253. Sorin A, Rosas G, Rao R: ***PMR1*, a Ca²⁺-ATPase in yeast Golgi, has properties distinct from sarco/endoplasmic reticulum and plasma membrane calcium pumps**. *J Biol Chem* 1997, **272**(15):9895-9901.

254. Culotta VC, Yang M, Hall MD: **Manganese transport and trafficking: lessons learned from *Saccharomyces cerevisiae***. *Eukaryot Cell* 2005, **4**(7):1159-1165.

255. Yu D, Danku JM, Baxter I, Kim S, Vatamaniuk OK, Vitek O, Ouzzani M, Salt DE: **High-resolution genome-wide scan of genes, gene-networks and cellular systems impacting the yeast ionome**. *BMC Genomics* 2012, **13**(1):623.

256. Van Bastelaere P, Vangrysperre W, Kersters-Hilderson H: **Kinetic studies of Mg²⁺-, Co²⁺-and Mn²⁺-activated D-xylose isomerases**. *Biochem J* 1991, **278**(1):285-292.

257. Bakker BM, Overkamp KM, van Maris AJA, Kötter P, Luttik MA, van Dijken JP, Pronk JT: **Stoichiometry and compartmentation of NADH metabolism in *Saccharomyces cerevisiae***. *FEMS Microbiol Rev* 2001, **25**(1):15-37.

258. Chang A, Schomburg I, Placzek S, Jeske L, Ulbrich M, Xiao M, Sensen CW, Schomburg D: **BRENDA in 2015: exciting developments in its 25th year of existence**. *Nucleic Acids Res* 2014, **43**(D1):D439-D446.

259. van den Brink J, Akeroyd M, van der Hoeven R, Pronk J, De Winde J, Daran-Lapujade P: **Energetic limits to metabolic flexibility: responses of *Saccharomyces cerevisiae* to glucose–galactose transitions**. *Microbiology* 2009, **155**(4):1340-1350.

260. Devasahayam G, Ritz D, Helliwell SB, Burke DJ, Sturgill TW: **Pmr1, a Golgi Ca²⁺/Mn²⁺-ATPase, is a regulator of the target of rapamycin (TOR) signaling pathway in yeast**. *Proc Natl Acad Sci* 2006, **103**(47):17840-17845.

261. Cui Y, Zhao S, Wu Z, Dai P, Zhou B: **Mitochondrial release of the NADH dehydrogenase Ndi1 induces apoptosis in yeast**. *Mol Biol Cell* 2012, **23**(22):4373-4382.

262. Li W, Sun L, Liang Q, Wang J, Mo W, Zhou B: **Yeast AMID homologue Ndi1p displays respiration-restricted apoptotic activity and is involved in chronological aging**. *Mol Biol Cell* 2006, **17**(4):1802-1811.

263. Hartley BS, Hanlon N, Jackson RJ, Rangarajan M: **Glucose isomerase: insights into protein engineering for increased thermostability**. *Biochim Biophys Acta, Protein Struct Mol Enzymol* 2000, **1543**(2):294-335.

264. Klaassen P, Gielesen BEM, Van Suylekom GP, Sarantinopoulos P, Heijne WHM, Greeve A: **Yeast cell capable of converting sugars including arabinose and xylose**. In.; 2012.

265. Ko JK, Um Y, Lee S-M: **Effect of manganese ions on ethanol fermentation by xylose isomerase expressing *Saccharomyces cerevisiae* under acetic acid stress**. *Bioresour Technol* 2016, **222**:422-430.

266. Nijkamp JF, van den Broek M, Datema E, de Kok S, Bosman L, Luttik MA, Daran-Lapujade P, Vongsangnak W, Nielsen J, Heijne WH: **De novo sequencing, assembly and analysis of the genome of the laboratory strain *Saccharomyces cerevisiae* CEN. PK113-7D, a model for modern industrial biotechnology**. *Microb Cell Fact* 2012, **11**(1):36.

267. Shevchuk NA, Bryksin AV, Nusinovich YA, Cabello FC, Sutherland M, Ladisch S: **Construction of long DNA molecules using long PCR-based fusion of several fragments simultaneously**. *Nucleic Acids Res* 2004, **32**(2):e19-e19.

268. Janke C, Magiera MM, Rathfelder N, Taxis C, Reber S, Maekawa H, Moreno-Borchart A, Doenges G, Schwob E, Schiebel E: **A versatile toolbox for PCR-based tagging of yeast genes: new**

fluorescent proteins, more markers and promoter substitution cassettes. *Yeast* 2004, **21**(11):947-962.

269.   Gietz RD, Woods RA: **Transformation of yeast by lithium acetate/single-stranded carrier DNA/polyethylene glycol method**. *Method Enzymol* 2002, **350**:87-96.

270.   Solis-Escalante D, Kuijpers NG, Bongaerts N, Bolat I, Bosman L, Pronk JT, Daran JM, Daran-Lapujade P: *amdSYM*, **a new dominant recyclable marker cassette for *Saccharomyces cerevisiae***. *FEMS Yeast Res* 2013, **13**(1):126-139.

271.   Verduyn C, Postma E, Scheffers WA, van Dijken JP: **Physiology of *Saccharomyces cerevisiae* in anaerobic glucose-limited chemostat cultures**. *Microbiology* 1990, **136**(3):395-403.

272.   Li H, Durbin R: **Fast and accurate short read alignment with Burrows–Wheeler transform**. *Bioinformatics* 2009, **25**(14):1754-1760.

273.   Walker BJ, Abeel T, Shea T, Priest M, Abouelliel A, Sakthikumar S, Cuomo CA, Zeng Q, Wortman J, Young SK: **Pilon: an integrated tool for comprehensive microbial variant detection and genome assembly improvement**. *PLoS One* 2014, **9**(11):e112963.

274.   Thorvaldsdóttir H, Robinson JT, Mesirov JP: **Integrative Genomics Viewer (IGV): high-performance genomics data visualization and exploration**. *Brief Bioinform* 2013, **14**(2):178-192.

275.   Nijkamp JF, van den Broek MA, Geertman JMA, Reinders MJ, Daran JMG, de Ridder D: *De novo* **detection of copy number variation by co-assembly**. *Bioinformatics* 2012, **28**(24):3195-3202.

276.   Eide DJ, Clark S, Nair TM, Gehl M, Gribskov M, Guerinot ML, Harper JF: **Characterization of the yeast ionome: a genome-wide analysis of nutrient mineral and trace element homeostasis in *Saccharomyces cerevisiae***. *Genome Biol* 2005, **6**(9):R77.

277.   Kersters-Hilderson H, Callens M, Van Opstal O, Vangrysperre W, De Bruyne CK: **Kinetic characterization of D-xylose isomerases by enzymatic assays using D-sorbitol dehydrogenase**. *Enzyme Microb Technol* 1987, **9**(3):145-148.

278.   Micard V, Renard C, Thibault J-F: **Enzymatic saccharification of sugar-beet pulp**. *Enzyme Microb Technol* 1996, **19**(3):162-170.

279.   Jansen ML, Bracher JM, Papapetridis I, Verhoeven MD, de Bruijn H, de Waal PP, van Maris AJA, Klaassen P, Pronk JT: *Saccharomyces cerevisiae* **strains for second-generation ethanol production: from academic exploration to industrial implementation**. *FEMS Yeast Res* 2017, **17**(5).

280.   Richard P, Verho R, Putkonen M, Londesborough J, Penttilä M: **Production of ethanol from L-arabinose by *Saccharomyces cerevisiae* containing a fungal L-arabinose pathway**. *FEMS Yeast Res* 2003, **3**(2):185-189.

281.   Leandro MJ, Fonseca C, Gonçalves P: **Hexose and pentose transport in ascomycetous yeasts: an overview**. *FEMS Yeast Res* 2009, **9**(4):511-525.

282.   Young E, Lee S-M, Alper H: **Optimizing pentose utilization in yeast: the need for novel tools and approaches**. *Biotechnol Biofuels* 2010, **3**(1):24.

283.   Özcan S, Johnston M: **Function and regulation of yeast hexose transporters**. *Microbiol Mol Biol Rev* 1999, **63**(3):554-569.

284.   Van Den Berg MA, Albang R, Albermann K, Badger JH, Daran J-M, Driessen AJ, Garcia-Estrada C, Fedorova ND, Harris DM, Heijne WH: **Genome sequencing and analysis of the filamentous fungus *Penicillium chrysogenum***. *Nat Biotechnol* 2008, **26**(10):1161-1168.

285.   Van den Berg MA: **Impact of the *Penicillium chrysogenum* genome on industrial production of metabolites**. *Appl Microbiol Biotechnol* 2011, **92**(1):45-53.

286.   Chiang C, Knight S: **L-Arabinose metabolism by cell-free extracts of *Penicillium chrysogenum***. *Biochim Biophys Acta* 1961, **46**(2):271-278.

287.   Chiang C, Knight S: **A new pathway of pentose metabolism**. *Biochem Biophys Res Commun* 1960, **3**(5):554-559.

288.   Sakamoto T, Ogura A, Inui M, Tokuda S, Hosokawa S, Ihara H, Kasai N: **Identification of a GH62 α-L-arabinofuranosidase specific for arabinoxylan produced by *Penicillium chrysogenum***. *Appl Microbiol Biotechnol* 2011, **90**(1):137-146.

289.   Lõoke M, Kristjuhan K, Kristjuhan A: **Extraction of genomic DNA from yeasts for PCR-based applications**. *Biotechniques* 2011, **50**(5):325.

290.   Inoue H, Nojima H, Okayama H: **High efficiency transformation of *Escherichia coli* with plasmids**. *Gene* 1990, **96**(1):23-28.

291. Solis-Escalante D, Kuijpers NG, Barrajon-Simancas N, van den Broek M, Pronk JT, Daran J-M, Daran-Lapujade P: **A minimal set of glycolytic genes reveals strong redundancies in** *Saccharomyces cerevisiae* **central metabolism**. *Eukaryot Cell* 2015, **14**(8):804-816.

292. Gueldener U, Heinisch J, Koehler G, Voss D, Hegemann J: **A second set of** *loxP* **marker cassettes for Cre-mediated multiple gene knockouts in budding yeast**. *Nucleic Acids Res* 2002, **30**(6):e23-e23.

293. Güldener U, Heck S, Fiedler T, Beinhauer J, Hegemann JH: **A new efficient gene disruption cassette for repeated use in budding yeast**. *Nucleic Acids Res* 1996, **24**(13):2519-2524.

294. Kuijpers NG, Solis-Escalante D, Luttik MA, Bisschops MM, Boonekamp FJ, van den Broek M, Pronk JT, Daran J-M, Daran-Lapujade P: **Pathway swapping: Toward modular engineering of essential cellular processes**. *Proc Natl Acad Sci* 2016:201606701.

295. Verhoeven MD, Lee M, Kamoen L, Van Den Broek M, Janssen DB, Daran J-MG, van Maris AJA, Pronk JT: **Mutations in** *PMR1* **stimulate xylose isomerase activity and anaerobic growth on xylose of engineered** *Saccharomyces cerevisiae* **by influencing manganese homeostasis**. *Sci Rep* 2017, **7**.

296. Roubos JA, Van Peij NNME: **A method for achieving improved polypeptide expression**. In.: WO Patent App. PCT/EP2007/055,943; 2008.

297. Klaassen P, Van Der Laan JM, Gielesen BEM, Van Suylekom GP: **Pentose sugar fermenting cell**. In., vol. US Patent 8.399.215 B2; 2013.

298. Kuijpers N, Solis-Escalante D, Bosman L, van den Broek M, Pronk JT, Daran J-M, Daran-Lapujade P: **A versatile, efficient strategy for assembly of multi-fragment expression vectors in** *Saccharomyces cerevisiae* **using 60 bp synthetic recombination sequences**. *Microb Cell Fact* 2013, **12**:47.

299. Bracher JM, de Hulster E, Koster CC, van den Broek M, Daran J-MG, van Maris AJA, Pronk JT: **Laboratory evolution of a biotin-requiring** *Saccharomyces cerevisiae* **strain for full biotin prototrophy and identification of causal mutations**. *Appl Environ Microbiol* 2017.

300. Harris DM, van der Krogt ZA, Klaassen P, Raamsdonk LM, Hage S, van den Berg MA, Bovenberg RA, Pronk JT, Daran J-M: **Exploring and dissecting genome-wide gene expression responses of** *Penicillium chrysogenum* **to phenylacetic acid consumption and penicillinG production**. *BMC Genomics* 2009, **10**(1):75.

301. Tusher VG, Tibshirani R, Chu G: **Significance analysis of microarrays applied to the ionizing radiation response**. *Proc Natl Acad Sci* 2001, **98**(9):5116-5121.

302. Katoh K, Rozewicki J, Yamada KD: **MAFFT online service: multiple sequence alignment, interactive sequence choice and visualization**. *Brief Bioinform* 2017:bbx108.

303. Katoh K, Kuma K-i, Toh H, Miyata T: **MAFFT version 5: improvement in accuracy of multiple sequence alignment**. *Nucleic Acids Res* 2005, **33**(2):511-518.

304. Letunic I, Bork P: **Interactive tree of life (iTOL) v3: an online tool for the display and annotation of phylogenetic and other trees**. *Nucleic Acids Res* 2016, **44**(W1):W242-W245.

305. Sakamoto T, Ihara H, Kozaki S, Kawasaki H: **A cold-adapted endo-arabinanase from** *Penicillium chrysogenum*. *Biochim Biophys Acta* 2003, **1624**(1):70-75.

306. Sloothaak J, Tamayo-Ramos JA, Odoni DI, Laothanacharoen T, Derntl C, Mach-Aigner AR, Martins dos Santos VAP, Schaap PJ: **Identification and functional characterization of novel xylose transporters from the cell factories** *Aspergillus niger* **and** *Trichoderma reesei*. *Biotechnol Biofuels* 2016, **9**(1):1-15.

307. Torchia T, Hamilton R, Cano C, Hopper JE: **Disruption of regulatory gene** *GAL80* **in** *Saccharomyces cerevisiae*: **effects on carbon-controlled regulation of the galactose/melibiose pathway genes**. *Mol Cell Biol* 1984, **4**(8):1521-1527.

308. Tani T, Taguchi H, Fujimori KE, Sahara T, Ohgiya S, Kamagata Y, Akamatsu T: **Isolation and characterization of xylitol-assimilating mutants of recombinant** *Saccharomyces cerevisiae*. *J Biosci Bioeng* 2016, **122**(4):446-455.

309. Baruffini E, Goffrini P, Donnini C, Lodi T: **Galactose transport in** *Kluyveromyces lactis*: **major role of the glucose permease Hgt1**. *FEMS Yeast Res* 2006, **6**(8):1235-1242.

310. Billard P, Ménart S, Blaisonneau J, Bolotin-Fukuhara M, Fukuhara H, Wésolowski-Louvel M: **Glucose uptake in K**luyveromyces lactis**: role of the** *HGT1* **gene in glucose transport**. *J Bacteriol* 1996, **178**(20):5860-5866.

311. Maier A, Völker B, Boles E, Fuhrmann GF: **Characterisation of glucose transport in** *Saccharomyces cerevisiae* **with plasma membrane vesicles (countertransport) and intact**

cells (initial uptake) with single Hxt1, Hxt2, Hxt3, Hxt4, Hxt6, Hxt7 or Gal2 transporters. *FEMS Yeast Res* 2002, **2**(4):539-550.

312. Weusthuis RA, Adams H, Scheffers WA, Van Dijken JP: **Energetics and kinetics of maltose transport in *Saccharomyces cerevisiae*: a continuous culture study**. *Appl Environ Microbiol* 1993, **59**(9):3102-3109.

313. Daran-Lapujade P, Daran J-M, van Maris AJA, de Winde JH, Pronk JT: **Chemostat-based micro-array analysis in baker's yeast**. *Adv Microb Physiol* 2008, **54**:257-417.

314. Cepeda-García C, Domínguez-Santos R, García-Rico RO, García-Estrada C, Cajiao A, Fierro F, Martín JF: **Direct involvement of the *CreA* transcription factor in penicillin biosynthesis and expression of the *pcbAB* gene in *Penicillium chrysogenum***. *Appl Microbiol Biotechnol* 2014, **98**(16):7113-7124.

315. Cubero B, Scazzocchio C: **Two different, adjacent and divergent zinc finger binding sites are necessary for CREA-mediated carbon catabolite repression in the proline gene cluster of *Aspergillus nidulans***. *EMBO J* 1994, **13**(2):407.

316. Jahn TP, Schulz A, Taipalensuu J, Palmgren MG: **Post-translational modification of plant plasma membrane H+-ATPase as a requirement for functional complementation of a yeast transport mutant**. *J Biol Chem* 2002, **277**(8):6353-6358.

317. Verho R, Penttilä M, Richard P: **Cloning of two genes (LAT1, 2) encoding specific L-arabinose transporters of the L-arabinose fermenting yeast *Ambrosiozyma monospora***. *Appl Biochem Biotechnol* 2011, **164**(5):604-611.

318. Teusink B, Diderich JA, Westerhoff HV, Van Dam K, Walsh MC: **Intracellular glucose concentration in derepressed yeast cells consuming glucose is high enough to reduce the glucose transport rate by 50%**. *J Bacteriol* 1998, **180**(3):556-562.

319. Knoshaug EP, Franden MA, Stambuk BU, Zhang M, Singh A: **Utilization and transport of L-arabinose by non-*Saccharomyces* yeasts**. *Cellulose* 2009, **16**(4):729-741.

320. Richard P, Putkonen M, Väänänen R, Londesborough J, Penttilä M: **The missing link in the fungal L-arabinose catabolic pathway, identification of the L-xylulose reductase gene**. *Biochem* 2002, **41**(20):6432-6437.

321. Wang C, Li Y, Qiu C, Wang S, Ma J, Shen Y, Zhang Q, Du B, Ding Y, Bao X: **Identification of Important Amino Acids in Gal2p for Improving the L-arabinose Transport and Metabolism in *Saccharomyces cerevisiae***. *Front Microbiol* 2017, **8**.

322. Bracher JM, Verhoeven MD, Wisselink HW, Crimi B, Nijland JG, Driessen AJM, Klaassen P, van Maris AJA, Daran J-MG, Pronk JT: **The *Penicillium chrysogenum* transporter *Pc*AraT enables high-affinity, glucose insensitive L-arabinose transport in *Saccharomyces cerevisiae***. *Biotechnol Biofuels* 2018, **11**(1):63.

323. Gietz RD, Schiestl RH, Willems AR, Woods RA: **Studies on the transformation of intact yeast cells by the LiAc/SS-DNA/PEG procedure**. *Yeast* 1995, **11**.

324. Ostergaard S, Walløe KO, Gomes CS, Olsson L, Nielsen J: **The impact of GAL6, GAL80, and MIG1 on glucose control of the GAL system in *Saccharomyces cerevisiae***. *FEMS Yeast Res* 2001, **1**(1):47-55.

325. Mangat S, Chandrashekarappa D, McCartney RR, Elbing K, Schmidt MC: **Differential roles of the glycogen-binding domains of β subunits in regulation of the Snf1 kinase complex**. *Eukaryot Cell* 2010, **9**(1):173-183.

326. Dickson RC, Nagiec EE, Wells GB, Nagiec MM, Lester RL: **Synthesis of mannose-(inositol-P) 2-ceramide, the major sphingolipid in *Saccharomyces cerevisiae*, requires the *IPT1* (YDR072c) gene**. *J Biol Chem* 1997, **272**(47):29620-29625.

327. Crowley JH, Leak FW, Shianna KV, Tove S, Parks LW: **A mutation in a purported regulatory gene affects control of sterol uptake in *Saccharomyces cerevisiae***. *J Bacteriol* 1998, **180**(16):4177-4183.

328. van Heusden GPH, Wenzel TJ, Lagendijk EL, De Steensma H, van den Berg JA: **Characterization of the yeast *BMH1* gene encoding a putative protein homologous to mammalian protein kinase II activators and protein kinase C inhibitors**. *FEBS Lett* 1992, **302**(2):145-150.

329. Van Hemert M, van Heusden G, Steensma H: **Yeast 14-3-3 proteins**. *Yeast* 2001, **18**(10):889-895.

330. Roberts RL, Mösch H-U, Fink GR: **14-3-3 proteins are essential for RAS/MAPK cascade signaling during pseudohyphal development in *S. cerevisiae***. *Cell* 1997, **89**(7):1055-1065.

331. Wang C, Skinner C, Easlon E, Lin S-J: **Deleting the 14-3-3 protein Bmh1 extends life span in *Saccharomyces cerevisiae* by increasing stress response**. *Genetics* 2009, **183**(4):1373-1384.

332. Wang C, Shen Y, Zhang Y, Suo F, Hou J, Bao X: **Improvement of L-arabinose fermentation by modifying the metabolic pathway and transport in *Saccharomyces cerevisiae***. *Biomed Res Int* 2013, **2013**.

333. Boender LG, de Hulster EA, van Maris AJA, Daran-Lapujade PA, Pronk JT: **Quantitative physiology of *Saccharomyces cerevisiae* at near-zero specific growth rates**. *Appl Environ Microbiol* 2009, **75**(17):5607-5614.

334. Weusthuis RA, Pronk JT, Van Den Broek P, Van Dijken J: **Chemostat cultivation as a tool for studies on sugar transport in yeasts**. *Microbiol Rev* 1994, **58**(4):616-630.

335. Ahuatzi D, Riera A, Peláez R, Herrero P, Moreno F: **Hxk2 regulates the phosphorylation state of Mig1 and therefore its nucleocytoplasmic distribution**. *J Biol Chem* 2007, **282**(7):4485-4493.

336. Raamsdonk LM, Diderich JA, Kuiper A, van Gaalen M, Kruckberg AL, Berden JA, Van Dam K: **Co-consumption of sugars or ethanol and glucose in a *Saccharomyces cerevisiae* strain deleted in the *HXK2* gene**. *Yeast* 2001, **18**(11):1023-1033.

337. Bro C, Knudsen S, Regenberg B, Olsson L, Nielsen J: **Improvement of galactose uptake in *Saccharomyces cerevisiae* through overexpression of phosphoglucomutase: example of transcript analysis as a tool in inverse metabolic engineering**. *Appl Environ Microbiol* 2005, **71**(11):6465-6472.

338. Sun L, Zeng X, Yan C, Sun X, Gong X, Rao Y, Yan N: **Crystal structure of a bacterial homologue of glucose transporters GLUT1-4**. *Nature* 2012, **490**(7420):361.

339. Jordan P, Choe J-Y, Boles E, Oreb M: **Hxt13, Hxt15, Hxt16 and Hxt17 from *Saccharomyces cerevisiae* represent a novel type of polyol transporters**. *Sci Rep* 2016, **6**.

340. Biswas C, Djordjevic JT, Zuo X, Boles E, Jolliffe KA, Sorrell TC, Chen SC-A: **Functional characterization of the hexose transporter Hxt13p: an efflux pump that mediates resistance to miltefosine in yeast**. *Fungal Genet Biol* 2013, **61**:23-32.

341. Fulton LM, Lynd LR, Körner A, Greene N, Tonachel LR: **The need for biofuels as part of a low carbon energy future**. *Biofuels, Bioprod Biorefin* 2015, **9**(5):476-483.

342. Gombert AK, van Maris AJA: **Improving conversion yield of fermentable sugars into fuel ethanol in 1ˢᵗ generation yeast-based production processes**. *Curr Opin Biotechnol* 2015, **33**:81-86.

343. Basso LC, Basso T, Nitsche Rocha S: **Ethanol production in Brazil: The industrial process and its impact on yeast fermentation**; 2011.

344. Lynd LR, Liang X, Biddy MJ, Allee A, Cai H, Foust T, Himmel ME, Laser MS, Wang M, Wyman CE: **Cellulosic ethanol: status and innovation**. *Curr Opin Biotechnol* 2017, **45**(Supplement C):202-211.

345. Shen Y, Chen X, Peng B, Chen L, Hou J, Bao X: **An efficient xylose-fermenting recombinant *Saccharomyces cerevisiae* strain obtained through adaptive evolution and its global transcription profile**. *Appl Microbiol Biotechnol* 2012, **96**.

346. Wei N, Oh EJ, Million G, Cate JHD, Jin Y-S: **Simultaneous utilization of cellobiose, xylose, and acetic acid from lignocellulosic biomass for biofuel production by an engineered yeast platform**. *ACS Synth Biol* 2015, **4**(6):707-713.

347. Shen M-H, Song H, Li B-Z, Yuan Y-J: **Deletion of D-ribulose-5-phosphate 3-epimerase (*RPE1*) induces simultaneous utilization of xylose and glucose in xylose-utilizing *Saccharomyces cerevisiae***. *Biotechnol Lett* 2015, **37**(5):1031-1036.

348. Aguilera A: **Deletion of the phosphoglucose isomerase structural gene makes growth and sporulation glucose dependent in *Saccharomyces cerevisiae***. *Mol Gen Genet* 1986, **204**(2):310-316.

349. Gawand P, Hyland P, Ekins A, Martin VJJ, Mahadevan R: **Novel approach to engineer strains for simultaneous sugar utilization**. *Metab Eng* 2013, **20**:63-72.

350. Boles E, Lehnert W, Zimmermann FK: **The role of the NAD-dependent glutamate dehydrogenase in restoring growth on glucose of a *Saccharomyces cerevisiae* phosphoglucose isomerase mutant**. *Eur J Biochem* 1993, **217**(1):469-477.

351. Dickinson JR, Sobanski MA, Hewlins MJE: **In *Saccharomyces cerevisiae* deletion of phosphoglucose isomerase can be suppressed by increased activities of enzymes of the hexose monophosphate pathway**. *Microbiology* 1995, **141**:385-391.

352. Papapetridis I, Goudriaan M, Vázquez Vitali M, de Keijzer NA, van den Broek M, van Maris AJA, Pronk JT: **Optimizing anaerobic growth rate and fermentation kinetics in *Saccharomyces***

cerevisiae strains expressing Calvin-cycle enzymes for improved ethanol yield. *Biotechnol Biofuels* 2018, **11**(1):17.

353.   Kuyper M, Harhangi HR, Stave AK, Winkler AA, Jetten MSM, de Laat WTAM, den Ridder JJJ, Op den Camp HJM, van Dijken JP, Pronk JT: **High-level functional expression of a fungal xylose isomerase: the key to efficient ethanolic fermentation of xylose by** *Saccharomyces cerevisiae*? *FEMS Yeast Res* 2003, **4**(1):69-78.

354.   Aung HW, Henry SA, Walker LP: **Revising the representation of fatty acid, glycerolipid, and glycerophospholipid metabolism in the consensus model of yeast metabolism**. *Ind Biotechnol* 2013, **9**(4):215-228.

355.   Becker SA, Feist AM, Mo ML, Hannum G, Palsson BØ, Herrgard MJ: **Quantitative prediction of cellular metabolism with constraint-based models: the COBRA Toolbox**. *Nat Protoc* 2007, **2**:727.

356.   Hucka M, Finney A, Sauro HM, Bolouri H, Doyle JC, Kitano H, Arkin AP, Bornstein BJ, Bray D, Cornish-Bowden A *et al*: **The systems biology markup language (SBML): a medium for representation and exchange of biochemical network models**. *Bioinformatics* 2003, **19**(4):524-531.

357.   Johansson B, Hahn-Hägerdal B: **The non-oxidative pentose phosphate pathway controls the fermentation rate of xylulose but not of xylose in** *Saccharomyces cerevisiae* **TMB3001**. *FEMS Yeast Res* 2002, **2**(3):277-282.

358.   Bruinenberg PM, Van Dijken JP, Scheffers WA: **A theoretical analysis of NADPH production and consumption in yeasts**. *Microbiology* 1983, **129**(4):953-964.

359.   Gonçalves DL, Matsushika A, de Sales BB, Goshima T, Bon EPS, Stambuk BU: **Xylose and xylose/glucose co-fermentation by recombinant** *Saccharomyces cerevisiae* **strains expressing individual hexose transporters**. *Enzyme Microb Technol* 2014, **63**(Supplement C):13-20.

360.   Westman JO, Bonander N, Taherzadeh MJ, Franzén CJ: **Improved sugar co-utilisation by encapsulation of a recombinant** *Saccharomyces cerevisiae* **strain in alginate-chitosan capsules**. *Biotechnol Biofuels* 2014, **7**(1):102.

361.   De Winde JH, Crauwels M, Hohmann S, Thevelein JM, Winderickx J: **Differential requirement of the yeast sugar kinases for sugar sensing in establishing the catabolite-repressed state**. *Eur J Biochem* 1996, **241**(2):633-643.

362.   Belgareh-Touzé N, Léon S, Erpapazoglou Z, Stawiecka-Mirota M, Urban-Grimal D, Haguenauer-Tsapis R: **Versatile role of the yeast ubiquitin ligase Rsp5p in intracellular trafficking**. *Biochemical Society Transactions* 2008, **36**(5):791.

363.   Nijland JG, Shin HY, Boender LGM, de Waal PP, Klaassen P, Driessen AJM: **Improved xylose metabolism by a** *CYC8* **mutant of** *Saccharomyces cerevisiae*. *Appl Environ Microbiol* 2017, **83**(11).

364.   Vincent O, Carlson M: **Sip4, a Snf1 kinase-dependent transcriptional activator, binds to the carbon source-responsive element of gluconeogenic genes**. *EMBO J* 1998, **17**(23):7002-7008.

365.   Rahner A, Schöler A, Martens E, Gollwitzer B, Schüller HJ: **Dual influence of the yeast Cat1p (Snf1p) protein kinase on carbon source-dependent transcriptional activation of gluconeogenic genes by the regulatory gene** *CAT8*. *Nucleic Acids Res* 1996, **24**(12):2331-2337.

366.   Vincent O, Carlson M: **Gal83 mediates the interaction of the Snf1 kinase complex with the transcription activator Sip4**. *EMBO J* 1999, **18**(23):6672-6681.

367.   Schmidt MC, McCartney RR: β **-subunits of Snf1 kinase are required for kinase function and substrate definition**. *EMBO J* 2000, **19**(18):4936-4943.

368.   Heux S, Cadiere A, Dequin S: **Glucose utilization of strains lacking** *PGI1* **and expressing a transhydrogenase suggests differences in the pentose phosphate capacity among** *Saccharomyces cerevisiae* **strains**. *FEMS Yeast Res* 2008, **8**(2):217-224.

369.   Grabowska D, Chelstowska A: **The** *ALD6* **gene product is indispensable for providing NADPH in yeast cells lacking glucose-6-phosphate dehydrogenase activity**. *J Biol Chem* 2003, **278**(16):13984-13988.

370.   Celton M, Sanchez I, Goelzer A, Fromion V, Camarasa C, Dequin S: **A comparative transcriptomic, fluxomic and metabolomic analysis of the response of** *Saccharomyces cerevisiae* **to increases in NADPH oxidation**. *BMC Genomics* 2012, **13**:317-317.

371.   Gottardi M, Reifenrath M, Boles E, Tripp J: **Pathway engineering for the production of heterologous aromatic chemicals and their derivatives in *Saccharomyces cerevisiae*: bioconversion from glucose**. *FEMS Yeast Res* 2017, **17**(4):fox035-fox035.

372.   Klug L, Daum G: **Yeast lipid metabolism at a glance**. *FEMS Yeast Res* 2014, **14**(3):369-388.

373.   Tehlivets O, Scheuringer K, Kohlwein SD: **Fatty acid synthesis and elongation in yeast**. *Biochim Biophys Acta Cell Biol Lipids* 2007, **1771**(3):255-270.

374.   Entian K-D: **Genetic and biochemical evidence for hexokinase PII as a key enzyme involved in carbon catabolite repression in yeast**. *Mol Gen Genet* 1980, **178**(3):633-637.

375.   Entian KD, Fröhlich K-U: ***Saccharomyces cerevisiae* mutants provide evidence of hexokinase PII as a bifunctional enzyme with catalytic and regulatory domains for triggering catabolite repression**. *J Bacteriol* 1984, **158**:29-35.

376.   Peláez R, Herrero P, Moreno F: **Functional domains of yeast hexokinase 2**. *Biochem J* 2010, **432**(Pt 1):181-190.

377.   Petit T, Diderich JA, Kruckeberg AL, Gancedo C, Van Dam K: **Hexokinase regulates kinetics of glucose transport and expression of genes encoding hexose transporters in *Saccharomyces cerevisiae***. *J Bacteriol* 2000, **182**(23):6815-6818.

378.   Miskovic L, Alff-Tuomala S, Soh KC, Barth D, Salusjärvi L, Pitkänen J-P, Ruohonen L, Penttilä M, Hatzimanikatis V: **A design–build–test cycle using modeling and experiments reveals interdependencies between upper glycolysis and xylose uptake in recombinant *S. cerevisiae* and improves predictive capabilities of large-scale kinetic models**. *Biotechnol Biofuels* 2017, **10**:166.

379.   Shcherbik N, Pestov DG: **The ubiquitin ligase Rsp5 is required for ribosome stability in *Saccharomyces cerevisiae***. *RNA* 2011, **17**(8):1422-1428.

380.   Huibregtse JM, Yang JC, Beaudenon SL: **The large subunit of RNA polymerase II is a substrate of the Rsp5 ubiquitin-protein ligase**. *Proc Natl Acad Sci* 1997, **94**(8):3656-3661.

381.   Kaliszewski P, Zołądek T: **The role of Rsp5 ubiquitin ligase in regulation of diverse processes in yeast cells**. *Acta Biochim Pol* 2008, **55**(4):649-662.

382.   Haguenauer-Tsapis R, André B: **Membrane trafficking of yeast transporters: mechanisms and physiological control of downregulation**. In: *Molecular Mechanisms Controlling Transmembrane Transport.* Berlin, Heidelberg: Springer Berlin Heidelberg; 2004: 273-323.

383.   Krampe S, Stamm O, Hollenberg CP, Boles E: **Catabolite inactivation of the high-affinity hexose transporters Hxt6 and Hxt7 of *Saccharomyces cerevisiae* occurs in the vacuole after internalization by endocytosis**. *FEBS Lett* 1998, **441**(3):343-347.

384.   Vincent O, Townley R, Kuchin S, Carlson M: **Subcellular localization of the Snf1 kinase is regulated by specific β subunits and a novel glucose signaling mechanism**. *Genes Dev* 2001, **15**(9):1104-1114.

385.   Erickson JR, Johnston M: **Genetic and molecular characterization of Gal83: Its interaction and similarities with other genes involved in glucose repression in *Saccharomyces cerevisiae***. *Genetics* 1993, **135**(3):655-664.

386.   Matsumoto K, Toh-e A, Oshima Y: **Isolation and characterization of dominant mutations resistant to carbon catabolite repression of galactokinase synthesis in *Saccharomyces cerevisiae***. *Mol Cell Biol* 1981, **1**(2):83-93.

387.   Momcilovic M, Iram SH, Liu Y, Carlson M: **Roles of the glycogen-binding domain and Snf4 in glucose inhibition of *SNF1* protein kinase**. *J Biol Chem* 2008, **283**(28):19521-19529.

388.   Wiatrowski HA, van Denderen BJW, Berkey CD, Kemp BE, Stapleton D, Carlson M: **Mutations in the Gal83 glycogen-binding domain activate the Snf1/Gal83 kinase pathway by a glycogen-independent mechanism**. *Mol Cell Biol* 2004, **24**(1):352-361.

389.   Schüller H-J: **Transcriptional control of nonfermentative metabolism in the yeast *Saccharomyces cerevisiae***. *Curr Genet* 2003, **43**(3):139-160.

390.   Gancedo JM: **Yeast carbon catabolite repression**. *Microbiol Mol Biol Rev* 1998, **62**(2):334-361.

391.   Canelas AB, Harrison N, Fazio A, Zhang J, Pitkänen J-P, van den Brink J, Bakker BM, Bogner L, Bouwman J, Castrillo JI *et al*: **Integrated multilaboratory systems biology reveals differences in protein metabolism between two reference yeast strains**. *Nat Comm* 2010, **1**:145.

392.   Walfridsson M, Hallborn J, Penttilä M, Keränen S, Hahn-Hägerdal B: **Xylose-metabolizing *Saccharomyces cerevisiae* strains overexpressing the *TKL1* and *TAL1* genes encoding the pentose phosphate pathway enzymes transketolase and transaldolase**. *Appl Environ Microbiol* 1995, **61**(12):4184-4190.

393. Bettiga M, Bengtsson O, Hahn-Hägerdal B, Gorwa-Grauslund MF: **Arabinose and xylose fermentation by recombinant *Saccharomyces cerevisiae* expressing a fungal pentose utilization pathway**. *Microb Cell Fact* 2009, **8**(1):40.

394. Wang C, Zhao J, Qiu C, Wang S, Shen Y, Du B, Ding Y, Bao X: **Coutilization of D-glucose, D-xylose, and L-arabinose in *Saccharomyces cerevisiae* by coexpressing the metabolic pathways and evolutionary engineering**. *Biomed Res Int* 2017, **2017**.

395. Berkhout J, Bosdriesz E, Nikerel E, Molenaar D, de Ridder D, Teusink B, Bruggeman FJ: **How biochemical constraints of cellular growth shape evolutionary adaptations in metabolism**. *Genetics* 2013, **194**(2):505-512.

396. Mans R, Daran J-MG, Pronk JT: **Under pressure: evolutionary engineering of yeast strains for improved performance in fuels and chemicals production**. *Curr Opin Biotechnol* 2018, **50**:47-56.

397. Hanly TJ, Urello M, Henson MA: **Dynamic flux balance modeling of *S. cerevisiae* and *E. coli* co-cultures for efficient consumption of glucose/xylose mixtures**. *Appl Environ Microbiol* 2012, **93**(6):2529-2541.

398. Eiteman MA, Lee SA, Altman E: **A co-fermentation strategy to consume sugar mixtures effectively**. *J Biol Eng* 2008, **2**(1):3.

399. Eiteman MA, Lee SA, Altman R, Altman E: **A substrate-selective co-fermentation strategy with *Escherichia coli* produces lactate by simultaneously consuming xylose and glucose**. *Biotechnol Bioeng* 2009, **102**(3):822-827.

400. Chen Y: **Development and application of co-culture for ethanol production by co-fermentation of glucose and xylose: a systematic review**. *J Ind Microbiol Biotechnol* 2011, **38**(5):581-597.

401. Laplace JM, Delgenes JP, Moletta R, Navarro JM: **Cofermentation of glucose and xylose to ethanol by a respiratory-deficient mutant of *Saccharomyces cerevisiae* co-cultivated with a xylose-fermenting yeast**. *J Ferment Bioeng* 1993, **75**(3):207-212.

402. Chandrakant P, Bisaria V: **Simultaneous bioconversion of cellulose and hemicellulose to ethanol**. *Crit Rev Biotechnol* 1998, **18**(4):295-331.

403. Luttik MA, Kötter P, Salomons FA, Van der Klei IJ, Van Dijken JP, Pronk JT: **The *Saccharomyces cerevisiae* ICL2 gene encodes a mitochondrial 2-methylisocitrate lyase involved in propionyl-coenzyme A metabolism**. *J Bacteriol* 2000, **182**(24):7007-7013.

404. Verhoeven MD, Bracher JM, Nijland JG, Bouwknegt J, Daran J-MG, Driessen AJM, van Maris AJA, Pronk JT: **Laboratory evolution of a glucose-phosphorylation-deficient, arabinose-fermenting *S. cerevisiae* strain reveals mutations in *GAL2* that enable glucose-insensitive L-arabinose uptake**. *FEMS Yeast Res* 2018, **18**(6).

405. Lee M, Rozeboom HJ, de Waal PP, de Jong RM, Dudek HM, Janssen DB: **Metal dependence of the xylose isomerase from *Piromyces* sp. E2 explored by activity profiling and protein crystallography**. *Biochem* 2017, **56**(45):5991-6005.

406. Chang Q, Griest TA, Harter TM, Petrash JM: **Functional studies of aldo-keto reductases in *Saccharomyces cerevisiae***. *Biochim Biophys Acta* 2007, **1773**(3):321-329.

407. Träff K, Jönsson LJ, Hahn-Hägerdal B: **Putative xylose and arabinose reductases in *Saccharomyces cerevisiae***. *Yeast* 2002, **19**(14):1233-1241.

408. Paalme T, Kevvai K, Vilbaste A, Hälvin K, Nisamedtinov I: **Uptake and accumulation of B-group vitamers in *Saccharomyces cerevisiae* in ethanol-stat fed-batch culture**. *World J Microbiol Biotechnol* 2014, **30**(9):2351-2359.

409. Boender LG, van Maris AJA, de Hulster EA, Almering MJ, van der Klei IJ, Veenhuis M, de Winde JH, Pronk JT, Daran-Lapujade P: **Cellular responses of *Saccharomyces cerevisiae* at near-zero growth rates: transcriptome analysis of anaerobic retentostat cultures**. *FEMS Yeast Res* 2011, **11**(8):603-620.

410. Kumar D, Singh V: **Dry-grind processing using amylase corn and superior yeast to reduce the exogenous enzyme requirements in bioethanol production**. *Biotechnol Biofuels* 2016, **9**(1):228.

411. La Grange DC, Pretorius IS, Claeyssens M, Van Zyl WH: **Degradation of Xylan to D-Xylose by Recombinant *Saccharomyces cerevisiae* Coexpressing the *Aspergillus niger* β -Xylosidase (xlnD) and the *Trichoderma reesei* Xylanase II (xyn2) Genes**. *Appl Environ Microbiol* 2001, **67**(12):5512-5519.

412. Katahira S, Fujita Y, Mizuike A, Fukuda H, Kondo A: **Construction of a xylan-fermenting yeast strain through codisplay of xylanolytic enzymes on the surface of xylose-utilizing *Saccharomyces cerevisiae* cells**. *Appl Environ Microbiol* 2004, **70**(9):5407-5414.

413. Lee JH, Heo S-Y, Lee J-W, Yoon K-H, Kim Y-H, Nam S-W: **Thermostability and xylan-hydrolyzing property of endoxylanase expressed in yeast *Saccharomyces cerevisiae***. *Biotechnol Bioprocess Eng* 2009, **14**(5):639-644.

414. Galazka JM, Tian C, Beeson WT, Martinez B, Glass NL, Cate JH: **Cellodextrin transport in yeast for improved biofuel production**. *Science* 2010, **330**(6000):84-86.

415. Hu M-L, Zha J, He L-W, Lv Y-J, Shen M-H, Zhong C, Li B-Z, Yuan Y-J: **Enhanced bioconversion of cellobiose by industrial *Saccharomyces cerevisiae* used for cellulose utilization**. *Front Microbiol* 2016, **7**.

416. Ryabova OB, Chmil OM, Sibirny AA: **Xylose and cellobiose fermentation to ethanol by the thermotolerant methylotrophic yeast *Hansenula polymorpha***. *FEMS Yeast Res* 2003, **4**(2):157-164.

417. Yuan WJ, Chang BL, Ren JG, Liu JP, Bai FW, Li YY: **Consolidated bioprocessing strategy for ethanol production from Jerusalem artichoke tubers by *Kluyveromyces marxianus* under high gravity conditions**. *J Appl Microbiol* 2012, **112**(1):38-44.

418. Goshima T, Tsuji M, Inoue H, Yano S, Hoshino T, Matsushika A: **Bioethanol production from lignocellulosic biomass by a novel *Kluyveromyces marxianus* strain**. *Biosci Biotechnol Biochem* 2013, **77**(7):1505-1510.

419. Scully S, Orlygsson J: **Recent advances in second generation ethanol production by thermophilic bacteria**. *Energies* 2015, **8**(1):1.

420. Lynd LR, van Zyl WH, McBride JE, Laser M: **Consolidated bioprocessing of cellulosic biomass: an update**. *Curr Opin Biotechnol* 2005, **16**(5):577-583.

Curriculum vitae

Maarten Dirk Verhoeven was born in Amersfoort, The Netherlands). on July 20, 1987, He attended pre-university education (VWO) at the Herman Jordan Lyceum in Zeist. In 2007, he enrolled in the BSc programme Life Science and Technology, which is jointly taught by Leiden University and the Delft University of Technology. In his BSc research thesis, Maarten conducted a chemostat-based transcriptome study of *Penicillium chrysogenum* strains used for semi-synthetic cephalosporin production under the supervision of Dr. Jean-Marc Daran and Dr. Tania Veiga. Subsequently, Maarten enrolled in the MSc Life Science and Technology at the Delft University of Technology, specializing in applied industrial and environmental microbiology by choosing the track 'Cell Factory'. As an MSc student, Maarten was actively involved in organizing a study tour for fellow students to companies and universities in South-Korea and Japan in 2011. During his MSc research thesis, Maarten characterized arginine catabolism in *Kluyveromyces lactis* through a combination of proteomics, transcriptomics and metabolomics, under the supervision of Dr. Jean-Marc Daran and Dr. Gabriele Romagnoli. Maarten completed his MSc studies with a 3- months industrial internship at HEINEKEN in Zoeterwoude, which focused on brewing-yeast production and characterization of beer fermentation processes. After graduating in 2013 (*cum laude*), he started his PhD project within the Industrial Microbiology group at the Delft University. This project, supervised by prof. dr. ir. Ton van Maris and prof. dr. Jack Pronk, focused on bioethanol production from lignocellulosic feedstocks using *Saccharomyces cerevisiae*. Being part of the BE-Basic partnership, his project allowed for close collaboration with industry and academic partners outside Delft. The results of this research are described in thesis.

Acknowledgements

The PhD thesis in front of you would not have been possible without the contribution of many people who I have met, got to know and became dear to me. I am tremendously grateful to all of you and I hope I can convey my gratitude to most of you below. I have had the enormous privilege to have worked within IMB for the majority of my time in academia. It was when I started my internship as a bachelor student, back in 2009, that my interest in conducting research kicked off. Not long after, I continued at IMB as an MSc student within a project that allowed me to get familiar with conducting science using a multitude of techniques and methods. Many thanks to my BSc- and MSc-thesis supervisors – Tania and Gabriele as well as Jean-Marc who also was closely involved during my PhD.

   With already quite some time spent at IMB I felt right at home when I started my PhD with Jack as promotor and Ton as daily supervisor. Ton – I thoroughly enjoyed working with you during the first three years of my PhD. Within 'ethanolics' you stimulated all of us to collaborate within our projects. I have always very much appreciated your approach towards science in which you always motivated me to pursue hypotheses while at the same staying on top of what was required to finish up the project. With you leaving for Sweden the TU-Delft has truly lost an irreplaceable scientist, supervisor and teacher. But I am thrilled that you are one of my promoters during my defense and as you have once told me: 'Don't worry, BE-Basic' ;). Jack – I have always been, and still am inspired by your never-ending enthusiasm and genuine excitement about everything science-related. From early on in my PhD you and Ton involved me with teaching BSc students, in which I learned a lot about both of you about how to convey and inspire about the inner workings of the cell. It was a lot of fun to join along in the exam corrections, the course evaluations or the general goofing around with the students during the lunch breaks (Jack; K3? Really? ;)). The final 1.5 years that you also became my daily supervisor (and a fellow ethanolic) were equally inspiring and productive as well! Thank you for keeping faith in the mixed culture story and for correcting all the manuscripts that are now part of this thesis! Jean-Marc – I have always appreciated, and very much valued, your input in my PhD project. During my time at IMB you have always been available for advice and guidance. Thanks for steering towards using CRISPR/Cas9 technology from very early on in the project!

   IMB would not function normally without the technical staff. Marijke - on many occasions your expertise in the lab helped me tremendously when I started up new experiments. Erik – aside from all the ins- and outs you taught me about fermentation, I enjoyed having you around as a fellow geek in the lab 8-|. Pilar – on several occasions you stepped in with your lightning-fast genome sequencing skills, thanks a lot! No company can provide such an incredible service ;). Thanks all three of you for all your invaluable help and for reminding me to clean up my stuff when I left it lying around in the most inconspicuous places in the lab :). Marcel – thanks for all your help in deciphering DNA sequencing data

from multiple laboratory evolution experiment I did within my thesis. Jannie, Astrid and Apilena; thank you for your flexibility on the occasions I suddenly decided that 8 reactors needed to be autoclaved on the same day!

As part of BE-Basic I had the fortune of interacting with colleagues from Groningen University and DSM. Within the OMNIYEAST group, several very fruitful collaborations were started that eventually resulted in two publications that are now part of this thesis. Misun and Dick – our manganese thriller would not have ended as well as it did without your help and input, thank you! Hanna – thank you for your valuable input during the first years of my PhD. Jeroen – many thanks for helping Jasmine and I with the transporter essay, despite you having a high fever! Thanks also to both you and Arnold for your regular input and suggestion during my research and during the writing process. One of the privileges of working within a public private partnership such as BE-Basic is the opportunity to collaborate with industrial parties, which in my case was DSM. Paul, Paul, Hans, Mickel and Sander – thank you very much for the many constructive discussions and collaborations! Besides the invaluable input on science, experimental design and IP, several of you also helped with writing the review that is now (slightly adapted) also part of this thesis. I thank Jim Lane from BiofuelsDigest and POET-DSM Advanced Biofuels for their kind permission to reproduce the photographs shown in Fig. 4 of the introduction of this thesis.

As mentioned above I was a member of the ethanolics during the main part of my PhD. I would like to thanks my fellow ethanolics; Laura, Jasmine and Ioannis. Your combined input has been paramount in my PhD project! Ioannis – I remember the wild ideas we had four years ago and I am really glad we have been able to work out at least one them! Without your perseverance and drive we would definitely not have achieved what we did in the co-consumption project, thanks you very much for that! Jasmine – from the beginning on, I always very much valued the discussions about both our projects. I am grateful for all the collaboration we have done on pentose transport and for the mutual understanding we shared about the challenges in pentose fermentation with yeast. We indeed experienced several high- and low points in terms of experimental results (#Pc20 ;)). I thoroughly enjoyed our trips to the OMNIYEAST meetings and I am very proud of what we were able to achieve, Thanks for everything!

I also would like to thank the students I had the privilege to supervise during their thesis. Tim, Lara, Lycka, Laurenz-Jan, Jildau, Jonna, Sanne, Sophie and Renzo – I had a great time supervising your projects and I can count myself lucky to have collaborated with such motivated students. You have contributed significantly to the results presented in this thesis. Thank you all very much!

Of course, everyday life at IMB involves a lot more people than the ones I thanked so far. It was a joy to work within a group in which you really feel part of a team! Harmen – I am grateful for our regular discussions about our project and your guidance on how to do research ('gewoon quenchen en weggooien' ;)), thanks! Niels – thank you for taking the time at the beginning of my project to help me make a plan for strain-construction! Xavier

- it was a pleasure to have you as an office mate during the final year. It was always a joy to exchange ideas about our research project and occasionally gossip about the ins and outs of BT. Wijb - thanks a lot for babysitting my reactors when I was on holidays. A big thank you to; Barbara, Marit, Dani, Daniel, Frank, Nick, Nick, Arthur, Mark, Jasper, Susan, Melanie, Tracey, Pascale, Sofia, Thomas, Anna, Jasmijn, Philip, Barbara, Francine, Maaike, Marloes, Aurin, Christiaan, Matthijs, Stefan, Tim, Angel, Anja, Eline, Ewout, Alex, Angelica, Thomas, Wesley & Paola for all the small things in the lab and for the great time at IMB!

Needless to say, I want to thank my two paranymphs Laura and Nicolo for all their efforts and for standing by my side during my defense. The members of the PhD committee are thanked for joining the defense and for reading my thesis.

Naast mijn activiteiten binnen IMB heb ik heel veel gehad aan de mensen om heen. Vrienden, familie, huisgenoten en clubgenoten heel erg bedankt voor al jullie steun! Jac, Joost en Thomas, bedankt voor de lange avonden of de bank! Wynze – het is altijd een genoegen om onder het genot van een kop koffie of een glas bier het reilen en zeilen van de wereld te bespreken.

Pap en Mam – Zonder jullie was ik nooit zover gekomen. Jullie oneindige vertrouwen in mij van jongs af aan hebben me ontzettend veel gebracht. Ik voel me enorm bevoorrecht om in ons gezin te zijn opgegroeid! Ook mijn beide broers; Willem en Steven – bedankt voor jullie steun en het af en toe eraan herinneren dat het leven meer is dan alleen je werk!

Laura – ik ben ontzettend blij dat ik jou heb ontmoet bij IMB! Het is geweldig om met jou s 'avonds op de bank na te praten, te lachen en te ontspannen. Het waren bewogen jaren waarin we lief en leed hebben gedeeld. Daar ben ik ontzettend dankbaar voor! Samen gaan we nog vele geweldige avonturen tegemoet!

List of publications

1. T. Veiga, A.K. Gombert, N. Landes, **Maarten D. Verhoeven**, J.A Kiel, A.M. Krikken, J.G. Nijland, H. Touw, M.A.H. Luttik, J.C. van der Toorn, A.J.M. Driessen, R.A. Bovenberg, M.A. van den Berg, I.J. van der Klei, J.T. Pronk and J.M.G. Daran. 'Metabolic engineering of β-oxidation in *Penicillium chrysogenum* for improved semi-synthetic cephalosporin biosynthesis'. *Metabolic Engineering* (2012). 14(4), 437-448.

2. G. Romagnoli, **Maarten D. Verhoeven**, R. Mans, Y. Fleury Rey, R. Bel- Rhlid, R. Zefar, A. ten Pierickx, M. Thompson, V. Müller, A. Wahl, J.T Pronk and J.M.G Daran. 'An alternative, arginase-independent pathway for arginine metabolism in *Kluyveromyces lactis* involves guanidinobutyrase as a key enzyme.' *Molecular Microbiology* (2014). 14(5), 562-586.

3. **Maarten D. Verhoeven***, M. Lee*, L. Kamoen, M. van den Broek, D.B. Janssen, J.M.G Daran, A.J.A. van Maris, and J.T Pronk. 'Mutations in *PMR1* stimulate xylose isomerase activity and anaerobic growth on xylose of engineered *Saccharomyces cerevisiae* by influencing manganese homeostasis.' *Scientific Reports* 7 (2017): 46155.

4. M.L.A. Jansen, J.M. Bracher, I. Papapetridis, **Maarten D. Verhoeven**, H. de Bruijn, P.P de Waal, A.J.A van Maris, P. Klaassen and J.T Pronk, '*Saccharomyces cerevisiae* strains for second-generation ethanol production: from academic exploration to industrial implementation'. *FEMS Yeast Research* (2017), *17* (5).

5. J.M. Bracher*, **Maarten D. Verhoeven***, H.W. Wisselink, B. Crimi, J.G. Nijland, A.J.M. Driessen, Paul Klaassen, A.J.A. van Maris, J.M.G. Daran and J.T. Pronk, 'The *Penicillium chrysogenum* transporter *Pc*AraT enables high-affinity, glucose insensitive l-arabinose transport in *Saccharomyces cerevisiae.*' *Biotechnology for Biofuels 11*(1), *63*, (2018).

6. **Maarten D. Verhoeven**, J.M. Bracher, J.G. Nijland, J. Bouwknegt, J.M.G. Daran, A.J.M. Driessen, A.J.A. van Maris and J.T. Pronk. 'Laboratory evolution of a glucose-phosphorylation-deficient, arabinose-fermenting *S. cerevisiae* strain reveals mutations in *GAL2* that enable glucose-insensitive ʟ-arabinose uptake'. *FEMS Yeast Research 18*(6), (2018).

7. I. Papapetridis*, **Maarten D. Verhoeven***, S.J. Wiersma, M. Goudriaan, A.J.A. van Maris and Jack T. Pronk. 'Laboratory evolution for forced glucose-xylose co-consumption enables identification of mutations that improve mixed-sugar fermentation by xylose-fermenting *Saccharomyces cerevisiae*'. *FEMS Yeast Research 18*(6), (2018),

8. **Maarten D. Verhoeven**, S.C. de Valk, J.M.G. Daran, A.J.A. van Maris & J.T. Pronk. 'Fermentation of glucose-xylose-arabinose mixtures in repeated batch cultures by a synthetic consortium of single-sugar- fermenting *Saccharomyces cerevisiae* strains.' *FEMS Yeast Research,* (2018).

9. Jasmine M. Bracher, Oscar A. Martinez, Wijb J.C. Dekker, **Maarten D. Verhoeven**, Antonius J.A. van Maris and Jack T. Pronk. 'Reassessment of requirements for anaerobic xylose fermentation by engineered, non-evolved *Saccharomyces cerevisiae* strains' *Manuscript submitted for publication.*

*Shared first authorship